Design, Synthesis and Evaluation of Novel N-linked Quinolone and Naphthyridone Analogs as Potential Anti-tubercular Agents

THESIS

Submitted in partial fulfilment

of the requirements for the degree of

DOCTOR OF PHILOSOPHY

by

SHAHUL HAMEED P
(2010PHXF012H)

Under the Supervision of
D. SRIRAM

BITS Pilani
Pilani | Dubai | Goa | Hyderabad

BIRLA INSTITUTE OF TECHNOLOGY AND SCIENCE, PILANI

2015

BIRLA INSTITUTE OF TECHNOLOGY AND SCIENCE, PILANI

CERTIFICATE

This is to certify that the thesis entitled "**Design, Synthesis and Evaluation of Novel N-linked Quinolone and Naphthyridone Analogs as Potential Anti-tubercular Agents**" and submitted by **SHAHUL HAMEED P** ID No. **2010PHXF012H** for award of Ph.D. of the institute embodies original work done by him under my supervision.

Signature of the Supervisor:

Name in capital letters   : **D. SRIRAM**

Designation   : **Professor**

Date:

Acknowledgement

It is a moment of gratification and pride to look back with a sense of contentment at the long travelled path, to be able to recapture some of the fine moments and to be able to thank the infinite number of people, some of whom were with me from the beginning, some who joined me at some stage during the journey, whose rally around kindness, love and blessings have brought me to this day. I wish to thank each and every one of them with all my heart.

encouragement, it would not have been possible for me to move a single step forward during my research work towards my goal. You have supported me in the darkest times and believed in me even when I did not believe in myself. Your tireless effort enabled me to take the time necessary to complete this work. I've always loved your joyful spirit and this spirit provided the boost that made even the longest hours enjoyable.

*I would like to begin by dedicating this piece of work to my parents (**Mr. Peer Mohamed and Mrs. Fathima Peer Mohamed**), my wife and children, whose dreams had come to life with me getting the highest degree in education.*

Lastly, and above all, I would like to thank the God Almighty; for all that he has given to me.

Date: **Shahul Hameed**

Abstract

DNA gyrase is a clinically validated target for developing drugs against *Mycobacterium tuberculosis* (*Mtb*). Despite the promise of fluoroquinolones (FQs) as anti-TB drugs, the prevalence of pre-existing resistance to FQs is likely to restrict their clinical value. In this study, we describe a novel class of N-linked quinolones and naphthyridones, which killed *Mtb* by inhibiting DNA gyrase activity. The mechanism of inhibition of DNA gyrase was distinct from the fluoroquinolones as shown by their ability to inhibit the growth of fluoroquinolone-resistant *Mtb*. Biochemical studies demonstrated that this class of compounds exertetd its action *via* single-strand cleavage rather than double-strand cleavage as seen with fluoroquinolones. The compounds were highly bactericidal against extracellular *Mtb*. Lead optimization resulted in the identification of potent compounds with improved oral bioavailability and reduced cardiac ion channel liability. Compounds from this series were efficacious in acute murine model of tuberculosis. A scaffold hopping approach using the binding mode of novel bacterial topoisomerase inhibitors (NBTIs) led to the identification of a novel class of benzimidazoles as DNA gyrase inhibitors with potent anti-TB activity. Docking of benzimidazoles to a NBTI bound crystal structure suggested that this class of compound made key contacts in the enzyme active site similar to the reported NBTIs. This observation was further confirmed through the measurement of DNA gyrase inhibition, activity against *Mtb* strains harboring mutations that conferred resistance to aminopiperidines based NBTIs and *Mtb* strains resistant to moxifloxacin.

Structure activity relationship (SAR) study of left hand side (LHS) ring provided a novel class of bacterial topoisomerase inhibitors that led to significant improvement in the selectivity against hERG cardiac channel binding with concomitant potent antimycobacterial activity. Bulky polar substituents at the C-7 position of the naphthyridone ring did not disturb its positioning between the two base pairs of DNA. Further optimization of the polar substituents on the LHS of the naphthyridone ring led to potent antimycobacterial activity (MIC = 0.03 μM) against *Mtb*. Additionally, this knowledge provided a robust SAR understanding to mitigate the hERG risk

With new anti-tubercular agents desperately needed, we believe that the present class of inhibitors reported in this work would be interesting as initial leads for further medicinal chemistry optimization to develop potential anti-tubercular agents.

Table of contents

_____

Contents	Page No.

Contents	Page No.

Contents	Page No.

Contents	Page No.

Contents	Page No.

List of Tables

List of Figures

List of Abbreviations

µg	:	Microgram
µM	:	Micromolar
HRMS	:	High resolution mass spectrometry
^{1}H NMR	:	Proton Nuclear Magnetic Resonance
ADMET	:	Absorption, Distribution, Metabolism, Elimination and Toxicity
AMK	:	Amikacin
ATP	:	Adenosine Triphosphate
CAP	:	Capreomycin
$CDCl_3$	:	Chloroform deuterated
CDI	:	1,1'-Carbonyldiimidazole
CoMFA	:	Comparative Molecular Field Analysis
d	:	Doublet
DCM	:	Dichloromethane
NBTIs	:	Novel bacterial topoisomerase inhibitors
DMF	:	*N*,*N*-Dimethylformamide
DMSO	:	Dimethyl sulfoxide
DMSO-d_6	:	Dimethyl sulphoxide deuterated
DNA	:	Deoxyribonucleic acid
DOTS	:	Directly Observed Treatment, Short course
EDC	:	1-Ethyl-3-(3-dimethylaminopropyl)carbodiimide
LHS	:	Left hand side
EMB	:	Ethambutol
ETH	:	Ethionamide
RHS	:	Right hand side
Mtb	:	*Mycobacterium tuberculosis*
hERG	:	human Ether-a-go-go-Related Gene
HIV	:	Human Immuno Deficiency Virus
HOBT	:	Hydroxybenzotriazole
IC_{50}	:	Half Maximal Inhibitory Concentration
INH	:	Isoniazid
FQ	:	Fluro Quinolones

J	:	Coupling constant
KAN	:	Kanamycin
MOX	:	Moxifloxacin
LCMS	:	Liquid chromatography–Mass Spectrometry
m	:	Multiplet
M.p	:	Melting point
MDCK	:	Madin-Darby canine kidney (MDCK) epithelial cell line
MDR-TB	:	Multidrug-Resistant *Mycobacterium tuberculosis*
mg	:	Milligram
MIC	:	Minimum Inhibitory Concentration
mL	:	Milliliter
mmol	:	Millimole
NADH	:	Nicotinamide Adenine Dinucleotide
nM	:	Nanomolar
PAS	:	*para*-Aminosalicylic acid
PCR	:	Polymerase Chain Reaction
PDB	:	Protein Data Bank
AP	:	Aminopiperidines
ppm	:	Parts per million
RB	:	Round bottam
PZA	:	Pyrazinamide
RIF	:	Rifampicin
RNA	:	Ribonucleic acid
BI	:	Benzimidazole
rt	:	Room temperature
s	:	Singlet
SAR	:	Structure Activity Relationship
SDS-PAGE	:	Sodium Dodecyl Sulphate- Polyacrylamide Gel Electrophoresis
STM	:	Streptomycin
t	:	Triplet
TB	:	Tuberculosis
HAR	:	Heteroaryloxy
TDR-TB	:	Totally Drug-Resistant *Mycobacterium tuberculosis*

TEA	:	Triethylamine
TFA	:	Trifluoroacetic acid
THF	:	Tetrahydrofuran
TLC	:	Thin-layer chromatography
IN	:	Indole
WHO	:	World Health Organisation
XDR-TB	:	Extensively Drug-Resistant *Mycobacterium tuberculosis*
OI	:	Oxyindole
δ	:	Chemical shift
BID	:	Bis in die
ABT	:	1-Aminobenzotriazole
CFU	:	Colony forming unit
DMA	:	N,N-Dimethylactamide
HBSS	:	Hank's Balanced Salt Solution
HPMC	:	Hydroxypropyl methycellulose
BSL	:	Biosafety level
DCE	:	1,2-Dichloro ethane
LCMS	:	Liquid chromatography–mass spectrometry
HPLC	:	High-performance liquid chromatography
h	:	hours
ANOVA	:	Analysis of variance
CTD	:	Carboxy-terminal domain
SOS	:	Save Our Soul
TOPRIM	:	Topoisomerase-primase
SC	:	Subcutaneuous
Msm	:	*Mycobacterium smegmatis*
MOA	:	Mechanism of action
PK	:	Pharmacokinetics
PD	:	Pharmacodynamics
SPR	:	Structute property relationship
Papp	:	Apparent permeability coefficient
RM	:	Reaction mixture

Introduction Chapter 1

Tuberculosis (TB) is a chronic bacterial infection caused by *Mycobacterium tuberculosis* (*Mtb*), a gram positive bacterium. TB continues to claim about 1.5 million lives each year (WHO report, 2014) and results in huge morbidity with a concomitant huge economic burden on resource constrained countries. The World Health Organisation (WHO) recommends a regimen containing four drugs administered for six months (Zumla, A, *et al*., 2013) to treat drug susceptible TB. The prolonged treatment results in poor patient compliance and severe toxicity arising from some of these drugs. Over the years most of the drugs have become ineffective due to the global evolution and spread of *Mtb* strains resistant to these frontline drugs resulting in multidrug resistant (MDR) and extremely drug resistant (XDR) strains of *Mtb*. A *Mtb* strain resistant to isoniazid and rifampicin is termed as a multi drug resistant (MDR) strain. A MDR strain resistant to fluoroquinolone and an injectable aminoglycoside is termed as an extremely drug resistant (XDR) strain. The global emergence of MDR and XDR-TB strains have greatly derailed the TB control and eradication efforts. WHO recommends a combination of 6-8 drugs for a period of 12-24 months (WHO report 2013) for patients infected with MDR or XDR strain of *Mtb*. It has been estimated that 4% of new TB cases and 20% of treated cases fall under the category of MDR or XDR TB. Over 95% of TB cases and deaths due to TB have been reported from developing countries. A huge chunk of infections (~60%) have been reported from India, China, and the Russian Federation. (Bridgen. G, *et al*., 2014. Bull. World Health Organ. 92: 68-74). Emergence of MDR strains has made current TB drugs relatively ineffective.

It is believed that the prolonged use of numerous drug regimens for several decades, coupled with poor patient compliance have led to the development of drug resistance. WHO recommended regimen to treat MDR-TB involves daily injections of poorly effective second line drugs for a duration of upto twenty months. The cost of treating MDR-TB has been estimated to be ~USD 4000/patient. Recent published reports have estimated the rate of success in treating MDR-TB to be around 54% while the rate of treatment default, mortality and treatment failure were 23%, 15% and 8% respectively. The treatment outcome for XDR-TB is an abysmal 13% (Brigden 2014; WHO reprt 2014) only in XDR tuberculosis patients. The grim global picture demands an urgent need to develop new drugs with novel mechanism of

action to treat drug resistant forms of *Mtb*. In order to minimise the drug related toxicity and improve patient compliance, it is imperative to develop novel drug regimens to minimise the duration of treatment.

The last decade has witnessed a concerted effort globally to discover and develop novel therapeutic agents against *Mtb*. In order to initiate a drug discovery program, it is imperative to understand the complex physiology of *Mtb* infection in humans. The key stages of TB infection in humans are depicted in figure 1 below:
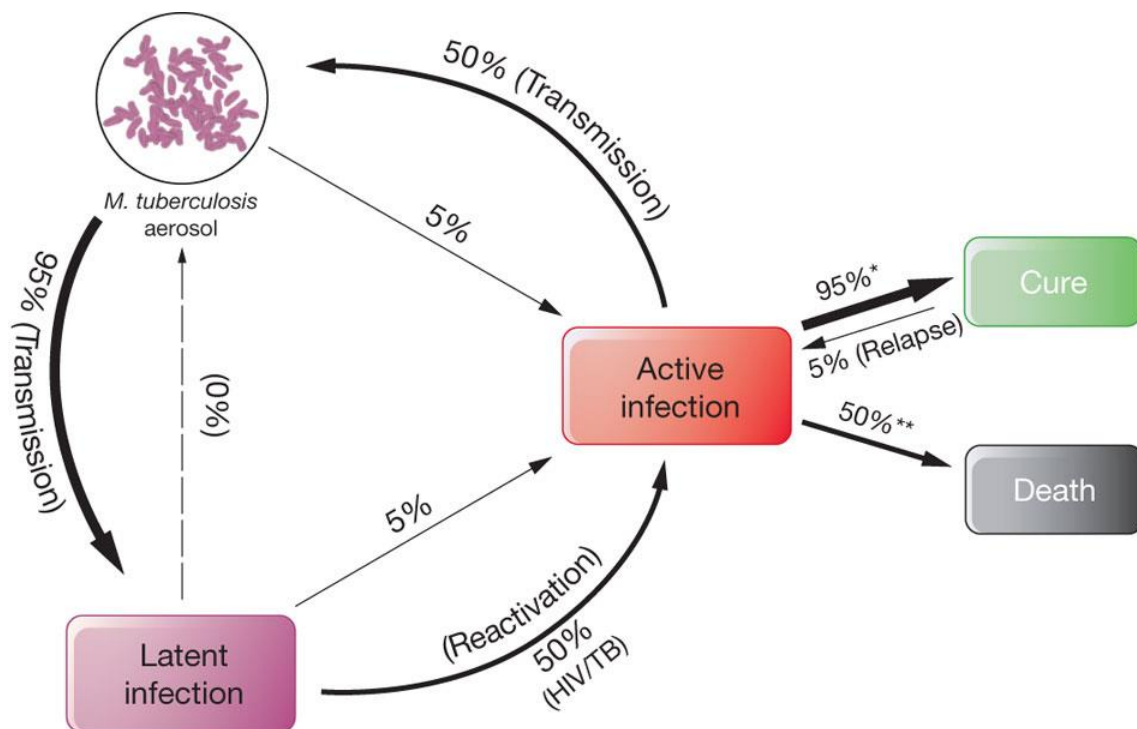
Figure 1.1: The various stages of *Mycobacterium tuberculosis* infection in humans [Koul A. *et al.*, 2011]. Transmission of *Mycobacterium tuberculosis* via aerosol route results in progression to infectious TB or non-infectious (latent) disease. It has been shown that a sizeable pool of latently infected people may relapse into active TB, years after their first exposure to *Mtb*. The latent form of TB is reactivated by immune suppression, in patients who are infected with HIV or undering chemotherapy. In the case of drug-susceptible TB (denoted by an asterisk), 95% of patients recover following treatment, whereas 5% relapse during their life time. If TB is left untreated (denoted by two asterisks), could result in high mortality.

1.1 Standard of care for treating TB

The currently used frontline drugs isoniazid, rifampicin, ethambutol and pyrazinamide were discovered during early 1960s.   The molecular target of these drugs along with the year of discovery (Zumla, A. *et al.*, 2013) is shown in Table 1.1

Drug (year of discovery)	Target	Effect
First-line drugs		
Isoniazid (1952)	Enoyl-[acyl-carrier-protein] reductase	Inhibits mycolic acid synthesis
Rifampicin (1963)	RNA polymerase, beta subunit	Inhibits transcription
Pyrazinamide (1954)	S1 component of 30S ribosomal subunit	Inhibits translation and *trans*-translation, acidifies cytoplasm
Ethambutol (1961)	Arabinosyl transferases	Inhibits arabinogalactan biosynthesis
Second-line drugs		
Para-amino salicylic acid (1948)	Dihydropteroate synthase	Inhibits folate biosynthesis
Streptomycin (1944)	S12 and 16S rRNA components of 30S ribosomal subunit	Inhibits protein synthesis
Ethionamide (1961)	Enoyl-[acyl-carrier-protein] reductase	Inhibits mycolic acid biosynthesis
Ofloxacin (1980)	DNA gyrase and DNA topoisomerase	Inhibits DNA supercoiling
Capreomycin (1963)	Interbridge B2a between 30S and 50S ribosomal subunits	Inhibits protein synthesis
Kanamycin (1957)	30S ribosomal subunit	Inhibits protein synthesis
Amikacin (1972)	30S ribosomal subunit	Inhibits protein synthesis
Cycloserine (1955)	D-alanine racemase and ligase	Inhibits peptidoglycan synthesis

Table 1.1: Molecular target of TB drugs (Zumla, A. *et al.*, 2013)

The currently used TB drug classes are categorised into three groups (first line, second line and third line drug) and the details of their nomenclature are shown in figure 1.2

First-line anti-TB drugs
Group 1. Oral: isoniazid (H/Inh), rifampicin/rifampin (R/Rif), pyrazinamide (Z/Pza), ethambutol (E/Emb), rifapentine (P/Rpt) or rifabutin (Rfb).

Second-line anti-TB drugs
Group 2. Injectable aminoglycosides: streptomycin (S/Stm), kanamycin (Km), amikacin (Amk). Injectable polypeptides: capreomycin (Cm), viomycin (Vim).

Group 3. Oral and injectable fluoroquinolones: ciprofloxacin (Cfx), levofloxacin (Lfx), moxifloxacin (Mfx), ofloxacin (Ofx), gatifloxacin (Gfx).

Group 4. Oral: *para*-aminosalicylic acid (Pas), cycloserine (Dcs), terizidone (Trd), ethionamide (Eto), prothionamide (Pto), thioacetazone (Thz), linezolid (Lzd).

Third-line anti-TB drugs
Group 5. Clofazimine (Cfz), linezolid (Lzd), amoxicillin plus clavulanate (Amx/Clv), imipenem plus cilastatin (Ipm/Cln), clarithromycin (Clr).

Figure 1.2: Classification of drugs used to treat drug-susceptible and drug-resistant tuberculosis (Zumla, A. *et al.*, 2013)

These drugs when used as monotherapy were poorly efficacious and have led to rapid emergence of drug resistance. A significant improvement in the management of TB was achieved by introducing combination treatments with the rationale to minimise the emergence of drug resistance. The introduction of Directly Observed Treatment, Short course (DOTS) strategy by WHO envisions a broad TB control strategy that focuses on four principal elements (Haydel S.E., 2010): (*i*) proper case detection with robust microbiological laboratory support, (*ii*) standard TB treatment regimen with patient support and supervision including directly observed therapy, (*iii*) availability of TB drugs continuously to patients during the course of treatment, and (*iv*) implementation of thorough monitoring and periodic evaluation system with impact measurements.

The first line anti-tubercular drugs target the actively replicating forms of *Mtb* in lungs resulting in bacterial killilng thereby significantly reducing the transmission rates to other persons within the first two months of treatment initiation. Interestingly, isoniazid targets only replicating Mtb resulting in early bactericidal activity within the first 48 hours following treatment initiation. On the contrary, rifampicin kills both replicating as well as non-replicating *Mtb*, thus accounting for sterilizing properties during the treatment course (Hafner R. *et al.*, 1997; Dickinson J.M. *et al.*, 1981). Pyrazinamide, an interesting drug exerts maximum activity against non-replicating *Mtb* localized within macrophages or the acidic environment of the pulmonary lesions (Girling D.J., 1984). The inclusion of ethambutol to the first line regimen

was intended to prevent the emergence of resistance to rifampicin, when the infecting strain was believed to be isoniazid resistant.

The second-line drugs are added to the regimen when resistance to isoniazid or rifampicin is suspected or confirmed using microbiological techniques (Dorman S.E. and Chaisson R.E., 2007). However, it has been shown that the second-line drugs are poorly efficacious and have higher toxicity profile compared to the first line drugs. Among the second line drugs, fluoroquinolones and aminoglycosides, targeting DNA replication and protein synthesis, respectively, are the main stay of the second line regimen (Mukherjee J.S. *et al.*, 2004). The remaining drugs in the cocktail are the most bacteriostatic in nature and have higher toxicity and high costs (Dorman S.E. and Chaisson R.E., 2007).

1.2 Pipeline of TB drugs in development

With the advent of AIDS and increased incidence of MDR-TB, a concerted global initiative involving several pharmaceutical and academic collaborations have led a promising portfolio of new anti-tubercular drugs.(**Figure 1.3**). The new drugs in development include drugs with novel mechanism of action and proven activity against MDR and XDR *Mtb* isolates. The most advanced front runner is Bedaquiline, a recently approved drug that targets adenosine triphosphate (ATP) synthase inhibitor in *Mtb* which has shown promising antimycobacterial activity in preclinical animal models as well in TB patients (Cohen J., 2013).   Recently, the European Medicines Agency (EMA)) has approved Delamanid, a nitroimidazole drug that has entered phase 3 trials for the treatment of MDR-TB.

Significant progress has also been made by re-purposing or re-dosing known anti-tubercular drugs such as rifamycins (RIF, rifapentine) and fluoroquinolones (moxifloxacin and gatifloxacin). These drugs have all entered phase 3 clinical studies [Zumla A. *et al.*, 2014].
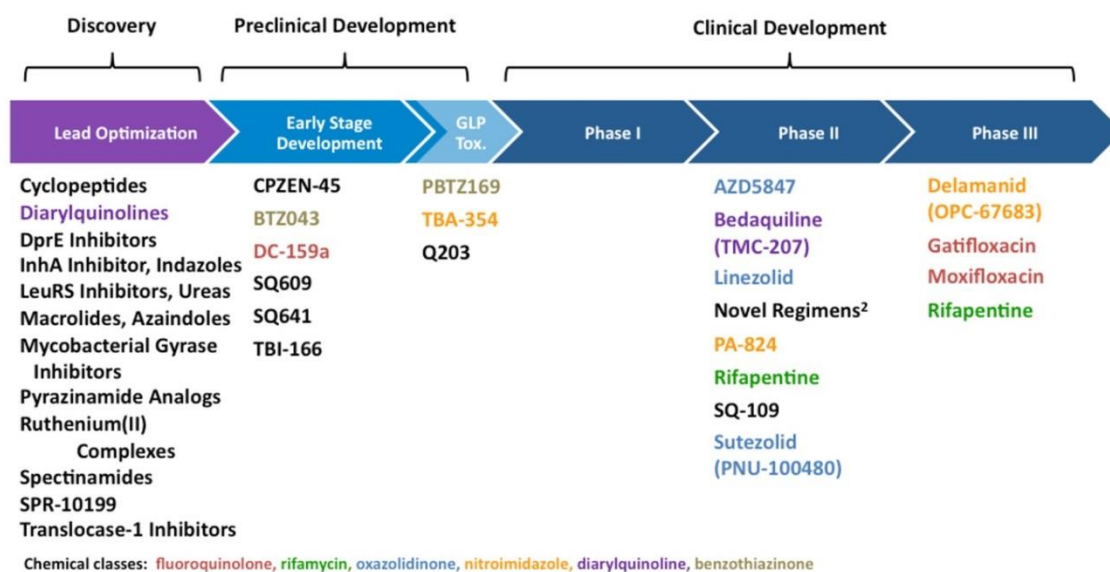
Figure 1.3: The current global pipeline of TB drugs in clinical development [Source: Stop TB Partnership Working Group on New Drugs http://www.newtbdrugs.org/pipeline-discovery.php]

Literature review Chapter **2**

The rise in drug-resistant *Mtb* and relatively few candidates in drug development pipeline signify the urgent need for novel anti-tubercular agents, ideally with clinical efficiency in MDR, XDR, and TDR isolates.

The availability of the genome sequence of *Mtb* has propelled a huge effort towards target-based discovery of anti-mycobacterial compounds (Cole, S.T. *et al.*, 1998). However, numerous efforts aimed at the essential targets in Mtb have highlighted many inherent challenges in identifying attractive chemical leads (Sharma, U. *et al.*, 2011). Clinically validated targets of known anti-mycobacterial agents offer great promise in terms of designing novel inhibitors that are likely to be bactericidal under the in *vitro* and *in vivo* growth conditions. Among the extensively studied bacterial targets, DNA gyrase, belonging to the Type II topoisomerase family, has been validated clinically by the fluoroquinolone (FQ) class of drugs (Burman, W. J. et al, 2006 and Conde, M. B. *et al.*, 2009). Combination regimens containing moxifloxacin have shown the potential to shorten duration of TB treatment (Diacon, A. H. *et al.*, 2011). However, pre-existing resistance to fluoroquinolones (FQs) is likely to limit the clinical utility of this class of drugs for treating TB in the long run (Duong, D. A. *et al.*, 2009).

FQs bind to the GyrA subunit of bacterial DNA gyrase and trap the double strand cleaved DNA-gyrase complex, inducing a save our soul (SOS) response that leads to bacterial cell death (Drlica, K. *et al.*, 2008). Hence, a novel inhibitor of DNA gyrase with a unique binding site is likely to have activity against FQ-resistant TB.

2.1 Bacterial DNA gyrase

DNA gyrase, a type II topoisomerase enzyme is involved in DNA replication and repair. This enzyme is essential in all bacteria and is absent in eukaryotes (Champoux, J.J. *et al.*, 2011). DNA gyrase catalyzes the critical step of maintaining the various topological forms of DNA during DNA replication. DNA gyrase performs an ATP-dependent reaction to introduce a negative supercoiling into circular DNA (Corbett, K.D. *et al.*, 2004). This enzyme exists in a heterotetrameric form, comprising of a GyrA and a GyrB sub-unit (A2B2). The DNA breakage

reunion function resides in the GyrA subunit, while the GyrB subunit catalyses the ATP-dependent hydrolysis to generate the energy required for enzyme activity. A very similar organization is observed for topoisomerase IV, which is composed of dimers of the ParC and ParE subunits. Interestingly, the *Mtb* genome encodes a functional DNA gyrase, but no topoisomerase IV. DNA gyrse subunits is made of twostructural domains, the N-terminal breakage−reunion domain (depicted in blue in figure 2.1) and the carboxy-terminal domain (CTD, depicted in green) for the GyrA or ParC subunits and the ATPase domain (depicted in yellow) along with topoisomerase-primase(TOPRIM) domain (depicted in red) for the GyrB or ParE subunits (Mayer, C. *et al.*, 2014).
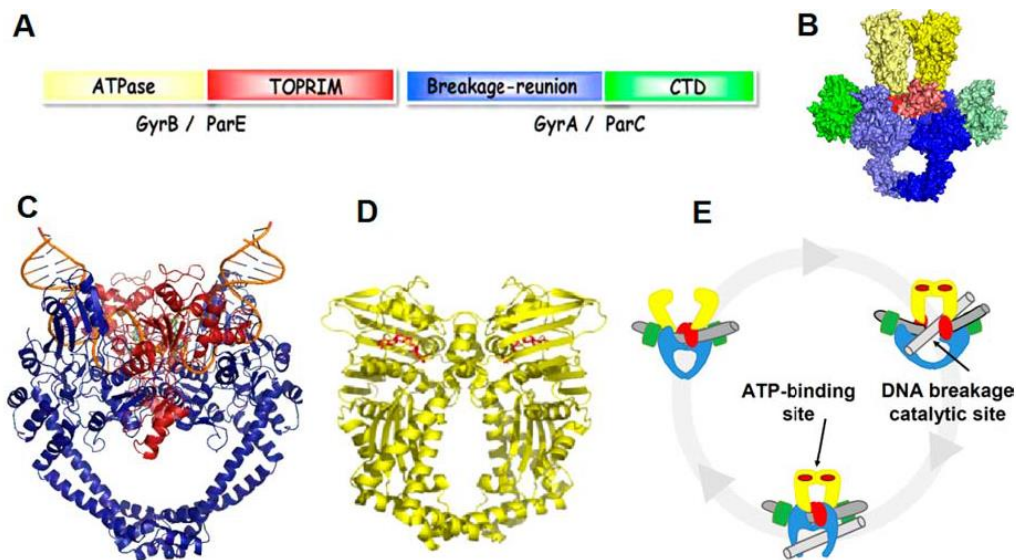
Figure 2. 1: Structural overview of bacterial type IIA topoisomerase architecture and catalytic cycle (Mayer, C. *et al*, 2014)

DNA gyrase binds to DNA as a tetramer in which two A and two B subunits wrap DNA into a negative supercoil, followed by passage of the DNA through the interior of the enzyme complex via double- stranded DNA cleavage and rejoining. This supercoiling reaction is an ATP-dependent process, with ATP hydrolysis essential for further catalytic cycles of gyrases
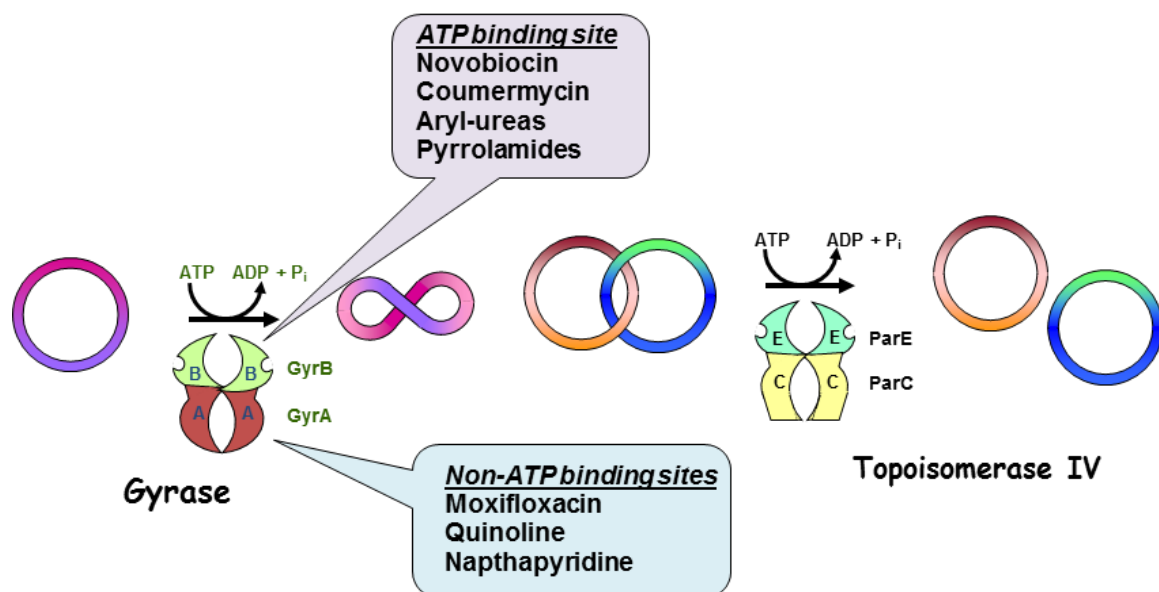
Figure 2.2: Schematic diagram of bacterial type II topoisomerases (Shirude, P and Hameed, S. 2012)

Several inhibitors targeting DNA gyrase have been reported to exhibit activity against *Mtb*. A class of inhibitors that target ATP recognition site of GyrB enzyme and block ATP hydrolysis have shown antimycobacterial activity (**Figure 2.2**). Examples of this type include aminopyrazinamides (Shirude, P. *et al.*, 2013), benimidazole ureas (Chopra, S. *et al.*, 2012), thiazolopyridine ureas (Kale, M.G *et a.l*, 2013), pyrrolamides (Hameed, P. S. *et al.*, 2013) and thiazolopyridone urea (Kale, R. *et al.*, 2014) with potent antmycobacterial activity. Representative structure of mycobacterial GyrB inhibitors are given in **Figure 2.3**

A second type of inhibitors that target GyrA subunit have been shown to inhibit DNA breakage–reunion function of the enzyme. This category of inhibitors include fluoroquinolones (FQs), novel bacterial topoisomerase inhibitors (NBTIs) and aminopiperidines. As our proposed work focuses around non fluroquinolone based novel bacterial topoisomerase inhibitors (NBTIs), it has been dicussed in great detail.

Structures mycobcterial GyrB inhibitors
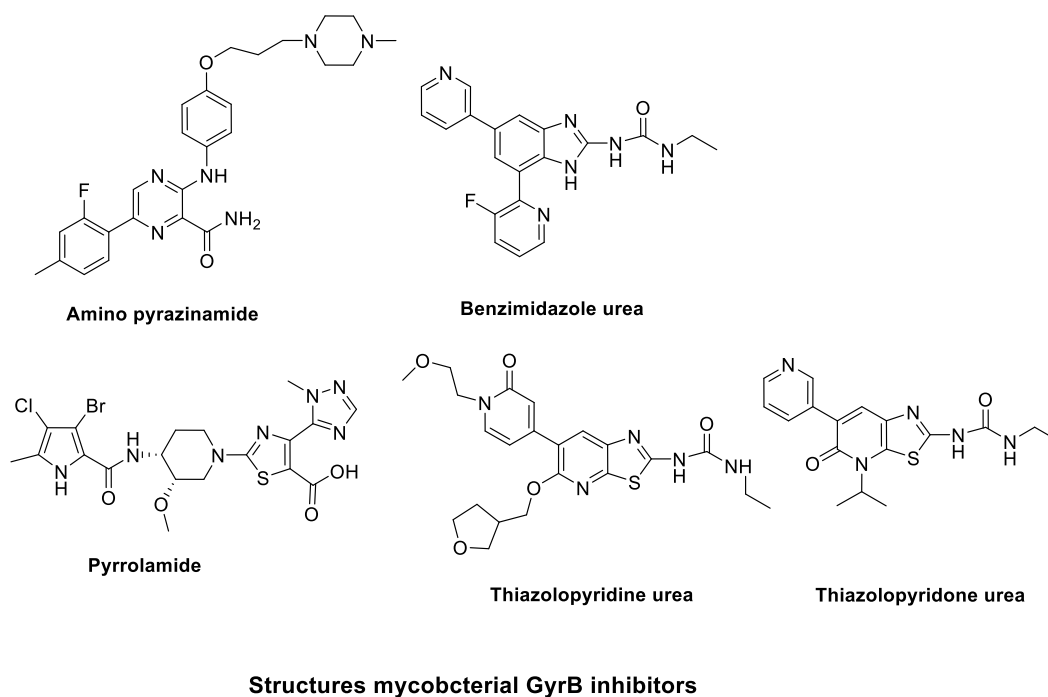
Figure 2.3: Structures of mycobacterial GyrB inhibitors

2.2 Bacterial novel topoisomerase inhibitors (NBTIs)

The generic chemical structures of NBTIs including the N-linked amino piperidines consist of three parts, namely a bicyclic aromatic left-hand side (LHS), a mono or bicyclic right- hand side (RHS), and a linker region joining the RHS and LHS (**Figure 2.4**).
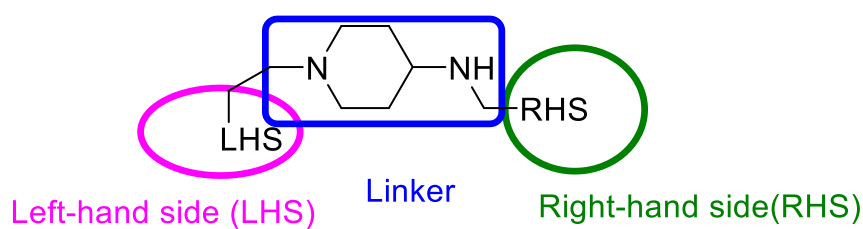
Figure 2.4: Generic structure of novel bacterial topoisomerase inhibitors (NBTIs)

The mechanism of inhibition and the binding mode of NBTIs for the antibacterial series has been reported (Bax, B.D. *et al.*, 2010). From the crystal structure studies of methoxyquinoline-3-carbonitrile (**GSK299423**, **Figure 2.5**), one could infer that the LHS portion of the NBTIs bind to DNA substrate, whereas the RHS portion interact with the protein dimer interface of GyrA subunits. The binding site of NBTIs was distinct from the FQ binding and they were reported to be active against FQ-resistant strains of *S. aureus*.
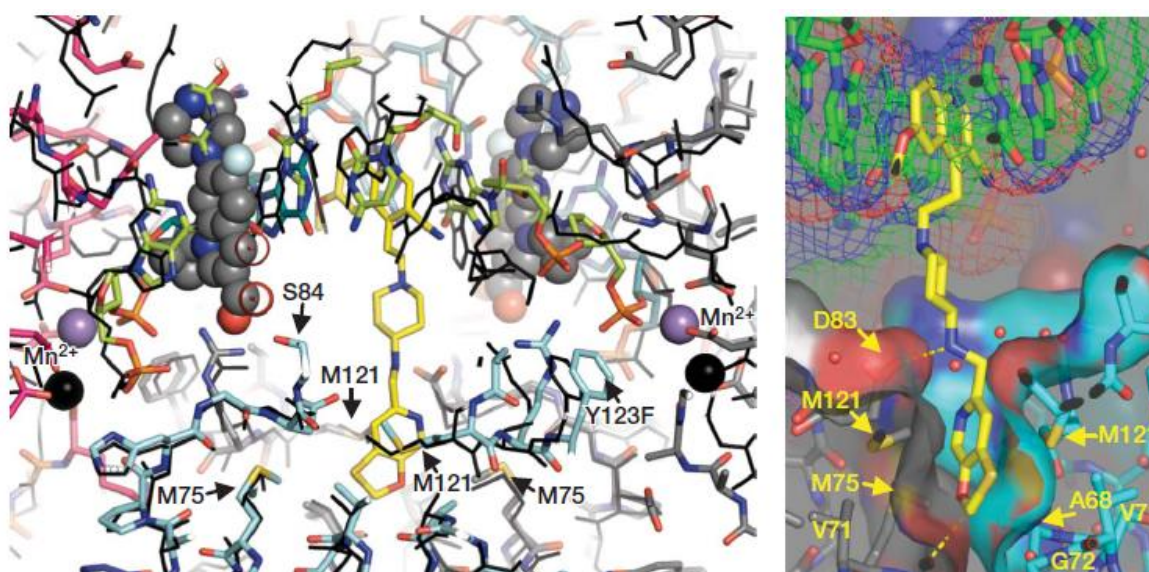
Figure 2.5: The 2.1A° GyrB27–A56 complex with GSK299423 and DNA (Bax, B.D. *et al.*, 2010). (a) The 2.1A ° GSK299423 complex is shown in stick representation with GSK299423 (yellow) half-way between the two Mn^{2+} ions (purple) at the active site. The 3.35A ° ciprofloxacin structure (black lines) is shown superposed with ciprofloxacin in space filling (grey carbons) representation, and Mn^{2+} ions are shown in black. (B) The oxathiolopyridine ring of **GSK299423** sits in a largely hydrophobic pocket at the dimer interface (Bax, B.D. *et al.*, 2010)

The simplified schematic representation of mechanism of inhibition of gyrase by NBTIs and FQ is shown in **figure 2.6** (Bax, B.D. *et al.*, 2010) for better clarity

Inference could drawn from the figure 2.6 that NBTI do not directly inhibit DNA cleavage–religation reaction as it do not bind in the active site (allosteric inhibition), with some single-strand cleavage. It stabilize a precleavage enzyme–DNA complex and inhibit strand separation, which was different from FQ, which cause double strand breakage. The unique binding mode provided a structural basis for why NBTIs were able to overcome target-mediated FQresistance.

As far as *Mtb* gyrase is concerned, it is believed to be have only DNA gyrase and no Topo IV. So far, the mode of binding of NBTIs to the *Mtb* GyrA subunit is not known. As the active site of DNA gyrases are highly conserved across the bacterial species, we assume that the binding mode could be similar to what was reported for *S. aureus* DNA gyrase.
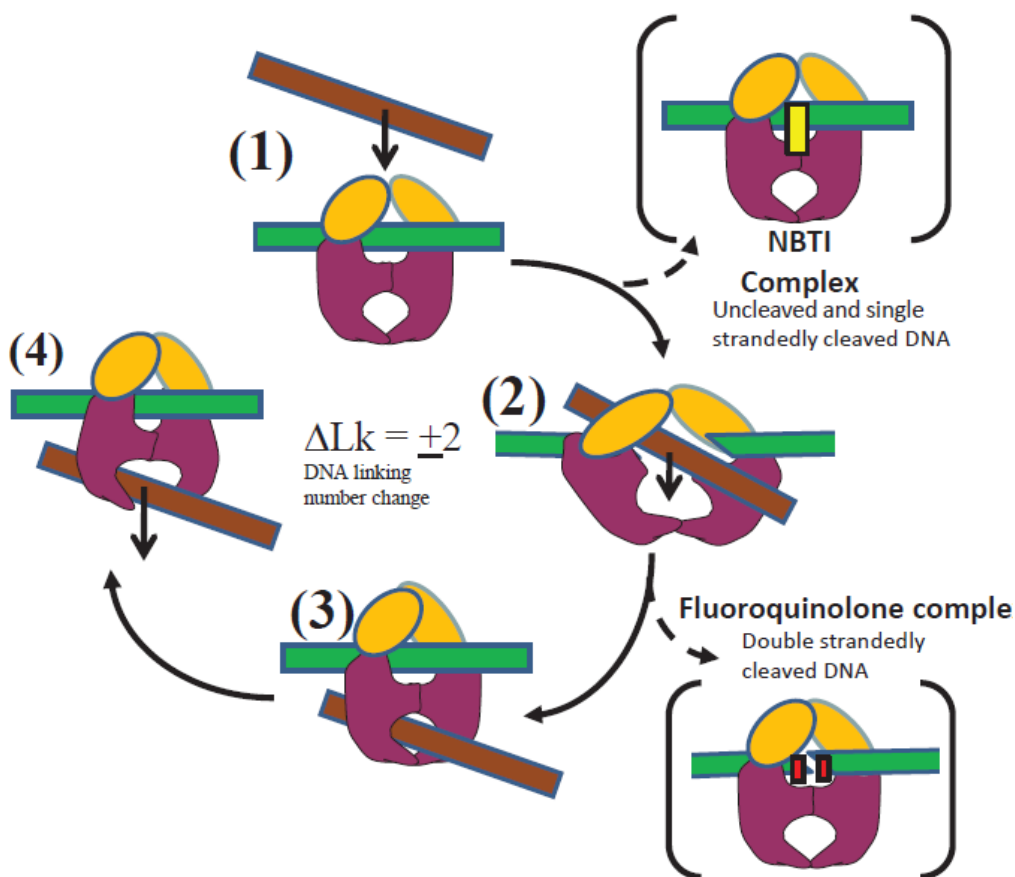
Figure 2.6: Mechanism of action of FQ drugs and NBTIs; Simplified schematic representations of type IIA topoisomerase action (1) to (4), and inhibitor complexes of NBTI and fluoroquinolone antibacterial agents (Bax, B.D. *et al.*, 2010).

Type IIA topoisomerases create a double-stranded break in one DNA duplex (green) and pass another DNA duplex (brown) through a break before resealing the break, to alter DNA topology (and change the DNA linking number by 2). NBTI complex - a single NBTI inhibitor molecule (yellow) binds to an uncleaved G-segment DNA and GyrA. FQ complex- two FQs (red) bind in the cleaved G-segment DNA(3). ParE/GyrB = orange subunits; ParC/GyrA = purple subunits; green bar = gate or G-segment DNA; brown bar =translocated T-segment; black arrows indicate the direction of DNA segment translocation.

The various novel bacterial topoisomerase inhibitors reported in literature are shown in **Figure 2.7**
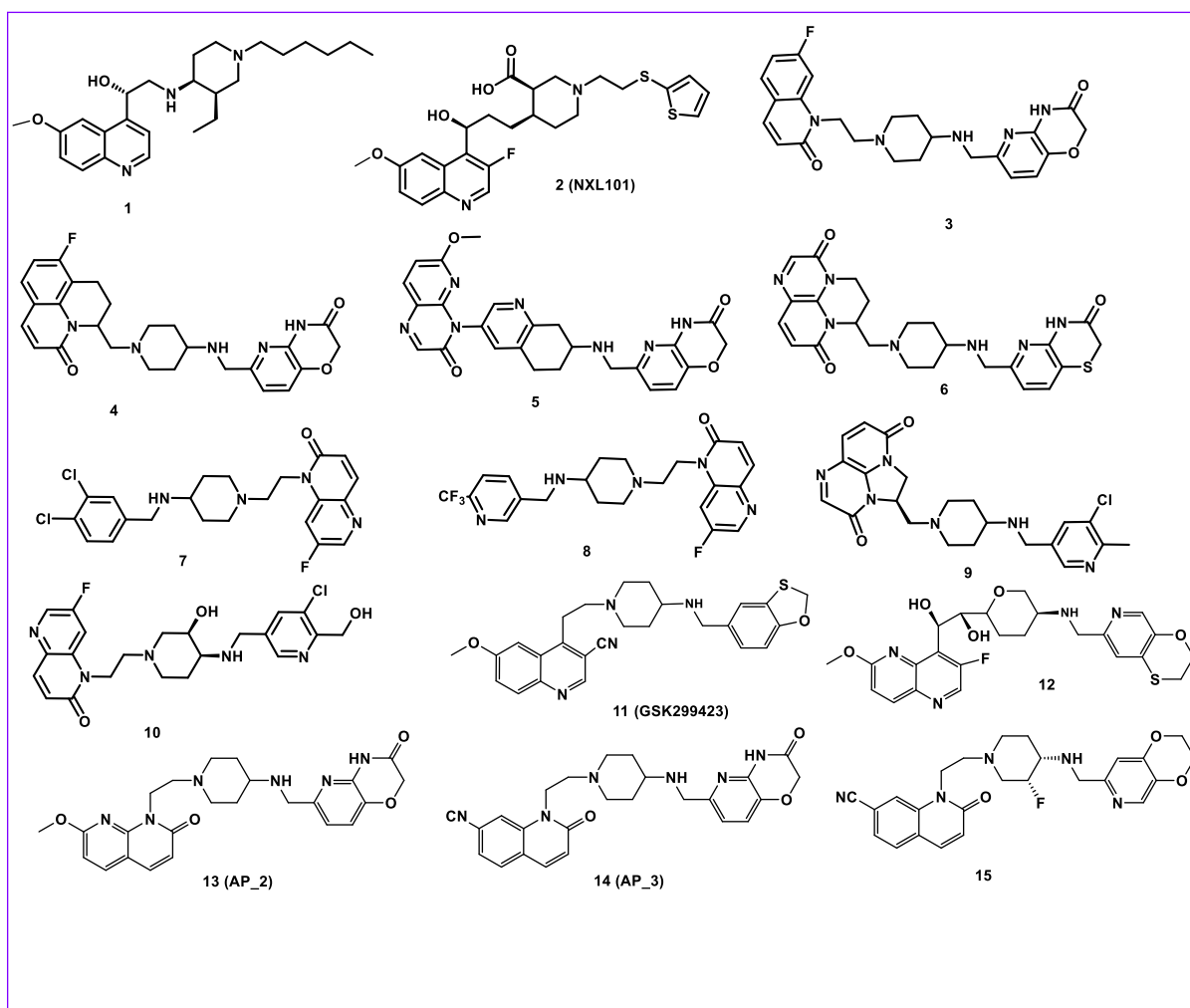
Figure 2.7: Known novel bacterial topoisomerase inhibitors **1 -15**

First compound (**1**) from piperidinyl alkyl quinoline derivative was reported by GSK in 1999 for antibacterial activity without disclosing the target information (W. J. Coates. *et al.*, 1999). Compound **1** showed MIC of 4 µg/ml against *E. coli* strain and this served as a starting point to develop a new class of broad-spectrum antibacterial agents. After disclosure of this new class of antibacterial scaffold, quite a few pharmaceutical companies worked around this scaffold to develop novel antibacterial agents and created their own chemical space. Novexel advanced a first clinical candidate **2** (NXL101) from this series and reported target information for this class as DNA gyrase. The compound **2** acted through inhibition of type II topoisomerase (both Topo IV and gyrase) in *E. coli* and *S. pneumoniae.* Compound **2** also showed good activity against FQ-resistant strains of *S. aureus* with known mutations in the quinolone resistance-determining region (QRDR). This indicated that mechanism of inhibition of topoisomerases by compound **2** was very different from that of FQ mechanism (Black, M.T. *et al.*, 2007). The compound **2** was advanced to Phase I studies but discontinued from the clinical trial due to QT

prolongation signals in healthy volunteers (Press release, June 30, 2008; http://www.novexel.com/).

Majority of the research work around quinoline and napthapyridine based gyrase inhibitors were reported for developing broad spectrum antibacterial agents. Scientist at GSK disclosed antimycobacterial activity for quinoline and napthapyrdine series of compounds as an extension of their antibacterial projects (Ballell, L. *et al.*, 2008, Brown, P. *et al.*, 2008 and Barfoot, C. *et al.*, 2008). Compounds **3-6** from quinolone, quinoxazolinone and naphthyridone series with bicyclic right hand side (RHS) fragments showed *Mtb* MICs ranging from 0.3 – 2 µg/ml. However there were no data related to *Mtb* gyrase inhibition reported for this set of compounds. Although this was believed to be through *Mtb* gyrase inhibition as they were structurally very close to compound **11**, for which potent inhibition of DNA gyrase in *E. coli* and *S. aureus* with crystal structures reported (Bax, B.D. *et al.*, 2010). Further medicinal chemistry efforts aimed towards improving *Mtb* activity for monocyclic RHS subseries werevreported. For example, compounds **7-10** were reported with improved *Mtb* MIC of 0.01- 0.3 µg/ml against *Mtb* (Alemparte-Gallardo, C. *et al.*, 2009 and Alemparte-Gallardo, C. *et al.*, 2010). Compound **8** (MGI1794) and it's closely related analogs maintained wild-type *Mtb* MICs and improved MICs versus FQ-resistant strains with well-characterized mutations in the QRDR region (S91P, A90V and D94G), where in ofloxacin and ciprofloxacin showed 5-30 fold increase in *Mtb* MICs (Barrows, D. *et al.*, 2009). These compounds also retained *Mtb* MIC against 8 XDR clinical isolates, which were completely resistant to first line and second line TB agents including ciprofloxacin and moxifloxacin. The above study indicated that quinoline and naphthyridine based antimycobacterial mechanism of gyrase inhibition might be similar to what was reported for broad-spectrum antibacterials and was distinctly different from FQ mode of inhibition.

Preliminary pharmacokinetic profiling of compound **7** (MGI1793) in mouse showed 28% bioavailability and also demonstrated an excellent efficacy with clear dose response (limit of quantification at 75 mg/kg BID, *SC*) in acute mouse model by BID dosing through subcutaneous (*SC*) route of administration. However, the NBTIs with monocyclic RHS (compounds **7-10**) were also potent inhibitors of the cardiac hERG channel and optimization of this series towards reducing hERG liability is underway (Barrows, D. *et al.*, 2009).

Scientists at AstraZeneca had reported novel N-linked aminopiperidines compound (compounds **13-15**) as potent inhibitors of the bacterial type II topoisomerases with potent anti-

bacterial activity (Reck, F. *et al.*, 2011 and 2012). It was shown that N-linked aminopiperidines with a bicyclic RHS and an optimised linker (compound **15**), showed lesser hERG liability (Reck, F. *et al.*, 2012).

Very recently, scientists at Merck reported oxabicyclooctane-linker based novel bacterial topoisomerase inhibitors (compound **12**) as broad spectrum antibacterial agents (Sing, S.B, *et al.*, 2014). However, compound **12** also suffers from cardiac ion channel liability with hERG IC$_{50}$ of 18 μM.

From an extensive literature review data it was clear that compounds (compounds **7-10)** with monocyclic RHS showed improved *Mtb* potency and linker modification with pKa modulation showed promise in terms of improving hERG selectivity (Reck, F. *et al.*, 2012). So we decided to exploit combination of both the approaches to identify a lead series with improved *Mtb* potency, hERG selectivity and optimal oral bioavailability for TB treatment.

The search for new TB drugs remain challenging albeit vitally important task. The failing effectiveness of current anti-tubercular drugs to combat infection signifies urgent need to identify new and potent agents.

3.1 Objectives

Clinically validated targets of known anti-mycobacterial agents offer a great promise in terms of designing novel inhibitors that are likely to be bactericidal under the *in vitro* and *in vivo* growth conditions. Hence newer anti-TB agents with novel mechanism of action (MOA) and improved safety profile will be an ideal agent for effective TB treatment. A thorough review of literature higligted the importance of mycobacterial DNA gyrase as clinically validated drug target with huge potential for TB drug discovery with novel MOAs. Inhibition of such targets with new mechanism which is different from FQ class of mechanism will be a good option for treatment of sensitive and resistance forms TB. A novel inhibitor of DNA gyrase with a unique binding site is likely to have activity against FQ-resistant TB. Numerous non FQ based bacterial Type II topoisomerase inhibitors for both GyrA and GyrB class have been reported as antibacterial agents and highlighted their potential for TB treatment in the literature survey report. Novel N-linked quinolone and napthyridone based bacterial typeII topoisomerase inhibitor was one such class of compounds with limited exploitation for antimycobacterial activity with potent hERG liability. The present study, thus focuses on identifying and optimizing a promising lead series within antibacterial N-linked quinolone and napthyridone series with improved anti-TB activity and hERG selectivity as *Mycobacterium tuberculosis* DNA GyrA inhibitors.

The main objectives of the proposed work were:

1. To design and synthesize novel N-linked quinolone and naphthyridones using SAR studies, scaffold morphing and homology model approach as *Mycobacterium tuberculosis* GyrA inhibitors with a view to improve antimycobacterial activity and hERG selectivity

2. To evaluate synthesized compounds by *in vitro* hERG inhibition assay for building selectivity SAR

3. To explore the protein –ligand interaction using homology model to identify new SAR handle to improve poetncy

4. To embark *in vitro* antimycobacterial screening of the synthesized compounds against *Mycobacterium tuberculosis*

5. To profile the *in vitro Mtb* DNA gyase supercoiling assay of the representative synthesized compounds to link the observed *Mtb* MIC to target inhibition

6. To profile representative compounds from the synthesized set for *in vitro* metobolic stability, Caco2 permeability and *in vivo* pharmacokinetic study to demonstarate oral bioavailability potential of the series and

7. To demonstarate *in vivo* proof for gyrase inhibition in a mouse TB model for advanced compounds from the synthesized set.

3.2 Plan of work

The plan of work was classified into the following categories:

3.2.1 Synthesis and characterization

Our research in collaboration with AstraZeneca initiated screening of a focused library of N-linked quinolones and napthyridones from the antibacterial drug discovery program at AstraZeneca against replicating *Mtb* in broth. This screening effort led to the identification of compounds with submicromolar MIC against *Mtb* with hERG liability

Lead optimization efforts were primarily focused on improving the *Mtb* MIC, Caco2 permeability and reducing the hERG liability. During lead optimization, we tracked the SAR based on *Mtb* MIC assuming that the mechanism of gyrase inhibition was retained across newly synthesized compounds in this series.

Thus, we decided to take these *Mtb* MIC active hits as lead molecules for further optimization of potency and hERG selectivity. Based on initial SAR hint and inputs from homology model developed with lead molecules, further optimization efforts were primarily focused on improving the *Mtb* MIC, reducing the hERG liability and demonstrating oral bioavailability by improving Caco2 permeability. Further modifications (and combinations thereof) were explored in a ligand expansion step using newly designed RHS, linker and expanded LHS fragments. The designed molecules were further synthesized in laboratory at AstraZeneca utilizing previously reported methodology available in literature for structurally related

molecules. All reactions were monitored using thin layer chromatography and LCMS. The synthesized compounds were fully characterized using modern analytical techniques. LCMS, ^{1}H-NMR and HRMS were recorded and analysed to confirm the structure of the compounds. Purity of the compounds was evaluated by HPLC.

The synthesized compounds were evaluated for their *Mtb* DNA gyrase inhibitory potency by *in vitro* gel based *Mtb* DNA gyrase supercoiling (SC) inhibition assay.

3.2.2 Understanding of protein-ligand interaction studies using homology model technique

The binding modes of active compounds to *Mtb* DNA gyrase protein was assessed by building a *Mtb* homology model using published crystal structures of NBTIs bounds to *S.au* DNA gyrase subunit. The build *Mtb* homology model was used for understanding key interaction involved and for developing SAR for antimycobacterial activity.

3.2.3 *In vitro Mycobacterium tuberculosis* activity studies

All the synthesized compounds were further screened for their *in vitro* antimycobacterial activity against *Mycobacterium tuberculosis* H37Rv (ATCC27294) by using agar dilution method.

3.2.4 *In vitro Mtb* DNA gyrase screening

Representative compounds from the synthesized set were also screened for their inhibition of *Mtb* gyrase supercoiling activity using gel based *Mtb* DNA gyrase SC assay and *Mycobacterium smegmatis* (*Msm*) GyrB ATPase assay.

3.2.5 *In vitro* hERG inhibition studies

Majority of the synthesized compounds were tested on voltage-gated ion channels using the medium-throughputelectrophysiology IonWorks™ device as described previously (Schroeder *et. al.,* 2003).

3.2.6 Advanced microbiological profiling

Few representative key compounds from the synthesized set were tested for *Mtb* killing patern in a time-dependent kill kinetic assay, resistance frequency and cross-resistant pattern by raising resistant mutant against one of the synthesized compound from the series and moxifloxacin

3.2.7 ADMET Properties

All the synthesized derivatives were further evaluated for their predicted ADMET properties using AstrZeneca developed predictive tools and representative compounds from the series were screened for logD, solubolity, Caco2 permeability, *in vitro* metabolic stability and *in vivo* pharmacokinetic studies to access their drug-like characteristics and oral bioavailability of a promising drug candidate from drug development point of view.

3.2.8 *In vivo* efficacy and TB animal model studies

Advanced key compounds with attractive *Mtb* MIC, improved hERG selectivity and oral bioavailability were screened in acute TB animal models to demonstrate *in vivo* proof of principle for the gyrase mechanism with positive efficacy.

4.1 Design of novel N-linked quinolone and naphthyridone based *Mycobacterium tuberculosis* DNA gyrase inhibitors

4.1.1 Identification of lead molecules through screening of focused antibacterial library set

A focused library of N-quinolone and naphthyridones from antibacterial library set of AstraZeneca corporate collection was screened for MIC against replicating *Mtb* in broth. This screening effort led to the identification of compounds **AP_1**, **AP_2** and **AP_3** with moderate *Mtb* MIC with gyrase inhibiton and hERG liability.

The stuctures and biological profiles of initial lead compounds with both bicyclic and monocyclic RHS shown in **Figure 4.1**

AP_1

Mtb MIC: 1 µM
Mtb Gyrase SC IC$_{50}$: 1.05 µM
hERG IC$_{50}$: 44 µM
Caco2: Papp : 1.9/38.3

AP_2

Mtb MIC: 0.13 µM
Mtb Gyrase SC IC$_{50}$: 0.15 µM
Caco2: Papp : 1.1/25

AP_3

Mtb MIC: 0.06 µM
Mtb Gyrase SC IC$_{50}$: 0.11 µM
Caco2: Papp : 2/12.6

Initial screening leads

Novel Monocyclic RHS design

AP_4

Mtb MIC: >15µM
Mtb Gyrase SC IC$_{50}$: >100 µM
hERG IC$_{50}$: 5.3 µM
Caco2: Papp : 17.1/9.1

AP_5

Mtb MIC: 0. 0 03 µM
Mtb Gyrase SC IC$_{50}$: 0.25 µM
hERG IC$_{50}$: 26 µM
Caco2: Papp : 13.6/7.4

Monocyclic RHS leads

Figure 4. 1: Chemical structure of selected aminopiperidine (AP) based leads for further optimization.

4.1.2 Identification of lead molecules through scaffold hopping

In order to identify a scaffold with novel RHS group and expand the chemical scope of quinolone and naphthyridone based NBTIs in order to mitigate hERG liability , we embarked on a scaffold hopping approach based on the literature reported NBTIs and its bound crystal structure with the *S. aureus* DNA gyrase (**Figure 4.2**).
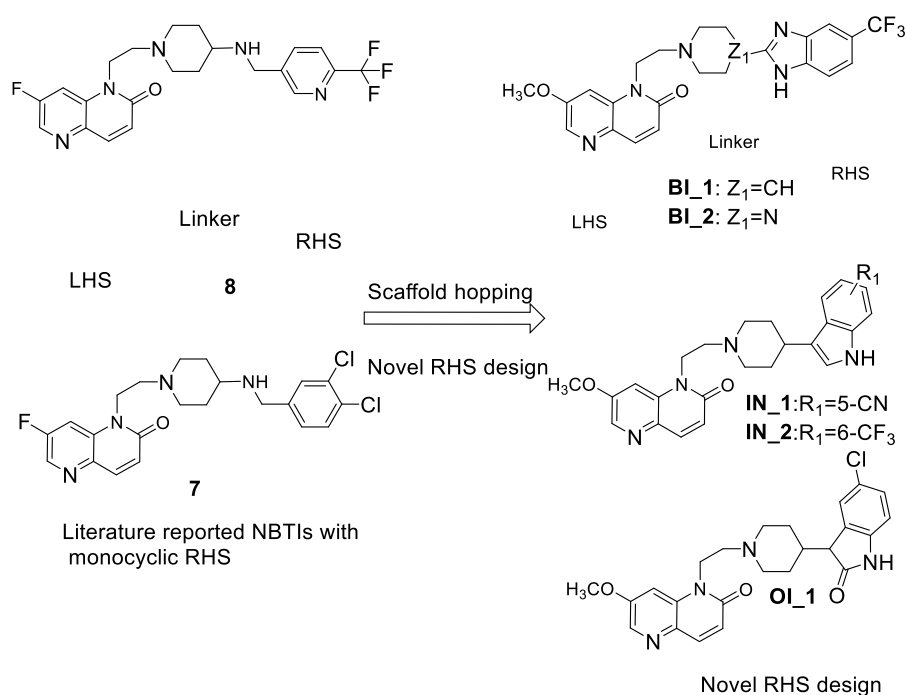
Figure 4.2: Scaffold hopping of NBTIs and design of novel RHS series.

4.1.3 Identification of lead molecules through expansion of left hand side of naphthyridones

To expand the chemical diversity and build a structural handle to mitigate the hERG liability, we explored the bulky substituents as R_1 instead of small flouro or methoxy group at the C-7 position of naphthyridone LHS. We hypothesized that by lowering the logD and modulation the polarity *via* bulky polar substitutions on LHS ring may provide structural diversity to mitigate hERG liability. Based on this hypothesis, several compounds with bulky polar substitutions were synthesized and their hERG IC_{50}s were determined. The new design strategy to exploit R_1substitution with bulky polar group at the C-7 position of naphthyridone LHS is shown in **figure 4.3**.
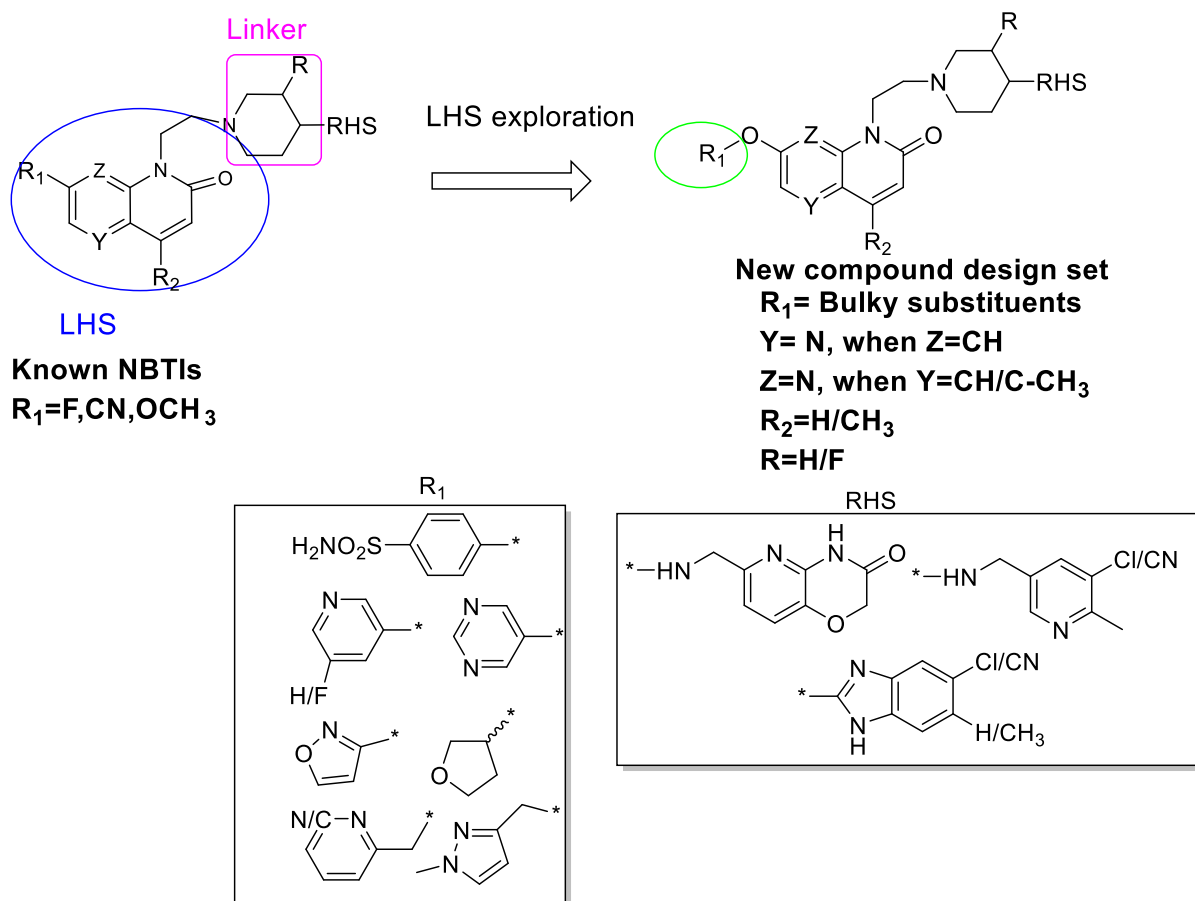
Figure 4.3: SAR exploration of LHS to improve hERG selectivity

4.2 Synthesis and characterization

All commercial reagents and solvents were used without further purification. Analytical thin-layer chromatography (TLC) was performed on SiO_2 plates on alumina. Visualization was accomplished by UV irradiation at 254 and 220 nm. Flash column chromatography was performed using the Biotage Isolera flash purification system with SiO_2 60 (particle size 0.040−0.055 mm, 230−400 mesh). Purity of all final derivatives for biological testing was confirmed to be >95% as determined using the following conditions: a Shimadzu HPLC instrument with a Hamilton reverse phase column (HxSil, C18, 3μm, 2.1 mm × 50 mm (H2)). Eluent A: 5% CH_3CN in H_2O, eluent B: 90% CH_3CN in H_2O. A flow rate of 0.2 mL/min was used with UV detection at 254 and 214 nm. The structure of the intermediates and end products was confirmed by ^{1}H NMR and mass spectroscopy. Proton magnetic resonance spectra were determined in DMSO- d_6 unless otherwise stated, using Bruker DRX-300 or Bruker DRX-400 spectrometers, operating at 300 MHz, or 400 MHz, respectively. Splitting patterns are indicated

as follows: s, singlet; d, doublet; t, triplet; m, multiplet; br, broad peak. LCMS data was acquired using Agilent LCMS VL series. Source: ES ionization, coupled with an Agilent 1100 series HPLC system and an Agilent 1100 series PDA as the front end. HRMS data was acquired using an Agilent 6520, Quadrupole-Time of flight tandem mass spectrometer (Q-Tof MS/MS) coupled with an Agilent 1200 series HPLC system.

Lead optimization of the selected three lead series through above mentioned approaches were achieved using the following synthetic schemes.

4.2.1 Synthesis of N-linked aminopeperidinyl alkyl Quinolones and Naphthyridones with substituted pyridines as RHS (Aminopiperidine series)

24a: R1= CN; R2= H; R3= H; X= C; Y= C; A= C
24b: R1= F; R2= H; X= N; Y= C; A= C
24c: R1= H; R2= OMe; X= N; Y= C; A= C
24d: R1= OMe; R2= H; R3= Br; X= C; Y= C; A= C
24f: R1= OMe; R2= H; R3= H; X= C; Y= N; A= N
24g: R1= F; R2= H; X= N; Y= C; A= N
24h: R1= OMe; R2= H; X= N; Y= C; A= N

26a: R1= CN; R2= H; R3= H; X= C; Y= C; A= C
26b: R1= F; R2= H; X= N; Y= C; A= C
26c: R1= H; R2= OMe; X= N; Y= C; A= C
26d: R1= OMe; R2= H; R3= Br; X= C; Y= C; A= C
26e: R1= OMe; R2= H; X= N; Y= C; A= C
26f: R1= OMe; R2= H; R3= H; X= C; Y= N; A= N
26h: R1= OMe; R2= H; X= N; Y= C; A= N
26i: R1= OMe; R2= H; R3= CN; X= C; Y= C; A= C

27a: R1= CN; R2= H; R3= H; X= C; Y= C; A= C
27b: R1= F; R2= H; X= N; Y= C; A= C
27c: R1= H; R2= OMe; X= N; Y= C; A= C
27e: R1= OMe; R2= H; X= N; Y= C; A= C
27f: R1= OMe; R2= H; R3= H; X= C; Y= N; A= N
27h: R1= OMe; R2= H; X= N; Y= C; A= N
27i: R1= OMe; R2= H; R3= CN; X= C; Y= C; A= C

RHS	31, RHS 1	32, RHS 2	33, RHS 3	34, RHS 4
Structure				
Reaction Condition	c	a	e	c

AP_4: R1= CN; R2= H; R3= H; X= C; Y= C; A= C; W= CH2; RHS 1
AP_5: R1= CN; R2= H; R3= H; X= C; Y= C; A= C; W= CH2;RHS 2
AP_6: R1= F; R2= H; X= N; Y= C; A= C; W= CH2; RHS 2
AP_7: R1= OMe; R2= H; X= N; Y= C; A= C; W= CH2; RHS 2
AP_7a: R1= H; R2= OMe; X= N; Y= C; A= C; W= CH2; RHS 2
AP_9: R1= OMe; R2= H; R3= CN; X= C; Y= C; A= C; W= CH2; RHS 2
AP_10: R1= OMe; R2= H; X= N; Y= C; A= C; W= CO; RHS 3
AP_11: R1= OMe; R2= H; X= N; Y= C; A= C; W= CH2; RHS 4
AP_12: R1= OMe; R2= H; R3= H; X= C; Y= N; A= N; W= CH2; RHS 2
AP_13: R1= OMe; R2= H; X= N; Y= C; A= N; W= CH2; RHS 2

Reagents: (a) Na$_2$CO$_3$, DMF, 70 ^{o}C (b) 4N HCl in Dioxane, 55 ^{o}C (c) NaBH$_3$CN, DCE or CHCl$_3$ /EtOH, 65-80 ^{o}C (d) NaOMe, MeOH, 75 ^{o}C (e) **33**, HATU, DIPEA, DMF, RT (f) ZnCN$_2$, Zn(OAc)$_2$, Zn, Pd$_2$(dba)$_3$, dppf, DMF, 100 ^{o}C, 23 % (g) Pd$_2$(dba)$_3$, dppf, CuCN, DMF, 110 ^{o}C, 68 %

Figure 4.4: Synthetic scheme utilised for synthesis of amino piperidine based molecules with substituted pyridines RHS
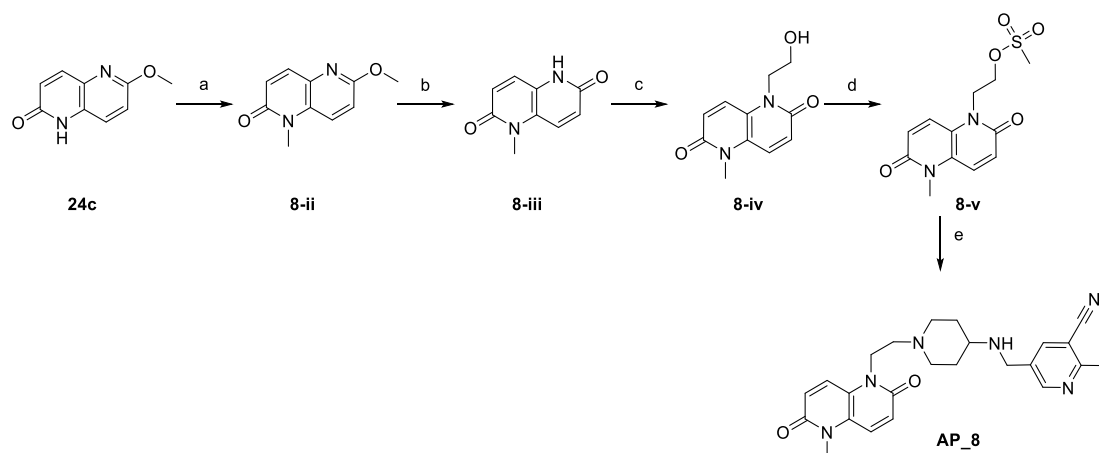
Reagents: (a) MeI, Cs_2CO_3, DMSO, 60 °C, 83 % (b) 48% HBr, 80 °C, > 95% (c) 2-Bromoethanol, Cs_2CO_3, DMSO, 95 °C, > 95% (d) MsCl, TEA, DCM, 0 °C, > 95% (e) **29e**, Na_2CO_3, DMF, 70 °C, 98 %

Figure 4.5: Synthetic scheme utilised for synthesis 1, 5-naphthyridine dione LHS derivative

4.2.2 Synthesis of methoxy/fluoro substituted aminopiperdine linker derivatives
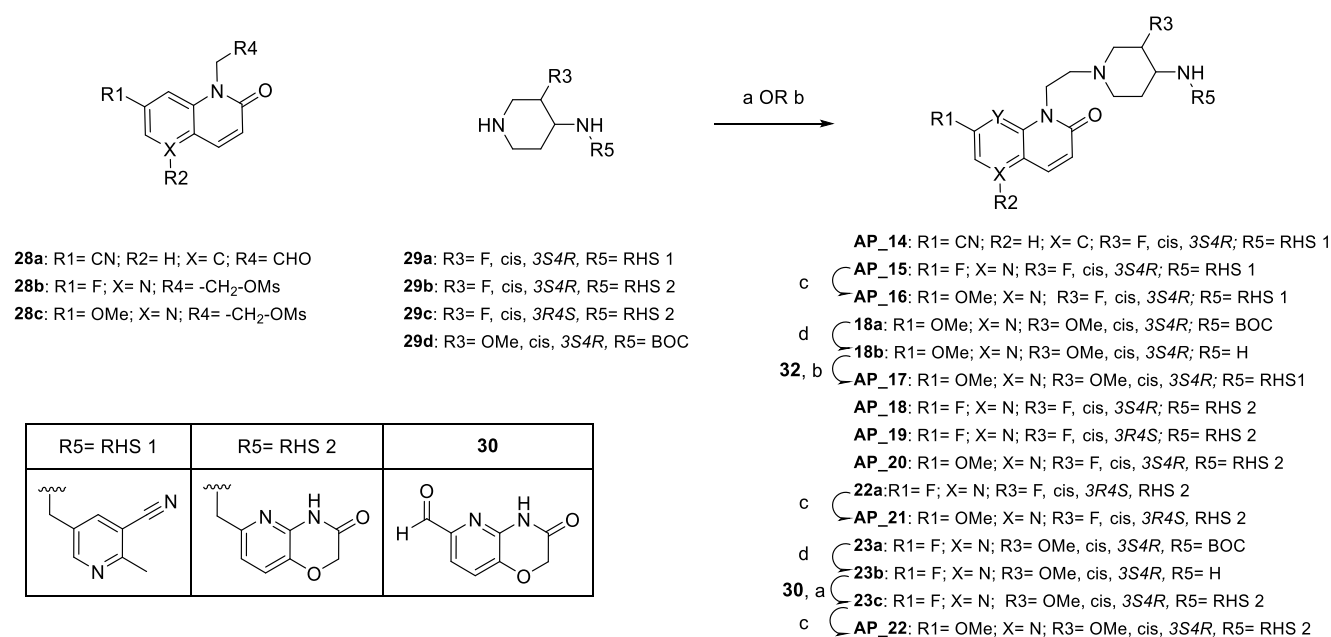
Reagents: For R4= CHO (a) $NaBH(OAc)_3$, DMF, 70 °C; For R4= -CH_2-OMs (b) Na_2CO_3, DMF, 70 °C (c) NaOMe, MeOH, 75 °C (d) 4N HCl in Dioxane, 55°C or TFA/DCM, RT

Figure 4.6: Synthetic scheme utilised for synthesis of fluoro/ methoxy substituted aminopiperidine linker derivatives.
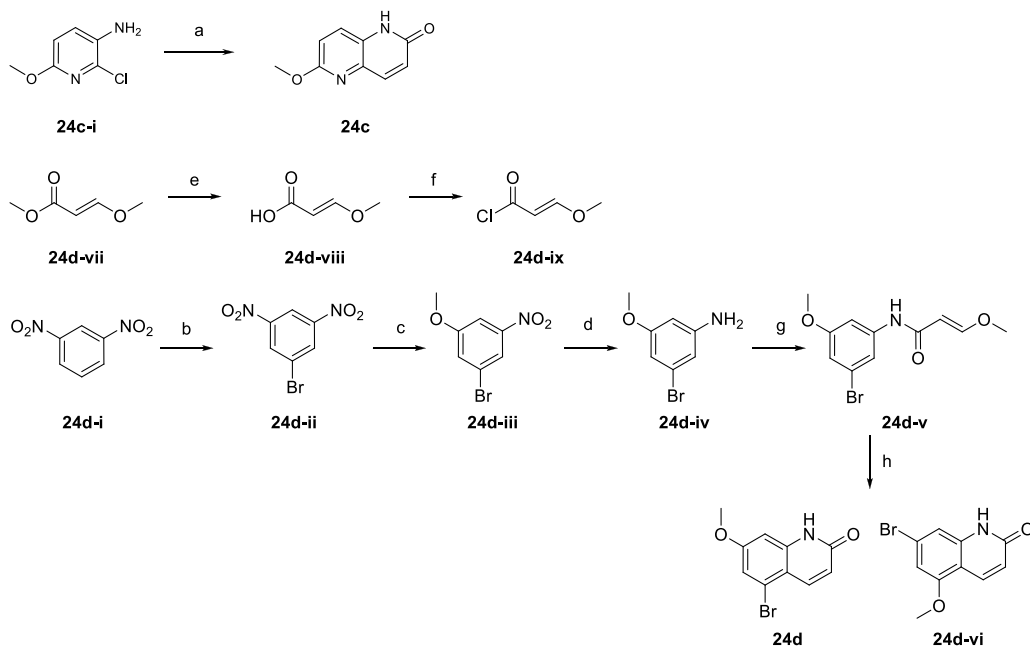
Reagents: (a) Butyl acrylate, Pd(OAc)$_2$, N,N-Dicyclohexylmethylamine, [(t-Bu)$_3$PH]BF$_4$, Cumene, 150 °C, 33 % (b) conc. H$_2$SO$_4$, NBS, 85 °C, 68 % (c) NaOMe, MeOH, Reflux, 90 % (d) Fe, NH$_4$Cl, MeOH:water, 95 °C, 75 % (e) 2N NaOH, Reflux, 84 % (f) SOCl$_2$, Reflux (g) **24d-ix**, Pyridine, 0 °C, 78 % (h) conc. H$_2$SO$_4$, 5-10 °C, 91%

Figure 4.7: Synthetic scheme utilised for synthesis of novel LHS
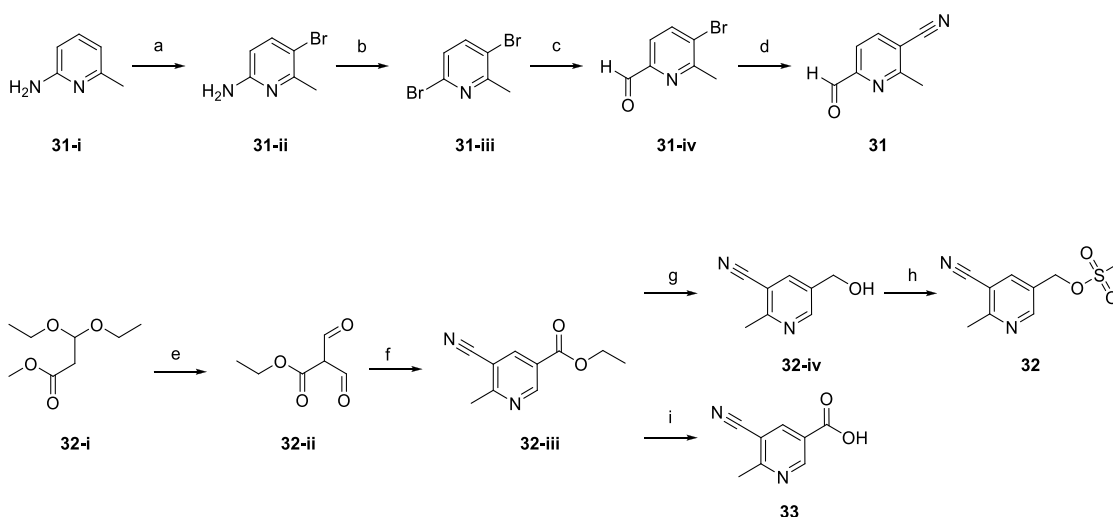
Reagents:(a) 1,3-Dibromo-5,5-dimethylhydantoin, DCM, -5 °C, 98% (b) HBr, NaNO$_2$, -5 °C, 65%, (c) n-BuLi, DMF, -78 °C, 68 % (d) CuCN, DMF, 130 °C, 32 % (e) Ethyl formate, NaH, Ether, -10 °C, 80 % (f) TEA, p-TSA, 3-amino crotononitrile, ether/DMF/pyridine 80 % (g)

LAH, THF, -78 °C, 22 % (h) MsCl, TEA, DCM, 0 °C, 92 % (i) LiOH, THF/Water/MeOH, 60 °C, 50 %

Figure 4.8: Synthetic scheme utilised for synthesis of (5-cyano-6-methylpyridin-3-yl) methyl methanesulfonate as RHS fragment.
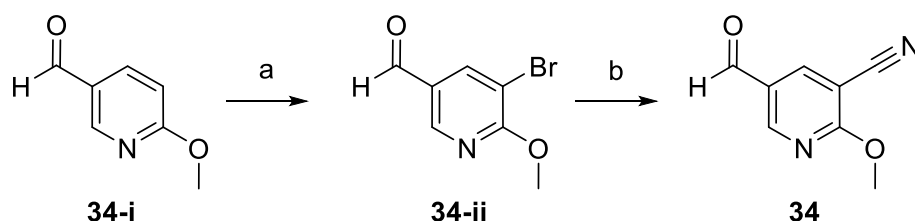
Reagents: (a) CH$_3$COONa, Br$_2$, AcOH, 90 °C, 30% (b) Pd$_2$(dba)$_3$, dppf, CuCN, DMF, 110 °C, 40 %

Figure 4.9: Synthetic scheme utilised for synthesis of (5-cyano-6-methylpyridin-3-yl) methyl methanesulfonate as RHS fragment.
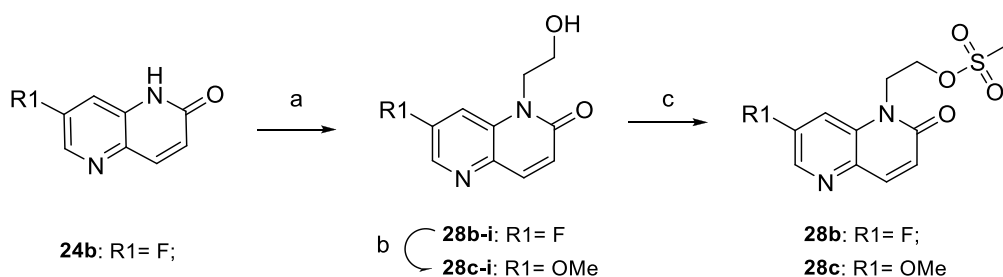
Reagents: (a) Cs$_2$CO$_3$, 2-Bromoethanol, DMSO, 90 °C (b) NaOMe, MeOH, 75 °C (d) MsCl, DIPEA, DCM, 0 °C

4. 2.3 Procedure for the synthesis LHS fragments

7-Fluoro-1, 5-naphthyridin-2(1H)-one (24b)

In 100ml RB flask, butyl acrylate (45.0 ml, 314.13 mmol), 2-bromo-5-fluoropyridin-3-amine (60g, 314.13 mmol), Pd(OAc)$_2$ (1.411 g, 6.28 mmol), P(t-Bu)$_3$ (3.64 g, 12.57 mmol), N-Methyldicyclohexylamine (202 ml, 942.40 mmol) was taken in Cumene (189 g, 1570.67 mmol).The RM was heated to 150 °C for overnight. RM was diluted with diethyl ether and solid obtained was filtered. The solid was suspended in water and filtered to get **24b** (45.0 g,

87 %). ¹H NMR (300 MHz, DMSO-d_6) δ 6.71 (d, 1H), 7.47 (dd, 1H), 7.94 (d, 1H), 8.49 (d, 1H), 11.95 (bs, 1H). m/z (ES⁻), (M-H) = 163.12 for $C_8H_5FN_2O$.

6-Methoxy-1, 5-naphthyridin-2(1H)-one (24c)

In a 250ml R. B. Flask, 2-chloro-6-methoxypyridin-3-amine, **24c-i** (1.900 g, 11.98 mmol), Pd(OAc)₂ (0.054 g, 0.24 mmol), Tri-t-butylphosphonium tetrafluoroborate (0.139 g, 0.48 mmol), N,N-Dicyclohexylmethylamine (6.35 mL, 29.95 mmol) were taken in Cumene (150 mL, 11.98 mmol) to give a brown suspension. The resulting RM was stirred at 150 °C overnight. Diethyl ether was added to the reaction mixture and sonicated well. Solid was filtered and washed with ether. The solid was suspended in water and filtered, washed with water and hexane, dried to obtain **24c** (0.700 g, 33.2 %) as brown solid. ¹H NMR (300 MHz, DMSO-d_6) δ 3.89 (s, 3 H) 6.68 (d, J=9.80 Hz, 1 H) 7.03 (d, J=8.85 Hz, 1 H) 7.66 (d, J=8.85 Hz, 1 H) 7.80 (d, J=9.80 Hz, 1 H) 11.77 (br. s., 1 H). m/z (ES+), (M+H)+ = 177.19 for $C_9H_8N_2O_2$.

3-Methoxy acrylic acid (24d-viii)

3-Methoxy acrylic acid methyl ester, **24d-vii** (50 g, 0.431 moles) was dissolved in 2N NaOH (275 mL) and the resulting solution was refluxed for two hours. The reaction mixture was cooled to room temperature, acidified with citric acid and extracted with ethyl acetate (3 × 250 mL). The combined organic layers were washed with water, brine, dried over Na_2SO_4 and concentrated to give **24d-viii** (37 g, 84%) as a yellow solid. ¹H NMR (400 MHz, DMSO-d_6) δ 3.66 (s, 3H), 5.16 (d, 1H, J = 12.52 Hz), 7.54 (d, 1H, J = 12.53 Hz), 11.91 (br. s, 1H).

3-Methoxy-acryloyl chloride (24d-ix)

24d-viii (30 g, 0.293 moles) was dissolved in thionyl chloride (300 mL) and refluxed for two hours. The reaction mixture was concentrated in vacuo to give 3-methoxy acryloyl chloride, **24d-ix** 32g (Crude) as a dark brown liquid, which was used as such for next step without further purification.

1-Bromo-3, 5-dinitro-benzene (24d-ii)

To the solution of **24d-i** (50 g, 0.297 moles) in conc. sulphuric acid (600 mL) was added N-Bromo succinimide (74 g, 0.416 moles) at 85 °C portion wise for a period of one hour. The

reaction mixture was allowed to stir at the same temperature for an hour and poured into ice water. The solid precipitated was filtered and washed with water and recrystallised from methanol to give **24d-ii** (50g, 68%). ^{1}H NMR (400 MHz, CDCl$_3$) δ 8.72 (s, 2H), 9.01 (s, 1H).

1-Bromo-3-methoxy-5-nitro-benzene (24d-iii)

Sodium methoxide (16.39 g, 0.303 moles) was added in one portion to the solution of **24d-ii** (50 g, 0.202 moles) in dry methanol (500 mL) at room temperature. The resulting solution was refluxed overnight and the progress of the reaction was monitored by NMR. The reaction mixture was quenched with 1.5N HCl (500 mL) and concentrated in vacuo to remove methanol. The aqueous layer was extracted with DCM (3 × 250 mL) and the combined organic layers were washed with water, brine, dried over Na$_2$SO$_4$ and concentrated. The crude product was purified by column chromatography using ethyl acetate in pet. ether (1 : 10) as eluent to give **24d-iii** (44g, 93%) as a yellow solid. ^{1}H NMR (400 MHz, CDCl$_3$) δ 3.90 (s, 3H), 7.37 (s,1H), 7.68 (s, 1H), 7.96 (s, 1H).

3-Bromo-5-methoxy-phenylamine (24d-iv)

To the solution of **24d-iii** (45 g, 0.193 moles) in methanol: water (1 : 1, 500 mL) was added ammonium chloride (67 g, 1.55 moles) and iron powder (55 g, 0.969 moles). The resulting mixture was heated at 95 °C overnight, filtered through celite and concentrated to remove methanol. The aqueous solution was extracted with ethyl acetate (3 × 250 mL) and the combined organic layers were washed with water, brine, dried over Na$_2$SO$_4$ and concentrated. The crude product was purified by column chromatography using 15% ethyl acetate in pet. ether as eluent to give **24d-iv** (30g, 76.5%) as a brown oil. ^{1}H NMR (400 MHz, DMSO-d_6) δ 3.65 (s, 3H), 5.40 (br. s, 2H), 6.09 (s, 1H), 6.22 (s, 1H), 6.33 (s, 1H).

N-(3-Bromo-5-methoxyphenyl)-3-methoxyacrylamide (24d-v)

24d-ix (27 g, 0.166 moles) was added drop wise to the solution of **24d-iv** (30 g, 0.148 moles) in pyridine (300 mL) at 0 °C and stirred at 0 − 10 °C for an hour. The reaction mixture was concentrated to remove pyridine and the residue was dissolved in ethyl acetate (750 mL), washed with 1.5N HCl (2 × 250 mL), water, brine, dried over Na$_2$SO$_4$ and concentrated. The crude product was triturated with ether, cooled and filtered to obtain **24d-v** (35g, 78.5%) as a dark brown solid. ^{1}H NMR (300 MHz, DMSO- d_6) δ 3.67 (s, 3H), 3.72 (s, 3H), 5.46 (d, 1H, J = 12.27 Hz), 6.78 (s, 1H), 7.17 (s, 1H), 7.47 (s, 1H), 7.50 (d, 1H, J = 12.24 Hz), 9.89 (s, 1H).

5-Bromo-7-methoxy-1H-quinolin-2-one (24d)

To the stirring solution of concentrated sulfuric acid (120 mL) was added **24d-v** (35 g, 0.107 moles) portion wise at 5 – 10 °C and stirred for 15 - 20 minutes. The reaction mixture was poured into ice water. The precipitated solid was filtered, washed with water and dried. The resulting solid was suspended in saturated sodium carbonate solution and filtered to give 5-Bromo-7-methoxy-1H-quinolin-2-one and **7**-Bromo-5-methoxy-1H-quinolin-2-one as a pale brown solid. This solid was tried to dissolve in CHCl$_3$: MeOH (1: 1, 750 mL) at 60° C and cooled to room temperature. The precipitated solid was filtered to obtain **24d** (8.85 g, 91%) and 5% of **7**-Bromo-5-methoxy-1H-quinolin-2-one. ^{1}H NMR (400 MHz, DMSO- d_6) δ 3.82 (s, 3H), 6.43 (d, 1H, J = 9.76 Hz), 6.83 (s, 1H), 7.14 (s, 1H), 7.91 (d, 1H, J = 9.76 Hz), 11.73 (s, 1H). m/z (ES+) (M+H)+: 256 for C$_{10}$H$_8$BrNO$_2$

7-Fluoropyrido (2, 3-b) pyrazin-2(1H)-one (24g)

A solution of 5-fluoro-2,3-pyridinediamine (12g, 0.0944 moles) and glyoxylic acid monohydrate (13.02 g, 0.141 moles) in EtOH (100 mL) was stirred at RT for 12 hrs and the precipitated solid was filtered to afford grey solid as a mixture of two isomers 7-fluoropyrido[3,2-b]pyrazin-2(1H)-one compound with 7-fluoropyrido[3,2-b]pyrazin-3(4H)-one (1:1) **24g** Crude yield : 12g (76%). This crude was taken as such for next step without purification. m/z (ES+) (M+H)+: 166.2 for C$_7$H$_4$FN$_3$O

7-Methoxypyrido[3,2-b]pyrazin-2(1H)-one (24h)

To a solution of 7-fluoropyrido[3,2-b]pyrazin-2(1H)-one compound with 7-fluoropyrido[3,2-b]pyrazin-3(4H)-one (1:1), **24g** (12 g, 0.0722 moles) in methanol (100 mL), sodium methoxide (19.51 g, 0.361 moles) was added and heated to 100° C in a sealed tube for 12 hrs. The reaction mixture was cooled to room temperature and poured into 500g of ice-water. The pH of the reaction mixture brought to 2-3 using 6N HCl solution. The precipitated solid was filtered, dried and the crude product was triturated with hot DMSO (3 volumes), filtered and washed with ethyl acetate to afford **24h** (6.2 g). ^{1}H NMR (400 MHz, DMSO- d_6) δ 3.90 (s, 3H), 7.12 (s, 1H), 8.15 (s, 1H), 8.25 (s, 1H), 12.48 (s, 1H). m/z (ES+), (M+H)+ : 178 for C$_8$H$_7$N$_3$O$_2$

***Tert*-butyl 1-(2-(7-fluoro-2-oxo-1,5-naphthyridin-1(2H)-yl)ethyl)piperidin-4-yl**

carbamate(26b)

In a 500 mL round-bottomed flask **25** (10.80 g, 33.51 mmol), **24b** (5 g, 30.46 mmol) and Cs_2CO_3 (13.90 g, 42.65 mmol) were taken in DMF (100 mL) to give a brown suspension. The reaction mixture was stirred at 90 °C overnight. All the DMF was removed and suspended the crude in 10% Methanol in DCM and washed with water, brine, dried, concentrated and chromatographed with DCM/MeOH. Title compound elutes out between 4%-6% Methanol in DCM. Pooled all pure fractions and concentrated to get the required product **26b** (9.30 g, 78 %). m/z (ES$^+$), (M+H)$^+$ = 391.42 for $C_{15}H_{19}FN_4O$

1-(2-(4-Aminopiperidin-1-yl) ethyl)-7-fluoro-1, 5-naphthyridin-2(1H)-one (27b)

In a 100 mL round-bottomed flask **26b** (1.5 g, 3.84 mmol) was taken in HCl (4N in Dioxane) (25 mL, 100.00 mmol). The RM was then heated at 80 °C for two hours. The RM was evaporated to dryness. The residue was then neutralised with saturated Na_2CO_3 solution. The suspension was evaporated to dryness. The residue was then dissolved in 5 % MeOH in DCM and the suspension was filtered. The solid was then washed with 5 % MeOH in DCM twice. The filterate was then evaporated to obtain **27b** (1.400 g, 126 %). m/z (ES$^+$), (M+H)$^+$ = 291.36 for $C_{15}H_{19}FN_4O$.

Tert-butyl 1-(2-(6-methoxy-2-oxo-1,5-naphthyridin-1(2H)-yl)ethyl)piperidin-4-yl carbamate(26c)

In a 100 mL round-bottomed flask, **24c** (700 mg, 3.97 mmol) and **25** (1281 mg, 3.97 mmol) and cesium carbonate (1554 mg, 4.77 mmol) were taken in DMF (15 mL) to give a brown solution. The resulting reaction mixture was heated to 90 °C overnight. DMF was evaporated from the reaction mass and water was added to it. This was extracted using 10% methanol in DCM (3X 50ml).The combined organic fractions were concentrated to dryness and purified by Silica gel chromatography using 0 to 10% methanol in DCM to obtain **26c** (1800 mg, 113 %) as brown liquid which was a mixture of both N and O alkylated. m/z (ES$^+$), (M+H)$^+$ = 403.45 for $C_{21}H_{30}N_4O_4$.

1-(2-(4-Aminopiperidin-1-yl) ethyl)-6-methoxy-1, 5-naphthyridin-2(1H)-one (27c)

In a 100 mL round-bottomed flask, **26c** (1.600 g, 3.98 mmol) and 4N HCL in Dioxane (10 mL, 329.12 mmol) were taken to give a yellowish solution. The resulting reaction mixture was stirred at 55 °C for 1 hr. The reaction mass was concentrated to dryness. This hydrochloride salt was washed with ethyl acetate. Then it was cooled to 5-10°C and basified using sodium

hydroxide solution. This was extracted using 10% methanol in DCM (3 X 25ml). The combined organic layers was concentrated to dryness to obtain **27c** (0.800 g, 66.6 %) as light yellow gel. m/z (ES$^+$), (M+H)$^+$ = 303.37 for $C_{16}H_{22}N_4O_2$.

Tert-butyl 1-(2-(5-bromo-7-methoxy-2-oxoquinolin-1(2H)-yl) ethyl) piperidin-4-ylcarbamate (26d)

In a 250 mL round-bottomed flask, **24d** (600 mg, 2.36 mmol) and **25** (838 mg, 2.60 mmol) and cesium carbonate (923 mg, 2.83 mmol) were taken in DMF (10 mL) to give a brown solution. The resulting reaction mixture was heated to 90 °C overnight. DMF was evaporated from the reaction mass and water was added to it. This was extracted using 10% methanol in DCM (3X 50ml).The combined organic fractions were concentrated to dryness and purified by Silica gel chromatography using 0 to 10% methanol in DCM to obtain **26d** (1000 mg, 88 %) as yellow gel which was a mixture of both N and O alkylated products. m/z (ES+), (M+)$^+$/(M+2H)$^+$ = 480.3/482.3 for $C_{22}H_{30}BrN_3O_4$

Tert-butyl 1-(2-(5-cyano-7-methoxy-2-oxoquinolin-1(2H)-yl)ethyl)piperidin-4-yl carbamate (26i)

In a 15 mL sealed vial, **26d** (1.100 g, 2.29 mmol), Pd2(dba)$_3$ (0.042 g, 0.05 mmol), dppf (0.051 g, 0.09 mmol) and CuCN (1.025 g, 11.45 mmol) were taken in DMF (10 mL) to give a brown suspension . The resulting reaction mixture was heated at 110 °C overnight. DMF was evaporated from the reaction mixture. Water and ammonia were added to it. This was extracted using 5% Methanol in DCM. The combined Organic layers were concentrated and purified using 0 to 15% Methanol in DCM to obtain **26i** (0.670 g, 68.6 %) as brown solid, which was impure. m/z (ES$^+$), (M+H)$^+$ = 427.42 for $C_{23}H_{30}N_4O_4$

Tert-butyl 1-(2-(7-methoxy-2-oxo-1, 5-naphthyridin-1(2H)-yl)ethyl)piperidin-4-yl carbamate (26e)

In a 100 mL round-bottomed flask **26b** (1.3 g, 3.33 mmol) was taken in methanol (25 mL) under N$_2$. The resulting solution was stirred at 60 °C for 1.5 hrs. Reaction was allowed to cool at RT, methanol was evaporated to dryness. Obtained solid was diluted with water and extracted with 5 % methanol in DCM. Organic layer was concentrated and chromatographed using Methanol/DCM to get **26e** (1.000 g, 74.6 %) as a product. m/z (ES$^+$), (M+H)$^+$ = 403.49 for $C_{21}H_{30}N_4O_4$

1-(2-(4-Aminopiperidin-1-yl)ethyl)-7-methoxy-1,5-naphthyridin-2(1H)-one (27e)

In a 100 mL round-bottomed flask **26e** (1.2 g, 2.98 mmol) was taken in 4 N HCl in Dioxane (20 mL) .The resulting reaction was stirred at 70 °C for 30 min. Reaction was cooled to RT and solvent was evaporated to dryness. Obtained solid was neutralised with $NaHCO_3$ to pH 8 and it was again evaporated to dryness. Obtained solid was diluted with 5 % methanol in DCM and filtered. Filtrate was concentrated to obtain **27e** (0.750 g, 83 %) as a gummy material ,which was taken for next reaction as such without further purification. m/z (ES$^+$), (M+H)$^+$ = 303.4 for $C_{16}H_{22}N_4O_2$.

Tert-butyl 1-(2-(6-methoxy-3-oxopyrido[3,2-b]pyrazin-4(3H)-yl)ethyl)piperidin-4-yl carbamate (26f)

In a 200 mL round-bottomed flask 6-methoxypyrido[3,2-b]pyrazin-3(4H)-one (CAS No-917344-37-7, commercial) (2 g, 11.29 mmol) and Cs_2CO_3 (4.78 g, 14.68 mmol) was taken in DMF (15 mL) under N2 and stirred. After 3 min **25** (5.46 g, 16.93 mmol) was added. The resulting reaction mixture was stirred at 90 °C for 12 hrs. Reaction was allowed to cool RT and DMF was evaporated to dryness. Crude solid was diluted with water and extracted with 10 % methanol in DCM to get crude product. Purification was done using methanol/DCM as a mobile phase to get product **26f** as a mixture tert-butyl 1-(2-(6-methoxy-3-oxopyrido[3,2-b]pyrazin-4(3H)-yl)ethyl)piperidin-4-ylcarbamate compound with tert-butyl 1-(2-(6-methoxypyrido[3,2-b]pyrazin-3-yloxy)ethyl)piperidin-4-ylcarbamate (1:1) (2.100 g, 23.05 %). m/z (ES$^+$), (M+H)$^+$ = 404.5 for $C_{20}H_{29}N_5O_4$

4-(2-(4-Aminopiperidin-1-yl)ethyl)-6-methoxypyrido[3,2-b]pyrazin-3(4H)-one (27f)

In a 100ml RB flask, crude mix of tert-butyl 1-(2-(6-methoxy-3-oxopyrido[3,2-b]pyrazin-4(3H)-yl)ethyl)piperidin-4-ylcarbamate compound with tert-butyl 1-(2-(6-methoxypyrido[3,2-b]pyrazin-3-yloxy)ethyl)piperidin-4-ylcarbamate (1:1), **26f** (2 g, 4.96 mmol) was taken in DCM (10ml). Slowly Trifluoroacetic acid (15.18 ml, 198.28 mmol) was added to the RM and RM was heated to 60°C for 1hr. The RM was evaporated and taken in aqueous Sodium bicarbonate solution. The aqueous layer was evaporated and taken in dcm /methanol the inorganic solid was filtered. The filtrate was evaporated to obtain **27f** (1.600 g, 106 %) as crude mix which was taken for next step without purification. m/z (ES$^+$), (M+H)$^+$ = 304.35 for $C_{15}H_{21}N_5O_2$.

Tert-butyl 1-(2-(7-methoxy-2-oxopyrido[3,2-b]pyrazin-1(2H)-yl)ethyl)piperidin-4-yl carbamate (26h)

In a 250 mL round-bottomed flask, 24h (3.00 g, 16.93 mmol) and **25** (6.01 g, 18.63 mmol) and cesium carbonate (6.07 g, 18.63 mmol) were taken in DMF (50 mL) to give a brown solution. The resulting reaction mixture was heated to 90 °C 3hrs. DMF was evaporated from the reaction mass and water was added to it. This was extracted using 10% methanol in DCM (3X 100ml).The combined organic fractions were concentrated to dryness and purified by Silica gel chromatography using 0 to 9% methanol in DCM to obtain **26h** (8.10 g, 119 %) as orange solid which was a mixture of N and O- alkylated product. m/z (ES$^+$), (M+H)$^+$ = 404.52 for C$_{20}$H$_{29}$N$_5$O$_4$.

1-(2-(4-Aminopiperidin-1-yl)ethyl)-7-methoxypyrido[3,2-b]pyrazin-2(1H)-one (27h)

In a 100 mL round-bottomed flask, **26h** (3.00 g, 7.44 mmol) and TFA (11.46 mL, 148.71 mmol) were taken in DCM (50 mL) to give a yellowish solution. The resulting reaction mixture was stirred at 55 °C overnight. The reaction mass was concentrated to dryness. This was TFA salt, which was co-evaporated with toluene thrice to obtain TFA salt of **27h** (3.00 g, 133 %) as yellow gel, which was directly used for the next step. m/z (ES$^+$), (M+H)$^+$ = 304.41 for C$_{15}$H$_{21}$N$_5$O$_2$.[TFA]

1-(2-(4-Aminopiperidin-1-yl)ethyl)-7-methoxy-2-oxo-1,2-dihydroquinoline-5-carbonitrile(27i)

 In 100 mL round-bottomed flask **26i** (670 mg, 1.57 mmol) and 4N HCl in Dioxane (10 mL, 329.12 mmol) were taken to give a yellowish solution. The resulting reaction mass was heated to 55 °C for 30 mins. The reaction mass was concentrated to dryness. This hydrochloride salt was washed with ethyl acetate. Then it was cooled to 5-10 °C and basified using sodium hydroxide solution. This was extracted using 10% methanol in DCM (3 X 25ml). The combined organic layers was concentrated to dryness to obtain **27i** (500 mg, 98 %) as yellow gel. m/z (ES$^+$), (M+H)$^+$ = 327.34 for C$_{18}$H$_{22}$N$_4$O$_2$

6-Methoxy-1-methyl-1,5-naphthyridin-2(1H)-one (8-ii)

 In a 100 mL round-bottomed flask, **24c** (2.000 g, 11.35 mmol) and cesium carbonate (4.07 g, 12.49 mmol) were taken in DMSO (20 mL) to give a tan suspension. Then to this methyl iodide (1.065 mL, 17.03 mmol) was added and the resulting reaction mixture was heated to 60 °C for

2 hrs. Water was added to the reaction mixture and this was extracted using EtOAc (5 X50ml). The resulting organic layers were washed with water, dried over sodium sulphate and concentrated under vacuum to obtain crude solid. The crude product was purified by silica gel column using 0 to 9% Methanol in DCM to obtain **8-ii** (1.800 g, 83 %) as solid. ^{1}H NMR (300 MHz, DMSO- d_6) δ 3.61 (s, 3 H) 3.91 (s, 3 H) 6.80 (d, J=9.61 Hz, 1 H) 7.12 (d, J=9.23 Hz, 1 H) 7.79 (d, J=9.61 Hz, 1 H) 8.00 (d, J=9.04 Hz, 1 H); m/z (ES$^+$), (M+H)$^+$ = 191.23 for $C_{10}H_{10}N_2O_2$

1-Methyl-1,5-naphthyridine-2,6(1H,5H)-dione (8-iii)

In a 250 mL round-bottomed flask, **8-ii** (1.700 g, 8.94 mmol) was taken in 48 % HBr in Water (15 ml, 276.23 mmol) to give a yellow solution. The resulting reaction mass was stirred at 80 °C for 2hr. The reaction mass was concentrated to dryness and pH was adjusted to ~7. Yellow solid obtained, was filtered, washed with hexane and dried to obtain **8-iii** (1.800 g, 114 %) as yellow solid. ^{1}H NMR (300 MHz, DMSO- d_6) δ 3.49 (s, 3 H) 6.33 (d, J=9.23 Hz, 1 H) 6.50 (d, J=9.61 Hz, 1 H) 7.43 (d, J=9.42 Hz, 1 H) 7.36 (d, J=9.61 Hz,1 H); m/z (ES+), (M+H)$^+$ = 177.19 for $C_9H_8N_2O_2$.

1-(2-Hydroxyethyl)-5-methyl-1,5-naphthyridine-2,6(1H,5H)-dione (8-iv)

In 100 mL round-bottomed flask, **8-iii** (1.000 g, 5.68 mmol) and cesium carbonate (2.034 g, 6.24 mmol) were taken in DMSO (10 mL) under nitrogen atmosphere to give a yellowish solution. To it was added 2-bromoethanol (0.561 mL, 7.95 mmol) and the resulting reaction mass was heated to 95 °C overnight. Water was added to the reaction mass and extracted using ethyl acetate (5X 40ml). The combined organic fractions were washed with water, dried with sodium sulfate and concentrated to dryness to obtain **8-iv** (1.300 g, 104 %) as light yellow solid. m/z (ES$^+$), (M+H)$^+$ = 221.26 for $C_{11}H_{12}N_2O_3$

2-(5-Methyl-2,6-dioxo-5,6-dihydro-1,5-naphthyridin-1(2H)-yl)ethyl methanesulfonate (8-v)

In 50 mL round-bottomed flask, **8-iv** (400 mg, 1.82 mmol) and TEA (0.759 mL, 5.45 mmol) were taken in DCM (10 mL) under nitrogen atmosphere to give a yellowish solution. The resulting reaction mass was cooled to 0°C and Mesyl-Cl (0.184 mL, 2.36 mmol) was added to it very slowly. Then the RM was stirred at 0°C for 45 mins. DCM was added to the reaction mass and washed with water (2 X20ml). The combined organic fractions were dried over

sodium sulfate and concentrated to dryness to obtain **8-v** (600 mg, 111 %) as yellow gel. m/z (ES^+), $(M+H)^+ = 299.27$ for $C_{12}H_{14}N_2O_5S$.

Procedure for the synthesis RHS fragments

2-Amino-5-bromo-6-methylpyridine (31-ii)

To a 5L flask was added **31-i** (75 g, 0.693 moles) and DCM (2 L) and the solution was cooled to -5 °C. 1,3-Dibromo-5,5-dimethylhydantoin (99 g, 0.346 mol) was added portion wise during a 2 hrs period while maintaining the temperature below -5 °C. The reaction was stirred at -5 °C for 1 h after addition, and monitored by ^{1}H-NMR and TLC. After completion of the reaction, the mixture was quenched with cold 30% Na_2SO_3 solution (120 mL) and brine (150 mL). The layers were separated and the aqueous was extracted with DCM. The combined organic layers were dried over sodium sulphate and concentrated under reduced pressure. The residue was purified by flash chromatography on silica gel (EtOAc/hexanes, 1:4 in v/v) to afford **31-ii** (131 g, quantitative yield). ^{1}H NMR (300 MHz, DMSO- d_6) δ 2.29 (s, 3H), 6.03 (br s, 2H), 6.20 (d, 1H, J= 8.46 Hz), 7.43 (d, 1H, J= 8.64 Hz). m/z (ES^+) $(M+H)^+$: 189 for $C_6H_7BrN_2$

3, 6-Dibromo-2-methyl-pyridine (31-iii)

To a solution of **31-ii** (100 g, 0.534 moles) in aqueous HBr (48%, 540 mL), cooled at 0 °C, was added bromine (169.80 g, 1.068 moles), forming a yellow suspension. A solution of $NaNO_2$ (92.2 g, 1.336 moles) in water (107 mL) was then added drop-wise. After addition the mixture was brought to room temperature and stirred for 1.5 hrs, and was poured into ice (500 mL). The aqueous mixture was neutralized with NaOH, and extracted with DCM (4 x 200 mL). The combined extracts were dried (Na_2SO_4), filtered and concentrated under reduced pressure. The residue was purified by flash chromatography on silica gel (EtOAc/hexanes, 1 : 10 in v/v), to obtain **31-iii** as white solid 87 g, (64.8%). ^{1}H NMR (400 MHz, DMSO- d_6) δ 2.54 (s, 3H), 7.43 (d, 1H, J= 8.14 Hz), 7.94 (d, 1H, J= 8.28 Hz). m/z (ES^+) $(M+H)^+$: 254 for $C_6H_5Br_2N_2$

5-Bromo-6-methyl-pyridine-2-carbaldehyde (31-iv)

To a solution of **31-iii** (87g, 0.346 moles) in anhydrous ether (2 L), n-BuLi (2.5M solution in hexanes, 159 mL, 0.398 moles) was added slowly at -78 °C, forming a yellow suspension. The reaction mixture was stirred at the same temperature for 1 hour and DMF (44.67g, 0.612 mL) was added dropwise. After stirring for 1 hr at -78 °C, the mixture was allowed to warm to room

temperature and stirred for 1 hour. Aqueous HCl (0.5N, 350 mL) was added and the organic layer was separated. The aqueous layer was extracted with ethyl acetate and the combined organic layers were dried over sodium sulfate and concentrated. The residue was purified by flash column chromatography on silica gel (EtOAc/hexanes, 15: 100) to afford **31-iv** as yellow solid. (47g, 67.8%). ^{1}H NMR (400 MHz, DMSO- d_6) δ 2.75 (s, 3H), 7.70 (d, 2H, J = 8.10 Hz), 8.06 (d, 2H, J = 8.10 Hz), 10.22 (s, 1H). m/z (ES$^+$) (M+H)$^+$: 202 for C_7H_6BrNO

6-Formyl-2-methylnicotinonitrile (31)

Cuprous cyanide (24.7g, 0.274 moles) was added to a solution of **31-iv** (46 g, 0.228 moles) in DMF (1 L) and degassed with nitrogen. The reaction mixture was heated at 130 °C for 8 hours and cooled to room temperature. The mixture was filtered through celite and washed with ethyl acetate. The combined organic layers were washed with brine, dried over sodium sulfate and concentrated. The crude product was purified by flash column chromatography on silica gel (EtOAc/hexanes, 15: 100) to afford **31** as white solid. (11 g, 32%). ^{1}H NMR (400 MHz, DMSO-$d6$) δ 2.83 (s, 3H), 8.10 (d, 2H, J = 7.88 Hz), 8.38 (d, 2H, J = 7.84 Hz), 10.30 (s, 1H). GCMS (M$^+$): 146 for C_7H_6BrNO.

2-Formyl-3-oxo-propionic acid ethyl ester (32-ii)

Ethyl formate (2219 mL, 27.59 moles) was added dropwise to a suspension of sodium hydride (158.9 g, 3.31 moles, 60% dispersion in mineral oil) in diethyl ether (4 L) at -10 °C under nitrogen atmosphere. Then ethyl 3,3-diethoxy propionate, **32-i** (525 g, 2.759 moles) in diethyl ether (2 L) was added dropwise to the reaction mixture and stirred at 0 – 5 °C for 15 hrs and at room temperature for 6 hours. The mixture was added to ice water and organic layer was separated. The aqueous layer was acidified to pH 3 using 1.5 N HCl and extracted with MTBE. The combined organic layers were dried over sodium sulphate and concentrated under reduced pressure. The crude product was purified by distillation to afford **32-ii** as colorless liquid. (320 g, 80%). ^{1}H-NMR (300MHz, DMSO- d_6) δ 1.20 (t, 3H, J = 7.08 Hz), 4.14 (q, 2H, J = 7.11 Hz), 8.89 (s, 2H), 11.60 (brs, 1H).

5-Cyano-6-methyl-nicotinic acid ethyl ester (32-iii)

To a solution of **32-ii** (180 g, 1.2503 moles) in diethyl ether (1 L), triethyl amine (192 mL, 1.37 moles) was added dropwise at 0° C and stirred for one hour. The solvent was evaporated and

the residue was dissolved in dry DMF (1.5 L). *p*-Toluene sulfonyl chloride (260 g, 1.36 moles) in dry DMF (1 L) was added drop wise at -15 °C and the reaction mixture was allowed to warm to room temperature. After stirring for overnight, 3-amino crotononitrile (101.8 g, 1.242 moles) in pyridine (400 mL, 4.96 moles) was added at 0 °C. After the addition is complete the mixture was allowed to warm to RT and heated at 70 °C for 10 hours. The solvent was evaporated under reduced pressure and the residue was dissolved in dichloromethane. The organic layer was washed with water, brine and dried over sodium sulphate. The solvent was concentrated and the residue was purified by column chromatography using 100% pet. ether to obtain **32-iii** as light brown solid. (188 g, 79%). ^{1}H-NMR (400MHz, CDCl$_3$) δ: 1.41 (t, 3H, J = 7.16 Hz), 2.84 (s, 3H), 4.43 (q, 2H, J = 7.16 Hz), 8.48 (s, 1H), 9.23 (s, 1H). m/z (ES$^+$) (M+H)$^+$: 191 for C$_{10}$H$_{10}$N$_2$O$_2$.

5-Hydroxymethyl-2-methyl-nicotinonitrile (32-iv)

A solution of **32-iii** (29 g, 0.1517 moles) in dry THF (300 mL) was added dropwise to a suspension of lithium aluminum hydride (5.75 g, 0.1517 moles) in dry THF (300 mL) at -78° C. The progress of the reaction was monitored by TLC. After 1 hour and 45 minutes, the reaction mixture was quenched with water, 10% NaOH and water (1:1:3). The solid was filtered and washed with ethyl acetate. The combined filtrates were concentrated and the residue was purified by column chromatography using pet. ether /ethyl acetate (1 : 1) to obtain **32-iv** as light yellow solid. This reaction was done in batches (6 x 29 g) and the crude material from these six batches were purified together to afford compound **32-iv**. (30 g, 22%). ^{1}H-NMR (400MHz, DMSO) δ 2.65 (s, 3H), 4.55 (d, 2H, J = 5.68 Hz), 5.47 (t, 1H, J = 5.68 Hz), 8.10 (s, 1H), 8.66 (s, 1H). m/z (ES$^+$) (M+H)$^+$: 149 for C$_8$H$_8$N$_2$O.

(5-Cyano-6-methylpyridin-3-yl) methyl methanesulfonate (32)

In a 100mL round-bottomed flask **32-iv** (6 g, 40.50 mmol) and Triethylamine (16.93 mL, 121.49 mmol) were taken in DCM (150 mL) under N2. The RM was then cooled with ice and then Methanesulfonyl chloride (4.70 mL, 60.74 mmol) was added dropwise to RM. The RM was stirred at cold for 1 hr. The RM was then diltued wth DCM and was washed with water. The organic layer was dried and evaporated to get a residue as **32** (8.40 g, 92 %). It was not purified and taken for next step as such. m/z (ES$^+$), (M+H)$^+$ = 227 for C$_9$H$_{10}$N$_2$O$_3$S.

5-Cyano-6-methylnicotinic acid (33)

In a 50 ml RBF, **32-iii** (0.7 g, 3.68 mmol) was taken in THF (8 ml), methanol (2.000 ml), water (1.000 ml). Slowly Lithium hydroxide (0.881 g, 36.80 mmol) was added to the RM. The RM was heated to 60°C for 2 hrs. RM was evaporated and taken in little amount of water. The aqueous layer was acidified with dil. HCl, the solid obtained was filtered to get **33** (0.300 g, 50.3 %). m/z (ES-), (M-H)$^-$ = 161.09 for $C_8H_6N_2O_2$

34-i   a →   **34-ii**   b →   **34**
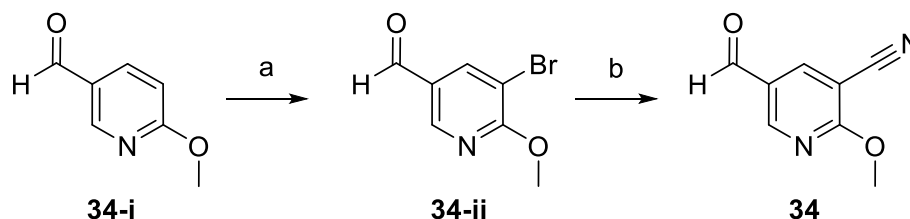
Reagents: (a) CH$_3$COONa, Br$_2$, AcOH, 90 °C, 30% (b) Pd$_2$(dba)$_3$, dppf, CuCN, DMF, 110 °C, 40 %

5-Bromo-6-methoxynicotinaldehyde (34-ii)

To a mixture of **34-i** (2 g, 14.58 mmol) and sodium acetate (2.393 g, 29.17 mmol) in AcOH (10 mL) was added a solution of bromine (1.127 mL, 21.88 mmol)in AcOH (10 mL) over 30 mins via an additional funnel. The mixture was heated to 90 °C for 5h, cooled to rt. The reaction was added ice water, neutralized to pH = 7.5 with aqueous NaOH (5 N), extracted with ethyl acetate, washed with brine, dried over Na$_2$SO$_4$, filtered and concentrated. The residue was purified via flash column using dichloromethane as an eluent. Pure fractions were collected and concentrated to give **34-ii** (1.000 g, 31.7 %). ^{1}H NMR (300 MHz, CDCl$_3$) δ 4.17 (s, 3H), 8.35 (s, 1H), 8.6 (s, 1H), 9.97 (s, 1H)

5-Formyl-2-methoxynicotinonitrile (34)

In a 50ml reaction RB flask **34-ii** (.100 g, 0.46 mmol), dppf (0.103 g, 0.19 mmol), Pd$_2$(dba)$_3$ (0.085 g, 0.09 mmol) and CuCN (0.187 g, 2.08 mmol) was taken in DMF (20 mL) under N2. A resulting reaction mixture was stirred at 110 °C for 12 hrs. Reaction was cooled to RT, and passed through celite and washed with 5% methanol in DCM. Obtained filtered was concentrated and purified using EtOAc and hexane as a mobile phase to obtain product **34** (0.030 g, 40.0 %).^{1}H NMR (300 MHz, CDCl$_3$) δ 4.11 (s, 3 H) 8.30 (d, J=2.26 Hz, 1 H) 8.75 (d, J=2.07 Hz, 1 H) 9.92 (s, 1 H)

Synthetic schemes and procedures for synthesis LHS and linker fragments

7-Fluoro-1-(2-hydroxyethyl)-1,5-naphthyridin-2(1H)-one (28b-i)

In a 250 mL round-bottomed flask **24b** (10 g, 60.92 mmol) and Cesium carbonate (23.82 g, 73.11 mmol) were taken in DMSO (50 mL) to get a suspension. The suspension was then stirred at RT for 10 mins. Then to this 2-bromoethanol (6.02 mL, 85.29 mmol) was added drop wise through a dropping funnel over a period of 15 minutes. The resulting reaction mixture was heated to 90 °C overnight. Water was added to the reaction mixture and this was extracted using ethylacetate. The organic layer was washed with water, dried over sodium sulphate and concentrated under vacuum to obtain crude solid. The crude product was purified on silica with DCM/MeOH. Title compound eluted out between 3% -5% MeOH in DCM. Pure fractions were pooled and concentrated to obtain **28b-i** (9.10 g, 71.7 %) as off white solid. m/z (ES$^+$), (M+H)$^+$ = 209.19 for $C_{10}H_9FN_2O_2$

2-(7-Fluoro-2-oxo-1,5-naphthyridin-1(2H)-yl)ethyl methanesulfonate (28b)

In a 100mL round-bottomed flask **28b-i** (300 mg, 1.44 mmol) and Triethylamine (0.603 mL, 4.32 mmol) were taken in DCM (4 mL) under N2. The RM was then cooled with ice and then Methanesulfonyl chloride (0.167 mL, 2.16 mmol) was added dropwise to RM. The RM was stirred at cold for 30 mins. Solid precipitated out in the RM was then filtered, dried to obtain **28b** (412 mg, 100 %). m/z (ES$^+$), (M+H)$^+$ = 287.16 for $C_{11}H_{11}FN_2O_4S$.

1-(2-Hydroxyethyl)-7-methoxy-1,5-naphthyridin-2(1H)-one (28c-i)

In a 100 mL round-bottomed flask, **28b-i** (3.50 g, 16.81 mmol) was taken in MeOH (30 mL) to give a yellow solution. To it was added sodium methoxide (3.63 g, 67.25 mmol) and heated to 75 °C for 2 hrs. Solvent was evaporated from the reaction mixture, water was added to it. Solid precipitated out was filtered, washed with water and Hexane to obtain **28c-i** (3.00 g, 81 %) as white solid. m/z (ES$^+$), (M+H)$^+$ = 221.26 for $C_{11}H_{12}N_2O_3$

2-(7-Methoxy-2-oxo-1,5-naphthyridin-1(2H)-yl)ethyl methanesulfonate (28c)

In 100 mL round-bottomed flask, **28c-i** (1.100 g, 4.99 mmol) and TEA (2.089 mL, 14.98 mmol) were taken in DCM (20 mL) under nitrogen atmosphere to give a white suspension. The

resulting reaction mass was cooled to 0°C and Methanesulfonyl chloride (0.467 mL, 5.99 mmol) was added to it very slowly. Then the RM was stirred at 0°C for 45 mins. Solid precipitated out from RM was filtered, washed with little DCM and dried to obtain **28c** (1.800 g, 121 %) as white solid. m/z (ES+), $(M+H)^+ = 229$ for $C_{12}H_{14}N_2O_5S$

29a-i: R3= F, cis, 3S4R
29c-i: R3= F, cis, 3R4S
29e-i: R3= H

29a-ii: R3= F, cis, 3S4R, R5= RHS 1
29b-ii: R3= F, cis, 3S4R, R5= RHS 2
29c-ii: R3= F, cis, 3R4S, R5= RHS 2
29e-ii: R3= H, R5= RHS 1

29a: R3= F, cis, 3S4R, R5= RHS 1
29b: R3= F, cis, 3S4R, R5= RHS 2
29c: R3= F, cis, 3R4S, R5= RHS 2
29e: R3= H, R5= RHS 1
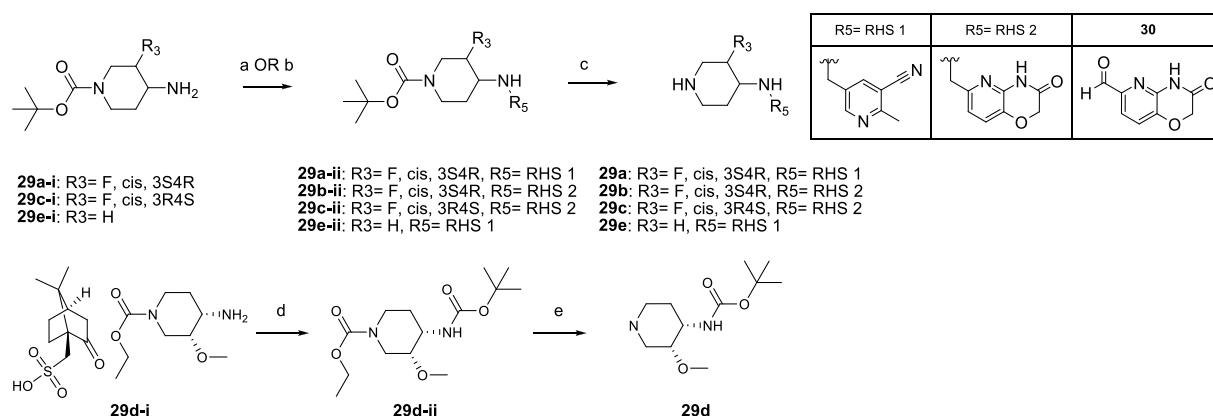
Reagents: (a) **32**, Na$_2$CO$_3$, DMF, 70°C, 30% (b) **30**, NaBH$_3$CN, DIPEA, DCE/EtOH, 80 °C 40 % (c) 4N HCl in Dioxane, 80 °C or TFA/DCM, 55 °C (d) Boc$_2$O, TEA, DCM, RT, 93% (e) NaOH, EtOH/Water, 80 °C, > 95%

Figure 4.10: Synthetic scheme utilised for synthesis of linker fragment.

(3S, 4R)-*Tert*-butyl 4-((5-cyano-6-methylpyridin-3-yl)methylamino)-3-fluoropiperidine-1-carboxylate (29a-ii)

In a 50 mL round-bottomed flask, (3S, 4R)-tert-butyl 4-amino-3-fluoropiperidine-1-carboxylate, **29a-i** (1.200 g, 5.50 mmol) and Na$_2$CO$_3$ (1.748 g, 16.49 mmol) were taken in DMF (20 mL) and stirred at room temperature for 5 mins. Then **32** (1.493 g, 6.60 mmol) was added and the resulting RM was heated to 70 °C for 2 hours. DMF was evaporated from the RM and the residue obtained was triturated with sodium bicarbonate solution and extracted using 5% Methanol in DCM (2X25ml). The combined organic fractions were concentrated to dryness and purified with DCM/MeOH on silica to get **29a-ii** (0.550 g, 28.7 %). m/z (ES$^+$), (M-tBu)$^+$ = 293.32 for $C_{18}H_{25}FN_4O_2$

5-(((3S, 4R)-3-Fluoropiperidin-4-ylamino)methyl)-2-methylnicotinonitrile (29a)

In a 100ml RB flask **29a-ii** (4.00 g, 11.48 mmol) was dissolved in DCM (15.00 mL) and TFA (15 mL) and stirred at 50°C for 1 hour. The solvent was evaporated under vacuum and co-evaporated with toluene to get the crude product **29a** (6.55 g, 97 %), as TFA salt which was taken for further step without purification. m/z (ES$^+$), (M+H)$^+$ = 249.33 for C$_{13}$H$_{17}$FN$_4$. [TFA]

(3S, 4R)-*Tert*-butyl 3-fluoro-4-((3-oxo-3,4-dihydro-2H-pyrido[3,2-b][1,4]oxazin-6-yl)methylamino)piperidine-1-carboxylate (29b-ii)

In a 250 mL round-bottomed flask, (3S, 4R)-tert-butyl 4-amino-3-fluoropiperidine-1-carboxylate, **29a-i** (1.225 g, 5.61 mmol), **30** (1.000 g, 5.61 mmol) were taken in EtOH (20 mL) and CHCl$_3$ (20.00 mL). Acetic acid (0.321 mL, 5.61 mmol) was added and the resulting RM was heated to 70 °C for 1 hour. Then, the reaction mass was cooled to RT and sodium cyanoborohydride (1.058 g, 16.84 mmol) was added to it. This reaction mass was heated at 70 °C overnight. Solvent was evaporated from the reaction mixture and water was added to it. This was basified using dilute sodium hydroxide solution to pH~8. This was extracted using 5% Methanol in DCM (5X50ml). The combined organic layers were concentrated to dryness and purified by silica gel chromatography with 0 to 7% Methanol in DCM to obtain **29b-ii** (2.200 g, 103 %) as light yellow gel. m/z (ES$^+$), (M+H)$^+$ = 381.44 for C$_{18}$H$_{25}$FN$_4$O$_4$

6-(((3S, 4R)-3-Fluoropiperidin-4-ylamino)methyl)-2H-pyrido[3,2-b][1,4]oxazin-3(4H)-one (29b)

In a 100 mL round-bottomed flask, **29b-ii** (2.100 g, 5.52 mmol) and TFA (0.425 mL, 5.52 mmol) were taken to give a yellowish solution. The resulting reaction mixture was stirred at 55 °C for 1 hr. The reaction mass was concentrated to dryness. The residue was co-evaporated with toulene thrice to obtain TFA salt of **29b** (1.400 g, 90 %) as yellow gel and directly used for the next step. m/z (ES$^+$), (M+H)+ = 281.32 for C$_{13}$H$_{17}$FN$_4$O$_2$.[TFA]

(3R, 4S)-*Tert*-butyl 3-fluoro-4-((3-oxo-3,4-dihydro-2H-pyrido[3,2-b][1,4]oxazin-6-yl)methylamino)piperidine-1-carboxylate (29c-ii)

In a 250 ml RB flask **29c-i** (3.68 g, 8.42 mmol) and **30** (1.500 g, 8.42 mmol) was dissolved in 1,2-dichloroethane (50 mL) and ethanol (10.00 mL). To this acetic acid (0.289 mL, 5.05 mmol) was added and stirred and then heated to 70°C for 2 hr and then sodium triacetoxyborohydride (4.46 g, 21.05 mmol) was added at RT and stirred for overnight. Reaction mixture was concentrated and basified with saturated sodium bicarbonate solution and extracted with 10% MeOH/DCM and the solvent was evaporated under vacuum and the

crude compound was purified on silica with DCM/MeOH to get **29c-ii** (2.80 g, 87 %). m/z (ES$^+$), (M+H)$^+$ = 381.44 for C$_{18}$H$_{25}$FN$_4$O$_4$

6-(((3R, 4S)-3-Fluoropiperidin-4-ylamino)methyl)-2H-pyrido[3,2-b][1,4]oxazin-3(4H)-one (29c)

In a 100ml RB flask **29c-ii** (2.80 g, 7.36 mmol) was dissolved in DCM (15.00 mL) and TFA (15 mL) and stirred at 50°C for 1 hour. The solvent was evaporated under vacuum and co-evaporated with toluene to get the crude product as TFA salt of **29c** (4.50 g, 98 %) which was taken for further step without purification. m/z (ES$^+$), (M+H)$^+$ = 281.32 for C$_{13}$H$_{17}$FN$_4$O$_2$.[TFA]

(3S, 4R)-Ethyl 4-(tert-butoxycarbonylamino)-3-methoxypiperidine-1-carboxylate (29d-ii)

In a 500 mL round-bottomed flask, (3S,4R)-ethyl 4-amino-3-methoxypiperidine-1-carboxylate ((1S,4R)-7,7-dimethyl-2-oxobicyclo[2.2.1]heptan-1-yl)methanesulfonate **29d-i** [1] (10.00 g, 23.01 mmol) was taken in DCM (250 mL) to give a colourless solution. To it was added TEA (9.62 mL, 69.04 mmol), followed by slow addition of di-tert-butyl dicarbonate (5.61 mL, 24.16 mmol) in DCM (25ml). The resulting reaction mixture was stirred at room temperature overnight. The RM was thoroughly washed with water (5X 100ml). Then, it was dried over sodium sulfate and concentrated under vaccum to give **29d-ii** (6.50 g, 93 %) as white solid. m/z (ES$^+$), (M-tBu)$^+$ = 247.27 for C$_{14}$H$_{26}$N$_2$O$_5$.

Tert-butyl (3S, 4R)-3-methoxypiperidin-4-ylcarbamate (29d)

In a 100ml RB flask **29d-ii** (32.2 g, 106.49 mmol) was dissolved in ethanol (200 mL)/ water (100 mL) and NaOH (42.6 g, 1064.93 mmol) in water (10 mL) was added to it. The resulting reaction mass was heated to 90°C overnight. Solvent was evaporated from the reaction mixture. The pH was adjusted to ~9 using 6N HCl. The mix was extracted using 10% Methanol in DCM (5X50ml). The combined organic fractions were concentrated to dryness to obtain **29d** (22.00 g, 90 %) as colourless gel. m/z (ES$^+$), (M+H)$^+$ = 231.36 for C$_{11}$H$_{22}$N$_2$O$_3$.

Tert-butyl 4-((5-cyano-6-methylpyridin-3-yl)methylamino)piperidine-1-carboxylate (29e-ii)

In a 100 mL round-bottomed flask, tert-butyl 4-aminopiperidine-1-carboxylate (1.000 g, 4.99 mmol), **32** (1.186 g, 5.24 mmol) and Na$_2$CO$_3$ (1.588 g, 14.98 mmol) were taken in DMF (10

mL) and the resulting reaction mixture was heated to 70 °C for 1 hour. DMF was evaporated from the reaction mixture and water was added to it. This was extracted using 5% Methanol in DCM (3X 25ml). The combined organic layers were concentrated to dryness and purified by silica gel chromatography to obtain **29e-ii** (1.500 g, 91 %) as yellow gel. m/z (ES$^+$), (M+H)$^+$ = 331.40 for $C_{18}H_{26}N_4O_2$.

2-Methyl-5-((piperidin-4-ylamino)methyl)nicotinonitrile (29e)

In a 50 mL round-bottomed flask, **29e-ii** (1.500 g, 4.54 mmol) and 4N HCL in Dioxane (10 ml, 329.12 mmol) were taken to give a yellowish solution. The resulting reaction mixture was stirred at 55 °C for 1 hr. The reaction mass was concentrated to dryness. This hydrochloride salt was washed with ethyl acetate. Then it was cooled to 5-10°C and basified using sodium hydroxide solution. This was extracted using 10% methanol in DCM (3 X 25ml). The combined organic layers was concentrated to dryness to obtain **29e** (0.862 g, 82 %) as yellow gel. m/z (ES$^+$), (M+H)$^+$ = 231.34 for $C_{13}H_{18}N_4$.

Tert-butyl (3S, 4R)-3-methoxy-1-(2-(7-methoxy-2-oxo-1,5-naphthyridin-1(2H)-yl)ethyl)piperidin-4-ylcarbamate (18a)

In a 100 ml RB flask **29d** (300 mg, 1.30 mmol) was dissolved in DMF (30mL) and then Na_2CO_3 (681 mg, 6.42 mmol) followed by **28c** (389 mg, 1.30 mmol) was added and heated to 70°C for 2 hours. Reaction mixture was concentrated under vacuum and the residue basified with saturated $NaHCO_3$ solution and concentrated under vacuum and it was purified by column chromatography to get **18a** (250 mg, 44.4 %). m/z (ES$^+$), (M+H)$^+$ = 433.37 for $C_{22}H_{32}N_4O_5$.

1-(2-((3S, 4R)-4-Amino-3-methoxypiperidin-1-yl)ethyl)-7-methoxy-1,5-naphthyridin-2(1H)-one (18b)

In a 50 mL round-bottomed flask, **18a** (250 mg, 0.58 mmol)was dissolved in 4N HCl in dioxane (10 mL) and the resulting reaction mixture was stirred at 55 °C for 1 hr. The reaction mass was concentrated and basified using aqueous sodium hydroxide solution. This was extracted using 10% methanol in DCM (2 X 50ml). The combined organic layers was concentrated to dryness to obtain **18b** (170 mg, 88 %). m/z (ES$^+$), (M+H)$^+$ = 333.29 for $C_{17}H_{24}N_4O_3$.

6-(((3R, 4S)-3-Fluoro-1-(2-(7-methoxy-2-oxo-1,5-naphthyridin-1(2H)-yl)ethyl)piperidin-4-ylamino)methyl)-2H-pyrido[3,2-b][1,4]oxazin-3(4H)-one (22a)

In a 250 ml RB flask **29c** (3.50 g, 12.49 mmol) was dissolved in DMF (50mL) and Na_2CO_3 (3.97 g, 37.46 mmol) was added and stirred for 2 minutes and then **28b** (4.29 g, 14.98 mmol) was added and heated to 70°C for 2 hours. Reaction mixture was concentrated under vacuum and the residue basified with saturated $NaHCO_3$ solution and concentrated under vacuum and it was purified by reverse phase preparative HPLC to get **22a** (2.90 g, 49.4 %). m/z (ES+), (M+H)+ = 471.44 for $C_{23}H_{24}F_2N_6O_3$.

Tert-butyl (3S, 4R)-1-(2-(7-fluoro-2-oxo-1,5-naphthyridin-1(2H)-yl)ethyl)-3-methoxypiperidin-4-ylcarbamate (23a)

In a 250 mL round-bottomed flask, **28b** (7.93 g, 27.70 mmol), **29d** (5.80 g, 25.18 mmol) and Na_2CO_3 (5.34 g, 50.37 mmol) were taken in DMF (50 mL) to give a yellowish solution under nitrogen atmosphere and heated to 70 °C for 1hr. Solvent was evaporated from the reaction mixture. Water was added to it and extracted using 10% methanol in DCM (3 X 100ml). The combined organic layers were concentrated to dryness and purified by silica gel chromatography using 0 to 9% Methanol in DCM to obtain **23a** (9.90 g, 93 %) as yellow gel. m/z (ES$^+$), (M+H)$^+$ = 421.51 for $C_{21}H_{29}FN_4O_4$.

1-(2-((3S, 4R)-4-Amino-3-methoxypiperidin-1-yl)ethyl)-7-fluoro-1,5-naphthyridin-2(1H)-one (23b)

In a 100 mL round-bottomed flask, **23a** (7.60 g, 18.07 mmol) and 4N HCL in Dioxane (25 ml, 822.80 mmol) were taken to give a yellowish solution. The resulting reaction mixture was stirred at 55 °C for 1 hr. The reaction mass was concentrated to dryness. This hydrochloride salt was washed with ethyl acetate. Then it was cooled to 5-10°C and basified using sodium hydroxide solution. This was extracted using 10% methanol in DCM (3 X 75ml). The combined organic layers was concentrated to dryness to obtain **23b** (4.60 g, 79 %) as yellow gel. m/z (ES+), (M+H)+ = 321.43 for $C_{16}H_{21}FN_4O_2$.

6-(((3S, 4R)-1-(2-(7-Fluoro-2-oxo-1,5-naphthyridin-1(2H)-yl)ethyl)-3-methoxypiperidin-4-ylamino)methyl)-2H-pyrido[3,2-b][1,4]oxazin-3(4H)-one (23c)

In a 250 mL round-bottomed flask, **23b** (3.50 g, 10.93 mmol), **30** (1.946 g, 10.93 mmol) were taken in EtOH (50 mL) and CHCl3 (50.0 mL). Acetic acid (0.625 mL, 10.93 mmol) was added and the resulting reaction miture was heated to 70 °C for 1 hour. Then, the reaction mass was cooled to RT and sodium cyanoborohydride (2.060 g, 32.78 mmol) was added to it. This reaction mass was heated at 70 °C for 2 hrs. Solvent was evaporated from the reaction mixture

and water was added to it. This was basified using dilute sodium hydroxide to pH~8. This was extracted using 5% Methanol in DCM (5X25ml). The combined organic layers were concentrated to dryness and purified by silica gel chromatography using 1 to 12% methanol in DCM to obtain **23c** (3.40 g, 64.5 %) as off white solid. ^{1}H NMR (300 MHz, DMSO-d_6) δ 1.35 - 1.51 (m, 1 H) 1.52 - 1.68 (m, 1 H) 2.12 - 2.37 (m, 2 H) 2.52 (t, J=6.12 Hz, 2 H) 2.60 - 2.91 (m, 2 H) 3.09 (s, 3 H) 3.58 - 3.78 (m, 2 H) 4.16 - 4.37 (m, 2 H) 4.56 (s, 2 H) 6.77 (d, J=9.80 Hz, 1 H) 6.96 (d, J=8.10 Hz, 1 H) 7.26 (d, J=7.91 Hz, 1 H) 7.89 (d, J=9.80 Hz, 1 H) 7.98 (dd, J=11.11, 2.07 Hz, 1 H) 8.50 (d, J=2.26 Hz, 1 H) 11.17 (s, 1 H). m/z (ES$^+$), (M+H)$^+$ = 483.51 for $C_{24}H_{27}FN_6O_4$.

4.2.3 Synthesis of N-linked quinolones and napthyridones with indole, benzimidazoles and oxindole RHS

2a: R1= F,Y=N,X=CH
2b: R1=OCH₃,Y=CH, X=N
2c: R1=OCH₃,Y=N,X=N

3a: R1= F,Y=N,X=CH
3b: R1=OCH₃,Y=N,X=CH
3c: R1=OCH₃,Y=CH, X=N
3d: R1=OCH₃,Y=N,X=N

4a: R1= F,Y=N,X=CH
4b: R1=OCH₃,Y=N,X=CH
4c: R1=OCH₃,Y=CH,X=N
4d: R1=OCH₃,Y=N,X=N

5a: R2=CF₃,R3=H
5b: R2=Cl,R3=H
5c R2=CN,R3=H
5d: R2=Cl,R3=F
5e; R2=Cl,R3=CH₃
5f: R2=CN,R3=CH₃

6a: R2=CF₃,R3=H
6b: R2=Cl,R3=H
6c: R2=CN,R3=H
6d: R2=Cl,R3=F
6e R2=Cl,R3=CH₃
6f: R2=CN,R3=CH₃

7a-f

4a-d

7a-f

BI_1, BI_5 to 15
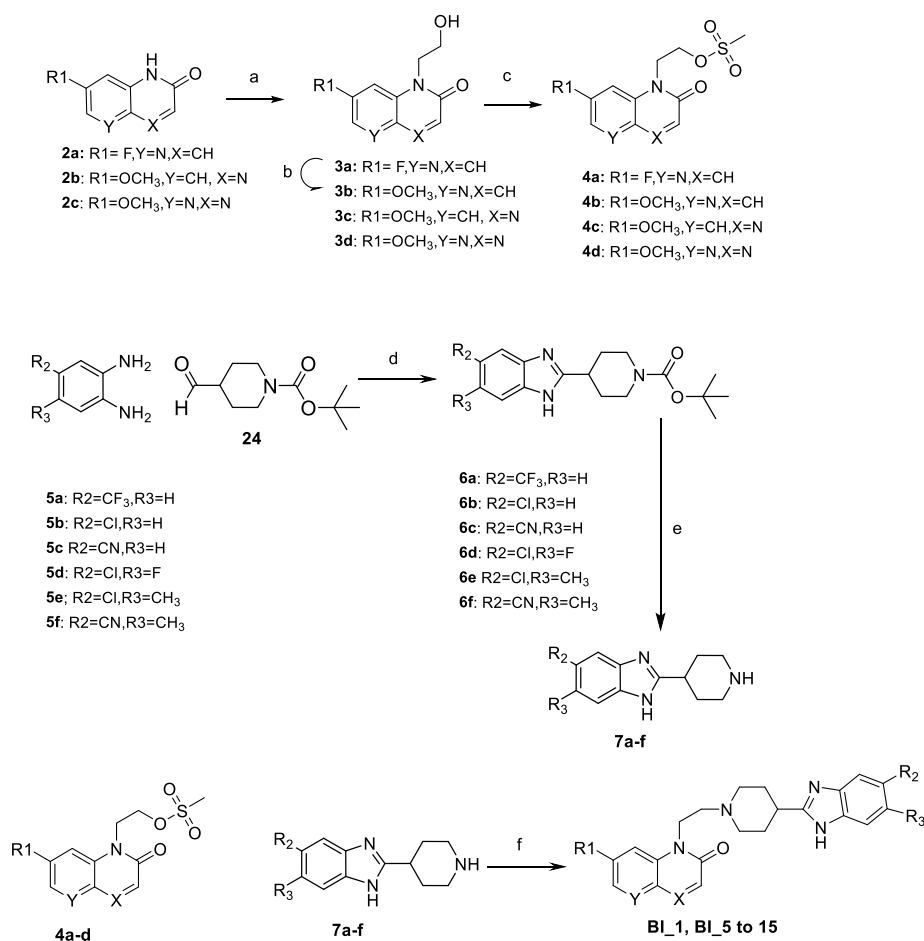
Reagents (a) CsCO₃, DMSO, 90 ºC; (b) NaOMe, MeOH, 75 ºC; c) Mesyl chloride, DIPIEA, DCM, 0 ºC; (d) PTSA, Ethanol, 90 ºC; (e) 4N HCl in Dioxane, 50 ºC; (f) Na₂CO₃, DMF, 130 ºC

Figure 4.11: Synthetic scheme utilised for synthesis of compounds with piperidinyl benzimidazoles RHS

7-Fluoro-1,5-naphthyridin-2(1H)-one (2a)

In 100ml RB flask, Butyl acrylate (45.0 ml, 314.13 mmol), 2-bromo-5-fluoropyridin-3-amine (60g, 314.13 mmol), Pd(OAc)$_2$ (1.411 g, 6.28 mmol), P(t-Bu)$_3$ (3.64 g, 12.57 mmol), N-Methyldicyclohexylamine (202 ml, 942.40 mmol) was taken in Cumene (189 g, 1570.67 mmol). Reaction mixture was heated to 150 °C for overnight. RM was diluted with diethyl ether and solid obtained was filtered. The solid was suspended in water and filtered to get **2a** (45.0 g, 87 %). ^{1}H NMR (300 MHz, DMSO-d_6) δ 6.71 (d, 1H), 7.47 (dd, 1H), 7.94 (d, 1H), 8.49 (d, 1H), 11.95 (bs, 1H). m/z (ES$^-$), (M-H)$^-$ = 163.12 for C$_8$H$_5$FN$_2$O.

7-Methoxypyrido[3,2-b]pyrazin-2(1H)-one (2b)

7-Fluoropyrido (2, 3-b) pyrazin-2(1H)-one

A solution of 5-fluoro-2,3-pyridinediamine (12g, 0.0944 moles) and glyoxylic acid monohydrate (13.02 g, 0.141 moles) in EtOH (100 mL) was stirred at RT for 12 hrs and the precipitated solid was filtered to afford grey solid as a mixture of two isomers 7-fluoropyrido[3,2-b]pyrazin-2(1H)-one compound with 7-fluoropyrido[3,2-b]pyrazin-3(4H)-one (1:1) **.** Crude yield : 12g (76%). This crude was taken as such for next step without purification. m/z (ES$^+$) (M+H)$^+$: 166.2 for C$_7$H$_4$FN$_3$O

7-Methoxypyrido[3,2-b]pyrazin-2(1H)-one (2b)

To a solution of 7-fluoropyrido[3,2-b]pyrazin-2(1H)-one compound with 7-fluoropyrido[3,2-b]pyrazin-3(4H)-one (1:1), (12 g, 0.0722 moles) in methanol (100 mL), sodium methoxide (19.51 g, 0.361 moles) was added and heated to 100° C in a sealed tube for 12 hrs. The reaction mixture was cooled to room temperature and poured into 500g of ice-water. The pH of the reaction mixture brought to 2-3 using 6N HCl solution. The precipitated solid was filtered, dried and the crude product was triturated with hot DMSO (3 volumes), filtered and washed with ethyl acetate to afford **2b** (6.2 g). ^{1}H NMR (400 MHz, DMSO- d_6) δ 3.90 (s, 3H), 7.12 (s, 1H), 8.15 (s, 1H), 8.25 (s, 1H), 12.48 (s, 1H). m/z (ES$^+$), (M+H)$^+$: 178 for C$_8$H$_7$N$_3$O

7-Fluoro-1-(2-hydroxyethyl)-1,5-naphthyridin-2(1H)-one (3a)

In a 250 mL round-bottomed flask **2a** (10 g, 60.92 mmol) and Cesium carbonate (23.82 g, 73.11 mmol) were taken in DMSO (50 mL) to get a suspension. The suspension was then stirred at RT for 10 mins. Then to this 2-bromoethanol (6.02 mL, 85.29 mmol) was added drop wise through a dropping funnel over a period of 15 minutes. The resulting reaction mixture was heated to 90 °C overnight.Water was added to the reaction mixture and this was extracted using ethylacetate. The organic layer was washed with water, dried over sodium sulphate and concentrated under vacuum to obtain crude solid. The crude product was purified on silica with DCM/MeOH. Title compound eluted out between 3% -5% MeOH in DCM. Pure fractions were pooled and concentrated to obtain 3a (9.10 g, 71.7 %) as off white solid. m/z (ES$^+$), (M+H)$^+$ = 209.19 for $C_{10}H_9FN_2O_2$

1-(2-Hydroxyethyl)-7-methoxy-1,5-naphthyridin-2(1H)-one (3b)

In a 100 mL round-bottomed flask, **28b-i** (3.50 g, 16.81 mmol) was taken in MeOH (30 mL) to give a yellow solution.To it was added sodium methoxide (3.63 g, 67.25 mmol) and heated to 75 °C for 2 hrs. Solvent was evaporated from the reaction mixture, water was added to it. Solid precipitated out was filtered, washed with water and Hexane to obtain **28c-i** (3.00 g, 81 %) as white solid. m/z (ES$^+$), (M+H)$^+$ = 221.26 for $C_{11}H_{12}N_2O_3$

1-(2-Hydroxyethyl)-7-methoxypyrido[2,3-b]pyrazin-2(1H)-one (3c)

Intermediate **3c** was prepared from 7-methoxypyrido[3,2-b]pyrazin-2(1H)-one **(2b)** and 2-bromoethanol using procedure analogous to **intermediate 3a**

m/z (ES$^+$), (M+H)$^+$ = 222.22 for $C_{10}H_{11}N_3O_3$

1-(2-Hydroxyethyl)-7-methoxy quinazolin-2(1H)-one (3d)

Intermediate **3d** f was prepared from 7-methoxy quinazolin-2(1H)-one **(2c,** Activate scientific) and 2-bromoethanol using procedure analogous to **intermediate 3a**

1H NMR (300 MHz, DMSO-d$_6$) δ 3.68 (q, *J*=6.03 Hz, 2 H) 4.28 (t, *J*=6.03 Hz, 2 H) 4.92 (t, *J*=6.03 Hz, 1 H) 6.98 (dd, *J*=8.85, 2.45 Hz, 1 H) 7.12 (d, *J*=2.45 Hz, 1 H) 7.72 (d, *J*=8.85 Hz, 1 H) 8.03 (s, 1 H). m/z (ES+), (M+H)+ : 221 for $C_{11}H_{12}N_2O_3$

2-(7-Fluoro-2-oxo-1,5-naphthyridin-1(2H)-yl)ethyl methanesulfonate (4a)

In a 100mL round-bottomed flask **28b-i** (300 mg, 1.44 mmol) and Triethylamine (0.603 mL, 4.32 mmol) were taken in DCM (4 mL) under N2. The RM was then cooled with ice and then Methanesulfonyl chloride (0.167 mL, 2.16 mmol) was added dropwise to RM. The RM was stirred at cold for 30 mins. Solid precipitated out in the RM was then filtered, dried to obtain **28b** (412 mg, 100 %). m/z (ES$^+$), (M+H)$^+$ = 287.16 for $C_{11}H_{11}FN_2O_4S$.

2-(7-Methoxy-2-oxo-1, 5-naphthyridin-1(2H)-yl)ethyl methanesulfonate (4b)

In 100 mL round-bottomed flask, **3b** (1.100 g, 4.99 mmol) and TEA (2.089 mL, 14.98 mmol) were taken in DCM (20 mL) under nitrogen atmosphere to give a white suspension. The resulting reaction mass was cooled to 0°C and methanesulfonyl chloride (0.467 mL, 5.99 mmol) was added to it very slowly. Then the RM was stirred at 0°C for 45 mins. Solid precipitated out from RM was filtered, washed with little DCM and dried to obtain **4b** (1.800 g, 121 %) as white solid. m/z (ES$^+$), (M+H)$^+$ = 299 for $C_{12}H_{14}N_2O_5S$.

2-(7-Methoxy-2-oxopyrido[2,3-b]pyrazin-1(2H)-yl)ethyl methanesulfonate (4c)

Intermediate 4c was prepared from **intermediate 3c** using procedure analogous to **intermediate 4a**

m/z (ES$^+$), (M+H)$^+$ = 300 for $C_{11}H_{13}N_3O_5S$.

2-(7-Methoxy-2-oxoquinoxalin-1(2H)-yl)ethyl methanesulfonate (4d):

Intermediate 4d was prepared from **intermediate 3d** using procedure analogous to **intermediate 4a**

m/z (ES$^+$), (M+H)$^+$ = 299 for $C_{12}H_{14}N_2O_5S$.

General proecedures for synthesis of intermediates 5a-f

In a 50 mL round-bottomed flask, substituted benzene-1,2-diamine(5a-5f) (2 mmol)was taken in ethanol (10 mL)added to give a brown solution. To it was added tert-butyl 4-formylpiperidine-1-carboxylate (427 mg, 2 mmol)and catalytic amount of para toluene solphonic acid. Resulting reaction mass was heated to 95 °C for overnight and the reaction was monitored by LCMS, which indicated required product formation.

Ethanol from the reaction mixture was evaporated and the residue adsorbed on slicagel. The crude product was purified by flash column chromatography using hexane and ethylacetate as

eluent.The pruduct was eluted from column at 70% ethyl acetate in hexane. The fraction were pooled and concentrated under vacum afforded pure products (**6a-f**).

Substituted benzene-1, 2- diamines (**5a-f**) from commercial sources were used for the preparation intermediate **6a-f**

Tert-butyl 4-(5-(trifluoromethyl)-1H-benzo[d]imidazol-2-yl)piperidine-1-carboxylate(6a)

Yield: 320 mg, 43.3 %; ^{1}H NMR (300 MHz, DMSO-d_6) δ 1.42 (s, 9 H), 1.58 - 1.78 (m, 2 H), 2.01 (d, J = 9.98 Hz, 2 H), 2.93 (br. s., 2 H), 3.04 - 3.20 (m, 1 H), 4.01 (d, J =13.00 Hz, 2 H), 7.35 - 7.52 (m, 1 H), 7.62 (d, J = 8.48 Hz, 1 H), 7.67 - 7.82 (m, 1 H), 7.90 (s, 1 H), 12.68 (s, 1 H). m/z (ES[+]), (M+H)[+] : 370.69 for $C_{18}H_{22}F_3N_3O_2$

Tert-butyl 4-(5-chloro-1H-benzo[d]imidazol-2-yl)piperidine-1-carboxylate (6b)

Yield: 276 mg, 40.9 %; 1H NMR (300 MHz, DMSO-d_6) δ 1.41 (s, 9 H), 1.57 - 1.80 (m, 2 H), 2.02(d, J = 9.98 Hz, 2 H), 2.93 (br. s., 2 H), 3.03 - 3.19 (m, 1 H), 4.03 (d, J =13.00 Hz, 2 H), 7.41 - 7.53 (m, 1 H), 7.62 (d, J = 8.48 Hz, 1 H), 7.67 - 7.82 (m, 1 H), 7.90 (s, 1 H), 12.70 (s, 1 H). m/z (ES[+]), (M+H)[+] : 336.33 for $C_{17}H_{22}ClN_3O_2$.

Tert-butyl 4-(5-cyano-1H-benzo[d]imidazol-2-yl)piperidine-1-carboxylate (6c)

Yield: 160mg, 25 %; ^{1}H NMR (DMSO-d_6 ,300MHz): δ1.43 (s, 9H), 1.59 - 1.78 (m, 2H), 1.95 - 2.07 (m, 2H), 2.94 (br. s., 2H), 3.05 - 3.20 (m, 1H), 4.02 (d, J=7.3 Hz, 2H), 7.54 - 7.77 (m, 2H), 7.97 -8.08 m, 1H), 12.81 (br. s., 1H). m/z (ES[+]), (M+H)[+] : 326.29 for $C_{18}H_{22}N_4O_2$.

Tert-butyl 4-(5-chloro-6-fluoro-1H-benzo[d]imidazol-2-yl)piperidine-1-carboxylate (6d)

Yield: 566mg, 80 %;^{1}H NMR (DMSO-d_6, 300MHz): δ1.47 (s, 9H), 1.54 - 1.77 (m, 2H), 1.88 - 2.11 (m, 2H), 2.92 (br. s., 2H), 3.05 - 3.10 (m, 1H), 3.98-4.02 (d, J=7.2 Hz, 2H), 7.40 - 7.70 (m, 2H), 12.50 (br. s., 1H). m/z (ES+), (M+H)+ : 354.39 for $C_{17}H_{21}FClN_3O_2$.

Tert-butyl 4-(5-chloro-6-methyl-1H-benzo[d]imidazol-2-yl)piperidine-1-carboxylate (6e)

Yield: 420mg, 60 %; ^{1}H NMR (DMSO-d_6 ,300MHz): δ1.48 (s, 9H), 1.55 - 1.75 (m, 2H), 1.90 - 2.03 (m, 2H), 2.39(s,3H), 2.91 (br. s., 2H), 2.97 - 3.10 (m, 1H), 3.98-4.00 (d, J=12.6 Hz, 2H), 7.43 (s, 1H), 7.52(s,1H), 12.24 (br. s., 1H). m/z (ES+), (M+H)+ : 350.36 for $C_{18}H_{24}ClN_3O_2$

***Tert*-butyl 4-(5-cyano-6-methyl-1H-benzo[d]imidazol-2-yl)piperidine-1-carboxylate (6f)**

Yield: 400mg, 58.8 %; ^{1}H NMR (DMSO-d_6 ,300MHz): δ1.43 (s, 9H), 1.61 - 1.72 (m, 2H), 1.95 - 2.01 (m, 2H), 2.54(s,3H), 2.92 (br. s., 2H), 3.08 (t, J=11.4 Hz,1H), 4.00 (d, J=12.81 Hz, 2H), 7.58-7.70(m, 1H), 7.87-7.98(m,1H), 12.60 (br. s., 1H). m/z (ES+), (M+H)+ : 341.29 for $C_{19}H_{24}N_4O_2$

General proecedures for synthesis of intermediates 7a-f

In a 25 mL round-bottomed flask, **intermediate 6a-f** (1mmol) was taken in HCl (4N in Dioxane) (5ml). Reaction mixture was then heated at 60 °C for two hours. The reaction was monitored by LCMS. The profile showed completion of reaction. Reaction mixture was evaporated to dryness under vacuo afford the **intermediate 6a-f** as hydrochloride salt and they were taken for next step without further purification.

2-(Piperidin-4-yl)-5-(trifluoromethyl)-1H-benzo[d]imidazole hydrochloride (7a)

Yield: 260mg, 97 %; m/z (ES$^+$), (M+H)$^+$: 270.2 for $C_{13}H_{14}F_3N_3$

5-Chloro-2-(piperidin-4-yl)-1H-benzo[d]imidazole hydrochloride (7b)

Yield: 240mg, 95 %; m/z (ES$^+$), (M+H)$^+$: 236.22 for $C_{12}H_{14}ClN_3$

2-(Piperidin-4-yl)-1H-benzo[d]imidazole-5-carbonitrile hydrochloride (7c)

Yield: 270mg, 97 %; m/z (ES$^+$), (M+H)$^+$: 227.25 for $C_{13}H_{14}N_4$

5-Chloro-6-fluoro-2-(piperidin-4-yl)-1H-benzo[d]imidazole hydrochloride (7d)

Yield: 255mg, 98 %; m/z (ES$^+$), (M+H)$^+$: 254.13 for $C_{12}H_{13}ClFN_3$

5-Chloro-6-methyl-2-(piperidin-4-yl)-1H-benzo[d]imidazole hydrochloride (7e)

Yield: 245mg, 95 %; m/z (ES$^+$), (M+H)$^+$: 250.27 for $C_{13}H_{16}ClN_3$

6-Methyl-2-(piperidin-4-yl)-1H-benzo[d]imidazole-5-carbonitrile hydrochloride (7f)

Yield: 245mg, 98%; m/z (ES$^+$), (M+H)$^+$: 241.26 for $C_{14}H_{16}N_4$
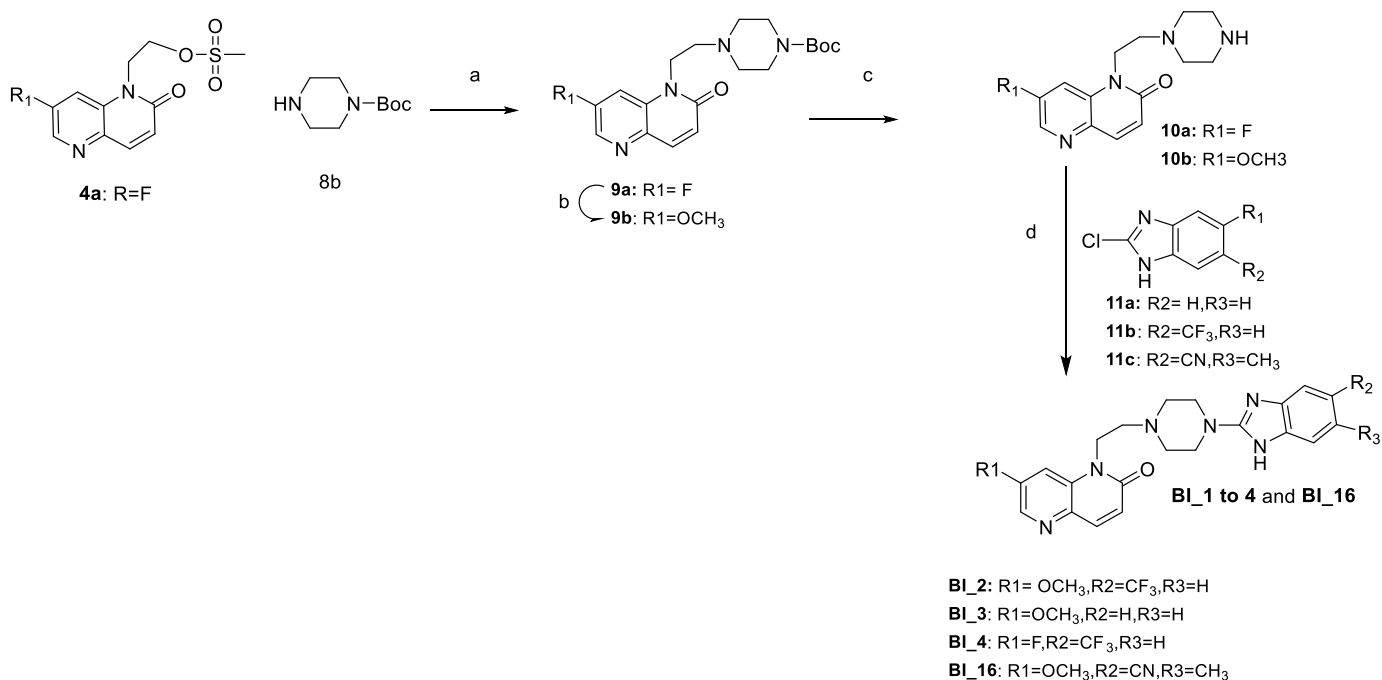
Figure 4.13: Synthetic scheme utilised for synthesis of compounds with piperazinyl benzimidazoles RHS

Tert-butyl 4-(2-(7-fluoro-2-oxo-1, 5-naphthyridin-1(2H)-yl)ethyl)piperazine-1-carboxylate(9a)

In a 100 mL round-bottomed flask 2-(7-fluoro-2-oxo-1,5-naphthyridin-1(2H)-yl)ethyl methanesulfonate (**4a**, 2.4 g, 8.4 mmol), tert-butyl piperazine-1-carboxylate (**8b**, 1.88 g, 10.06 mmol) and sodium carbonate (3.012 g, 25 mmol) were taken in DMF (50 mL). The resulting suspension was stirred at 92 ^{0}C for 3hrs.The reaction was monitored by LCMS and LCMS proofile showed the formation of product. The organic layer was then separated, dried (Na2SO4) and evaporated to get a residue. The crude material was purified on silica gel using methanol/DCM as eluent. The fraction were pooled and concentrated under vacuo afforded the pure product.

Yield: 1800mg, 57%; ^{1}H NMR (DMSO-d$_6$,300MHz): δ1.38 (s, 9H), 2.43 (t, _J_=4.80 Hz, 4H), 2.56 (t, _J_ = 6.69 Hz, 2 H), 3.16 - 3.32 (m, 4 H), 4.33 (t, J = 6.69 Hz, 2H), 6.83 (d, J = 9.61 Hz, 1 H), 7.91 - 8.11 (m, 2 H), 8.56 (d, J = 2.45 Hz, 1 H). m/z (ES$^+$), (M+H)$^+$: 377.40 for C$_{19}$H$_{25}$FN$_4$O$_3$.

***Tert*-butyl 4-(2-(7-methoxy-2-oxo-1,5-naphthyridin-1(2H)-yl)ethyl)piperazine-1-carboxylate(9b)**

In a 100 mL round-bottomed flask tert-butyl 4-(2-(7-fluoro-2-oxo-1,5-naphthyridin-1(2H)-yl)ethyl)piperazine-1-carboxylate (**9a**, 0.8g, 2.13 mmol) was taken in methanol (50 mL) under nitrogen. To this Sodium methoxide (0.459 g, 8.50 mmol) was added while stirring.The resulting reaction was stirred at 70 °C for overnight. LCMS showed formation of title product. Reaction was cooled to RT, solvents was evapourated to dryness.Obtained solid was diluted with water and extracted with 5 % methanol in DCM. Organic layer was separted, washed with brine and dried to get a residue. The residue was then purified on silica with with DCM/MeOH to tert-butyl 4-(2-(7-methoxy-2-oxo-1,5-naphthyridin-1(2H)-yl)ethyl)piperazine-1-carboxylate.

Yield: 600mg, 72.7%; ^{1}H NMR (DMSO-d$_6$,300MHz): δ1.38 (s, 9H), 2.44 (t, *J*=4.80 Hz, 4H), 2.57(t, *J* = 6.69 Hz, 2 H), 3.16 - 3.32 (m, 4 H), 3.86(s,3H), 4.35 (t, J = 6.69 Hz, 2H), 6.84 (d, J = 9.61 Hz, 1 H), 7.92 - 8.07 (m, 2 H), 8.41 (d, J = 2.45 Hz, 1 H). m/z (ES$^+$), (M+H)$^+$: 389.29 for C$_{20}$H$_{28}$N$_4$O$_4$.

7-Fluoro-1-(2-(piperazin-1-yl) ethyl)-1,5-naphthyridin-2(1H)-one (10a)

In a 50 mL round-bottomed flask, tert-butyl 4-(2-(7-fluoro-2-oxo-1,5-naphthyridin-1(2H)-yl)ethyl)piperazine-1-carboxylate (**9a**, 753 mg, 2mmol) was taken in HCl in Dioxane (4N,20 ml). Resulting reaction mixture was then heated at 80 °C for two hours. Reaction was monitored by LCMS and LCMS profile showed completion of reaction. Reaction mixture was evaporated to dryness. The residue was then neutralised with saturated Na$_2$CO$_3$ solution. The suspension was evaporated to dryness and the residue was then dissolved in 5 % MeOH in DCM and filtered.. The filterate was then evaporated to get 7-fluoro-1-(2-(piperazin-1-yl)ethyl)-1,5-naphthyridin-2(1H)-one.

Yield: 400mg, 72.4%; ^{1}H NMR (DMSO-d$_6$, 300MHz): δ 2.42 (m, 4H), 2.67 (m, 4 H), 3.4 (m,Hz, 2H), 4.31 (t, *J* = 6.7 Hz, 2H), 6.83 (d, *J* = 9.8 Hz, 1 H), 7.93 - 8.02 (m, 2 H), 8.56 (d, J = 2.45 Hz, 1 H). m/z (ES$^+$), (M+H)$^+$: 277.22 for C$_{14}$H$_{17}$FN$_4$O$_3$.

7-Methoxy-1-(2-(piperazin-1-yl)ethyl)-1,5-naphthyridin-2(1H)-one (10b)

Intermediate 10b was prepared from **intermediate 9b** using procedure analogous to **intermediate 10a**

m/z (ES$^+$), (M+H)$^+$ = 289.35 for $C_{15}H_{20}N_4O_2$.

2-Chloro-6-methyl-1H-benzoimidazole-5-carbonitrile(11c)

To the solution of 6-Methyl-2-oxo-2,3-dihydro-1H-benzoimidazole-5-carbonitrile (1.08 g, 0.0062 mole) in POCl$_3$ (10 mL) was added concentrated HCl (3 drops) in a sealed tube and stirred at 150° C for 2-3 hrs. The reaction mixture was concentrated and the resulting solid was suspended in water, basified and extracted with EtOAc (200 mL). The solid was filtered, washed with cold ether and dried under vacuum. The crude product was purified by column chromatography using 15% EtOAc in Pet. ether as eluent to give 2-Chloro-6-methyl-1H-benzoimidazole-5-carbonitrile as a off white solid.

Yield : 530mg, 45%; ^{1}H NMR (300 MHz, DMSO-d$_6$): δ 2.55 (s, 3H), 7.56 (s, 1H), 8.03 (s, 1H), 13.75 (s, 1H). MS (ES) (M+H)$^+$: 192 for $C_9H_6ClN_3$

Synthesis of 6-Methyl-2-oxo-2,3-dihydro-1H-benzoimidazole-5-carbonitrile

To the solution of 4,5-Diamino-2-methyl-benzonitrile (1.6 g, 10.87 mmoles, FCH Group Reagents for Synthesis) in THF (20 mL) was added CDI (3.56 g, 21.7 mmole) and the resulting solution was stirred at RT for overnight. The reaction mixture was concentrated and the residue was suspended in water. The solid was filtered, washed with cold ether and dried under vacuum to give 6-Methyl-2-oxo-2,3-dihydro-1H-benzoimidazole-5-carbonitrile.

Yield : 1080 mg, 60%; ^{1}H NMR (400 MHz, DMSO-d$_6$): δ 2.44 (s, 3H), 6.96 (s, 1H), 7.21 (s, 1H), 10.90 (s, 1H), 11.10 (s, 1H).
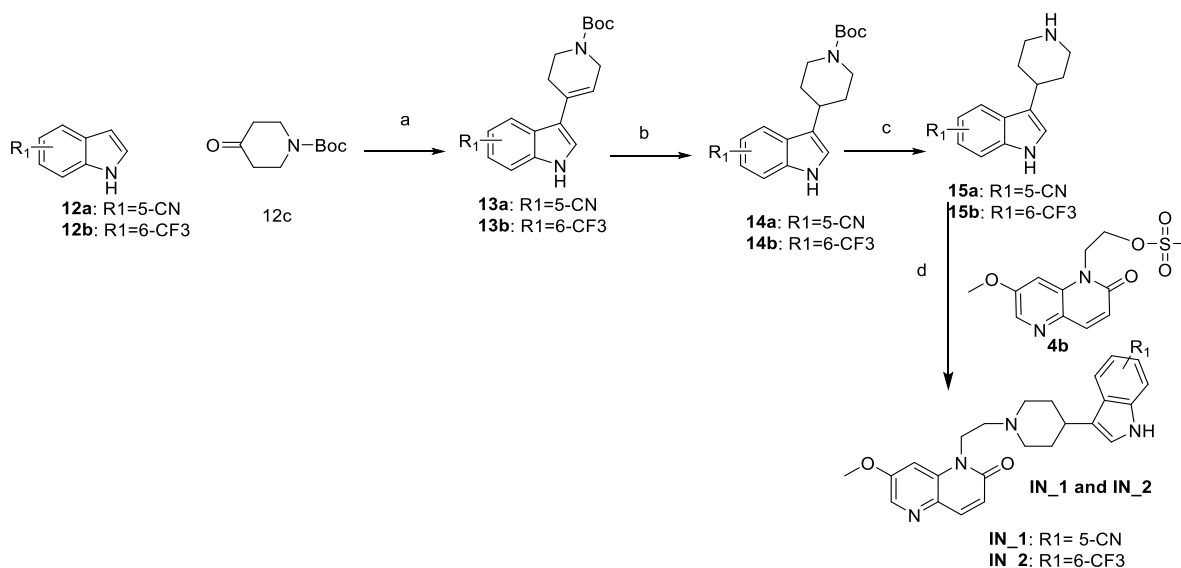
Reagents : (a) NaOH, Ethanol, 70 °C, 85 % (b) HCOONH$_4$, Ethanol, 10%Pd-C, 75 °C, 90 %

(c) 4N HCl in Dioxane, 50 °C, >95% (d) Na$_2$CO$_3$, DMF, 130 °C, 30 %

Figure 4.14: Synthetic scheme utilised for synthesis of compounds with RHS indole derivatives.

Tert-butyl 4-(5-cyano-1H-indol-3-yl)-5, 6-dihydropyridine-1(2H)-carboxylate (13a)

Potassium hydroxide (3.37 g, 60.00 mmol) was added to 1H-indole-5-carbonitrile (2.132 g, 15 mmol) and tert-butyl 4-oxopiperidine-1-carboxylate (5.98 g, 30.00 mmol) in methanol (30 mL) at room temperature and the resulting solution stirred at 65 °C for 18 hours. The mixture was then cooled to room temperature, quenched in dilute NH4Cl(aq.) (80 ml) and extracted with ethyl acetate. The extract was washed sequentially with water and sat. brine, dried over MgSO4 and concentrated by evaporation then purified by flash silica chromatography, elution gradient 30 to 50% EtOAc in isohexane. Pure fractions were combined and concentrated by evaporation then triturated with ether to give a colourless ppt.. The precipitate was collected by filtration, washed with Et2O and air dried to afford tert-butyl 4-(5-cyano-1H-indol-3-yl)-5,6-dihydropyridine-1(2H)-carboxylate (3.20 g, 66.0 %) as a colourless solid, which was used without further purification.

^{1}H NMR (DMSO-d$_6$,300MHz): δ 1.44 (s, 9H), 3.56 (t, *J*=5.7Hz, 2 H), 4.05 (br.s., 2H), 6.22 (br.s., 1H), 7.39 – 7.51 (m, 1 H), 7.51-7.60 (m, 1 H),7.63(s, 1H), 8.35 (s,1H), 11.73 (br.s., 1H) . m/z (ES$^+$), (M+H)$^+$: 323.22 for C$_{19}$H$_{21}$N$_3$O$_2$.

***Tert*-butyl 4-(6-(trifluoromethyl)-1H-indol-3-yl)-5,6-dihydropyridine-1(2H)-carboxylate (13b)**

Intermediate 13b was prepared from 6-(trifluoromethyl)-1H-indole (1.851 g, 10 mmol) and tert-butyl 4-oxopiperidine-1-carboxylate (1.992 g, 10.00 mmol) using procedure analogous to **intermediate 13a**

Yield : 2100 mg, 70.1%; ^{1}H NMR (DMSO-d$_6$,300MHz): δ 1.45 (s, 10H), 3.57 (t, *J*=5.6Hz, 2 H), 4.05 (br.s., 2H), 6.18 (br.s., 1H), 7.30 – 7.33 (d, J=9Hz, 1 H), 7.68-7.73 (d, *J*=13.8 Hz, 2 H), 8.01-8.04 (d, *J*=9 Hz,1H), 11.61 (br.s., 1H) . m/z (ES$^+$), (M+H)$^+$: 367.25 for C$_{19}$H$_{21}$F$_3$N$_2$O$_2$.

***Tert*-butyl 4-(5-cyano-1H-indol-3-yl)piperidine-1-carboxylate (14a)**

Tert-butyl 4-(5-cyano-1H-indol-3-yl)-5,6-dihydropyridine-1(2H)-carboxylate (**13a**, 1.45 g, 4.48 mmol), ammonium formate (1.412 g, 22.42 mmol) and Pd (5% on activated carbon) (50 mg) in ethanol (30 mL) were stirred and refluxed for 1 hour. The resulting mixture was cooled to room temperature and filtered through Celite. The filtrate was concentrated by evaporation then treated with dilute NH4Cl(aq.) (50 ml) and extracted with DCM. The extract was washed with water, dried over MgSO4 and evaporated to a colourless solid which was triturated with Et2O then collected by filtration and air-dried to give tert-butyl 4-(5-cyano-1H-indol-3-yl)piperidine-1-carboxylate (1.120 g, 77 %) as a colourless solid.

^{1}H NMR (CDCl, 300MHz): δ 1.45 (s, 9H), 1.6-1.7 (m, 2H), 2.01 (d, *J*=11.8 Hz, 2 H), 2.85-3.0 (m, 2H),4.26(d, *J*=12.0 Hz, 2H), 7.07 (s, 1H), 7.42 (m, 2 H),8.0(s, 1H), 8.47(br.s., 1H) . m/z (ES$^+$), (M+H)$^+$: 326.21 for C$_{19}$H$_{23}$N$_3$O$_2$.

***Tert*-butyl 4-(6-(trifluoromethyl)-1H-indol-3-yl)piperidine-1-carboxylate (14b)**

Tert-butyl   4-(6-(trifluoromethyl)-1H-indol-3-yl)-5,6-dihydropyridine-1(2H)-carboxylate (**13b**, 733 mg, 2 mmol), ammonium formate (630 mg, 10.00 mmol) and Pd (5% on activated carbon) (50 mg) in ethanol (20 mL) were stirred and refluxed for 1.5 hours. The resulting mixture was cooled to room temperature and filtered through Celite. The filtrate was concentrated by evaporation then treated with dilute NH4Cl(aq.) (50 ml) and extracted with DCM. The extract was washed with water, dried over MgSO4 and evaporated to a colourless solid. The solid was triturated with Et2O then collected by filtration and dried under vacuum

to give tert-butyl 4-(6-(trifluoromethyl)-1H-indol-3-yl)piperidine-1-carboxylate (500 mg, 67.9 %) as a colourless solid.

^{1}H NMR (DMSO-d$_6$,300MHz): δ 1.42 (s, 9H), 1.45-1.59(m,2H), 1.92 (d, J=12 Hz, 2 H), 2.75-3.03 (m, 2H),4.05(d, J=12.2 Hz, 2H), 6.87 (d, J=8.29 Hz, 1H) 7.04 (d, J=2.07 Hz, 1H), 7.21 (d, J=8.29 Hz,1 H),7.32(s, 1H),10.64 (br.s., 1H) . m/z (ES[+]), (M+H)[+] : 369.21 for C$_{19}$H$_{23}$F3N$_2$O$_2$.

3-(piperidin-4-yl)-1H-indole-5-carbonitrile (15a)

Intermediate 15a was prepared from **intermediate 14a** using procedure analogous to **intermediate 10a.**

Yield: 900mg, 98 %; m/z (ES[+]), (M+H)[+] : 226.25 for C$_{14}$H$_{15}$N$_3$.

3-(piperidin-4-yl)-6-(trifluoromethyl)-1H-indole (15b)

Intermediate 15b was prepared from **intermediate 14b** using procedure analogous to **intermediate 10a.**

Yield: 390mg, 97 %; m/z (ES+), (M+H)[+] : 269.24 for C$_{14}$H$_{15}$N$_3$
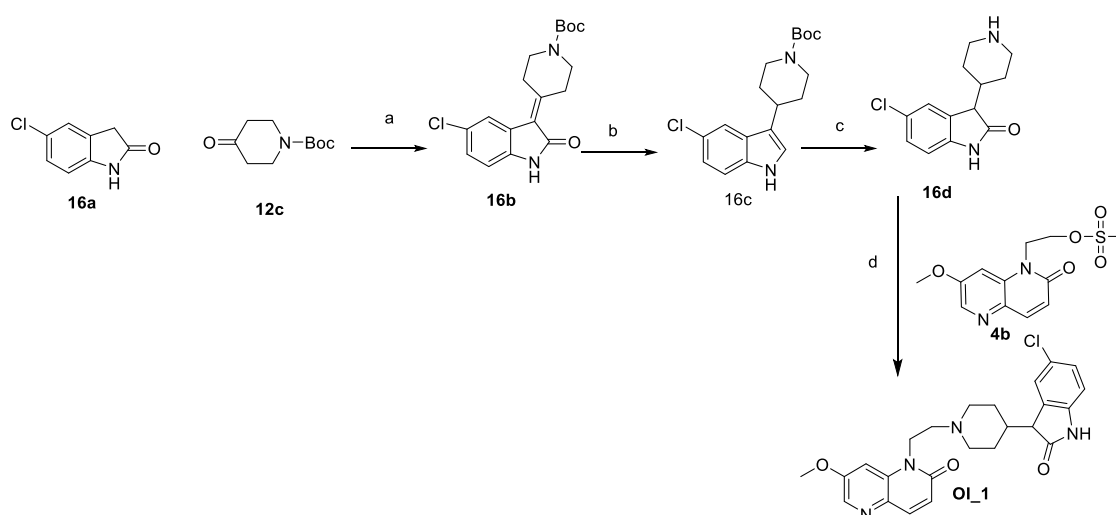
Reagents : (a) NaOH, Ethanol, 70 °C, 85 % (b) (b) NaBH$_3$, Ethanol, 0-RT °C, 70 % (c) 4N HCl in Dioxane, 50 °C, >95% (d) Na2CO3, DMF, 130 °C, 50 %

Figure 4.15: Synthetic scheme utilised for synthesis of compound with RHS oxindole

Tert-butyl 4-(5-chloro-2-oxoindolin-3-ylidene)piperidine-1-carboxylate (16b)

Potassium hydroxide (2.244 g, 40.00 mmol) was added to 5-chloroindolin-2-one (**16a**, 1.676 g, 10 mmol, Aldrich) and tert-butyl 4-oxopiperidine-1-carboxylate (**12c**,1.992 g, 10.00 mmol) in methanol (30 mL) at room temperature and the resulting solution stirred at 65 °C for 6 hours. The mixture was then cooled to room temperature, quenched in dilute NH4Cl(aq.) (80 ml) and extracted with ethyl acetate. The extract was washed sequentially with water and sat. brine, dried over sodium and concentrated under vacuo. The residue was purified by flash silica chromatography, using 2% MeOH in DCM eluent. Pure fractions were combined and concentrated by evaporation then triturated with ether to give a colourless ppt.. The precipitate was collected by filtration, washed with Et2O and air dried to afford tert-butyl 4-(5-chloro-2-oxoindolin-3-ylidene)piperidine-1-carboxylate (2.1 g, 70.1 %) as a offwhite solid.

^{1}H NMR (DMSO-d_6 ,300MHz): δ 1.43 (s, 9H), 2.95 (t, *J*=5.84 Hz, 2 H), 3.43 (br.s., 4H), 3.59 (t, J=5.84 Hz, 2H), 6.81-6.84 (d, *J*=9 Hz ,1H), 7.22 – 7.25 d, *J*=9 Hz, 1 H), 7.57(s, 1 H), 10.64 (br.s., 1H) . m/z (ES$^+$), (M+H)$^+$: 349.18 for $C_{18}H_{21}ClN_2O_3$.

Tert-butyl 4-(5-chloro-2-oxoindolin-3-yl)piperidine-1-carboxylate (16c)

Tert-butyl 4-(5-chloro-2-oxoindolin-3-ylidene)piperidine-1-carboxylate (698 mg, 2 mmol), ammonium formate (630 mg, 10.00 mmol) and Pd (5% on activated carbon) (50 mg) in ethanol (20 mL) were stirred and refluxed for 1.5 hours. The resulting mixture was cooled to room temperature and filtered through Celite. The filtrate was concentrated by evaporation then treated with dilute NH4Cl(aq.) (50 ml) and extracted with DCM. The extract was washed with water, dried over MgSO4 and evaporated to a colourless solid. The solid was triturated with Et2O then collected by filtration and dried under vacuum to give tert-butyl 4-(5-chloro-2-oxoindolin-3-yl)piperidine-1-carboxylate (450 mg, 64.1 %) as a colourless solid.

^{1}H NMR (DMSO-d_6 ,300MHz): δ 1.37-50 (m,12), 2.15-2.18 (m, 1H), 2.64(br.s., 2H), 3.17 (m, 2H), 3.44(br.s, 1H), 4.04 (m, 2H), 6.79 – 6.82(d, *J*=8.3 Hz, 1 H), 7.22 – 7.30(d, *J*=7.5 Hz, 1 H), 7.29 (br.s., 1H) . m/z (ES$^+$), (M+H)$^+$: 351.15 for $C_{18}H_{23}ClN_2O_3$.

5-Chloro- 3-(piperidin-4-ylindolin-2-one (16d)

Intermediate 16a was prepared from **intermediate 16c** using procedure analogous to **intermediate 10a.**

Yield: 370mg, 98 %; m/z (ES+), (M+H)+ : 251.2for $C_{13}H_{15}ClN_2O$.

4.2.4 Synthesis of N-linked quinolones and napthyridones with heteroaryloxy extention on LHS (HAR series)
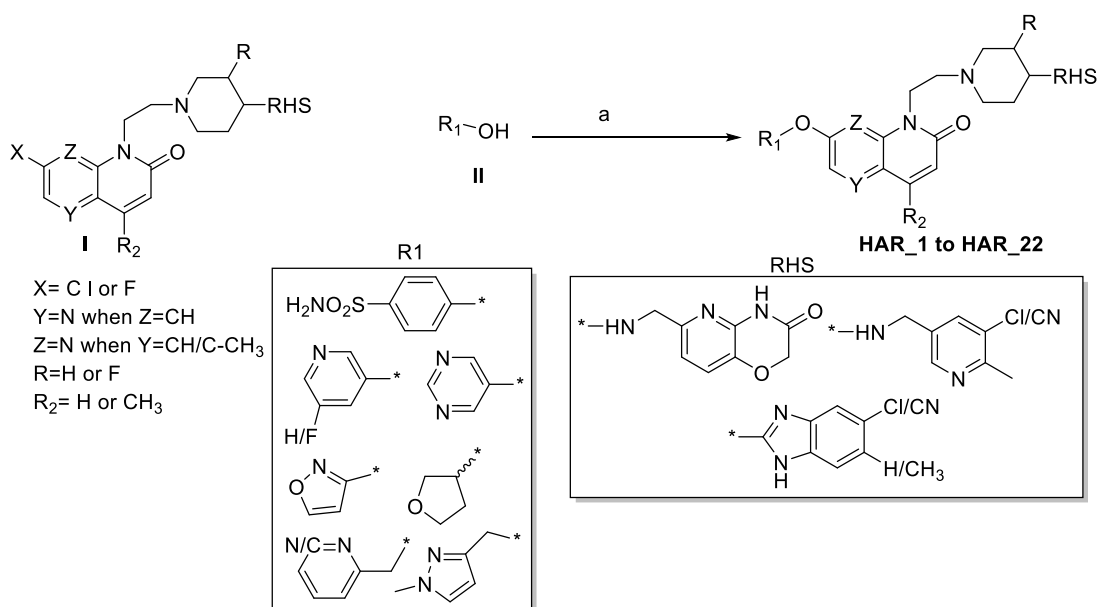
Reagents and conditions: a) Cs_2CO_3, DMSO, 130ºC

Figure 4.16: Synthetic scheme utilised for synthesis of compounds with heteroaryl ether LHS derivatives (HAR series)

6-((1-(2-(7-Chloro-2-oxo-1, 8-naphthyridin-1(2H)-yl)ethyl)piperidin-4-ylamino)methyl)-2H-pyrido[3,2-b][1,4]oxazin-3(4H)-one (AP_Ia)
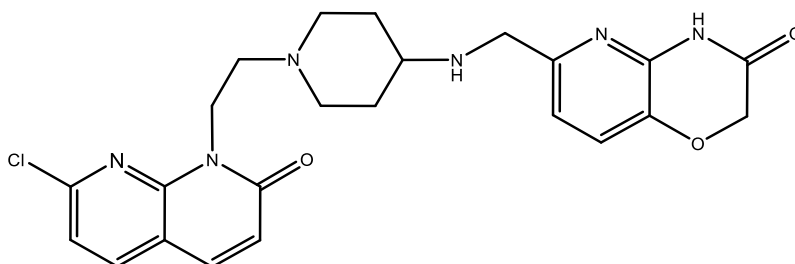
The 6-((1-(2-(7-chloro-2-oxo-1, 8-naphthyridin-1(2H)-yl)ethyl)piperidin-4-ylamino)methyl)-2H-pyrido[3,2-b][1,4]oxazin-3(4H)-one (**AP_Ia**) (CAS: 1033589-08-0) was synthesized as reported earlier (WO 2008071964)

6-(((1-(2-(7-Fluoro-2-oxo-1,5-naphthyridin-1(2H)-yl)ethyl)piperidin-4 yl)amino)methyl)-

2H-pyrido[3,2-b][1,4]oxazin-3(4H)-one (AP_Ib)
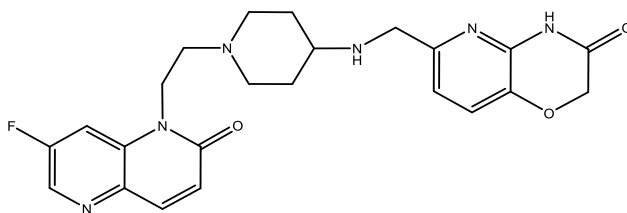
The compound **AP_Ib** (CAS: 1003943-19-8) was synthesized as reported earlier (WO 2008009700)

1-(2-(4-(((5-chloro-6-methylpyridin-3-yl)methyl)amino)piperidin-1-yl)ethyl)-7-fluoro-

1,5-naphthyridin-2(1H)-one (AP_Ic)
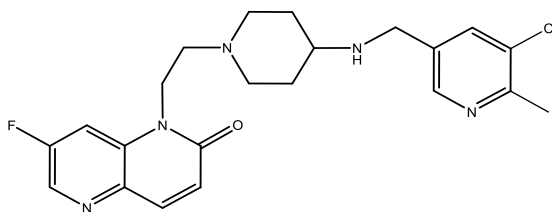
The compound **AP_ Ic** (CAS: 1173896-62-2) was synthesized as reported earlier (WO 009090222)

5-(((1-(2-(7-chloro-2-oxo-1,8-naphthyridin-1(2H)-yl)ethyl)piperidin-4-ylamino)methyl)-2-methylnicotinonitrile (**AP_Id**)
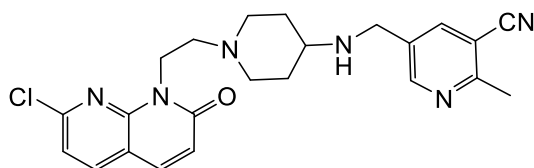
The compound 5-((1-(2-(7-chloro-2-oxo-1,8-naphthyridin-1(2H)-yl)ethyl)piperidin-4-ylamino)methyl)-2-methylnicotinonitrile (**AP_Id**) was synthesized from intermediate 1-(2-(4-aminopiperidin-1-yl)ethyl)-7-chloro-1,8-naphthyridin-2(1H)-one (CAS: 1033589-09-1, WO 2008071964) and (5-cyano-6-methylpyridin-3-yl)methyl methanesulfonate (Intermediate **32**)

In a 50 mL round-bottomed flask, 1-(2-(4-aminopiperidin-1-yl)ethyl)-7-chloro-1,8-naphthyridin-2(1H)-one (0.9 g, 2.93 mmol), (5-cyano-6-methylpyridin-3-yl)methyl methanesulfonate (**32**, 0.730 g, 3.23 mmol, from step1) and Sodium carbonate (0.728 g, 5.87 mmol) were taken in DMF (10 mL) to give a brown solution. The resulting reaction mixture was heated to 70 °C for 1hr. The progress of the reaction was monitored by LCMS and the profile showed the formation of required product. The reaction mixture was concentrated under vacuum and the residue was diluted with 15% MeOH/DCM and washed with saturated sodium bicarbonate solution. Organic layer was separated, concentrated under vacuum and purified by column chromatography using DCM/Methanol to afford the title compound (0.45 g, 35.1 %)

MS (ES$^+$) (M)$^+$: 437.36 for C$_{23}$H$_{25}$ClN$_6$O

The synthesis of intermediate **AP_If** and **AP_Ig** were synthesized using procedure anlogues to **AP_Ia** (WO 2008071964)

6-((1-(2-(7-Chloro-5-methyl-2-oxo-1,8-naphthyridin-1(2H)-yl)ethyl)piperidin-4-ylamino)methyl)-2H-pyrido[3,2-b][1,4]oxazin-3(4H)-one (AP_If)
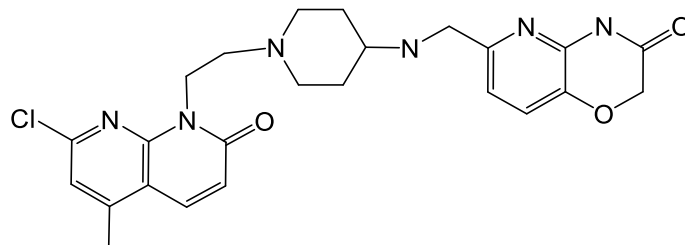
Step1: Synthesis of tert-butyl 1-(2-(7-chloro-5-methyl-2-oxo-1,8-naphthyridin-1(2H)-yl)ethyl)piperidin-4-ylcarbamate
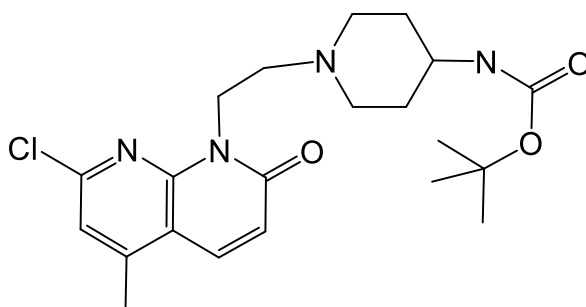
In a 100 mL round-bottomed flask, 7-chloro-5-methyl-1,8-naphthyridin-2(1H)-one (8 g, 41.11 mmol Aces Pharma, Inc), tert-butyl 1-(2-(methylsulfonyl)ethyl)piperidin-4-ylcarbamate (15.12 g, 49.33 mmol) and cesium carbonate (20.09 g, 61.66 mmol) were taken in DMF (30 mL) to give a brown solution. The resulting reaction mixture was heated to 90 °C for 1hr. The progress of the reaction was monitored by LCMS and the profile showed the formation of required product The reaction mixture was concentrated under vacuum and the residue was diluted with 10% MeOH/DCM and washed with saturated sodium bicarbonate solution. Organic layer was separated, concentrated under vacuum to afford the title compound (4.50 g, 26.0 %). The compound was taken for next step.

MS (ES$^+$) (M)$^+$: 421.40 for $C_{21}H_{29}ClN_4O_3$

Step2: Synthesis of 1-(2-(4-aminopiperidin-1-yl) ethyl)-7-chloro-5-methyl-1, 8-naphthyridin-2(1H)-one bis(2,2,2-trifluoroacetate)
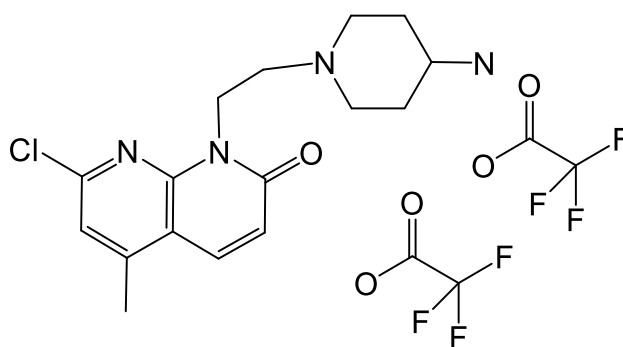
In a 250 mL round-bottomed flask, tert-butyl 1-(2-(7-chloro-5-methyl-2-oxo-1,8-naphthyridin-1(2H)-yl)ethyl)piperidin-4-ylcarbamate (1 g, 2.38 mmol, from step1) was taken in DCM (50ml) to give a yellowish solution. To this TFA (9.15 mL, 118.78 mmol) in dichloromethane (20 mL) was added and the resulting reaction mixture was stirred at 40°C for 1 hr. The reaction was monitored by LCMS, which indicated completion of reaction. The reaction mass was concentrated to dryness, till TFA was removed completely. The residue was then triturated with ethyl acetate, the solvent was decanted and the residue concentrated to dryness to obtain afford the title compound (1.20 g, 92 %) as TFA salt. The intermediate was taken for next step.

MS (ES+) (M)$^+$: 321.32 for $C_{20}H_{23}ClF_6N_4O_5$

Step3: Synthesis of 6-((1-(2-(7-chloro-5-methyl-2-oxo-1,8-naphthyridin-1(2H)-yl)ethyl)piperidin-4-ylamino)methyl)-2H-pyrido[3,2-b][1,4]oxazin-3(4H)-one (**AP_If**)

In a 250 mL round-bottomed flask, 1-(2-(4-aminopiperidin-1-yl)ethyl)-7-chloro-5-methyl-1,8-naphthyridin-2(1H)-one (1.2 g, 3.74 mmol, Intermediate from step2) and 3-oxo-3,4-dihydro-2H-pyrido[3,2-b][1,4]oxazine-6-carbaldehyde (0.733 g, 4.11 mmol , AfferChem, Inc) was taken in ethanol (34 mL)and 1,2-dichloroethane (80 mL). DIPEA (2.61 mL, 14.96 mmol) was added to the reaction mixture and it was heated to 70°C for 30 minutes to clear solution. Then the reaction was cooled to RT, sodium triacetoxyborohydride (2.378 g, 11.22 mmol) was added to it and stirred at 70°C for 12hrs. The progress of the reaction was monitored by LCMS and the profile showed the formation of required product. The reaction mixture was concentrated under vacuum and the residue was diluted with 15% MeOH/DCM and washed with saturated sodium bicarbonate solution. Organic layer was separated, concentrated under vacuum and purified by column chromatography using CHCl3/Methanol with0.2% aq. ammonia to afford the title compound (0.850 g, 47.1 %)

MS (ES+) (M)$^+$: 483.41 for $C_{24}H_{27}ClN_6O_3$

6-((1-(2-(7-chloro-4-methyl-2-oxo-1,8-naphthyridin-1(2H)-yl)ethyl)piperidin-4-ylamino)methyl)-2H-pyrido[3,2-b][1,4]oxazin-3(4H)-one (AP_Ig)
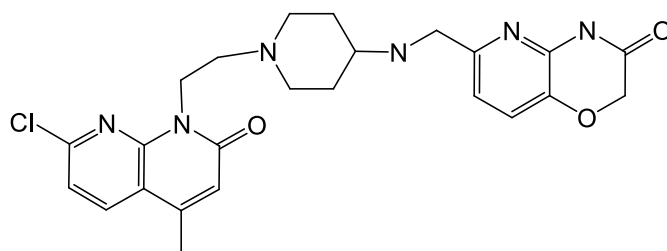

Step1: Synthesis of 7-Amino-4-methyl-1(H)-(1, 8) naphthyridin-2-one
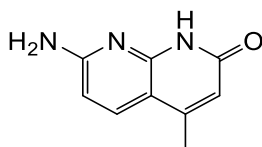
A mixture of 2,6-diaminopyridine (20 g, 184 mmol) and ethyl acetoacetate (28 g, 215 mmol) was refluxed for 2 hours using Dean-Stark water separator. After cooling the crystalline precipitate was filtered, washed with ether and dried. Yield : 18.5 g (46.2%).

^{1}H NMR (300 MHz, DMSO-d_6) δ2.26 (s, 3H), 5.97 (s, 1H), 6.32 (d, 1H, $J = 8.70$ Hz), 6.67 (s, 2H), 7.68 (d, 1H, $J = 8.70$ Hz), 11.34 (s, 1H). MS (ES) (M)$^+$: 176 (M$^+$) for $C_9H_9N_3O$.

Step 2: Synthesis of 7-Chloro-4-methyl-1(H)-(1,8)naphthyridin-2-one
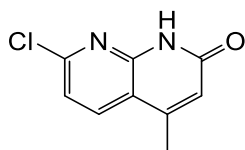
7-Amino-4-methyl-1(H)-(1,8)-naphthyridin-2-one (75 g, 428 mmol) was added to a mixture of acetic acid and conc. hydrochloric acid (300 ml : 300 ml) at 0° C. Sodium nitrite (82.3 g, 1193 mmol) dissolved in water was added dropwise and the resulting solution was maintained the same temperature for 1 hr. Then aqueous urea was added dropwise for half an hour. The resulting mixture was quenched with saturated sodium bicarbonate solution and extracted with ethyl acetate and brine wash dried over sodium sulphate. The crude product was washed with solvents to get pure 7-Chloro-4-methyl-1(H)-(1, 8) naphthyridin-2-one. Yield :10g (12%).

^{1}H NMR (400 MHz, DMSO-d_6) δ 2.39 (s, 3H), 6.46 (s, 1H), 7.31 (d, 1H, J = 8.28 Hz), 8.15 (d, 1H, J = 8.28 Hz). MS (ES) (M)$^+$: 196 (M$^+$) for $C_9H_7ClN_2O$. HPLC purity : 98.40%

Step 3: Synthesis of tert-butyl 1-(2-(7-chloro-4-methyl-2-oxo-1, 8-naphthyridin-1(2H)-yl) ethyl) piperidin-4-ylcarbamate
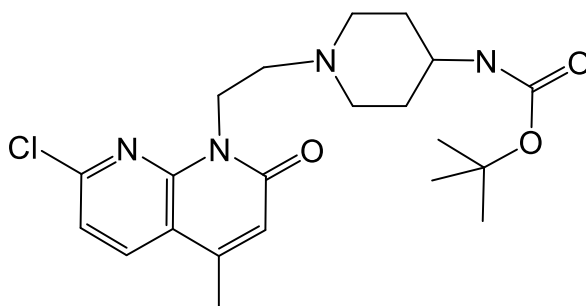
In a 100 mL round-bottomed flask, 7-Chloro-4-methyl-1(H)-(1,8)naphthyridin-2-one (8 g, 41.11 mmol), tert-butyl 1-(2-(methylsulfonyl)ethyl)piperidin-4-ylcarbamate (15.12 g, 49.33 mmol) and cesium carbonate (20.09 g, 61.66 mmol) were taken in DMF (30 mL) to give a brown solution. The resulting reaction mixture was heated to 90 °C for 1hr. The progress of the reaction was monitored by LCMS and the profile showed the formation of required product The reaction mixture was concentrated under vacuum and the residue was diluted with 10% MeOH/DCM and washed with saturated sodium bicarbonate solution. Organic layer was separated, concentrated under vacuum to afford the title compound (4.50 g, 26.0 %)

MS (ES+) (M)$^+$: 421.40 for $C_{21}H_{29}ClN_4O_3$

Step 4: Synthesis of 1-(2-(4-aminopiperidin-1-yl)ethyl)-7-chloro-4-methyl-1,8-naphthyridin-2(1H)-one
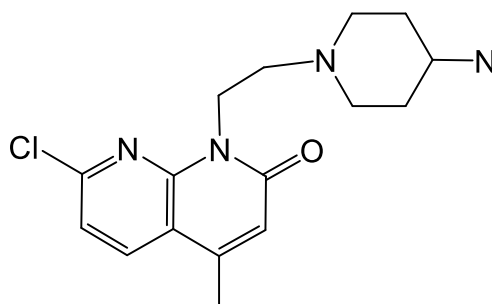
In a 250 mL round-bottomed flask, tert-butyl 1-(2-(7-chloro-4-methyl-2-oxo-1,8-naphthyridin-1(2H)-yl)ethyl)piperidin-4-ylcarbamate (1 g, 2.38 mmol, from step1) was taken in DCM (50ml) to give a yellowish solution. To this TFA (9.15 mL, 118.78 mmol) in dichloromethane (20 mL) was added and the resulting reaction mixture was stirred at 40°C for 1 hr. The reaction was monitored by LCMS, which indicated completion of reaction. The reaction mass was concentrated to dryness, till TFA was removed completely. The residue was then triturated with ethyl acetate and the solvent was decanted and the residue concentrated to dryness to obtain afford the title compound (1.20 g, 92 %) as TFA salt.

MS (ES+) (M)$^+$: 321.32 for $C_{20}H_{23}ClF_6N_4O_5$

Step5: Synthesis of 6-((1-(2-(7-chloro-4-methyl-2-oxo-1, 8-naphthyridin-1(2H)-yl) ethyl) piperidin-4-ylamino) methyl)-2H-pyrido [3, 2-b][1,4]oxazin-3(4H)-one (**AP_Ig**)
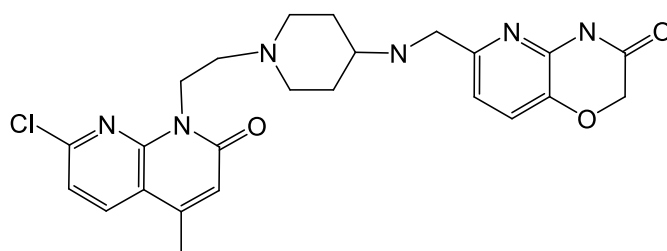

Compound **Ig** was synthesized using procedure similar to compound **If**

MS (ES+) (M)$^+$: 483.41 for $C_{24}H_{27}ClN_6O_3$

4.3 Computational methods

4.3.1 Ligand preparation

Throughout the studies, CORINA (http://www.molecular-networks.com/products/corina) was used for generating 3D structures from smiles and Omega 2.2.0 (OpenEye Scientific Software, Santa Fe, New Mexico 87507) was used for generating conformers. Default settings were retained for both the tools.

4.3.2 Molecular alignment of compound AP_4 and AP_5

ROCS, a shape based molecular alignment tool (Version 3.2, OpenEye Sci. Software Open Eye) was used for molecular alignment. Shape Tanimoto score was used to rank the overlays. The omega generated multi-conformers (max number of output conformers per molecule = 30) of compound **AP_1** and **AP_2** were aligned to the crystal bound conformation of **GSK299423** (PDB ID:2XCS). The best scoring conformation of compound **AP_1** and **AP_2** was further utilized as reference to derive the best possible conformer of compound **AP_4** and **AP_5** from the pool of multiple conformers.

4. 3.3 Homology modeling

Mycobacterium tuberculosis Gyrase subunit A (*Mtb* GyrA) was built by homology modeling using MOE (Molecular Operating Environment, Version 2013.12, Chemical computing group, Montreal, Canada). The published *Staphylococcus aureus* DNA gyrase Subunit A (Sau GyrA) crystal structure was retrieved from Protein Data Bank (PDB ID: 2XCS 2.1Å) and examined for 1) ligand interaction and followed by 2) similarity with *Mtb* GyrA.

The NBTI binds to a site adjacent to FQ binding site (**Figure 4.15**) as evident in the published crystal structure (Bax,B.D. *et al.*, 2010). The NBTI binds midway between the two active sites, with the quinoline-carbonitrile group sitting in between the two central base pairs of the stretched DNA and the oxathiolo-pyridine group occupying the non-catalytic pocket that opens up between the two GyrA subunits.
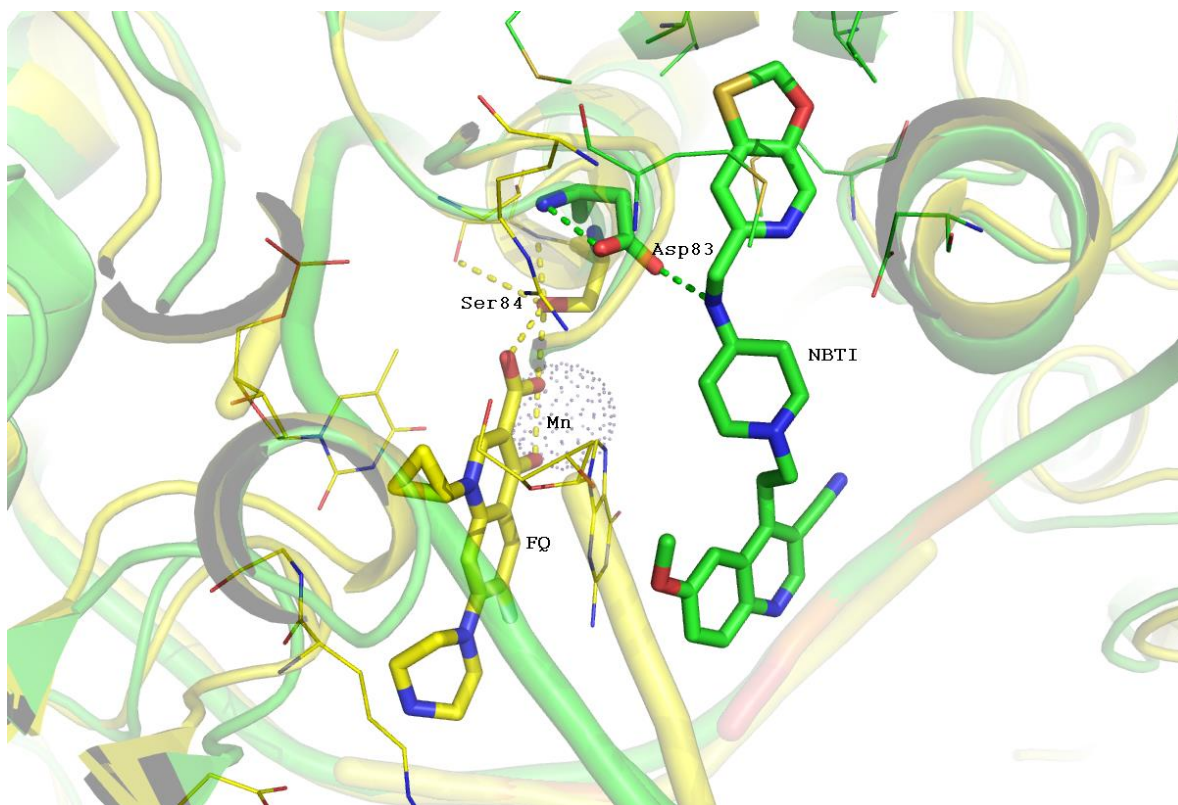
Figure 4.17. Comparison of binding mode of Fluoroquinolone (FQ) as represented by Ciprofloxacin (Stick model, yellow color, PDB id; 2XCT) and NBTIs as represented by GSK299423 (Stick model, green color PDB id; 2XCS) in Sau DNA gyrase. The NBTIs binds to a site adjacent to FQ binding site.

Overall primary sequence similarity of *Mtb* with *Sau* GyrA was found to be 42% whereas the active site similarity was >95% (Figure 4.22) and thus *Sau* GyrA served as template for the *Mtb* GyrA model generation (GeneDoc Ver 2.6.002; http://www.nrbsc.org/gfx/genedoc/ with default options was used for multiple alignments of sequences).

Sequence aligment

```
                *              80              *              100              *              120              *
Sau_GyrA : PDKSYKKSARIVGDVMGKYHPHGDSSIYEAMVRMAQDFSYRYPLVDGQGNFGSMDGDGAAAMRYT
Mtb_GyrA : PDRSHAKSARSVAETMGNYHPHGDASIYDSLVRMAQPWSLRYPLVDGQGNFGSPGNDPPAAMRYT
           PD S  KSAR V   MG YHPHGD SIY    VRMAQ  S RYPLVDGQGNFGS   D  AAMRYT
```

Figure 4.18. Sequence alignment of *Sau*-GyrA and *Mtb*-GyrA residues. The active site residues spanning 5Å radius from ligand bound to *Sau*-GyrA crystal structure (2XCS) are

shown. The conserved active site residues are hightleted in green and G72/A78 in *Sau* and

Mtb GyrA respectively is highlighted in orange.

Model generation Steps: 10 different models of Mtb GyrA were generated with the default settings as implemented in MOE. The bound ligand and DNA were used as environment for induced fit. Out of the 10 different models, the model with lowest RMSD (C-α) to the average position of all of the intermediate models was selected. Analysis of the Ramachandran plot of the selected model indicated that > 95% residues were in the allowed region. The coordinates of DNA and the ligand from the 2XCS were merged into the homology model of *Mtb* GyrA. The resultant complex of model was further analyzed and minimized in Maestro (version 8; Schrödinger, LLC: New York.) using default parameters of Protein Preparation Tool. The RMSD (C-α) of the *Mtb* GyrA model and *Sau* GyrA was found be less than 2Å. No major structural differences were observed between the *Mtb* GyrA model and *Sau* GyrA crystal structure and the overall architecture remains same (**Figure 4.17**). The active site (5Å radius from ligand:2XCS) is very well conserved except Gly72 of Sau GyrA is occupied by Ala78 in Mtb GyrA. This difference is not disturbing the architecture of active site and provides additional hydrophobicity to active site of *Mtb* GyrA (**Figure 4.18**). The energy minimized model was used for docking.

4.3.4 Molecular docking

Molecular dockings were performed using FRED (Version 2, OpenEye Sci. Software) in to the *Sau* GyrA and *Mtb* GyrA model. Fred Receptor tool was used to prepare the receptor input file for docking. The active site was defined by selecting the ligand and a docking constrain involving Asp83/89 of Sau and *Mtb* GyrA as a hydrogen bond acceptor was added. The Asp is found to be involved in critical hydrogen bond interaction with the ligand and mutation of it found to affect the activity of NBTIs (Bax, B.D. *et al.*, 2010). The docking protocol was validated by extracting the bound conformation of the ligand and re-docking into the receptor. Best agreement was found between docked pose and crystal bound conformation (RMSD < 0.8Å in both the receptor). After this validation the receptor was used for docking. Apart from the default Chemgauss3 scoring function, CGO scoring (based on the shape overlay of ligands) was used.

Figure 4.19. Overlay of secondary structure represntation of *Mtb* GyrA (Yellow) homology model on to *Sau* GyrA (Green: PDB ID: 2XCS).

Figure 4.20. Comparision of active site residues (dimer) of *Mtb* model (cyan and orange color) and *Sau* GyrA (green and pink color) spanning 5Å radius from ligand (green color,

stick model) bound to *Sau*-GyrA crystal structure (2XCS). The differing residue Gly72 (*Sau*) and Ala78 (*Mtb*) are shown in stick model with green and orange color respectively.

The docking of designed molecules was done in two steps. In the first step the multiple conformers of compound to be docked were aligned using ROCS on to the best aligned conformation of compound 2a on to crystal ligand. Maximum of 5 conformations per compound were opted as an output from ROCS. In the second step the resultant conformations of designed compounds were docked using FRED protocol as described above. Consensus scoring and visual inspection were used to select the pose. The complex of selected pose and protein was subjected to constrained minimization using Macromodel (Schrodinger) and OPLS force field to remove unfavorable contacts.

4.4 Enzyme inhibition studies

4.4.1 *Mycobacterium tuberculosis* DNA gyrase supercoiling inhibition assay

Determination of IC_{50} for the supercoiling activity of *Mtb* H37Rv gyrase holoenzyme was performed as reported earlier (Hameed, P. S. *et al*., 2013). DNA supercoiling assay was performed in 96-well PCR plates (Bio-rad) in 30 µL volume. Assay mix contained 12.5 nM of *Mtb* H37Rv holoenzyme, 50 ng of relaxed pBR322 DNA, 40 mM HEPES-KOH pH 7.5, 100 mM potassium glutamate, 15 mM KCl, 1 mM spermidine, 10 mM $MgCl_2$, 4 mM DTT, 8% glycerol, 0.36 mg/mL BSA and 75 µM ATP. The assay was started with the addition of DNA and ATP mix and continued for 90 min at 37°C. The reaction was stopped by addition of 0.75 µL Proteinase K (20 mg/mL, 40 U/mg) and 3 µL of 2% SDS followed by incubation at 37 ºC for 1 hour. This was followed by the addition of 4 µL of 10 X DNA-loading dye to samples followed by loading onto the gel. Supercoiled and relaxed forms of DNA were separated by gel electrophoresis for 16 h at 1 V/cm, on a 0.8 % agarose in buffer containing 45 mM Tris-borate and 1 mM EDTA. The gel was stained for 10 min with a solution containing 0.7 µg/mL ethidium bromide in water, destained in water for 30 min followed by imaging and quantitation of the gel bands.

4.4.2 Cleavable complex assay with *Mtb* H37Rv gyrase holoenzyme

The cleavable complex assay was performed in 96-well PCR plates (Bio-rad) in 30 µL volume as reported earlier with minor modifications. (Aubry, A. *et al*., 2004). Assay mix contained 400 nM - *Mtb* H37Rv holoenzyme, 105 ng of relaxed pBR322 DNA, 40 mM HEPES-KOH pH

7.5, 100 mM potassium glutamate, 25 mM KCl, 1 mM spermidine, 10 mM $MgCl_2$, 4 mM DTT, 6% glycerol and 0.35 mg/mL BSA. The assay was started with the addition of DNA and carried out for 60 min at 37°C. The reaction was stopped by addition of 0.75 µL proteinase K (20 mg/mL, 40 U/mg) and 3 µL of 2% SDS followed by incubation at 37 ºC for 1 hour. This was followed by the addition of 4 µL of 10 X DNA-loading dye to samples followed by loading onto the gel. Nicked, linear and supercoiled forms of DNA were separated by gel electrophoresis for 16 h at 1 V/cm, on a 0.8 % agarose in buffer containing 45 mM Tris-borate, 1 mM EDTA and 0.3 µg/ml ethidium bromide. An image of the gel was captured using a Fujifilm FLA 5100 Phosphorimager and used for quantitation of the DNA using Bio-rad's Quantity One software.

4.5 Microbiological studies

4.5.1 Bacterial growth inhibition with *Mycobacterium tuberculosis* H37Rv strain

All the synthesized compounds were evaluated for anti-mycobacterial screening as per previously reported procedure [Ramesh *et al.,* 2003]. The MICs of synthesized compounds for *Mtb* were determined in broth by a standard microdilution method according tothe guidelines of NCCLS using *Mycobacterium tuberculosis* H37Rv ATCC 27294 strain. The assay was performed in a 96-well microtiter plate (catalog no. 900196; Tarsons, Kolkata, India), in which all the peripheral wells were filled with sterile distilled water. Serial twofold dilutions of test compound were placed in the remaining wells, with the concentrations ranging from 32 to 0.06mg/liter. For determination of the MIC in broth, BACTEC 7H12B medium was used as the diluent. Each well was inoculated with a final inoculum of approximately 5 x 10^5 CFU/ml. The plates were incubated at 37°C for 16 to 18 days, and the wells were assessed for visible turbidity. The lowest concentration at which there was no visible turbidity was defined as the MIC.

4.5.2 Time kill studies against *Mtb* in 7H9 broth

This assay was performed in a 200 µL volume using 96-well micro plates with Middlebrook 7H9 broth supplemented with 0.2% glycerol, 0.05% Tween 80 (Sigma) and 10% albumin dextrose catalase (Difco Laboratories, Detroit, Mich.) as described earlier (Shirude, P. S *et al*., 2013). Serial two-fold dilutions of aminopiperidines spanning a wide concentration range were added to each of the 96-wells containing approximately 3 X 10^7 CFU/mL of Mtb H37Rv. The plates were incubated at 37ºC. Bacterial enumeration was performed on Middlebrook 7H11

70

agar plates at 0, 3, 7 and 10 days post drug exposure. The plates were incubated for upto 28 days at 37°C, in 5% CO_2 in a humidified atmosphere. The bacterial colonies were enumerated and data expressed as the $log_{10}CFU$ for each drug concentration.

4.5.3 Resistance frequency, genetic mapping and cross resistance studies

Spontaneous resistant mutants were raised against compound **AP_3**, **AP_16**, ciprofloxacin and moxifloxacin using a single step selection method (Shirude, P. S *et al*., 2013). Briefly, a mid-logarithmic phase culture of Mtb H37Rv was centrifuged and concentrated 100-fold to achieve a bacterial number of ~10^{10} CFU/mL. Varying dilutions of the bacterial culture were plated on to compound-containing plates. Appropriate dilutions of the bacterial culture were also plated on drug-free Middlebrook 7H11 agar to enumerate the bacterial numbers in the culture. Plates were incubated for 4 weeks at 37°C and the CFUs in drug-free plates were enumerated. The drug-containing plates were incubated for up to 6-8 weeks at 37°C to enumerate the number of resistant colonies.

The spontaneous rate of resistance was calculated by dividing the number of colonies on drug-containing plates (at a given concentration) divided by the total number of viable bacteria estimated on drug-free plates. Resistant colonies were randomly picked from the drug containing plates and grown in complete 7H9 broth to determine their level of resistance against the parent compound, close analogs and TB drugs with different mechanisms of action.

In order to map the genetic mutations arising following compound exposure and mutant selection, genomic DNA from microbiologically well characterized colonies were isolated. The entire *gyrA* gene of resistant mutants and wild-type *Mtb* H37Rv were PCR amplified using standard conditions from boiled supernatants using specific *Mtb* primers to amplify the entire *gyrA* gene. PCR was performed with cycling parameters of 94 °C for 30 s, 60°C for 30 s, and 72°C for 2 min for 30 cycles in a DNA Engine Dyad cycler (Bio-Rad). PCR products were purified from the gel (PCR purification kit, Qiagen), quantitated, and sequenced (Microsynth). The sequences from the resistant clones were aligned against the wild-type H37Rv *gyrA* gene using Vector NTI software to detect mutations in the target gene.

4.6 Cytotoxicity studies

All the synthesized compounds were further examined for cytotoxicity using A549 human lung carcinoma cells as described earlier (Eakin *et al.*, 2012). Briefly, A549 cells (ATCC) were grown in RPMI medium (GIBCOBRL) containing 10% heat-inactivated fetal bovine serum (GIBCO-BRL) and 1mM L-glutamine (GIBCO-BRL) at a density of ~ 1,000 cells/well. After incubation of the cells with compound in a CO_2 atmosphere at 37°C for 72 hours, cell viability was determined following addition of 10μM of resazurin solution (Sigma), by measuring fluorescence (excitation at 535 nm, emission at 590 nm) using a fluorimeter. The concentration at which growth is inhibited by 50% is taken as IC_{50} value.

4.7 hERG IC_{50} determination

All the synthesized compounds were tested on voltage-gated ion channels using the medium-throughput electrophysiology IonWorks™ device as described previously and detailed methods regarding the running of IonWorks™ have been published (Schroeder *et al.,* 2003). For carrying out the experiment, a boat in the "Cells" position of the IonWorks™ instrument was loaded with the cell suspension, and a 96-well PBS destination plate was placed in the "Plate 1" position. A 384-well PatchPlate™ was placed in the IonWorks™ plenum and held in position using the plenum clamp. From this point the experiment progress is automated and ultimately reports a non-cumulative concentration-effect curve for test compound.

4.8 ADMET Properties

4.8.1 Determination of LogD

All the synthesized derivatives were further evaluated for octanol-water partition coefficient (Log *D*) was measured by shake-flask method (Berthod, A. et *al.*, 1999). A 10 mM sodium phosphate buffer pH 7.4 was used as aqueous solution. A 10 mM compound solution was made in DMSO and subsequently DMSO was removed using GeneVac. A 435 μL of octanol was added using Tomtec, stirred for 5 minutes. Further mixing was done by inversion for 5 h at 25 ºC, subsequently centrifuged for 30 minutes at 3000 RPM. LC/UV/APPI/MS quantitation of both aqueous and octanol layers was performed to calculate Log *D* value according to the following equation.

LogD = *Log* (Octanol/Octanol inj volume/ Buffer/Buffer inj volume)

The method has been validated for log *D* ranging from -2 to 5.0.

4.8.2 Solubility determination

Solubility of the compounds in 0.1M phosphate buffer, pH 7.4 was determined as described (Baka, E.*et al*., 2008) Glyburide was used as QC standard in the assay. Briefly, compounds were diluted in ACN/water (40:60) to desired concentration, samples were dried using Genevac for 4 hrs and subsequently 800μl of buffer was added. Compound containing plates were stirred for 24 hrs at 25ºC on Eppendorf Thermomix R at 750rpm. Finally, compound concentration was estimated using UV and MS analysis.

4.8. 3 Caco2 permeability assay

The permeability (A to B) in Caco-2 cells was measured using the intestinal lumen/blood pH6.5/7.4 gradient (Tavelin, S. *et al*., 2003)The assay was carried in the presence of inhibitors of three major efflux transporters; quinidine (P-gp), sulfasalazine (BCRP), and benzbromarone (MRP2)), to measure passive permeability. The reference compounds were metoprolol, rosuvastatin and erythromycin. The Caco-2 cell monolayer was washed once with HBSS prior to start. Transepithelial electrical resistance (TEER) was measured both before and after performing all the transport experiments. Transport buffer, 800 µL, Hanks balanced salt solution (HBSS, pH 7.4) was first dispensed to the basal side of the monolayer. The assay was then initiated by adding 200 µL of compound solution in HBSS, pH 6.5 with 1% DMSO to the apical side. Final concentration of compound was 10 µM. Samples were withdrawn before and at 45 and 120 min post addition of test compound. 2 µL and 200 µL were withdrawn from the apical donor compartment and the basolateral receiver compartment, respectively. During incubation the transwell plates were placed in a shaking incubator at 480 rpm and 37°C between the sampling up to 120 min. All samples were immediately analysed by LC/MS/MS. The apparent permeability coefficient (Papp) was calculated according to the following equation: Papp = (ΔQ/Δt)/(A X CD) [cm/s] where (ΔQ/Δt) [cm/s] is the cumulative amount of test compound transported over time to the basolateral side, A is the surface area of the monolayer

membrane (cm2) and CD is the average drug concentration in the donor chamber over the period which (ΔQ/Δt) was determined.

4.9 *In vivo* animal studies

All animal experimentation protocols were approved by the Institutional Animal Ethics Committee registered with the Govt. of India (Reg. No. 5/1999/CPCSEA). Six to eight week old BALB/c mice, purchased from RCC laboratories, Hyderabad, India were used in the pharmacokinetic (PK) and pharmacodynamic (PD) studies. Animals randomly assigned to cages were allowed 2 weeks of acclimatization period before initiating the experiment. Feed and water were given *ad libitum*

4.9.1 Rat Pharmacokinetic studies

Pharmakinetic profile of representative key compounds were performed in rats to access the oral bioavailabity potential of the series. Wistar rats were administered test compounds in separate groups, via oral gavage. All oral administration was performed as suspensions in 0.5 % HPMC, and 0.1% Tween 80. In a separate groups, test compound (2 mg/kg) were administered intravenously as a solution (20 % v/v DMA in phosphate buffered saline). All blood samples were collected via sapheneous vein into Microvette CB300® (Starstedt, Germany) tubes coated with Lithium-Heparin, and plasma was prepared from the collected blood by centrifugation.

4.9.2 Pharmacokinetic and pharmacodynamic studies in mice

4.9.2a Pharmacokinetics. PK was analyzed in the infected mice during the efficacy study. Blood samples from infected mice were collected on the 18th or 19th day of dosing and processed in a BSL3 laboratory. Compound **AP_5, AP_7, AP_18, AP_19** & **AP_21** were formulated in a solution containing 5 % dextrose, pH adjusted to 4-5 with 5M acetic acid. Test compounds, or the corresponding vehicle, were orally administered through gavage at 10 mL/kg dose volume. 1-Aminobenzotriazole (ABT), a known cytochrome P450 Inhibitor, dissolved in water, was orally administered at a dose of 100 mg/kg (10 ml/kg) 2 h before dosing the compound to reduce the first pass metabolism and increase plasma exposure. Blood samples were collected by puncturing the saphenous vein at 5 min, 15 min, 30 min, 1 h, 2 h, 4 h, 6 h after dosing. The same formulation as above was used for intravenous PK at 5 mg/kg and per oral PK at 40 mg/kg dose in rats. Plasma samples from mice/rats were mixed with chilled acetonitrile (1:10 v/v) to precipitate proteins, vortexed and centrifuged at 4000 rpm for

30 min at 10°C. The resulting supernatant was mixed with mobile phase containing carbamazepine (internal standard, 10 ng/ml), and analysed for drug concentrations by liquid chromatography with tandem mass spectrometry (LC-MS/MS). Chromatographic separation was achieved on a Gemini C18 column (50 X 4.6 mm, particle size 5 μ, Phenomenex, USA) by isocratic elution with 40% 10 mM ammonium acetate buffer in acetonitrile at 500 μL/min flow rate over 4.5 minutes. AB Sciex API3000 triple quadrupole mass spectrometer (Applied Biosystems, USA) equipped with a turbo ionspray source was used for the quantitation. Area under the concentration (AUC) vs. time PK profile was calculated by non-compartmental analysis (WinNonLin 5.2.1, Pharsight Inc.).

4.9.2b Pharmacodynamics. BALB/c mice were infected in an aerosol chamber as described earlier (Hameed, P.S. *et al.*, 2014). Infected mice were housed in individually ventilated cages (Allentown technologies, USA) in a biosafety level three (BSL-3) facility. Treatment was initiated after 3 days and 4 weeks of infection in the acute and chronic model respectively. Vehicle or compound treated groups contained 3 mice each. An additional 3 mice were sacrificed just after infection to serve as early controls. Isoniazid was formulated in 0.5 % (w/v) hydroxy propyl methyl cellulose (HPMC) whereas test compounds were prepared in the same formulation as used for the PK study. ABT was orally administered before compound administration as described above. In the acute model, infected mice were treated with an oral dose of 20 or 40 or 80 or 160 mg/kg of compound **AP_5, AP_7, AP_18, AP_19** and **AP_21** given twice daily (8 h interval) for 20 days (7 days/wk). Mice were sacrificed after completion of treatment and suitable dilutions of lung homogenates were plated on 7H11 agar to determine viable CFU per mouse lung tissue. One-way analysis of variance (ANOVA) followed by the Bonferroni's Multiple Comparison Test was used for analyzing efficacy data.

Statistical Analysis

The colony counts obtained from plating were transformed to Log10 (X+1), where x equals the total number of viable bacilli present in a given sample. Prism software version 4 (Graph PadSoftware, Inc., San Diego, California) was used for plotting pharmacodynamic effects. Dunnet'smultiple-comparison test was used to differentiate statistical differences in lung CFU in treated versus untreated mice.

The attractiveness of DNA gyrase as a high quality anti-bacterial target has been validated by the clinical success of several generations of FQs to treat serious bacterial infections. The widespread emergence of FQ-resistant bacterial strains is likely to reduce the clinical value of FQs in the near future. The clinical benefit of combining FQs in the drug regimen to treat TB have been demonstrated in pre-clinical animal models as well as in TB patients. Numerous reports have highlighted the emergence of *Mtb* strains resistant to FQs, thereby limiting the life of these drugs in treating TB. The existing body of evidence around the clinical safety and efficacy of FQs, provide an opportunity to identify novel GyrA inhibitors. It was envisaged that a novel GyrA inhibitor class would have a distinct binding mechanism compared to the binding mode of FQs. Therefore, identification of a novel GyrA inhibitors with unique binding mechanism that is distinctly different from the binding mode of the FQ class is needed. This would lead to the discovery of novel gyrase agents that could act against FQ resistant *Mtb* strains. Thus in the present study, we focused on identifying promising antimycobacterial agents with improved potency, safety and *in vivo* efficacy by targeting mycobacterium *tuberculosis* DNA Gyrase A subunit.

The various novel bacterial type II topoisomerase inhibitors (NBTIs) belonging to N-linked aminopiperidine class with anti-bacterial activity were reported in literature. The published crystal structure of NBTIs (GSK299423) bound to *S. aureus* DNA gyrase provided key insights into the important interactions involved in the gyrase active site. A non-overlapping mechanism of binding distinct between FQs and NBTIs with the S. aureus DNA gyrase could be inferred from this study. The unique binding mechanism of NBTIs enabled them to retain their activity against FQ resistant strains of *S. aureus*. This salient observation has triggered the search for novel chemotypes and to expand the chemical scope of NBTI for treatment of TB. However, the reported cardiac ion channel (hERG) liability associated with NBTIs posed a significant challenge in the clinical advancement of several NBTIs, e.g NXL101.

The chemical structures of NBTIs including the N-linked piperidines consisted of three parts, namely a bicyclic aromatic left-hand side (LHS), a mono or bicyclic right- hand side (RHS), and a linker region joining the RHS and LHS (**Figure 2.4**).

Hence, the current focus of study was to expand the chemical scope of antibacterial NBTIs for improved anti TB activity and hERG selectivity. Additionally to demonstrate structure property relationship (SPR) for oral bioavailability with *in vivo* efficacy to progress the lead series towards clinical candidate selection. Herein, we report medicinal chemistry efforts to reduce the hERG liability and improve *Mtb* MIC as well as oral bioavailability of these lead molecules. Additionally, we also describe the mechanism of inhibition of *Mtb* gyrase, characterization of spontaneous resistant mutants and efficacy in the acute and chronic mouse model of TB.

5.1 Development N-linked aminopiperidinyl alkyl quinolone and naphthyridones as potential *Mtb* GyrA inhibitors.

A focused library screening of antibacterial NBTIs collection followed by initial design of novel aminopiperidines with monocyclic substituted pyridine RHS ring system resulted in identification attractive lead series with potent *Mtb* MIC, gyrase inhibition and Caco2 permeability. However, initial lead compound had shown moderate hERG inhibition and hence further SAR expansion directed towards improving poteny and hERG selectivity with new design sets through polarity modulation of quinolone LHS and pka modulation of aminopiperidine linker regions of identified lead series (e.g **AP_5**).

AP_5
Mtb MIC: 0.25 µg/ml
Mtb Gyrase SC IC$_{50}$: 0.25 µM
hERG IC$_{50}$: 26 µM
Caco2: Papp : 13.6/7.4
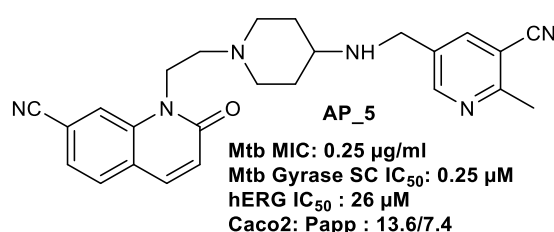
Figure 5.1: Chemical structure of novel lead molecule **AP_5**

5.1.1 Chemical synthesis and characterization of lead compounds

The synthesis of compounds with un-substituted aminopiperidine and methoxy or fluoro substituted aminopiperidine linker is described in **Scheme 5.1**, **5.2** and **5.3**, respectively. The alkylation of LHS (**24a-h**) with mesylate **25** in the presence of a base resulted in the formation of N-alkylated product (**26a-i**) as the major isomer along with a small amount of O-alkylated product. Wherever possible, the minor O-alkylated isomer was removed by column chromatography (Reck, F. *et al.*, 2011), otherwise the mixture was taken as such for N-Boc

deprotection. The free amines (**27a-i**) were obtained upon N-Boc deprotection of the intermediates 26a-i in the presence of an acid. Compounds **AP_4-AP_13** were synthesized from the amines **27a-i** either by reductive amination with RHS aldehydes (**31**, **34**) or an amide coupling with RHS acid (**33**) or alkylation with mesylate (**32**) (**Scheme 5.1**).

24a: R1= CN; R2= H; R3= H; X= C; Y= C; A= C
24b: R1= F; R2= H; X= N; Y= C; A= C
24c: R1= H; R2= OMe; X= N; Y= C; A= C
24d: R1= OMe; R2= H; R3= Br; X= C; Y= C; A= C
24f: R1= OMe; R2= H; R3= H; X= C; Y= N; A= N
24g: R1= F; R2= H; X= N; Y= C; A= N
24h: R1= OMe; R2= H; X= N; Y= C; A= N

26a: R1= CN; R2= H; R3= H; X= C; Y= C; A= C
26b: R1= F; R2= H; X= N; Y= C; A= C
26c: R1= H; R2= OMe; X= N; Y= C; A= C
26d: R1= OMe; R2= H; R3= Br; X= C; Y= C; A= C
26e: R1= OMe; R2= H; X= N; Y= C; A= C
26f: R1= OMe; R2= H; R3= H; X= C; Y= N; A= N
26h: R1= OMe; R2= H; X= N; Y= C; A= N
26i: R1= OMe; R2= H; R3= CN; X= C; Y= C; A= C

27a: R1= CN; R2= H; R3= H; X= C; Y= C; A= C
27b: R1= F; R2= H; X= N; Y= C; A= C
27c: R1= H; R2= OMe; X= N; Y= C; A= C
27e: R1= OMe; R2= H; X= N; Y= C; A= C
27f: R1= OMe; R2= H; R3= H; X= C; Y= N; A= N
27h: R1= OMe; R2= H; X= N; Y= C; A= N
27i: R1= OMe; R2= H; R3= CN; X= C; Y= C; A= C

RHS	**31**, RHS 1	**32**, RHS 2	**33**, RHS 3	**34**, RHS 4
Structure				
Reaction Condition	c	a	e	c

AP_4: R1= CN; R2= H; R3= H; X= C; Y= C; A= C; W= CH2; RHS 1
AP_5: R1= CN; R2= H; R3= H; X= C; Y= C; A= C; W= CH2; RHS 2
AP_6: R1= F; R2= H; X= N; Y= C; A= C; W= CH2; RHS 2
AP_7: R1= OMe; R2= H; X= N; Y= C; A= C; W= CH2; RHS 2
AP_7a: R1= H; R2= OMe; X= N; Y= C; A= C; W= CH2; RHS 2
AP_9: R1= OMe; R2= H; R3= CN; X= C; Y= C; A= C; W= CH2; RHS 2
AP_10: R1= OMe; R2= H; X= N; Y= C; A= C; W= CO; RHS 3
AP_11: R1= OMe; R2= H; X= N; Y= C; A= C; W= CH2; RHS 4
AP_12: R1= OMe; R2= H; R3= H; X= C; Y= N; A= N; W= CH2; RHS 2
AP_13: R1= OMe; R2= H; X= N; Y= C; A= N; W= CH2; RHS 2

Reagents: (a) Na₂CO₃, DMF, 70 °C (b) 4N HCl in Dioxane, 55 °C (c) NaBH₃CN, DCE or CHCl₃ /EtOH, 65-80 °C (d) NaOMe, MeOH, 75 °C (e) **33**, HATU, DIPEA, DMF, RT (f) ZnCN₂, Zn(OAc)₂, Zn, Pd₂(dba)₃, dppf, DMF, 100 °C, 23 % (g) Pd₂(dba)₃, dppf, CuCN, DMF, 110 °C, 68 %

Scheme 5.1: Synthesis of compounds **AP_4 – AP_13**.

The mesylate **25**, LHS fragment **24a** and **24f** were synthesized as reported (Reck,F *et al.*, 2011), whereas LHS fragments **24b** and **24c** synthesized using an optimized Heck protocol as described earlier (Eric, et al., 2010). The synthetic scheme for synthesis of **24c** and **24d** as shown in Figure **4.11**. The LHS **24h** was synthesized from its fluoro precursor **24g** using NaOMe (Lluis *et al*, 2008). Detailed synthesis of the precursor aldehydes **31 & 34**, the mesylates **32 &** and acid **33** are described in **Figures 4.12** and **4.13**

Compound **AP_8** was synthesized as described in **Scheme 5.2**. The intermediate naphthyridone **24c** was N-methylated with methyl iodide in the presence of cesium carbonate to generate intermediate **8-ii**. O-demethylation of **8-ii** with HBr provided the naphthyridine-1, 5 dione **8-iii**, which upon alkylation with 2-bromoethanol gave both the N & O-alkylated isomers. The N-alkylated isomer, **8-iv** was converted to a mesylate **8-v** with MsCl under basic conditions. The alkylation of **29e** with a mesylate **8-v** under basic conditions resulted in compound **AP_ 8.**
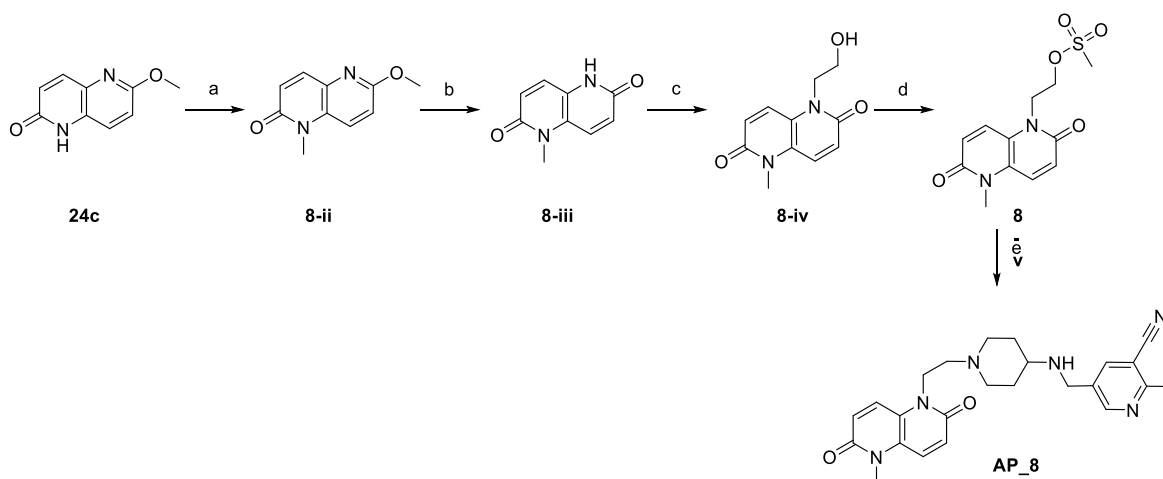
Reagents: (a) MeI, Cs$_2$CO$_3$, DMSO, 60 $^\circ$C, 83 % (b) 48% HBr, 80 $^\circ$C, > 95% (c) 2-Bromoethanol, Cs$_2$CO$_3$, DMSO, 95 $^\circ$C, > 95% (d) MsCl, TEA, DCM, 0 $^\circ$C, > 95% (e) **29e**, Na$_2$CO$_3$, DMF, 70 $^\circ$C, 98 %

Scheme 5.2: Synthesis of **AP_8**

The synthesis of compounds with substituted aminopiperidine linker is shown in **Scheme 5.3**. The reductive amination of the modified aminopiperidine linkers (**29a-d**) with the LHS aldehyde (**28a**) or alkylation with mesylates (**28b-c**) in the presence of a base provided the final compounds (**AP_15** to **AP_16**, **AP_18** to **AP_21**) in moderate to good yields. The compounds **AP_17** and **AP_22** were obtained by alkylation of **18b** with mesylate **32** and reductive amination of **23b** with aldehyde 30 respectively. Aldehyde **30** was synthesized as reported earlier (Hameed, P. S. *et al.*, 2013).

28a: R1= CN; R2= H; X= C; R4= CHO
28b: R1= F; X= N; R4= -CH₂-OMs
28c: R1= OMe; X= N; R4= -CH₂-OMs

29a: R3= F, cis, *3S4R,* R5= RHS 1
29b: R3= F, cis, *3S4R,* R5= RHS 2
29c: R3= F, cis, *3R4S,* R5= RHS 2
29d: R3= OMe, cis, *3S4R,* R5= BOC

AP_14: R1= CN; R2= H; X= C; R3= F, cis, *3S4R;* R5= RHS 1
AP_15: R1= F; X= N; R3= F, cis, *3S4R;* R5= RHS 1
AP_16: R1= OMe; X= N; R3= F, cis, *3S4R,* R5= RHS 1
18a: R1= OMe; X= N; R3= OMe, cis, *3S4R;* R5= BOC
18b: R1= OMe; X= N; R3= OMe, cis, *3S4R,* R5= H
32, b AP_17: R1= OMe; X= N; R3= OMe, cis, *3S4R;* R5= RHS1
AP_18: R1= F; X= N; R3= F, cis, *3S4R;* R5= RHS 2
AP_19: R1= F; X= N; R3= F, cis, *3R4S;* R5= RHS 2
AP_20: R1= OMe; X= N; R3= F, cis, *3S4R,* R5= RHS 2
22a: R1= F; X= N; R3= F, cis, *3R4S,* RHS 2
AP_21: R1= OMe; X= N; R3= F, cis, *3R4S,* RHS 2
23a: R1= F; X= N; R3= OMe, cis, *3S4R,* R5= BOC
23b: R1= F; X= N; R3= OMe, cis, *3S4R,* R5= H
30, a 23c: R1= F; X= N; R3= OMe, cis, *3S4R,* R5= RHS 2
AP_22: R1= OMe; X= N; R3= OMe, cis, *3S4R,* R5= RHS 2

R5= RHS 1	R5= RHS 2	30

Scheme 5.3: Synthesis of compounds **AP_14 – AP_22**.

5.1.2 Experimental protocol utilised for synthesis of final compounds

Procedure for the synthesis of final compounds from unsubstituted aminopiperidine linker (Scheme 5.1, AP_ 1 to AP_13)

The synthesis of compound **AP_1**, **AP_2** and **AP_3** were previously reported (Reck, F. *et al.*, 2011).

1-(2-(4-((5-Cyano-6-methylpyridin-2-yl)methylamino)piperidin-1-yl)ethyl)-2-oxo-1,2-dihydroquinoline-7-carbonitrile (AP_4)

In a 100 mL round-bottomed flask, **27a** (250 mg, 0.84 mmol) and **31** (185 mg, 1.27 mmol) were taken in DCE (8 mL) and ethanol (2.000 mL) mixture. Acetic acid (0.050 mL, 0.84 mmol) was added to it and the RM was then heated at 80 °C for 1 hr. The RM was then cooled to RT and then Sodium triacetoxyborohydride (536 mg, 2.53 mmol) was added to it portion wise. The RM was then stirred at RT for overnight. The reaction was monitored by LCMS. The profile showed formation of imine and only 20% product. Sodium cyanoborohydride (106 mg, 1.69 mmol) was added to RM and it was stirred at RT for 4 hrs. The RM was then evaporated and the residue was then neutralised with saturated NaHCO₃. It was then partitioned between DCM (5%MeOH) and water. The organic layer was then separated, dried (Na₂SO₄) and evaporated

to get a residue. It was then chromatographed with DCM/MeOH to get AP_4 (75 mg, 20.85 %). ^{1}H NMR (300 MHz, DMSO- d_6) δ1.24 (d, J=8.85 Hz, 2 H) 1.81 (d, J=10.74 Hz, 2 H) 2.04 (t, J=10.55 Hz, 2 H) 2.15 (br. s., 1 H) 2.38 (br. s., 1 H) 2.51 (s, 3 H) 2.55 (br. s., 2 H) 2.92 (d, J=11.11 Hz, 2 H) 3.76 (br. s., 2 H) 4.37 (t, J=6.50 Hz, 2 H) 6.79 (d, J=9.42 Hz, 1 H) 7.66 (d, J=8.10 Hz, 1 H) 7.84 (d, J=7.72 Hz, 1 H) 7.93 (t, J=8.29 Hz, 2 H) 8.01 (d, J=9.61 Hz, 1 H) 8.09 (s, 1 H); HRMS: m/z (ES[+]) = 427.21721(MH[+]) for $C_{25}H_{26}N_6O$.

1-(2-(4-((5-Cyano-6-methylpyridin-3-yl)methylamino)piperidin-1-yl)ethyl)-2-oxo-1,2-dihydroquinoline-7-carbonitrile (AP_5)

In a 500 ml RBF, **27a** (11 g, 37.12 mmol) and sodium carbonate, monohydrate (13.81 g, 111.35 mmol) were taken in DMF (100 mL). In another liquid addition funnel **32** (8.40 g, 37.12 mmol) was taken in DMF (100 mL) and the solution was then added slowly to the above RM. The RM was then stirred at RT for 4 hrs. The solvent was evaporated to dryness and the residue was then partitioned between DCM (5% MeOH) and water. The organic layer was then separated, dried and chromatographed with DCM/MEOH to get a slightly crude product. The solid was then triturated in succession with DCM/Hexane, MeOH/Ether to get slight impure AP_5 (9.30 g, 58.7 %), which was again triturated with water/MeOH to get 4.85 g pure compound. The remaining amount was later purified by preparative HPLC to get another 1.577 g of product. ^{1}H NMR (300 MHz, DMSO- d_6) δ 1.20 (d, J=12.43 Hz, 3 H) 1.76 (d, J=11.87 Hz, 2 H) 1.92 - 2.11 (m, 2 H) 2.30 (d, J=14.51 Hz, 2 H) 2.54 (br. s., 1 H) 2.65 (s, 3 H) 2.90 (d, J=11.68 Hz, 2 H) 3.74 (s, 2 H) 4.36 (t, J=6.59 Hz, 2 H) 6.78 (d, J=9.42 Hz, 1 H) 7.65 (d, J=7.91 Hz, 1 H) 7.91 (d, J=8.10 Hz, 1 H) 8.00 (d, J=9.61 Hz, 1 H) 8.08 (s, 1 H) 8.15 (d, J=1.88 Hz, 1 H) 8.66 (d, J=1.88 Hz, 1 H); HRMS: m/z (ES[+]) = 427.22570 (MH[+]) for $C_{25}H_{26}N_6O$.

5-((1-(2-(7-Fluoro-2-oxo-1,5-naphthyridin-1(2H)-yl)ethyl)piperidin-4-ylamino)methyl)-2-methylnicotinonitrile (AP_6)

In a 100 mL round-bottomed flask, **27b** (1.500 g, 5.17 mmol), **32** (1.286 g, 5.68 mmol) and sodium carbonate (1.095 g, 10.33 mmol) were taken in DMF (25 mL) to give a yellowish solution under nitrogen atmosphere and heated to 70 °C for 1h. Solvent was evaporated from the reaction mixture. Water was added to it and extracted using 10% methanol in DCM (4 X 25ml). The combined organic layers were concentrated to dryness and purified by silica gel chromatography using 0 to 18% Methanol in DCM to obtain 6 (1.400 g, 64.4 %) as brown solid. 200mg of the product was purified by preparative HPLC to obtain product as di-acetate

salt. ^{1}H NMR (300 MHz, DMSO- d_6) δ1.15 - 1.29 (m, 2 H) 1.73 - 1.83 (m, 2 H) 1.91 (s, 6 H) 1.97 - 2.10 (m, 2 H) 2.31 - 2.43 (m, 1 H) 2.53 - 2.59 (m, 2 H) 2.65 (s, 3 H) 2.90 (d, J=11.68 Hz, 3 H) 3.77 (s, 2 H) 4.31 (t, J=6.59 Hz, 2 H) 6.83 (d, J=9.80 Hz, 1 H) 7.95 (d, J=9.80 Hz, 1 H) 8.01 (dd, J=11.30, 2.07 Hz, 1 H) 8.16 (d, J=1.88 Hz, 1 H) 8.56 (d, J=2.45 Hz, 1 H) 8.67 (d, J=1.88 Hz, 1 H); HRMS: m/z (ES$^+$) = 421.21490 (MH$^+$) for $C_{23}H_{25}FN_6O$

5-((1-(2-(7-Methoxy-2-oxo-1,5-naphthyridin-1(2H)-yl)ethyl)piperidin-4-ylamino)methyl)-2-methylnicotinonitrile (AP_7)

In a 500 mL round-bottomed flask, **AP_6** (6.3 g, 14.98 mmol) was taken in methanol (100 mL) under N_2. To this sodium methoxide (3.24 g, 59.93 mmol) was added while stirring. The resulting reaction was stirred at 70 °C for 6 h. Reaction was cooled to RT, solvent was evaporated to dryness. Obtained solid was diluted with water and extracted with 5 % methanol in DCM. Organic layer was separated, washed with brine and dried to get a residue. The residue was then purified on silica with DCM/MeOH to a slightly crude compound, which on trituration with acetonitrile afforded the pure **AP_7** (4.01 g, 61.9 %). ^{1}H NMR (300 MHz, DMSO- d_6) δ 1.11 - 1.32 (m, 2 H) 1.76 (d, J=10.93 Hz, 2 H) 1.94 - 2.10 (m, 2 H) 2.28 (d, J=18.46 Hz, 2 H) 2.54 (br. s., 2 H) 2.64 (s, 3 H) 2.91 (d, J=11.30 Hz, 2 H) 3.34 (s, 2 H) 3.98 (s, 3 H) 4.35 (t, J=6.78 Hz, 2 H) 6.66 (d, J=9.80 Hz, 1 H) 7.41 (d, J=2.26 Hz, 1 H) 7.86 (d, J=9.61 Hz, 1 H) 8.15 (d, J=1.88 Hz, 1 H) 8.28 (d, J=2.26 Hz, 1 H) 8.66 (d, J=2.07 Hz, 1 H); HRMS: m/z (ES$^+$) = 433.23590(MH$^+$) for $C_{24}H_{28}N_6O_2$.

5-((1-(2-(6-Methoxy-2-oxo-1,5-naphthyridin-1(2H)-yl)ethyl)piperidin-4-ylamino)methyl)-2-methylnicotinonitrile (AP_7a)

In a 100 mL round-bottomed flask, **27c** (800 mg, 2.65 mmol), **32** (658 mg, 2.91 mmol) and sodium carbonate (561 mg, 5.29 mmol) were taken in DMF (20 mL) to give a yellowish solution under nitrogen atmosphere and heated to 70 °C for 1hr. Solvent was evaporated from the reaction mixture. Water was added to it and extracted using 10% methanol in DCM (3 X 50ml). The combined organic layers were concentrated to dryness and purified by silica gel chromatography using 0 to 15% Methanol in DCM to obtain product (270mg) which was impure. Therefore, it was repurified by preparative HPLC to obtain **AP_7a** (270 mg, 23.59 %) as white solid. ^{1}H NMR (300 MHz, DMSO- d_6) δ 1.11 − 1.33 (m, 2 H) 1.67 − 1.84 (m, 2 H) 2.01 (t, J=11.02 Hz, 2 H) 2.18 − 2.38 (m, 2 H) 2.64 (s, 3 H) 2.79 − 2.98 (m, 2 H) 3.73 (s, 2 H) 3.91 (s, 3 H) 4.31 (t, J=6.78 Hz, 2 H) 6.79 (d, J=9.80 Hz, 1 H) 7.12 (d, J=9.23 Hz, 1 H) 7.80

(d, J=9.80 Hz, 1 H) 8.00 (d, J=9.23 Hz, 1 H) 8.15 (d, J=1.88 Hz, 1 H) 8.66 (d, J=1.88 Hz, 1 H); HRMS: m/z (ES$^+$) = 433.23427(MH$^+$) for $C_{24}H_{28}N_6O_2$.

2-Methyl-5-((1-(2-(5-methyl-2,6-dioxo-5,6-dihydro-1,5-naphthyridin-1(2H)-yl)ethyl)piperidin-4-ylamino)methyl)nicotinonitrile (AP_8)

In a 100 mL round-bottomed flask, **8-v** (500 mg, 1.68 mmol), **29e** (386 mg, 1.68 mmol) and sodium carbonate (355 mg, 3.35 mmol) were taken in DMF (5 mL) to give a yellowish solution under nitrogen atmosphere and heated to 70 °C for 1h. Solvent was evaporated from the reaction mixture. Water was added to it and extracted using 10% methanol in DCM (3 X 25ml).The combined organic layers were concentrated to dryness and purified by preparative HPLC to obtain **AP_8** (160 mg, 22.07 %) as yellow solid. ^{1}H NMR (400 MHz, DMSO- d_6) δ 1.14 - 1.27 (m, 2 H) 1.70 - 1.80 (m, 2 H) 1.96 - 2.06 (m, 2 H) 2.25 - 2.36 (m, 2 H) 2.39 - 2.49 (m, 2 H) 2.65 (s, 3 H) 2.84 - 2.89 (m, 2 H) 3.62 (s, 3 H) 3.73 (s, 2 H) 4.31 (t, J=6.78 Hz, 2 H) 6.78 (s, 1 H) 6.76 (s, 1 H) 7.82 - 8.01 (m, 2 H) 8.15 (d, J=2.01 Hz, 1 H) 8.66 (d, J=2.01 Hz, 1 H); HRMS: m/z (ES+) = 433.23518(MH$^+$) for $C_{24}H_{28}N_6O_2$.

1-(2-(4-((5-Cyano-6-methylpyridin-3-yl)methylamino)piperidin-1-yl)ethyl)-7-methoxy-2-oxo-1,2-dihydroquinoline-5-carbonitrile (AP_9)

In a 100 mL round-bottomed flask, **27i** (500 mg, 1.53 mmol), **32** (416 mg, 1.84 mmol) and sodium carbonate(325 mg, 3.06 mmol) were taken in DMF (10 mL) to give a yellowish solution under nitrogen atmosphere and heated to 70 °C for 1h. Solvent was evaporated from the reaction mixture. Water was added to it and extracted using 10% methanol in DCM (3 X 25 ml). The combined organic layers were concentrated to dryness and purified by silica gel chromatography to obtain impure product (250mg). This was repurified by preparative HPLC to obtain **AP_9** (60.0 mg, 8.58 %) as white solid. ^{1}H NMR (400 MHz, DMSO- d_6) δ1.10 - 1.33 (m, 2 H) 1.75 - 1.78 (m, 2 H) 2.02 (t, J=10.54 Hz, 2 H) 2.15 - 2.39 (m, 2 H) 2.55 (m, 2H) 2.65 (s, 3 H) 2.89 -2.92 (m, 2 H) 3.74 (br. s., 2 H) 3.96 (s, 3 H) 4.37 (t, J=7.03 Hz, 2 H) 6.68 (d, J=9.54 Hz, 1 H) 7.31 (d, J=2.01 Hz, 1 H) 7.54 (d, J=2.51 Hz, 1 H) 7.92 (d, J=10.04 Hz, 1 H) 8.15 (d, J=2.01 Hz, 1 H) 8.66 (d, J=2.01 Hz, 1 H); HRMS: m/z (ES$^+$) = 457.23416 (MH$^+$) for $C_{26}H_{28}N_6O_2$.

5-Cyano-N-(1-(2-(7-methoxy-2-oxo-1,5-naphthyridin-1(2H)-yl)ethyl)piperidin-4-yl)-6-methylnicotinamide (AP_10)

In a 50 mL round-bottomed flask, **33** (0.161 g, 0.99 mmol) was dissolved in DMF (5 mL) under N_2. To this DIPEA (0.520 mL, 2.98 mmol) and HATU (0.754 g, 1.98 mmol) was added and stirred. After 5 min, **27e** (.300 g, 0.99 mmol) was added. The resulting reaction was stirred at RT for 3 h. DMF was evaporated to dryness and diluted with water and extracted with 10% methanol in DCM and concentrated. Purification was done by preparative HPLC to get pure product **AP_10** (0.200 g, 45.1 %). ^{1}H NMR (300 MHz, DMSO- d_6) δ1.41 - 1.61 (m, 2 H) 1.80 (d, J=9.98 Hz, 2 H) 2.05 - 2.22 (m, 2 H) 2.59 (t, J=6.59 Hz, 2 H) 2.73 (s, 3 H) 3.01 (d, J=11.30 Hz, 2 H) 3.77 (dd, J=7.63, 3.67 Hz, 1 H) 4.00 (s, 3 H) 4.39 (t, J=6.59 Hz, 2 H) 6.67 (d, J=9.61 Hz, 1 H) 7.44 (d, J=2.07 Hz, 1 H) 7.88 (d, J=9.61 Hz, 1 H) 8.29 (d, J=2.26 Hz, 1 H) 8.51 (d, J=7.54 Hz, 1 H) 8.59 (d, J=2.07 Hz, 1 H) 9.08 (d, J=2.26 Hz, 1 H); HRMS: *m/z* (ES[+]) = 447.21398(MH[+]) for $C_{24}H_{26}N_6O_3$.

2-Methoxy-5-((1-(2-(7-methoxy-2-oxo-1,5-naphthyridin-1(2H)-yl)ethyl)piperidin-4-ylamino)methyl)nicotinonitrile (AP_11)

In a 50 mL round-bottomed flask, **27e** (0.050 g, 0.17 mmol) and **34** (0.027 g, 0.17 mmol) was taken in a mixture of solvent ethanol (5 mL) and chloroform (5.00 mL) under N_2. To this acetic acid (0.095 µL, 1.65 µmol) was added reaction was stirred at 65 °C .A turbid solution was observed. After 1 h reaction was cooled to RT and sodium cyanoborohydride (0.021 g, 0.33 mmol) was added. The resulting reaction was stirred at RT for another 6 hrs. Reaction solvents was evaporated to dryness and diluted with sat. $NaHCO_3$ solution .Crude was extracted with 5 % methanol in DCM and washed with water and brine. Organic layer was separated and concentrated. Purification was done using methanol/DCM as a mobile phase to get pure product 11 (0.045 g, 60.7 %). ^{1}H NMR (300 MHz, DMSO- d_6) δ 1.13 - 1.28 (m, 2 H) 1.77 (d, J=11.30 Hz, 2 H) 2.04 (t, J=10.46 Hz, 2 H) 2.16 (br. s., 1 H) 2.30 (d, J=14.51 Hz, 1 H) 2.55 (m, 2H) 2.91 (d, J=11.68 Hz, 2 H) 3.68 (s, 2 H) 3.98 (s, 6 H) 4.35 (t, J=6.88 Hz, 2 H) 6.66 (d, J=9.61 Hz, 1 H) 7.41 (d, J=2.07 Hz, 1 H) 7.87 (d, J=9.61 Hz, 1 H) 8.19 (d, J=2.26 Hz, 1 H) 8.28 (d, J=2.45 Hz, 1 H) 8.39 (d, J=2.26 Hz, 1 H); HRMS: *m/z* (ES[+]) = 449.22926 (MH[+]) for $C_{24}H_{28}N_6O_3$.

5-((1-(2-(6-Methoxy-3-oxopyrido[3,2-b]pyrazin-4(3H)-yl)ethyl)piperidin-4-ylamino)methyl)-2-methylnicotinonitrile (AP_12)

In a 100 mL round-bottomed flask, 4-(2-(4-aminopiperidin-1-yl)ethyl)-6-methoxypyrido[3,2-b]pyrazin-3(4H)-one (**27f**) (1.5g, 4.94 mmol) and **32** (1.342 g, 5.93 mmol) and sodium carbonate (0.545 ml, 9.89 mmol) were taken in DMF (5 mL) to give a brown solution. The resulting reaction mixture was heated to 74 °C for 1h. The RM was evaporated and taken in water. The aqueous layer was extracted with DCM (3 times).The DCM layer was evaporated and the crude compound was purified by preparative HPLC to obtain **AP_12** (0.500 g, 20.49 %) as monoacetate salt. ^{1}H NMR (300 MHz, DMSO- d_6) δ 1.26 – 1.28 (m, 2 H) 1.56-1.57 (m, 2 H) 1.9 (s, 3 H) 2.0-2.1 (m, 2 H) 2.2-2.4 (m,1 H) 2.6-2.7 (m, 1 H) 2.8 (s, 3 H) 2.9-3.0 (m, 2 H) 3.7 (s, 2 H) 4.0 (s, 3 H) 4.2-4.5 (t, 2 H) 6.80 (d, 1 H) 8.0-8.2 (m, 3 H) 8.6 (s, 1H); HRMS: m/z (ES$^+$) = 434.23002 (MH$^+$) for $C_{23}H_{27}N_7O_2$•[CH$_3$COOH].

5-((1-(2-(7-Methoxy-2-oxopyrido[3,2-b]pyrazin-1(2H)-yl)ethyl)piperidin-4-ylamino)methyl)-2-methylnicotinonitrile (AP_13)

In a 250 mL round-bottomed flask, **27h** (2.000 g, 6.59 mmol), **32** (1.641 g, 7.25 mmol), DIPEA (3.45 mL, 19.78 mmol) and sodium carbonate (1.398 g, 13.19 mmol) were taken in DMF (25 mL) to give a yellowish solution under nitrogen atmosphere and heated to 70 °C for 1h. Solvent was evaporated from the reaction mixture. Water was added to it and extracted using 10% methanol in DCM (3 X 50ml). The combined organic layers were concentrated to dryness and purified by silica gel chromatography using 0 to 35% methanol in DCM and 0.1 % ammonia to obtain product (700 mg), which was impure. Therefore, it was re-purified by preparative HPLC to obtain **AP_13** (0.100 g, 3.50 %). ^{1}H NMR (300 MHz, DMSO- d_6) δ 1.07 – 1.26 (m, 2 H) 1.72 – 1.75 (m, 2 H) 1.92 – 2.09 (m, 2 H) 2.22 – 2.36 (m, 2H) 2.55 (t, J=6.59 Hz, 2 H) 2.64 (s, 3 H) 2.82 – 2.96 (m, 2 H) 3.72 (s, 2 H) 4.00 (s, 3 H) 4.34 (t, J=6.50 Hz, 2 H) 7.51 (d, J=2.45 Hz, 1 H) 8.14 (d, J=1.70 Hz, 1 H) 8.25 (s, 1 H) 8.32 (d, J=2.45 Hz, 1 H) 8.65 (d, J=1.88 Hz, 1 H); HRMS: m/z (ES+) = 434.23032 (MH+) for $C_{23}H_{27}N_7O_2$.

Procedure for the synthesis of final compounds from fluro and methoxy substituted aminopiperidine linker (Scheme 5.3, AP_ 14 to AP_22)

1-(2-((3S,4R)-4-((5-Cyano-6-methylpyridin-3-yl)methylamino)-3-fluoropiperidin-1-yl)ethyl)-2-oxo-1,2-dihydroquinoline-7-carbonitrile (AP_14)

In a 50 ml RB flask, **29a** (487 mg, 0.82 mmol) was dissolved in DMF (15 mL) and DIPEA (0.576 mL, 3.30 mmol) was added and stirred for 5 minutes and then **28a** (175 mg, 0.82 mmol) were added and heated to 70°C for 2 hr and then reaction mixture was brought to RT and added sodium triacetoxyborohydride (524 mg, 2.47 mmol), stirred at RT for overnight. Reaction mixture was filtered through sintered funnel and was washed with 20% MeOH in DCM and concentrated. The crude compound was basified with saturated sodium bicarbonate solution and extracted with 15% MeOH/DCM and the solvent was evaporated under vacuum to get crude product and the crude product was purified by preparative HPLC to get **AP_14** (200 mg, 54.6 %). ^{1}H NMR (400 MHz, DMSO- d_6) δ 1.64 (m., 2 H) 2.13 (t, 1 H) 2.40-2.20 (m, 1 H) 2.57 (t, 4 H) 2.87 (s, 3H) 3.14 (m,1H) 2.97(m,1H) 3.80 (s, 2 H) 4.28 – 4.44 (m, 2 H) 4.65 & 4.78 (s, 1 H) 6.79 (d, J=9.54 Hz, 1 H) 7.66 (d, J=8.03 Hz, 1 H) 7.91 (d, J=8.03 Hz, 1 H) 8.01 (d, J=9.54 Hz, 1 H) 8.10 (s, 1 H) 8.17 (d, J=2.01 Hz, 1 H) 8.68 (d, J=2.01 Hz, 1 H); HRMS: m/z (ES$^+$) = 445.21672 (MH$^+$) for $C_{25}H_{25}FN_6O$.

5-(((3S,4R)-3-Fluoro-1-(2-(7-fluoro-2-oxo-1,5-naphthyridin-1(2H)-yl)ethyl)piperidin-4-ylamino)methyl)-2-methylnicotinonitrile (AP_15)

In a 100 mL round-bottomed flask, **29a** (520 mg, 2.10 mmol), **28b** (500 mg, 1.75 mmol) and sodium carbonate (370 mg, 3.49 mmol) were taken in DMF (10 mL) to give a yellowish solution under nitrogen atmosphere and heated to 70 °C for 1h. Solvent was evaporated from the reaction mixture. Water was added to it and extracted using 10% methanol in DCM (3 X 25ml).The combined organic layers were concentrated to dryness and purified by silica gel chromatography to obtain **AP_15** (450 mg, 58.8 %) as yellow gel. ^{1}H NMR (400 MHz, DMSO-d_6) δ 1.48 - 1.63 (m, 1 H) 1.63 - 1.74 (m, 1 H) 2.10 - 2.23 (m, 1 H) 2.25 - 2.44 (m, 2 H) 2.46 - 2.54 (m, 1 H) 2.63 (t, J=6.53 Hz, 2 H) 2.70 (s, 3 H) 2.90 - 3.03 (m, 1 H) 3.11 - 3.23 (m, 1 H) 3.85 (s, 2 H) 4.26 - 4.45 (m, 2 H) 4.69 - 4.81 (2m, 1 H) 6.89 (d, J=9.54 Hz, 1 H) 8.00 (d, J=10.04 Hz, 1 H) 8.09 (dd, J=11.04, 2.01 Hz, 1 H) 8.21 (d, J=1.51 Hz, 1 H) 8.61 (d, J=2.51 Hz, 1 H) 8.73 (d, J=2.01 Hz, 1 H); HRMS: m/z (ES+) = 439.20623 (MH$^+$) for $C_{23}H_{24}F_2N_6O$.

5-(((3S,4R)-3-Fluoro-1-(2-(7-methoxy-2-oxo-1,5-naphthyridin-1(2H)-yl)ethyl)piperidin-4-ylamino)methyl)-2-methylnicotinonitrile (AP_16)

In a 500 mL round-bottomed flask, 16 (8.50 g, 19.39 mmol) and sodium methoxide (4.19 g, 77.54 mmol) were taken in MeOH (150 mL) to give a yellow solution. The resulting reaction mixture was heated to reflux for 2 h. Solvent was evaporated from the reaction mixture, water

was added to it. This was extracted using 10% methanol in DCM (3X200ml) and the combined organic layers were concentrated and purified by silica gel chromatography using 0 to 10% Methanol in DCM to obtain **AP_16** (5.5 g) as off white solid, which was low melting and hygroscopic. Therefore, freebase was dissolved in DCM (60ml) and HCl in ether (85ml) was added to it. The precipitated solid was stirred at RT for 2hrs and filtered. The filtered solid was further triturated with methanol/Acetonitrile ,filtered and dried to obtain HCl salt of **AP_16** (6.50 g, 64.1 %) as pale yellow solid. ^{1}H NMR (300 MHz, DMSO- d_6) δ 2.18 - 2.47 (m, 2 H) 2.72 (s, 3 H) 3.23 - 3.75 (m, 7 H) 4.07 (s, 3 H) 4.26 - 4.46 (m, 2 H) 4.63 - 4.86 (m, 2 H) 5.50 - 5.66 (d, J=45 Hz 1H), 6.73 (d, J=9.80 Hz, 1 H) 7.75 (s, 1 H) 7.95 (d, J=9.80 Hz, 1 H) 8.34 (d, J=2.07 Hz, 1 H) 8.57 (d, J=2.07 Hz, 1 H) 8.95 (d, J=2.07 Hz, 1 H) 10.22 - 10.33 (2br. s., 2 H) 11.25 (br. s., 1 H); HRMS: *m/z* (ES$^+$) = 451.22543 (MH$^+$) for $C_{24}H_{27}FN_6O_2$•2[HCl].

5-(((3S,4R)-3-Methoxy-1-(2-(7-methoxy-2-oxo-1,5-naphthyridin-1(2H)-yl)ethyl)piperidin-4-ylamino)methyl)-2-methylnicotinonitrile (AP_17)

In a 50 ml RB flask , **18b** (150 mg, 0.45 mmol) was dissolved in DMF (5mL) and sodium carbonate (143 mg, 1.35 mmol) was added and stirred for 2 minutes and then **32** (102 mg, 0.45 mmol) was added and heated to 70°C for 2 h. Reaction mixture was concentrated under vacuum and the residue basified with saturated NaHCO$_3$ solution and concentrated under vacuum and it was purified by preparative HPLC to get **AP_17** (30.0 mg, 12.42 %) as a gum. ^{1}H NMR (300 MHz, DMSO- d_6) δ 1.35 - 1.52 (m, 1 H) 1.58 - 1.74 (m, 1 H) 1.97 - 2.11 (m, 1 H) 2.20 - 2.44 (m, 2 H) 2.54 - 2.61 (m, 2 H) 2.61 - 2.85 (m, 6 H) 3.17 (s, 3 H) 3.25 - 3.32 (m, 1 H) 3.74 (d, J=4.33 Hz, 2 H) 3.98 (s, 3 H) 4.27 - 4.44 (m, 2 H) 6.66 (d, J=9.61 Hz, 1 H) 7.43 (s, 1 H) 7.86 (d, J=9.80 Hz, 1 H) 8.17 (s, 1 H) 8.27 (d, J=2.07 Hz, 1 H) 8.67 (s, 1 H); HRMS: *m/z* (ES+)= 463.24532 (MH$^+$) for $C_{25}H_{30}N_6O_3$.

6-(((3S,4R)-3-Fluoro-1-(2-(7-fluoro-2-oxo-1,5-naphthyridin-1(2H)-yl)ethyl)piperidin-4-ylamino)methyl)-2H-pyrido[3,2-b][1,4]oxazin-3(4H)-one (AP_18)

In a 250 mL round-bottomed flask, **28b** (7.86 g, 27.47 mmol), **29b** (7.00 g, 24.97 mmol) and sodium carbonate(5.29 g, 49.95 mmol) were taken in DMF (50 mL) to give a yellowish solution under nitrogen atmosphere and heated to 70 °C for 1h. Solvent was evaporated from the reaction mixture. Water was added to it and extracted using 10% methanol in DCM (5 X 75ml).The combined organic layers were concentrated to dryness and purified by silica gel column using 0 to 12% Methanol in DCM to obtain **AP_18** (5.40 g, 46.0 %) as white solid. ^{1}H

NMR (300 MHz, DMSO- d_6) δ 1.44 - 1.68 (m, 2 H) 2.2 - 2.39 (m, 3 H) 2.57 (t, J=6.59 Hz, 2 H) 2.84 - 2.97 (m, 1 H) 3.06 - 3.20 (m, 1 H) 3.60 - 3.82 (m, 2 H) 4.14 - 4.43 (m, 2 H) 4.61 (s, 3 H) 4.63 - 4.79 (d, J=45 Hz, 1 H) 6.83 (d, J=9.80 Hz, 1 H) 7.02 (d, J=8.10 Hz, 1 H) 7.30 (d, J=7.91 Hz, 1 H) 7.95 (d, J=9.80 Hz, 1 H) 8.04 (dd, J=11.21, 2.17 Hz, 1 H) 8.56 (d, J=2.26 Hz, 1 H) 11.20 (s, 1 H); HRMS: m/z (ES+) = 471.19674 (MH$^+$) for $C_{23}H_{24}F_2N_6O_3$.

6-(((3R,4S)-3-Fluoro-1-(2-(7-fluoro-2-oxo-1,5-naphthyridin-1(2H)-yl)ethyl)piperidin-4-ylamino)methyl)-2H-pyrido[3,2-b][1,4]oxazin-3(4H)-one (AP_19)

In a 250 ml RB flask, **29c** (3.50 g, 12.49 mmol) was dissolved in DMF (50mL) and Na$_2$CO$_3$ (3.97 g, 37.46 mmol) was added and stirred for 2 minutes and then **28b** (4.29 g, 14.98 mmol) was added and heated to 70°C for 2 h. Reaction mixture was concentrated under vacuum and the residue basified with saturated NaHCO$_3$ solution and concentrated under vacuum and it was purified by preparative HPLC to get **AP_19** (2.90 g, 49.4 %). ^{1}H NMR (300 MHz, DMSO) δ 1.41-1.70 (m, 2H), 1.93-2.19 (m, 3H), 2.19-2.42 (m, 1H), 2.57 (t, J=6.69 Hz, 3H), 2.90 (d, J=11.30 Hz, 1H), 3.02-3.22 (m, 1H), 3.71 (d, J=3.39 Hz, 2H), 4.30 (tq, J=13.10, 6.77 Hz, 2H), 4.60 (s, 1H), 4.64- 4.79 (d, J=45 Hz 1H), 6.83 (d, J=9.61 Hz, 1H), 7.02 (d, J=8.10 Hz, 1H), 7.30 (d, J=8.10 Hz, 1H), 7.95 (d, J=9.80 Hz, 1H), 7.99-8.11 (m, 1H), 8.56 (d, J=2.07 Hz, 1H), 11.19 (s, 1H); HRMS: m/z (ES$^+$)= 471.19693 (MH$^+$) for $C_{23}H_{24}F_2N_6O_3$.

6-(((3S,4R)-3-Fluoro-1-(2-(7-methoxy-2-oxo-1,5-naphthyridin-1(2H)-yl)ethyl)piperidin-4-ylamino)methyl)-2H-pyrido[3,2-b][1,4]oxazin-3(4H)-one (AP_20)

In a 50 mL round-bottomed flask, **28c** (350 mg, 1.17 mmol), **29b** (803 mg, 1.29 mmol), DIPEA (0.615 mL, 3.52 mmol) and sodium carbonate (249 mg, 2.35 mmol) were taken in DMF (5 mL) to give a yellowish solution under nitrogen atmosphere and heated to 70 °C for 1h. Solvent was evaporated from the reaction mixture. Water was added to it and extracted using 10% methanol in DCM (3 X 25ml).The combined organic layers were concentrated to dryness and purified by preparative HPLC to obtain **AP_20** (120 mg, 21.20 %) as white solid. ^{1}H NMR (300 MHz, DMSO- d_6) δ 1.46 - 1.74 (m, 2 H) 2.16 (t, J=10.27 Hz, 1 H) 2.24 - 2.45 (m, 2 H) 2.59 (t, J=6.88 Hz, 3 H) 2.86 - 2.98 (m, 1 H) 3.08 - 3.17 (m, 1 H) 3.73 (s, 2 H) 3.99 (s, 3 H) 4.27 - 4.44 (m, 2 H) 4.61 (s, 2 H) 4.65 -4.82 (2m, 1 H) 6.66 (d, J=9.61 Hz, 1 H) 7.02 (d, J=8.10 Hz, 1 H) 7.30 (d, J=7.91 Hz, 1 H) 7.42 (d, J=2.26 Hz, 1 H) 7.87 (d, J=9.61 Hz, 1 H) 8.28 (d, J=2.26 Hz, 1 H) 11.15 (br. s., 1 H); HRMS: m/z (ES$^+$) = 483.21593 (MH+) for $C_{24}H_{27}FN_6O_4$.

6-(((3R,4S)-3-Fluoro-1-(2-(7-methoxy-2-oxo-1,5-naphthyridin-1(2H)-yl)ethyl)piperidin-4-ylamino)methyl)-2H-pyrido[3,2-b][1,4]oxazin-3(4H)-one (AP_21)
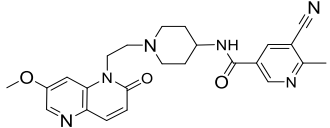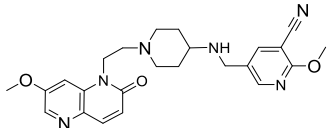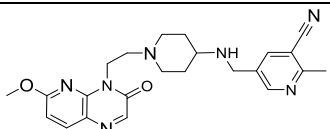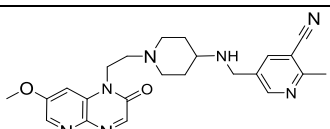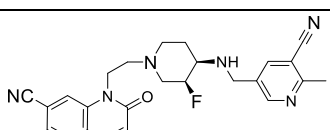
In a 100ml RB flask, 22a (1.5 g, 3.19 mmol) was dissolved in MeOH (30 mL) and sodium methoxide (0.689 g, 12.75 mmol) was added and heated to 80°C for overnight. The solvent was evaporated under vacuum and the residue was basified with saturated $NaHCO_3$ solution and extracted with 10% MEOH/DCM and the solvent was evaporated to get the crude compound. The crude product was purified by preparative HPL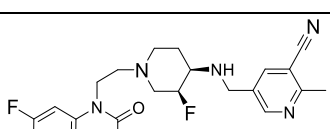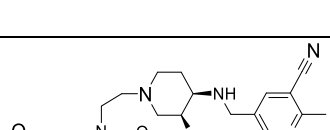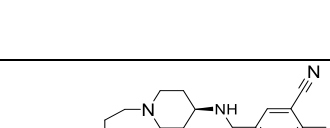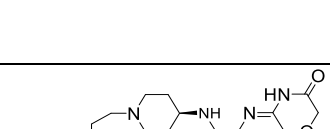C to get **AP_21** (1.2 g, 78 %). ^{1}H NMR (300 MHz, DMSO- d_6) δ 1.46-1.76 (m, 2H), 1.96-2.22 (m, 2H), 2.22-2.45 (m, 1H), 2.57 (t, J=6.78 Hz, 3H), 2.93 (d, J=11.30 Hz, 1H), 3.15 (br. s., 1H), 3.72 (s, 2H), 3.92-4.09 (m, 3H), 4.35 (t, J=6.22 Hz, 2H), 4.60 (s, 2H), 4.63-4.88 (d, J=51 Hz 1H), 6.66 (d, J=9.61 Hz, 1H), 7.02 (d, J=8.10 Hz, 1H), 7.30 (d, J=8.10 Hz, 1H), 7.42 (s, 1H), 7.87 (d, J=9.61 Hz, 1H), 8.28 (s, 1H), 11.19 (s, 1H); HRMS: m/z (ES[+])= 483.21640 (MH[+]) for $C_{24}H_{27}FN_6O_4$.
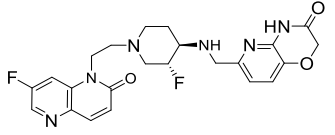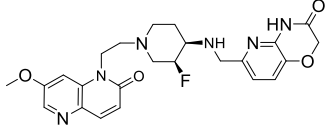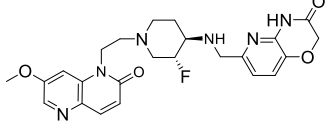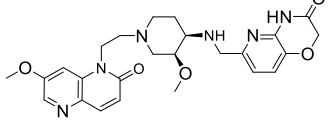
6-(((3S,4R)-3-Methoxy-1-(2-(7-methoxy-2-oxo-1,5-naphthyridin-1(2H)-yl)ethyl)piperidin-4-ylamino)methyl)-2H-pyrido[3,2-b][1,4]oxazin-3(4H)-one (AP_22)

In a 250 mL round-bottomed flask, 23c (2.300 g, 4.77 mmol), and sodium methoxide (1.288 g, 23.83 mmol) were taken in MeOH (50 mL) to give a white solution under nitrogen atmosphere and heated to 70 °C for 2h. Solvent was evaporated from the reaction mixture. Water was added to it and extracted using 10% methanol in DCM (3 X 100ml). The combined organic layers were concentrated to dryness and purified by silica gel chromatography using 0 to 10% Methanol in DCM and 0.1% ammonia to obtain **AP_22** (0.350 g, 14.85 %) as off white solid. ^{1}H NMR (300 MHz, DMSO) δ 1.73 (br. s., 2H), 1.99-2.20 (m, 2H), 2.51-2.71 (m, 2H), 2.99 (br. s., 1H), 3.09-3.23 (m, 4H), 3.62 (br. s., 1H), 3.94 (s, 3H), 3.95-4.10 (m, 3H), 4.21-4.47 (m, 2H), 4.63 (s, 2H), 6.61 (d, J=9.61 Hz, 1H), 7.06 (d, J=7.91 Hz, 1H), 7.30-7.47 (m, 2H), 7.83 (d, J=9.61 Hz, 1H), 8.24 (d, J=2.07 Hz, 1H), 8.75 (br. s., 1H), 11.30 (s, 1H); HRMS: m/z (ES[+])= 495.23061(MH[+]) for $C_{25}H_{30}N_6O_5$.

Table 5.1: Physicochemical properties of synthesized compounds (**AP_4** to **AP_13** and **AP_14 to AP_22)**

Compound	Structure	Molecular formula	Molecular weight	ClogP	LogD
AP_4		$C_{25}H_{26}N_6O$	426.216	1.30	1.1
AP_5		$C_{25}H_{26}N_6O$	426.216	1.30	1.3
AP_6		$C_{23}H_{25}FN_6O$	420.492	0.85	0.81
AP_7		$C_{24}H_{28}N_6O_2$	432.52	1.18	1.07
AP_7a		$C_{24}H_{28}N_6O_2$	432.528	1.58	ND
AP_8		$C_{24}H_{28}N_6O_2$	432.528	-0.2	-0.6
AP_9		$C_{26}H_{28}N_6O_2$	456.550	1.44	1.86

AP_10		$C_{24}H_{26}N_6O_3$	446.511	1.24	1.4
AP_11		$C_{24}H_{28}N_6O_3$	448.527	1.31	1.2
AP_12		$C_{23}H_{27}N_7O_2$	433.516	0.71	1.65
AP_13		$C_{23}H_{27}N_7O_2$	433.516	0.71	0.38
AP_14		$C_{25}H_{25}FN_6O$	444.514	1.42	1.29
AP_15		$C_{23}H_{24}F2N_6O$	438.482	1.14	0.92
AP_16		$C_{24}H_{27}FN_6O_2$	450.518	1.47	1.29
AP_17		$C_{25}H_3N_6O_3$	462.554	1.55	0.99
AP_18		$C_{23}H_{24}F_2N_6O_3$	470.480	0.80	0.47

AP_19		$C_{23}H_{24}F_2N_6O_3$	470.480	0.80	0.47
AP_20		$C_{24}H_{27}FN_6O_4$	482.516	1.13	0.64
AP_21		$C_{24}H_{27}FN_6O_4$	482.516	1.13	0.82
AP_22		$C_{25}H_{30}N_6O_5$	494.552	1.21	0.4

[ND] Not determined

5.2 Development piperidinyl/piperazinyl benzimidzoles as potent *Mtb* GyrA inhibitors with whole cell activity

Scaffold mophing effort on literature reported aminopiperidines based NBTIs using its bound crystal structure with the *S. aureus* DNA gyrase resulted in identification of piperidinyl benzimidazoles as one of the lead series with attractive antimycobacterial activity. Identified lead compound (**BI_1**) inhibits *Mtb* DNA gyrase with potent antimycobacterial activity (**Figure 5.2**). These compounds are bactericidal; retain their minimum inhibitory concentration (MIC) against FQ-resistant strains of *Mtb*. However, the initial lead has shown drawback of hERG liability, which is a known risk associated with NBTIs series. Furher chemistry optimization on benzimidazole RHS series was focused on building structure activity relationship (SAR) for hERG mitigation and improving anti TB activity in order to make it as attractive lead series for discovering a new preclinical candidate.
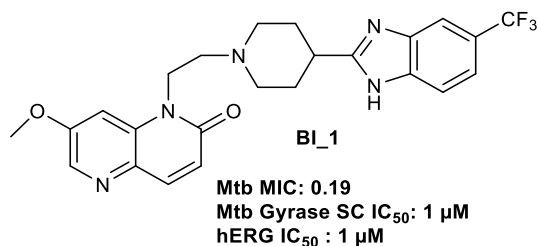
BI_1

Mtb MIC: 0.19
Mtb Gyrase SC IC$_{50}$: 1 µM
hERG IC$_{50}$: 1 µM

Figure 5.2: Chemical structure of novel benimidazole based molecule **BI_1**.

5.2.1 Chemical synthesis and characterization of benzimidazole, indole and oxindole RHS series compounds

Alkylation of LHS ring (**2a-c**) with 2-bromoethanol in the presence of cesium carbonate as a base provided N-alkylated product (**3a-d**) as the major isomer. Nucleophilic displacement of 3a with sodium methoxide in methanol under heating conditions resulted in intermediate 3b. The mesylates (**4a-d**) were obtained by treating **3a-d** with mesylchloride under basic conditions. The mesylates (**4a-d**) were freshly prepared and used immediately for the next step due to potential instability reasons. The N-BOC protected piperidinyl benzimidazoles (**6a-f**) were synthesized by treating corresponding ortho phenylene diamines (**5a-f**) with N-BOC piperidine-4-carboxaldehyde (**24**) in the presence of para-toluene sulphonic acid (catalytic amount) under open air condition. The secondary piperidines (**7a-f**) were obtained upon deprotection of N-BOC group under acidic conditions. Alkylation of secondary piperidines (**7a-f**) with mesylates (**4a-d**) in the presence of Na$_2$CO$_3$ as base under thermal heating conditions resulted in the title compounds (**BI_1**, **BI_5 to 15**).
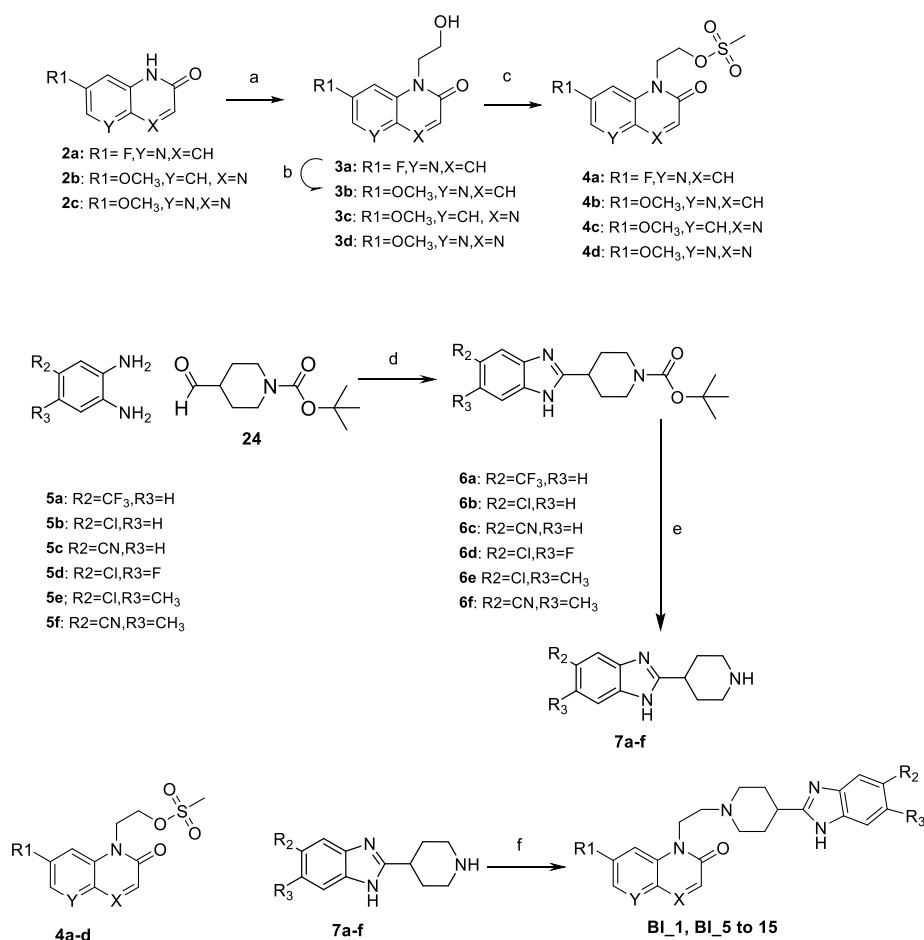
Reagents and conditions: (a) CsCO₃, DMSO, 90 °C; (b) NaOMe, MeOH, 75 °C; c) Mesyl chloride, DIPIEA, DCM, 0 °C; (d) PTSA, Ethanol, 90 °C; (e) 4N HCl in Dioxane, 50 °C; (f) Na₂CO₃, DMF, 130 °C

Scheme 5.4: Synthesis of compounds **BI_1**, **BI_5** to **BI_15**.

Treatment of mesylate **4a** with N-BOC protected piperazine (**8b**) under basic condition and heating provided **9a** Intermediate **9b** was obtained from **9a** using sodium methoxide. Alkylation of secondary piperazines (**7a-g**) with 2-choro benzimidazoles (**11a-c**) in the presence of a base under microwave condition resulted in the title compounds (**BI_2 to BI_4** and **BI_16**).
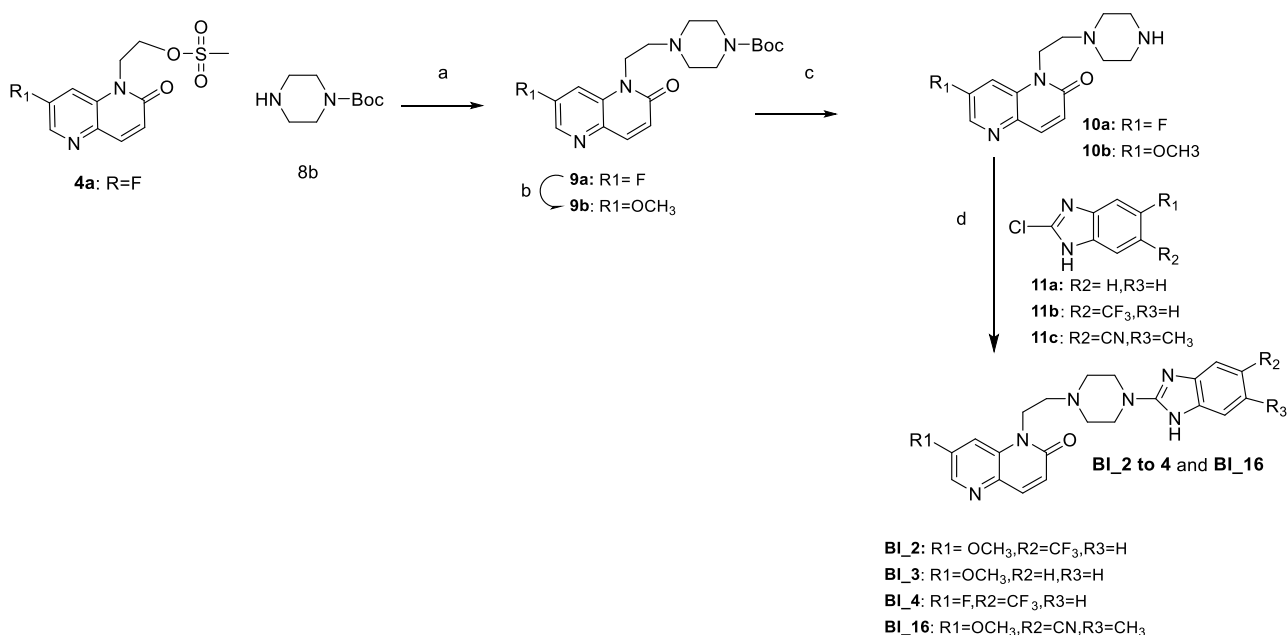
Scheme 5.5: Synthesis of compounds **BI_2** to **BI_4** and **BI_16**.

Compound from indole RHS series (**IN_1** and **IN_2**) and oxindole RHS (**OI_1**) were synthesized as per synthetic scheme shown in **figure 4.18** and **figure 4.19** respectively.

Procedure for the synthesis of final compounds from benzimidazole, indole and oxindole RHS series linker (BI_ 1 to BI_16, IN_1, IN_2 and OI_1)

3-(1-(2-(7-methoxy-2-oxo-1,5-naphthyridin-1(2H)-yl)ethyl)piperidin-4-yl)-1H-indole-5-carbonitrile (IN_1)

In a 25ml round-bottomed flask 2-(7-methoxy-2-oxo-1,5-naphthyridin-1(2H)-yl)ethyl methanesulfonate (97 mg, 0.33 mmol), 3-(piperidin-4-yl)-1H-indole-5-carbonitrile (56 mg, 0.25 mmol) and Sodium carbonate (155 mg, 1.25 mmol) were taken in DMF (3 mL). The resulting suspension was stirred at 90 0C for 2h. Progress of reaction was monitored by LCMS and LCMS proofile showed the formation of required product.The reaction mixture was diluted with ethylacetate and washed with water, brine and dried over anhydrous sodium sulphate. The organiuc fraction was evaporated under vacuum.The crude product was purified by reverse phase column chromatography

Yield: 35.0 mg, 54.6 %; ^{1}H NMR (300 MHz, DMSO- d$_6$) δ1.49 - 1.75 (m, 2 H), 1.79 – 2.02 (m, 2 H), 2.10-2.35 (m, 3 H), 2.55 - 2.67 (m, 3H), 3.15 (m, 1 H), 4.12 (s, 3 H), 4.30-4.45(m, 2 H), 6.7 (d, J=9.80 Hz, 1 H), 7.2-7.33 (m, 1 H), 7.40-7.61(m,3H), 7.74(m, 1 H), 8.10(br.s, 1 H), 8.40 (m, 1 H), 11.65 (br.s, 1 H); HRMS: m/z (ES$^+$) = 428.20867 (MH$^+$) for C$_{25}$H$_{25}$N$_5$O$_2$

7-Methoxy-1-(2-(4-(6-(trifluoromethyl)-1H-indol-3-yl)piperidin-1-yl)ethyl)-1,5-naphthyridin-2(1H)-one (IN_2)

Compound IN_2 was prepared from **intermediate 16d** and **4b** using procedure analogous to **compound IN_1**.

Yield: 50mg, 42.5 %; ^{1}H NMR (300 MHz, DMSO- d_6) δ1.40 - 1.75 (m, 2 H), 1.80– 2.01 (m, 2 H), 2.23 (t, J=11.4 Hz, 2H), 2.61 (t, J=11.1 Hz, 2H), 2.79 (t, J=11.96 Hz, 1 H), 3.10(d, J=11.1 Hz, 2H); 4.0 (s, 3 H), 4.22-4.54(m, 2H), 6.88 (d, J=9.80 Hz, 1 H), 7.24 (d, J=8.29 Hz, 1H), 7.34 (s, 1H), 7.46 (s, 1H), 7.67 (s, 1H), 7.73 (d, J=8.48 Hz, 1H), 7.88 (d, J=9.61 Hz, 1H), 8.30 (d, J=2.07 Hz, 1H), 11.25 (br. s., 1H); HRMS: m/z (ES$^+$) = 471.20089 (MH$^+$) for $C_{25}H_{25}F_3N_4O_2$

1-(2-(4-(5-Chloro-2-oxoindolin-3-yl) piperidin-1-yl)ethyl)-7-methoxy-1,5-naphthyridin-2(1H)-one (OI_1)

Compound OI_1 was prepared from **intermediate 15b** and **4b** using procedure analogous to **compound IN_1**.

Yield: 70mg, 38.6 %; ^{1}H NMR (300 MHz, DMSO- d6) δ1.41 - 1.74 (m, 2 H), 1.81– 2.02 (m, 2 H), 2.24 (t, J=11.4 Hz, 2H), 2.63 (t, J=11.1 Hz, 2H), 2.80 (t, J=11.96 Hz, 1 H), 3.12(d, J=11.1 Hz, 2H); 3.99 (s, 3 H), 4.23-4.45(m, 3H), 6.87 (d, J=9.80 Hz, 1 H), 7.26 (d, J=8.29 Hz, 1H), 7.33 (s, 1H), 7.45 (s, 1H), 7.62 (s, 1H), 7.74 (d, J=8.48 Hz, 1H), 7.81 (d, J=9.61 Hz, 1H), 8.21 (d, J=2.07 Hz, 1H), 11.1 (br. s., 1H); HRMS: m/z (ES$^+$) = 453.16891 (MH$^+$) for $C_{24}H_{25}ClN_4O_3$.

7-Methoxy-1-(2-(4-(5-(trifluoromethyl)-1H-benzo[d]imidazol-2-yl)piperidin-1-yl)ethyl)-1,5-naphthyridin-2(1H)-one (BI_1)

Compound BI_1 was prepared from **intermediate 7a** and **4b** using procedure analogous to **compound IN_1**.

Yield: 60mg, 25 %; ^{1}H NMR (300 MHz, DMSO- d6) δ1.75 - 1.85 (m, 2 H), 1.97– 2.02 (m, 2 H), 2.17 (t, J=11.4 Hz, 2H), 2.63 (t, J=11.1 Hz, 2H), 2.92 (t, J=11.96 Hz, 1 H), 3.13(d, J=11.1 Hz, 2H); 4.01 (s, 3 H), 4.23-4.44(m, 2H), 6.71 (d, J=9.80 Hz, 1 H), 7.4-7.40 (m, 2H), 7.6-7.80 (m, 2H), 7.90 (d, J=9.61 Hz, 1H), 8.31 (s, 1H), 12.65 (br. s., 1H); HRMS: m/z (ES$^+$) = 472.194631 (MH$^+$) for $C_{24}H_{24}F_3N_5O_2$.

7-Methoxy-1-(2-(4-(5-(trifluoromethyl)-1H-benzo[d]imidazol-2-yl)piperazin-1-yl)ethyl)-1,5-naphthyridin-2(1H)-one (BI_2)

In a 10ml microwave test tube, 7-methoxy-1-(2-(piperazin-1-yl)ethyl)-1,5-naphthyridin-2(1H)-one (100 mg, 0.35 mmol), DIPEA (0.182 mL, 1.04 mmol) and 2-chloro-5-(trifluoromethyl)-1H-benzo[d]imidazole (84 mg, 0.38 mmol) were taken in DMF (2 mL) and heated to 130°C for 2 h in Biotage microwave instrument. The progress of the reaction was monitored through LCMS and the LCMS profile showed the completion of reaction after heating to 130°C. The reaction mixture was diluted with ethylacetate and washed with water, brine and dried over sodium sulphate. The solvent was evaporated under vacuum and the crude compound was purified by revrese phase HPLC to get 7-methoxy-1-(2-(4-(5-(trifluoromethyl)-1H-benzo[d]imidazol-2-yl)piperazin-1-yl)ethyl)-1,5-naphthyridin-2(1H)-one (**BI_2**).

Yield: 35mg, 21.3 %; ^{1}H NMR (300 MHz, DMSO- d6) δ1.76 - 1.84 (m, 2 H), 1.96– 2.02 (m, 2 H), 2.16 (t, J=11.4 Hz, 2H), 2.65 (t, J=11.1 Hz, 2H), 3.14 (d, J=11.1 Hz, 2H); 4.02 (s, 3 H), 4.23-4.43(m, 2H), 6.68 (d, J=9.80 Hz, 1 H), 7.12-7.36 (m, 2H), 7.4-7.45 (m, 2H); 7.88 (d, J=9.61 Hz, 1H), 8.29 (s, 1H), 11.79 (br. s., 1H); HRMS: m/z (ES+) = 473.190299 (MH+) for $C_{23}H_{23}F_3N_6O_2$.

1-(2-(4-(1H-Benzo[d]imidazol-2-yl)piperazin-1-yl)ethyl)-7-methoxy-1,5-naphthyridin-2(1H)-one(BI_3)

Compound BI_3 was prepared from **intermediate 10b** and 2-chlorobenzimidazole using procedure analogous to **compound BI_2**.

Yield: 44mg, 31.2 %; ^{1}H NMR (300 MHz, DMSO- d6) δ1.75 - 1.80 (m, 2 H), 2.55-2.70 (m, 4H), 3.50 (m, 2H); 4.0 (s, 3 H), 4.40-4.49(m, 2H), 6.71 (d, J=9.80 Hz, 1 H), 6.92-7.0 (m, 2H), 7.15-7.25 (m, 2H); 7.47 (br.s, 1H), 7.90(d, J=9.7 Hz, 1H); 8.30 (s, 1H), 12.0 (br. s., 1H); HRMS: m/z (ES$^+$) = 405.203688 (MH$^+$) for $C_{22}H_{24}N_6O_2$.

7-Fluoro-1-(2-(4-(5-(trifluoromethyl)-1H-benzo[d]imidazol-2-yl)piperazin-1-yl)ethyl)-1,5-naphthyridin-2(1H)-one (BI_4)

Compound BI_4 was prepared from **intermediate 10a** and 2-chloro-5-(trifluoromethyl)-1H-benzo[d]imidazole using procedure analogous to **compound BI_2**.

Yield: 30mg, 18 %; ^{1}H NMR (300 MHz, DMSO- d6) δ 2.57-2.71 (m, 6H), 3.48 (m, 4H), 4.38 (t, J=6.59 Hz, 2 H), 6.85 (d, J=9.80 Hz, 1 H), 7.37.47 (m, 3H), 7.96 (d, J=9.8 Hz, 1H), 8.10 (d, J=1.88 Hz, 1H), 8.50 (s, 1H), 11.8 (br. s., 1H); HRMS: m/z (ES+) = 461.169951 (MH+) for $C_{22}H_{20}F_4N_6O$.

7-Fluoro-1-(2-(4-(5-(trifluoromethyl)-1H-benzo[d]imidazol-2-yl)piperidin-1-yl)ethyl)-1,5-naphthyridin-2(1H)-one (BI_5)

Compound **BI_5** was prepared from **intermediate 4a** and **7a** using procedure analogous to **compound IN_1**.

Yield: 55mg, 30 %; ^{1}H NMR (300 MHz, DMSO- d6) δ 1.65-1.85 (m, 2H), 1.92-2.06 (m, 2H), 2.20 (t, J=11.2 Hz, 2 H), 2.60 (t, J=6.4 Hz, 2 H), 2.88(m, 1H), 3.07(d, J=10.9 Hz, 2H); 4.37(t, J=6.7 Hz, 2H), 6.85 (d, J=9.80 Hz, 1 H), 7.39-7.73 (m, 2H), 7.89-8.04 (m, 3H), 8.57 (s, 1H), 12.61 (br. s., 1H); HRMS: m/z (ES$^+$) = 460.17642 (MH$^+$) for $C_{23}H_{21}F_4N_5O$.

2-(1-(2-(7-Fluoro-2-oxo-1,5-naphthyridin-1(2H)-yl)ethyl)piperidin-4-yl)-1H-benzo[d]imidazole-5-carbonitrile(BI_6)

Compound **BI_6** was prepared from **intermediate 4a** and **7c** using procedure analogous to **compound IN_1**.

Yield: 370mg, 59 %; ^{1}H NMR (300 MHz, DMSO- d6) δ 1.52-1.87 (m, 2H), 1.95-2.0 (m, 2H), 2.10-2.33 (m, 2 H), 2.60 (m. 2H), 2.73-2.99(m, 1H), 2.96-3.19(m, 2H), 4.40-4.50 (m, 2H), 6.85 (d, J=9.80 Hz, 1 H), 7.38-7.73 (m, 2H), 7.90-8.2 (m, 3H), 8.60 (s, 1H), 12.71 (br. s., 1H); HRMS: m/z (ES$^+$) = 417.18355 (MH$^+$) for $C_{23}H_{21}FN_6O$.

1-(2-(4-(5-chloro-1H-benzo[d]imidazol-2-yl)piperidin-1-yl)ethyl)-7-fluoro-1,5-naphthyridin-2(1H)-one (BI_7a)

Compound **BI_7a** was prepared from **intermediate 4a** and **7b** using procedure analogous to **compound IN_2**.

^{1}H NMR (300 MHz, DMSO- d_6) δ 1.52-1.87 (m, 2H), 1.95-2.0 (m, 2H), 2.10-2.33 (m, 2 H), 2.60 (m. 2H), 2.73-2.99(m, 1H), 2.96-3.19(m, 2H), 4.40-4.50 (m, 2H), 6.85 (d, J =9.80 Hz, 1 H), 7.38-7.73 (m, 2H), 7.90-8.2 (m, 3H), 8.60 (s, 1H), 12.71 (br s, 1H). HRMS (ESI-TOF): calcd for $C_{22}H_{21}Cl_FN_5O$ (M+H)$^{+,}$ 426.89240; obsd, 426. 83551.

1-(2-(4-(5-Chloro-1H-benzo[d]imidazol-2-yl)piperidin-1-yl)ethyl)-7-methoxy-1,5-naphthyridin-2(1H)-one (BI_7)

Compound BI_7 was prepared from **intermediate 4b** and **7b** using procedure analogous to **compound IN_2**.

Yield: 90mg, 41.1 %; ^{1}H NMR (300 MHz, DMSO- d6) δ1.65 - 1.75 (m, 2 H), 1.95− 2.03 (m, 2 H), 2.16 (t, J=11.4 Hz, 2H), 2.65 (t, J=11.1 Hz, 2H), 2-80-2.91 (m, 1 H), 3.11(d, J=11.1 Hz, 2H); 4.0 (s, 3 H), 4.45(m, 2H), 6.70 (d, J=9.80 Hz, 1 H), 7.0-7.20 (m, 1H), 7.4-7.60 (m, 3H), 7.85 (d, J=9.61 Hz, 1H), 8.30 (s, 1H), 12.40 (br. s., 1H); HRMS: m/z (ES$^+$) = 438.168303 (MH$^+$) for $C_{23}H_{24}ClN_5O_2$.

2-(1-(2-(7-Methoxy-2-oxo-1,5-naphthyridin-1(2H)-yl)ethyl)piperidin-4-yl)-1H-benzo[d]imidazole-5-carbonitrile (BI_8)

Compound BI_8 was prepared from **intermediate 4b** and **7c** using procedure analogous to **compound IN_1**.

Yield: 50mg, 39 %; ^{1}H NMR (300 MHz, DMSO- d6) δ1.73 - 1.80 (m, 2 H), 1.95− 2.08 (m, 2 H), 2.21 (t, J=11.4 Hz, 2H), 2.60 (t, J=11.1 Hz, 2H), 2-82-2.89 (m, 1 H), 3.10(d, J=10.7 Hz, 2H); 4.02 (s, 3 H), 4.41(t, J=6.8 Hz, 2H), 6.68 (d, J=9.80 Hz, 1 H), 7.45(s, 1H), 7.54-7.71 (m, 2H), 7.89 (d, J=9.61 Hz, 1H), 8.06 (br.s, 1H), 8.30 (s, 1H), 12.78 (br. s., 1H); HRMS: m/z (ES$^+$) = 429.20368 (MH$^+$) for $C_{24}H_{24}N_6O_2$.

1-(2-(4-(5-Chloro-6-fluoro-1H-benzo[d]imidazol-2-yl)piperidin-1-yl)ethyl)-7-methoxy-1,5-naphthyridin-2(1H)-one (BI_9)

Compound BI_9 was prepared from **intermediate 4b** and **7d** using procedure analogous to **compound IN_1**.

Yield: 70mg, 31 %; ^{1}H NMR (300 MHz, DMSO- d6) δ1.65 - 1.85 (m, 2 H), 1.95− 2.01 (m, 2 H), 2.22 (t, J=11.4 Hz, 2H), 2.62 (t, J=11.1 Hz, 2H), 2-83-2.88 (m, 1 H), 3.08 (d, J=10.7 Hz, 2H); 4.01 (s, 3 H), 4.42(t, J=6.8 Hz, 2H), 6.69(d, J=9.80 Hz, 1 H), 7.40-7.45(m, 1H), 7.54-7.60 (m, 1H), 7.71 (d, J=9.61 Hz, 1H), 7.91 (d, J=9.7 Hz, 1H), 8.31 (s, 1H), 12.5 (br. s., 1H); HRMS: m/z (ES$^+$) = 456.16039 (MH$^+$) for $C_{23}H_{23}ClFN_5O_2$.

1-(2-(4-(5-Chloro-6-methyl-1H-benzo[d]imidazol-2-yl)piperidin-1-yl)ethyl)-7-methoxy-1,5-naphthyridin-2(1H)-one (BI_10)

Compound **BI_10** was prepared from **intermediate 4b** and **7e** using procedure analogous to **compound IN_1**.

Yield: 130mg, 57.5 %; ^{1}H NMR (300 MHz, DMSO- d6) δ1.70 - 1.85 (m, 2 H), 1.95– 2.0 (m, 2 H), 2.20 (t, J=11.4 Hz, 2H), 2.61 (t, J=11.1 Hz, 2H), 2-84-2.87 (m, 1 H), 3.06 (d, J=10.7 Hz, 2H), 3.35 (s, 3H), 4.0 (s, 3 H), 4.43(t, J=6.8 Hz, 2H), 6.70(d, J=9.80 Hz, 1 H), 7.35-7.57(m, 3H), 7.90 (d, J=9.7 Hz, 1H), 8.30 (s, 1H), 12.20 (br. s., 1H); HRMS: m/z (ES[+]) = 452.184017 (MH[+]) for $C_{24}H_{26}ClN_5O_2$.

1-(2-(4-(5-Chloro-6-methyl-1H-benzo[d]imidazol-2-yl)piperidin-1-yl)ethyl)-7-fluoro-1,5-naphthyridin-2(1H)-one (BI_11)

Compound **BI_11** was prepared from **intermediate 4a** and **7e** using procedure analogous to **compound IN_1**.

Yield: 150mg, 57.5 %; ^{1}H NMR (300 MHz, DMSO- d6) δ1.68 - 1.80 (m, 2 H), 1.92– 1.98 (m, 2 H), 2.19 (t, J=11.3 Hz, 2H), 2.60 (t, J=11.1 Hz, 2H), 2.79-2.85 (m, 1 H), 3.07 (d, J=10.7 Hz, 2H), 3.36 (s, 3H), 4.38(t, J=6.8 Hz, 2H), 6.85(d, J=9.80 Hz, 1 H), 7.32-7.58(m, 2H), 7.95(d, J=9.7 Hz, 1H), 8.05-8.10 (m, 1H), 8.60 (s, 1H), 12.20 (br. s., 1H); HRMS: m/z (ES[+]) = 440.16557 (MH[+]) for $C_{23}H_{23}ClFN_5O$.

1-(2-(4-(5-Chloro-6-methyl-1H-benzo[d]imidazol-2-yl)piperidin-1-yl)ethyl)-7-methoxyquinoxalin-2(1H)-one (BI_12)

Compound **BI_12** was prepared from **intermediate 4c** and **7e** using procedure analogous to **compound IN_1**.

Yield: 27mg, 20 %; ^{1}H NMR (300 MHz, DMSO- d6) δ1.70- 1.80 (m, 2 H), 1.92– 2.0 (m, 2 H), 2.18 (t, J=11.3 Hz, 2H), 2.40 (s,3H0, 2.61 (t, J=11.1 Hz, 2H), 2.77-2.88(m, 1 H), 3.08 (d, J=10.7 Hz, 2H), 3.95(s, 3H), 4.40(t, J=6.8 Hz, 2H), 7.0-7.10 (m, 2H), 7.40-7.51 (m, 1H), (7.79(d, J=9.7 Hz, 1H), 8.05 (s, 1H), 12.10 (br. s., 1H); HRMS: m/z (ES[+]) = 452.18489 (MH[+]) for $C_{24}H_{26}ClN_5O_2$.

1-(2-(4-(5-Chloro-6-methyl-1H-benzo[d]imidazol-2-yl)piperidin-1-yl)ethyl)-7-methoxypyrido[2,3-b]pyrazin-2(1H)-one(BI_13)

Compound **BI_13** was prepared from **intermediate 4d** and **7e** using procedure analogous to **compound IN_1**.

Yield: 50mg, 36 %; ^{1}H NMR (300 MHz, DMSO- d_6) δ1.67- 1.75 (m, 2 H), 1.90– 2.0 (m, 2 H), 2.17 (t, J=11.3 Hz, 2H), 2.41 (s,3H), 2.62 (t, J=11.1 Hz, 2H), 2.75-2.87(m, 1 H), 3.11 (d, J=10.7 Hz, 2H), 4.0(s, 3H), 4.46(t, J=6.8 Hz, 2H), 7.35-7.60 (m, 3H), 8.27-8.32(m, 2H), 12.30 (br. s., 1H); HRMS: m/z (ES$^+$) = 453.18077 (MH$^+$) for $C_{23}H_{25}ClN_6O_2$.

2-(1-(2-(7-Fluoro-2-oxo-1, 5-naphthyridin-1(2H)-yl)ethyl)piperidin-4-yl)-6-methyl-1H-benzo[d]imidazole-5-carbonitrile (BI_14)

Compound BI_14 was prepared from **intermediate 4a** and **7f** using procedure analogous to **compound IN_1**.

Yield: 70mg, 32.5 %; ^{1}H NMR (300 MHz, DMSO- d_6) δ1.65- 1.84 (m, 2 H), 1.89– 2.05 (m, 2 H), 2.19 (t, J=11.3 Hz, 2H), 2.47 (s,3H), 2.59 (t, J=11.1 Hz, 2H), 2.77-2.91(m, 1 H), 3.07 (d, J=10.7 Hz, 2H), 4.36(t, J=6.8 Hz, 2H), 6.84(d, J=9.8 Hz, 1H), 7.48 (br.s, 1H), 7.94-8.07 (m, 3H), 8.56(s, 1H), 12.56 (br. s., 1H); HRMS: m/z (ES$^+$) = 431.19908 (MH$^+$) for $C_{24}H_{23}FN_6O$.

2-(1-(2-(7-methoxy-2-oxo-1, 5-naphthyridin-1(2H)-yl)ethyl)piperidin-4-yl)-6-methyl-1H-benzo[d]imidazole-5-carbonitrile(BI_15)

Compound BI_15 was prepared from **intermediate 4b** and **7f** using procedure analogous to **compound IN_1**.

Yield: 90mg, 25.4 %**;** ^{1}H NMR (300 MHz, DMSO- d_6) δ1.72- 1.79 (m, 2 H), 1.95– 2.05 (m, 2 H), 2.21 (t, J=11.3 Hz, 2H), 2.48 (s,3H), 2.61 (t, J=6.5 Hz, 2H), 2.81-2.87(m, 1 H), 3.09(d, J=10.7 Hz, 2H), 4.0(s, 3H), 4.41(t, J=6.6 Hz, 2H), 6.68(d, J=9.8 Hz, 1H), 7.44 (s, 1H), 7.58(s, 1H), 7.84-7.98(m, 2H), 8.30(s, 1H), 12.57 (br. s., 1H); HRMS: m/z (ES$^+$) = 443.21902 (MH$^+$) for $C_{25}H_{26}N_6O_2$.

2-(4-(2-(7-Methoxy-2-oxo-1, 5-naphthyridin-1(2H)-yl)ethyl)piperazin-1-yl)-6-methyl-1H-benzo[d]imidazole-5-carbonitrile (BI_16)

Compound BI_16 was prepared from **intermediate 10b** and**11c** using procedure analogous to **compound IN_1**.

Yield: 93mg, 26 %; ^{1}H NMR (300 MHz, DMSO- d6) δ 2.47 (s,3H), 2.65-2.72 (m, 6H), 3.60-3.70(m, 4H), 4.0(s, 3H), 4.43(t, J=6.6 Hz, 2H), 6.69(d, J=9.8 Hz, 1H), 7.15 (s, 1H), 7.42-

7.47(m, 2H), 7.90(d, J=9.4 Hz, 1H), 8.30(s, 1H), 11.70 (br. s., 1H); HRMS: m/z (ES$^+$) = 444.213302 (MH$^+$) for $C_{24}H_{25}N_7O_2$.

5.3 LHS exploration of NBTIs as heteroaryl ether (HAR) to improve hERG selectivity while retaining gyrase inhibition and *Mtb* MIC

Majority of the novel n-linked quinolone and naphthyridones with smaller substitutions on the LHS side reported to have cardiac ion channel (hERG) liability and this poses a significant challenge in the clinical advancement of NBTIs.This trend was true for some of the potent compounds from aminopeperidine and benzimidaole lead series emerged from this research work. A thorough literature analysis reveals that the chemical diversity of substituents at LHS has not been fully exploited and most of these attempts have confined to smaller substituents such as fluoro, cyano and methoxy groups. Therefore, we devised a strategy to exploit bulky polar groups (R1) on LHS of naphthyridone ring system to improve the hERG selectivity, while retaining antimycobacterial activity. We hypothesized that by lowering the logD and modulation the polarity *via* bulky polar substitutions on LHS ring may provide structural diversity to mitigate hERG liability. Based on this hypothesis, several compounds with bulky polar substitutions were synthesized and their hERG IC$_{50}$s were determined. Match pairs of identified lead compound from HAR series (**HAR_1** and **HAR_4**) shown in **Figure 5.3**.
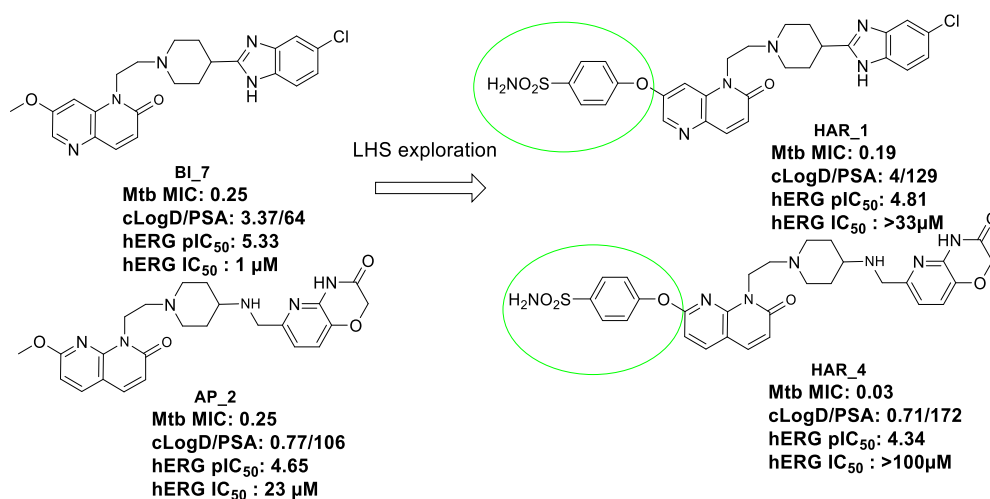

Figure 5.3: Match pair analysis and strcutures of identified leads from HAR series

From the match pair analysis, it is evident that compounds with polar bulky substitutions have shown better hERG selectivity (by both experimental determination and hERG pIC$_{50}$

102

prediction) compared to a smaller methoxy substituted counterpart (**BI_7** versus **HAR_1**, **AP_2** versus **HAR_4** in **figure 5.3**). This could be due to a higher polar surface area (PSA) combined with lower logD observed for compounds **HAR_1** and **HAR_4**. Hence, the better disturbance of hERG channel binding resulted in an improved hERG selectivity for compound **HAR_1** and **HAR_4**. A closer look at lipophilicity values for compound **AP_2** (ClogD 0.77) and **HAR_4** (ClogD 0.71) suggests that more polarity at the C-7 position of LHS confers better hERG selectivity than lipophilicity alone. Furthermore, compounds **HAR_1** and **HAR_4** retain their activity against Mtb (MIC of 0.19μM & 0.03μM, respectively).

Encouraged by the improved hERG selectivity for compounds **HAR_1** and **HAR_4** with 4-sulphamido phenyl substitution, we further expanded the SAR with various RHS combination to validate this hypothesis and synthesis of these set is given below.

5.3.1 Syntheis and characterization

The synthesis of compounds with smaller substituents like fluoro or chloro at the C-7 position of naphthyridone ring were reported earlier (Reck, F. *et al.*, 2011 and Reck, F. *et al.*, 2012). Nucleophilic displacement of halo substituted naphthyridones (**I**) with corresponding carbinol (**II**) using cesium carbonate under thermal heating condition resulted in title compounds **HAR_1** to **HAR_22** (**Scheme 5.6**).
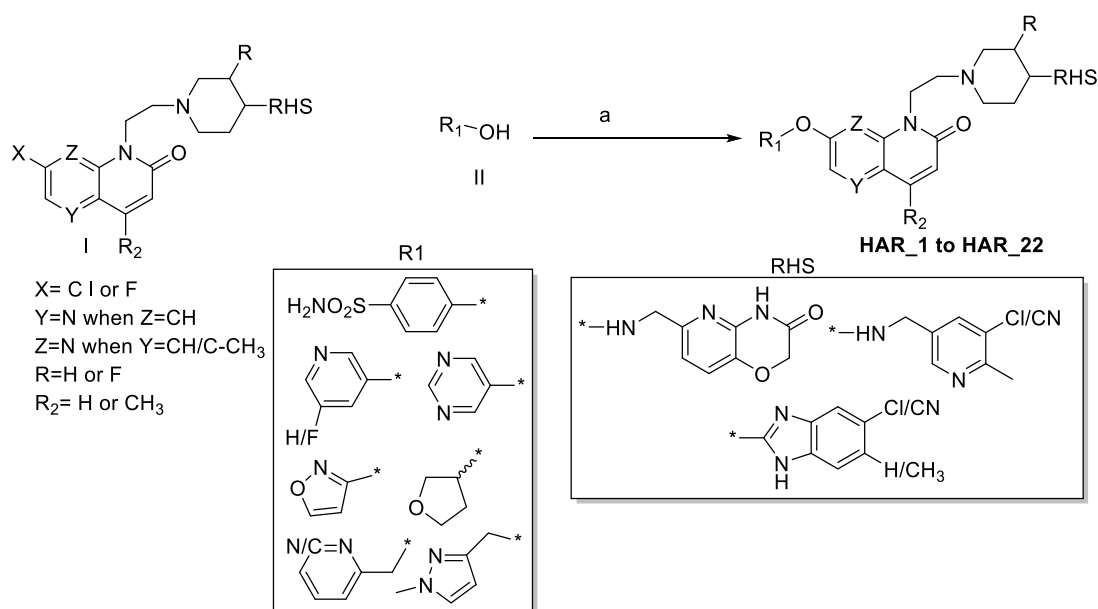
Reagents and conditions: a) Cs_2CO_3, DMSO, 130 °C

Scheme 5.6: Synthesis of compounds **HAR_1** – **HAR_22**

4-((5-(2-(4-(5-Chloro-1H-benzo[d]imidazol-2-yl) piperidin-1-yl) ethyl)-6-oxo-5, 6-dihydro-1, 5-naphthyridin-3-yl) oxy) benzenesulfonamide (HAR_1)

In a 10mL round-bottomed flask, 4-hydroxybenzenesulfonamide (0.18 mmol) and cesium carbonate (117 mg, 0.36 mmol) were taken in DMSO (25 mL) to give a colorless suspension and stirred at room temperature for 30 mins. Then, 1-(2-(4-(5-chloro-1H-benzo[d]imidazol-2-yl)piperidin-1-yl)ethyl)-7-fluoro-1,5-naphthyridin-2(1H)-one (**BI_7a**, 0 .18 mmol) was added and the resulting reaction miture was heated to 120 °C for overnight. Progress of reaction was monitored by LCMS, which indicated required product formation. Water was added to the reaction mixture and extracted using 10% Methanol in DCM (4X50ml). The combined organic layers were concentrated to dryness and purified by reverse phase chromatography (Gilson) to obtain 4-((5-(2-(4-(5-chloro-1H-benzo[d]imidazol-2-yl)piperidin-1-yl)ethyl)-6-oxo-5,6-dihydro-1,5-naphthyridin-3-yl)oxy)benzenesulfonamide.

Yield: 30mg, 34 %; ^{1}H NMR (300 MHz, DMSO- d_6) δ 1.66-1.77 (m, 2H), 1.93-1.97 (m, 2H), 2.10-2.19 (m, 4H), 2.81-2.93 (m, 3H), 4.28(t, *J*=6.4 Hz, 2H), 6.81(d, *J*=9.6 Hz, 1H), 7.43-7.71 (m, 5H), 7.95(d, *J*=9.8 Hz, 1H), 8.03 (s, 1H), 8.41-8.46 (m, 2H), 8.59 (s, 1H), 11.80 (br s, 1H). HRMS (ESI-TOF): calcd for $C_{28}H_{27}ClN_6O_4S$ (M+H)[+,] 579.15030; obsd, 579.15792.

4-((6-oxo-5-(2-(4-(5-(trifluoromethyl)-1H-benzo[d]imidazol-2-yl)piperidin-1-yl)ethyl)-5, 6-dihydro-1,5-naphthyridin-3-yl)oxy)benzenesulfonamide (HAR_2)

Compound **HAR_2** was synthesized from intermediate **BI_6** and 4-hydroxybenzene sulfonamide using procedure analogues to compound **HAR_1**.

Yield: 24mg, 30%; ^{1}H NMR (300 MHz, DMSO- d_6) δ 1.70-1.77 (m, 2H), 1.90-2.02 (m, 2H), 2.14 (t, *J*=10.8, 2H), 2.55-2.76 (m, 3H), 2.78-3.03 (m, 4H), 4.32(t, *J*=6.4 Hz, 2H), 6.83(d, *J*=9.8 Hz, 1H), 7.33-7.655 (m, 3H), 7.55-7.78(m, 3H), 7.86-7.98 (m, 3H), 8.41 (s, 1H), 12.2 (br. s., 1H); HRMS: m/z (ES[+]) = 613.18377 (MH[+]) for $C_{29}H_{27}F_3N_6O_4S$

4-(5-(2-(4-(5-Cyano-6-methyl-1H-benzo[d]imidazol-2-yl)piperidin-1-yl)ethyl)-6-oxo-5,6-dihydro-1,5-naphthyridin-3-yloxy)benzenesulfonamide (HAR_3)

Compound **HAR_3** was synthesized from intermediate **BI_14** and 4-hydroxybenzene sulfonamide using procedure analogues to compound **HAR_1**.

Yield: 30mg, 29%; ^{1}H NMR (300 MHz, DMSO- d_6) δ 1.57-1.81 (m, 2H), 1.87-2.02 (m, 2H), 2.10-2.19 (m, 2H), 2.45 (s, 3H), 2.55-2.764 (m, 3H), 2.74-3.03 (m, 3H), 4.30(t, *J*=6.4 Hz, 2H),

6.84(d, J=9.6 Hz, 1H), 7.53-7.66 (m, 2H), 7.40(d, J=9.7 Hz, 2H), 7.80(s, 1H), 7.82-8.10 (m, 4H), 8.45 (s, 1H), 12.1 (br s, 1H). HRMS (ESI-TOF): calcd for $C_{30}H_{29}N_7O_4S$ (M+H)$^+$, 584.20353; obsd, 584.20715.

4-(7-Oxo-8-(2-(4-((3-oxo-3,4-dihydro-2H-pyrido[3,2-b][1,4]oxazin-6-yl)methylamino)piperidin-1-yl)ethyl)-7,8-dihydro-1,8-naphthyridin-2-yloxy)benzenesulfonamide (HAR_4)

In a 50 mL round-bottomed flask, 4-hydroxybenzenesulfonamide (0.194 g, 1.12 mmol) was dissolved in DMF (1 mL) and K_2CO_3 (0.206 g, 1.49 mmol) was added and stirred for 2 minutes. Then, Intermediate **AP_Ia** (350mg, 0.75 mmol), was added and heated to 90°C for overnight. The progress of the reaction was monitored by LCMS and the profile showed the formation of required product. The reaction mixture was concentrated under vacuum and the residue was diluted with 15% MeOH/DCM and washed with saturated sodium bicarbonate solution. Organic layer was separated and concentrated under vacuum. The purification was done using reverse phase column chromatography (GILSON Prep system) using acetonitrile ammonium acetate buffer as eluent (gradient elution) afforded the title compound (25 mg, 5.53 %).

^{1}H NMR (500 MHz, DMSO-d_6) δ ppm 1.10 (d, J=10.09 Hz, 2 H) 1.68 (br s, 2 H) 1.76 (br s, 3 H) 1.91 (s, 2 H) 2.24 - 2.33 (m, 2 H) 3.18 (s, 3 H) 3.67 (s, 2 H) 4.04 - 4.18 (m, 3 H) 4.61 (s, 2 H) 6.57 (d, J=9.77 Hz, 2 H) 7.04 (dd, J=19.86, 8.20 Hz, 2 H) 7.30 (d, J=8.20 Hz, 1 H) 7.47 (d, J=8.20 Hz, 2 H) 7.92 (dd, J=15.13, 8.83 Hz, 2 H) 8.26 (d, J=8.51 Hz, 1 H). HRMS (ESI-TOF): calcd for $C_{29}H_{31}N_7O_6S$ (M+H)$^+$, 606.20565; obsd, 606.20583.

4-(4-Methyl-7-oxo-8-(2-(4-((3-oxo-3,4-dihydro-2H-pyrido[3,2-b][1,4]oxazin-6-yl)methylamino)piperidin-1-yl)ethyl)-7,8-dihydro-1,8-naphthyridin-2-yloxy)benzenesulfonamide (HAR_5)

Compound **HAR_5** was synthesized from intermediate **AP_If** and and 4-hydroxybenzene sulfonamide using procedure analogues to compound **HAR_1**.

Yield: 76 mg, 22.95 %; ^{1}H NMR (300 MHz, DMSO-d_6) δ ppm 1.02 - 1.19 (m, 2H) 1.61 - 1.79 (m, 7H) 1.85 (s, 4H) 2.20 - 2.35 (m, 3H) 2.55 (br s, 1H) 2.59 (s, 3 H) 3.66 (s, 2H) 4.12 (t, J=6.69 Hz, 2H) 4.61 (s, 2H) 6.56 (d, J=9.61 Hz, H) 6.95 (s, 1H) 7.01 (d, J=8.10 Hz, 1H) 7.30 (d, J=8.10 Hz, 1H) 7.44 (m, J=8.48 Hz, 2H) 7.89 (m, J=8.67 Hz, 2H) 8.04 (d, J=9.61 Hz, 1H). HRMS (ESI-TOF): calcd for $C_{30}H_{33}N7O_6S$ (M+H)$^+$, 620.22130; obsd, 620.22118.

4-(5-Methyl-7-oxo-8-(2-(4-((3-oxo-3,4-dihydro-2H-pyrido[3,2-b][1,4]oxazin-6-yl)methylamino)piperidin-1-yl)ethyl)-7,8-dihydro-1,8-naphthyridin-2-yloxy)benzenesulfonamide (HAR_6)

Compound **HAR_6** was synthesized from intermediate **AP_Ig** and and 4-hydroxybenzene sulfonamide using procedure analogues to compound **HAR_1**.

^{1}H NMR (300 MHz, DMSO-d_6) δ ppm 1.02 - 1.19 (m, 2H) 1.61 - 1.79 (m, 7H) 1.85 (s, 4H) 2.20 - 2.35 (m, 3H) 2.55 (br s, 1 H) 2.46 (s, 3H) 3.67 (s, 2H) 4.12 (t, J=6.69 Hz, 2H) 4.61 (s, 2H) 6.56 (d, J=9.61 Hz, 1H) 6.95 (s, 1H) 7.01 (d, J=8.10 Hz, 1H) 7.31 (d, J=8.10 Hz, 1H) 7.45 (m, J=8.48 Hz, 2H) 7.89 (m, J=8.67 Hz, 2H) 8.01 (d, J=9.61 Hz, 1H). HRMS (ESI-TOF): calcd for $C_{30}H_{33}N7O_6S$ (M+H)$^+$, 620.22130; obsd, 620.22117.

4-(5-(2-(4-((5-Chloro-6-methylpyridin-3-yl)methylamino)piperidin-1-yl)ethyl)-6-oxo-5,6-dihydro-1,5-naphthyridin-3-yloxy)benzenesulfonamide(HAR_7)

Compound **HAR_7** was synthesized from intermediate **AP_Ic** and 4-hydroxybenzene sulfonamide using procedure analogues to compound **HAR_1**.

^{1}H NMR (300 MHz, DMSO-d_6) δ ppm 1.04 - 1.21 (m, 2 H) 1.61 - 1.76 (m, 4H) 1.94 (t, J=10.36 Hz, 2 H) 2.24 - 2.35 (m, 3H) 2.42 - 2.48 (m, 2H) 2.77 (dd, J=5.93, 5.37 Hz, 2H) 3.69 (s, 2H) 4.25 (t, J=6.59 Hz, 2H) 6.81 (d, J=9.80 Hz, 1H) 7.26 - 7.50 (m, 4H) 7.70 (d, J=1.88 Hz, 1H) 7.77 - 7.83 (m, 1H) 7.89 (d, J=8.85 Hz, 2H) 7.95 (d, J=9.80 Hz, 1H) 8.40 (d, J=2.07 Hz, 1H) 8.34 (d, J=1.51 Hz, 1H). HRMS (ESI-TOF): calcd for $C_{28}H_{31}ClN_6O_4S$ (M+H)$^+$, 583.18160; obsd, 583.18991.

4-(8-(2-(4-((5-Cyano-6-methylpyridin-3-yl)methylamino)piperidin-1-yl)ethyl)-7-oxo-7,8-dihydro-1,8-naphthyridin-2-yloxy)benzenesulfonamide (HAR_8)

Compound **HAR_8** was synthesized from intermediate **AP_Id** and 4-hydroxybenzene sulphonamide using procedure analogues to compound **HAR_1**.

^{1}H NMR (300 MHz, DMSO-d_6) δ ppm 0.9 - 1.1 (m, 2H) 1.6-1.8 (m, 4H) 2.1-2.3 (m, 3H) 2.51-2.62(m, 4H) 3.7(m, 2H) 4.0-4.2(m, 4H) 6.6 (d, J=9.72 Hz, 1H) 7.0 (m, 1 H) 7.3-7.5(m, 3H) 7.9-8.0 (m, 3H) 8.1 (s,1H) 8.3 (d, J=1.63 Hz, 1H) 8.7(s, 1H) 11.2(br s, 1H). HRMS (ESI-TOF): calcd for $C_{29}H_{31}ClN_7O_4S$ (M+H)$^+$, 574.21918; obsd, 574.22355.

4-(5-(2-(4-((5-cyano-6-methylpyridin-3-yl)methylamino)piperidin-1-yl)ethyl)-6-oxo-5,6-dihydro-1,5-naphthyridin-3-yloxy)benzenesulfonamide (HAR_9)

Compound **HAR_9** was synthesized from intermediate **AP_6** and **4**-hydroxybenzene sulphonamide using procedure analogues to compound **HAR_1**.

^{1}H NMR (300 MHz, DMSO-d_6) δ ppm 1.10 - 1.30 (m, 2H) 1.65 - 1.85 (m, 4H) 1.88 - 2.03 (m, 2H) 2.36 - 2.47 (m, 2H) 2.66 (s, 3 H) 2.76 - 2.88 (m, 2H) 3.81 (br s, 2H) 4.26 (t, J=6.50 Hz, 2H) 6.82 (d, J=9.61 Hz, 1H) 7.28 - 7.37 (m, 2H) 7.40 (br s, 2H) 7.67 - 7.75 (m, 1H) 7.84 - 7.93 (m, 2H) 7.96 (d, J=9.80 Hz, 1H) 8.19 (br s, 1H) 8.41 (d, J=2.26 Hz, 1H) 8.69 (s, 1H). HRMS (ESI-TOF): calcd for $C_{29}H_{31}ClN_7O_4S$ (M+H)$^+$, 574.21918; obsd, 574.22337.

6-((1-(2-(2-Oxo-7-(pyridin-3-yloxy)-1,8-naphthyridin-1(2H)-yl)ethyl)piperidin-4-ylamino)methyl)-2H-pyrido[3,2-b][1,4]oxazin-3(4H)-one (HAR_10)

Compound **HAR_10** was synthesized from intermediate **AP_Ia** and 3-hydroxy pyridine using procedure analogues to compound **HAR_1**.

^{1}H NMR (300 MHz, DMSO-d_6) δ ppm 1.11 - 1.25 (m, 2H) 1.67 - 1.78 (m, 4H) 2.25 – 2.35 (m, 4H) 2.45 - 2.5 (m, 2H) 3.69 (s, 2H) 4.31 (t, J=7.06 Hz, 2H) 4.60 (s, 2H) 6.66 (d, J=9.61 Hz, 1H) 7.01 (dd, J=4.80, 1.70, 0.85 Hz, 2H) 7.29 (d, J=8.10 Hz, 1H) 7.51 (dd, J=7.54, 4.90, 1.13 Hz, 1H) 7.81 (d, J=2.07 Hz, 1H) 7.89(d, J=7.91 Hz, 1H) 8.32 (d, J=2.45 Hz, 1H) 8.51 (d, J=7.91Hz, 1H) 8.67 (d, J=2.07 Hz, 1H) 11.14 (br s, 1H). HRMS (ESI-TOF): calcd for $C_{28}H_{29}N_7O_4$ (M+H)$^+$, 528.22810; obsd, 528.22710.

6-((1-(2-(2-Oxo-7-(pyrimidin-5-yloxy)-1, 8-naphthyridin-1(2H)-yl) ethyl) piperidin-4-ylamino) methyl)-2H-pyrido [3, 2-b][1, 4] oxazin-3(4H)-one (HAR_11)

Compound **HAR_11** was synthesized from intermediate **AP_Ia** and 5-hydroxy pyrimidine using procedure analogues to compound **HAR_1**.

^{1}H NMR (300 MHz, DMSO-d_6) δ ppm 1.15 (m, 3H) 1.70 -1.83 (m, 4H) 1.89 (s, 3H) 2.35-2.40 (m, 3 H) 3.68 (s, 2H) 4.19 (t, J=6.97 Hz, 2H) 4.61 (s, 2 H) 6.79 (d, J=9.80 Hz, 1H) 7.02 (d, J=8.10 Hz, 1H) 7.25 (d, 1H) 7.30 (d, J=8.10 Hz, 1H) 7.89 (d, J=2.07 Hz, 1H) 8.31 (d, J=9.80 Hz, 1H) 8.92 (s, 2H) 9.12 (s, 1H). HRMS (ESI-TOF): calcd for $C_{27}H_{28}N_8O_4$ (M+H)$^+$, 529.22335; obsd, 529.23177.

6-((1-(2-(7-(Isoxazol-3-yloxy)-2-oxo-1,8-naphthyridin-1(2H)-yl)ethyl)piperidin-4-ylamino)methyl)-2H-pyrido[3,2-b][1,4]oxazin-3(4H)-one(HAR_12)

Compound **HAR_12** was synthesized from intermediate **AP_Ia** and 3-hydroxy isoxazole using procedure analogues to compound **HAR_1**

^{1}H NMR (300 MHz, DMSO-d_6) δ ppm 1.16 (d, J=9.80 Hz, 2H) 1.25 (br s, 1H) 1.72 (d, J=10.74 Hz, 2 H) 1.80 - 1.97 (m, 2H) 2.24 - 2.44 (m, 3H) 2.68 (d, J=11.11 Hz, 2H) 3.67 (s, 2H) 4.11 - 4.31 (m, 2H) 4.61 (s, 2H) 6.62 (d, J=9.42 Hz, 1H) 6.86 (d, J=1.88 Hz, 1H) 7.01 (d, J=8.10 Hz, 1H) 7.14 (d, J=8.29 Hz, 1H) 7.30 (d, J=8.10 Hz, 1H) 7.96 (d, J=9.61 Hz, 1H) 8.31 (d, J=8.48 Hz, 1H) 8.99 (d, J=1.88 Hz, 1H) 11.15 (br s, 1H). HRMS (ESI-TOF): calcd for $C_{26}H_{27}N_7O_5$ (M+H)$^+$, 518.21072; obsd, 518.21487

6-((1-(2-(7-(Isoxazol-3-yloxy)-2-oxo-1, 5-naphthyridin-1(2H)-yl) ethyl) piperidin-4-ylamino) methyl)-2H-pyrido [3, 2-b][1,4]oxazin-3(4H)-one (HAR_13)

Compound **HAR_13** was synthesized from intermediate **AP_Ib** and 3-hydroxy isoxazole using procedure analogues to compound **HAR_1**.

^{1}H NMR (400 MHz, DMSO-d_6) δ ppm 1.0-1.18 (m, 2H) 1.71 (br s, 1H) 1.9-2.05 (m, 3H) 2.33 (br s, 2H) 2.85 (d, J=11.54 Hz, 3H) 3.66 (br s, 2H) 4.30 (t, J=6.78 Hz, 2H) 4.61 (s, 3H) 6.71 (d, J=1.51 Hz, 1H) 6.85 (d, J=9.54 Hz, 1H) 7.01 (d, J=8.03 Hz, 1H) 7.30 (d, J=8.03 Hz, 1H) 7.91 - 8.09 (m, 2H) 8.57 (d, J=2.01 Hz, 1H) 8.95 (d, J=1.51 Hz, 1 H) 11.18 (s, 1H). HRMS (ESI-TOF): calcd for $C_{26}H_{27}N_7O_5$ (M+H)$^+$, 518.21072; obsd, 518.21482

6-((1-(2-(2-oxo-7-(pyridin-3-yloxy)-1,5-naphthyridin-1(2H)-yl)ethyl)piperidin-4-ylamino)methyl)-2H-pyrido[3,2-b][1,4]oxazin-3(4H)-one (HAR_14)

Compound **HAR_14** was synthesized from intermediate **AP_Ib and** 3-hyrdoxy pyridine using procedure analogues to compound **HAR_1**.

^{1}H NMR (300 MHz, DMSO-d_6) δ ppm 1.31 - 1.43 (m, 4H) 1.80 - 1.92 (m, 2H) 1.99 - 2.07 (m, 2 H) 2.33-2.36 (m, 2H) 2.82 - 2.93 (m, 2 H) 3.87 - 3.98 (m, 2 H) 4.24 - 4.34 (m, 2H) 4.70 (s, 2H) 6.84 (d, J=9.80 Hz, 1H) 7.13 (d, J=8.10 Hz, 2H) 7.41 (d, J=8.29 Hz, 1H) 7.52 - 7.64 (m, 2H) 7.74 (dd, J=7.63, 2.17 Hz, 1H) 8.00 (d, J=9.61 Hz, 1H) 8.46 (d, J=2.26 Hz, 1H) 8.54 (dd, J=4.62, 1.22 Hz, 1H) 8.62 (d, J=2.64 Hz, 1H). HRMS (ESI-TOF): calcd for $C_{28}H_{29}N_7O_4$ (M+H)$^+$, 528.22810; obsd, 528.23641.

6-((1-(2-(7-(5-fluoropyridin-3-yloxy)-2-oxo-1, 5-naphthyridin-1(2H)-yl)ethyl)piperidin-4-ylamino)methyl)-2H-pyrido[3,2-b][1,4]oxazin-3(4H)-one (HAR_15)

Compound **HAR_15** was synthesized from intermediate **AP_Ib and** 5-fluro-3-hydroxy pyridine using procedure analogues to compound **HAR_1**.

^{1}H NMR (300 MHz, DMSO-d_6) δ ppm 1.88 - 2.14 (m, 4H) 2.38 (d, J=12.62 Hz, 2H) 3.08 (d, J=10.55 Hz, 2H) 3.32 (br s, 1H) 3.77 (d, J=11.30 Hz, 2H) 4.19 (br s, 2H) 4.63 (t, J=6.22 Hz, 2 H) 4.71 (s, 2H) 6.89 (d, J=9.80 Hz, 1H) 7.22 (d, J=8.10 Hz, 1H) 7.46 (d, J=8.10 Hz, 1H) 7.74 (d, J=10.17 Hz, 1H) 8.03 (d, J=9.80 Hz, 1 H) 8.16 (br s, 1 H) 8.39 - 8.53 (m, 2 H) 9.55 (br s, 1 H) 10.75 (br s, 1H) 11.37 (s, 1H). HRMS (ESI-TOF): calcd for $C_{28}H_{28}FN_7O_4$ (M+H)$^+$, 546.22204; obsd, 546.22663.

(R)-6-((1-(2-(2-oxo-7-(tetrahydrofuran-3-yloxy)-1,5-naphthyridin-1(2H)-yl)ethyl)piperidin-4-ylamino)methyl)-2H-pyrido[3,2-b][1,4]oxazin-3(4H)-one (HAR_16)

Compound **HAR_16** was synthesized from intermediate **AP_Ib** and (R)-tetrahydrofuran-3-ol using procedure analogues to compound **HAR_1**.

^{1}H NMR (300 MHz, DMSO-d_6) δ ppm 1.1 - 1.3 (m, 3H) 1.7 - 1.8 (m, 2H) 1.9 - 2.1 (m, 4H) 2.3 - 2.5 (m, 3H) 2.8-3.0(m, 2H) 3.6(s, 2H) 3.7-3.8(m, 1H) 3.9-4.0 (m, 3H) 4.2-4.4 (m, 2H) 4.6 (s, 2H) 5.4(m, 1H) 5.8 (s, 1H) 6.6 (d, J=9.20 Hz, 1H) 7.1 (d, J=8.0 Hz, 1H) 7.25(d, J=8.15Hz, 1H) 7.9(d, J=9.90 Hz, 1H) 8.3(s, 1H) 11.25(br s, 1H). HRMS (ESI-TOF): calcd for $C_{27}H_{32}N_6O_5$(M+H)$^+$, 521.24342; obsd, 521.24313.

(S)-6-((1-(2-(2-oxo-7-(tetrahydrofuran-3-yloxy)-1,5-naphthyridin-1(2H)-yl)ethyl)piperidin-4-ylamino)methyl)-2H-pyrido[3,2-b][1,4]oxazin-3(4H)-one (HAR_17)

Compound **HAR_17** was synthesized from intermediate **AP_Ib** and (S)-tetrahydrofuran-3-ol using procedure analogues to compound **HAR_1**.

^{1}H NMR (300 MHz, DMSO-d_6) δ ppm 1.1 - 1.3 (m, 3H) 1.7 - 1.8 (m, 2H) 1.9 - 2.1 (m, 4H) 2.26 - 2.47 (m, 3H) 2.8-2.99(m, 2H) 3.69(s, 2H) 3.75-3.8(m,1H) 3.9-4.0 (m, 3H) 4.2-4.4 (m, 2 H) 4.6 (s, 2H) 5.39(m, 1H), 5.79(s, 1H) 6.61 (d, J=9.20 Hz, 1H) 7.01 (d, J=8.0 Hz, 1H) 7.27 (d, J=8.16Hz, 1H) 7.85(d, J=9.91 Hz, 1H) 8.3(s, 1H) 11.23(br s, 1H). HRMS (ESI-TOF): calcd for $C_{27}H_{32}N_6O_5$(M+H)$^+$, 521.24342; obsd, 521.24313.

6-((1-(2-(2-oxo-7-(pyridin-2-ylmethoxy)-1,5-naphthyridin-1(2H)-yl)ethyl)piperidin-4-ylamino)methyl)-2H-pyrido[3,2-b][1,4]oxazin-3(4H)-one (HAR_18)

Compound **HAR_18** was synthesized from intermediate **AP_Ib** and pyridin-2-yl methanol using procedure analogues to compound **HAR_1**.

^{1}H NMR (300 MHz, DMSO-d_6) δ ppm 1.20 - 1.32 (m, 2H) 1.70 - 1.81 (m, 2H) 1.93 - 2.05 (m, 2H) 2.31 - 2.39 (m, 2H) 2.40 - 2.48 (m, 2H) 2.80 - 2.92 (m, 2H) 3.69 (s, 2H) 4.31 (t, J=7.06 Hz, 2H) 4.60 (s, 2H) 5.46 (s, 2H) 6.66 (d, J=9.61 Hz, 1H) 7.01 (d, J=8.10 Hz, 1H) 7.29 (d, J=8.10 Hz, 1H) 7.37 (dd, J=7.54, 4.90, 1.13 Hz, 1H) 7.51 (d, J=2.07 Hz, 1H) 7.58 (d, J=7.91 Hz, 1H) 7.82 - 7.92 (m, 2H) 8.38 (d, J=2.45 Hz, 1H) 8.60 (dd, J=4.80, 1.70, 0.85 Hz, 1H) 11.14 (br s, 1 H). HRMS (ESI-TOF): calcd for $C_{29}H_{31}N_7O$ (M+H)$^+$, 542.24375; obsd, 542.24271.

6-((1-(2-(2-oxo-7-(pyridazin-3-ylmethoxy)-1, 5-naphthyridin-1(2H)-yl)ethyl)piperidin-4-ylamino)methyl)-2H-pyrido[3,2-b][1,4]oxazin-3(4H)-one (HAR_19)

Compound **HAR_19** was synthesized from intermediate **AP_Ib** and pyridazin-3-ylmethanol using procedure analogues to compound **HAR_1**.

^{1}H NMR (300 MHz, DMSO-d_6) δ ppm 1.21 - 1.3 (m, 2H) 1.70 - 1.80 (m, 2H) 1.93 - 2.1 (m, 2H) 2.31 - 2.39 (m, 2H) 2.40 - 2.48 (m, 2H) 2.80 - 2.92 (m, 2H) 3.68 (s, 2H) 4.31 (t, J=7.1 Hz, 2H) 4.59 (s, 2H) 5.80 (s, 2H) 6.50 (d, J=9.42 Hz, 1H) 6.87 (d, J=8.48 Hz, 1H) 7.00 (d, J=7.91 Hz, 1H) 7.27 (d, J=8.10 Hz, 1H) 7.70 - 7.76 (m, 3H) 7.86 (d, J=9.61 Hz, 1H) 8.11 (d, J=8.48 Hz, 1H) 8.28 (s, 1H). HRMS (ESI-TOF): calcd for $C_{28}H_{30}N_8O_4$ (M+H)$^+$, 543.24236; obsd, 543.24705.

6-((1-(2-(7-((1-Methyl-1H-pyrazol-3-yl)methoxy)-2-oxo-1,5-naphthyridin-1(2H)-yl)ethyl)piperidin-4-ylamino)methyl)-2H-pyrido[3,2-b][1,4]oxazin-3(4H)-one (HAR_20)

Compound **HAR_20** was synthesized from intermediate **AP_Ib** and (1-methyl-1H-pyrazol-3-yl)methanol using procedure analogues to compound **HAR_1**.

^{1}H NMR (300 MHz, DMSO-d_6) δ ppm 1.16 - 1.34 (m, 2H) 1.71 - 1.84 (m, 2H) 2.07 (t, J=10.46 Hz, 2H) 2.34 - 2.46 (m, 1H) 2.53 - 2.61 (m, 2H) 2.86 - 2.98 (m, 2H) 3.70 (s, 2H) 3.84 (s, 3H) 4.34 (t, J=6.59 Hz, 2H) 4.60 (s, 2H) 5.28 (s, 2H) 5.75 (s, 1H) 6.37 (d, J=2.07 Hz, 1H) 6.65 (d, J=9.61 Hz, 1H) 7.01 (d, J=8.10 Hz, 1H) 7.29 (d, J=8.10 Hz, 1H) 7.54 - 7.62 (m, 1H) 7.69 (d, J=1.88 Hz, 1H) 7.85 (d, J=9.61 Hz, 1H) 8.30 (d, J=1.88 Hz, 1H) 11.13 (br s, 1H). HRMS (ESI-TOF): calcd for $C_{28}H_{32}N_8O$ (M+H)$^+$, 545.25801; obsd, 545.25461.

6-(((3S,4R)-3-Fluoro-1-(2-(7-(isoxazol-3-yloxy)-2-oxo-1,5-naphthyridin-1(2H)-yl)ethyl)piperidin-4-ylamino)methyl)-2H-pyrido[3,2-b][1,4]oxazin-3(4H)-one (HAR_21)

Compound **HAR_21** was synthesized from intermediate **AP_18** and 3-hydroxy isoxazole using procedure similar to compound **HAR_1**.

^{1}H NMR (300 MHz, DMSO-d_6) d ppm 1.51-1.60 (m, 2H) 2.12 -2.35 (m, 4H) 2.41-2.45 (m, 1H) 2.82 -2.85 (m, 1H) 3.11 -3.18 (m, 1H), 3.75 -3.78 (m, 2H) 4.25 -4.30 (m , 2H) 4.7 (s, 3H) 6.65 (d, J=1.6 Hz, 1H) 6.85 (d, J=9.32 Hz 1H) 7.01 (d, J=8.1 Hz, 1H) 7.34 (d, J=8.11 Hz, 1H) 7.79 (d, J=9.65 Hz, 1H) 8.10 (d, J=2.05 Hz, 1H) 8.61(d, J=1.65 Hz 1H) 9.01 (s, 1H) 11.25 (s, 1H). HRMS (ESI-TOF): calcd for $C_{26}H_{26}FN_7O_5$ (M+H)$^+$, 536.19795; obsd, 536.19783.

6-(((3S,4R)-3-Fluoro-1-(2-(2-oxo-7-(pyridin-3-yloxy)-1,5-naphthyridin-1(2H)-yl)ethyl)piperidin-4-ylamino)methyl)-2H-pyrido[3,2-b][1,4]oxazin-3(4H)-one (HAR_22)

Compound **HAR_22** was synthesized from **AP_18** and 3-hydroxy pyridine using procedure similar to compound **HAR_1**.

^{1}H NMR (300 MHz, DMSO-d_6) δ1.70 - 1.85 (m, 2H), 1.95– 2.0 (m, 2H), 2.20 (t, J=11.4 Hz, 2H), 2.61 (t, J=11.1 Hz, 2H), 2-84-2.87 (m, 1H), 3.06 (d, J=10.7 Hz, 2H), 3.35 (s, 2H), 4.0 (s, 2H), 4.43(t, J=6.8 Hz, 2H), 6.70(d, J=9.80 Hz, 1H), 7.35-7.57(m, 5H), 7.90-7.95 (m, 3H), 8.30 (s, 1H), 12.20 (br s, 1H). HRMS (ESI-TOF): calcd for $C_{28}H_{28}FN_7O_4$ (M+H)$^+$, 546.22204; obsd, 546.22705.
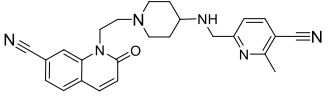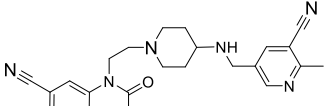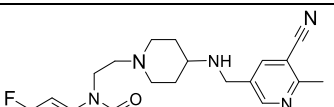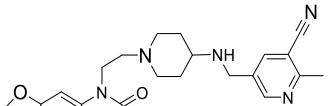
The spectral data (^{1}H NMR, and high resolution mass spectra-HRMS) of all the synthesized final compounds were in full agreement with the proposed structures and purity of all the final compounds were found to be >95% by HPLC method
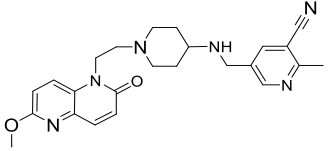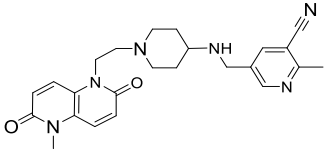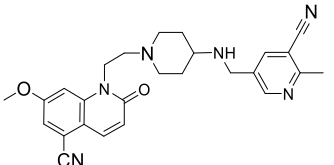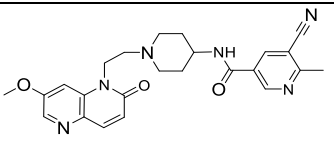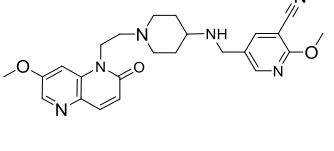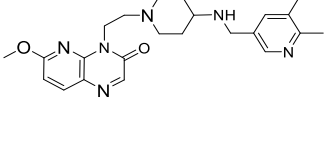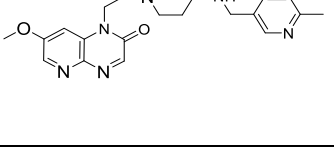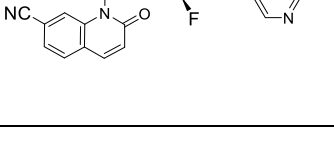
5. 4 *In vitro Mycobacterium tuberculosis* susceteptability testing (*Mtb* MIC), hERG inhibition potency, cytotoxicity and lipophilicity studies of the synthesised molecules

All the synthesized derivatives were first evaluated for their antimycobacterial potency (*Mtb* MIC), hERG inhibition and lipophilicty (logD) determination in order to build structure-activity relationship (SAR) and optimizatize identified lead series for improving potency and selectivity against hERG. Few representative compounds were further subjected to *Mtb* gyrase supercoiling and *Msm* GyrB ATPase activity inhibitions to link the observed Mtb MIC to Mtb GyrA inhibition and rule out any contribution of GyrB ATPase inhibition. Time dependent kill

kinetics were performed against *Mycobacterium tuberculosis* H37Rv strain to demonstrate bactericidal activity for the series. Resistant mutants were raised against representative compound and moxfloxacin using *Mtb* H37Rv strain to map the mutation on the *Mtb* gyrA subunit. Cross resistant studies were carried out using resitant mutants of moxifloxacin and amino piperidine based NBTIs to rule out the cross resistant against FQr strains and establish novel MOA, which is different from FQ mechanism. Further, majority of compound were profiled for Caco2 permeability assay to access the intestinal permeability and explaore SPR handle for oral bioavailability. All the final compounds were were evaluated for cytoxicity by checking them in a *in vitro* cytotoxicity assay against A549 cell line (human lung carcinoma) at 100 and 50 µM concentration and found to be inactive against both concentration tested. The results of in-vitro biological profile and physiochemical properties are summarized in the following Tables for SAR understanding.

Table 5.2: *In vitro* biological evaluation of the synthesized derivatives **AP_4 – AP_22**

Compound	Structure	Mtb MIC (µM)	LogD	hERG IC$_{50}$ (µM)	Caco-2:Papp A−B/B−A (1×10^{-6} cm/s)
AP_4		>15	1.1	5.3	17.1/9.4
AP_5		0.031	1.3	26	13.6/7.4
AP_6		0.13	0.81	69	18/9.8
AP_7		0.03	1.07	50.6	10.5/8.3

AP_7a		2	ND	10	ND
AP_8		>30	-0.6	>33	ND
AP_9		<0.01	1.86	2.5	10/4.7
AP_10		0.06	1.4	74	4.2/13
AP_11		0.03	1.2	12	13/9
AP_12		0.06	1.65	13	ND
AP_13		0.06	0.38	>100	ND
AP_14		0.13	1.29	>100	14.5/13
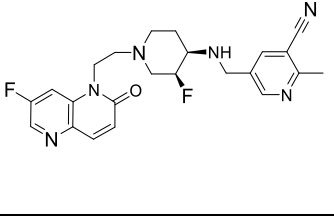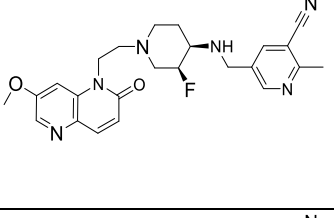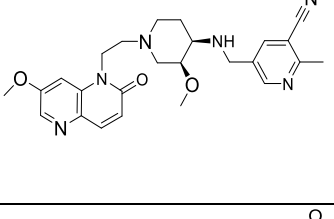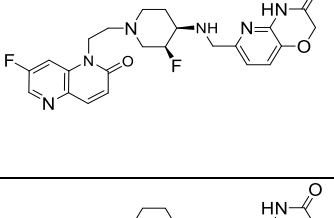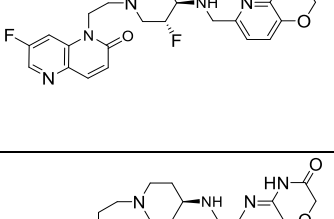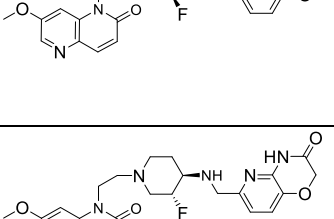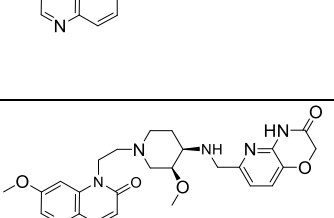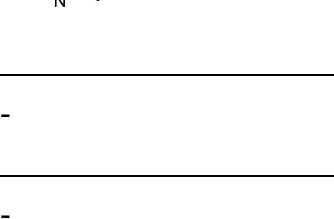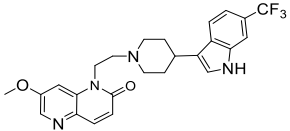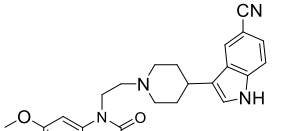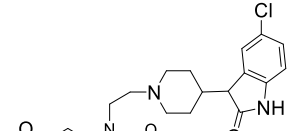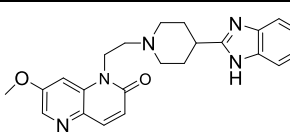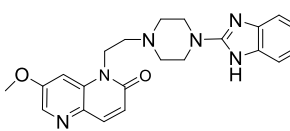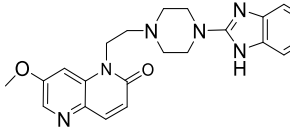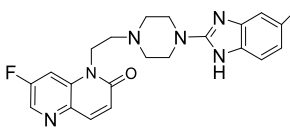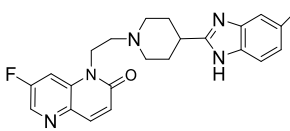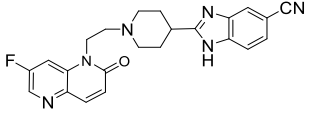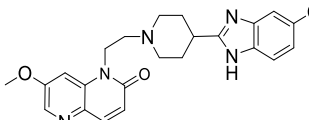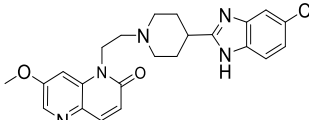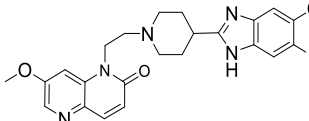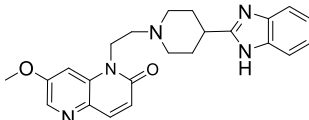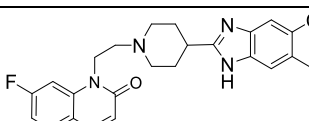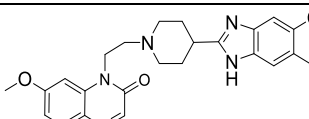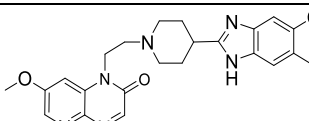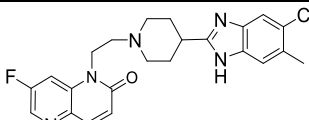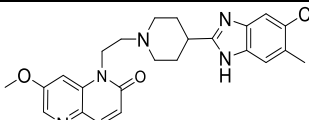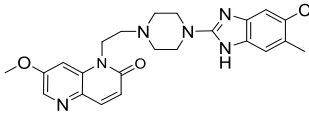
AP_15		0.13	0.92	133	17.7/15.4
AP_16		0.031	1.29	90	13.6/7.4
AP_17		0.031	0.99	151	11.7/9.9
AP_18		0.063	0.47	>100	7.6/11.2
AP_19		0.063	0.47	>100	8.1/12.3
AP_20		0.015	0.64	>100	4.1/10.8
AP_21		0.031	0.82	>100	3.4/12.7
AP_22		0.063	0.4	>100	ND
Rifampicin	-	0.031	ND	ND	ND
Moxifloxacin	-	0.15	ND	ND	ND

Table 5.3: *In vitro* biological evaluation of the synthesized derivatives **IN_1, IN_2, OI_1** and **BI_1– BI_16**

Compound	Structure	Mtb MIC (μM)	LogD	hERG IC$_{50}$ (μM)
IN_1		50	4	1.8
IN_2		100	3.3	2
OI_1		100	2.8	4.8
BI_1		0.19	4.0	1
BI_2		3.13	2.8	10
BI_3		100	2.4	7
BI_4		15	3.7	1
BI_5		0.78	ND	ND
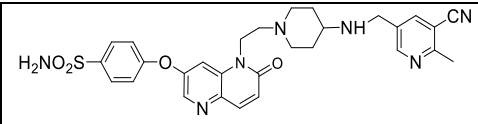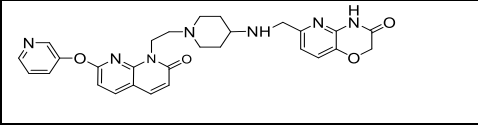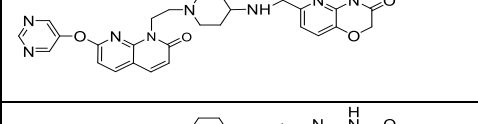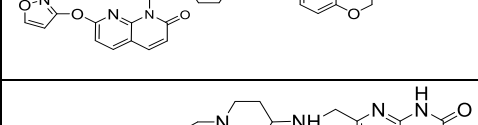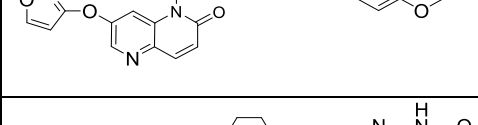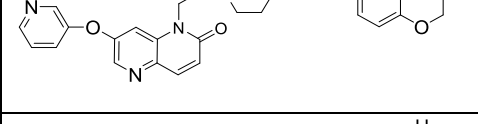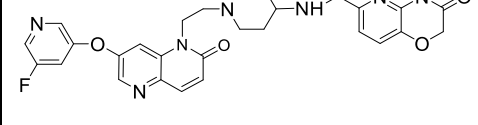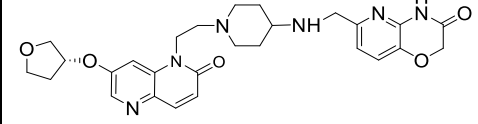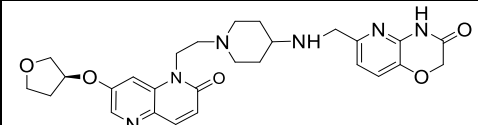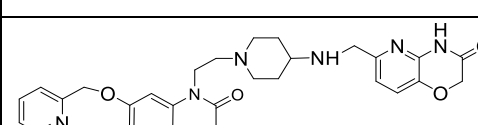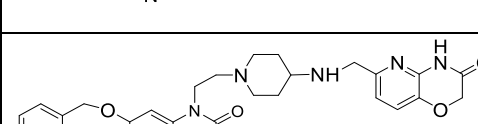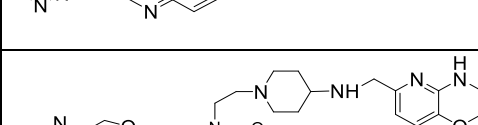
BI_6		50	ND	ND
BI_7		0.25	3.6	1
BI_8		3.13	2.4	4.5
BI_9		0.06	4	1.2
BI_10		0.13	3.8	1.4
BI_11		1.56	3.7	1.2
BI_12		0.13	ND	ND
BI_13		0.39	3.5	10
BI_14		3.15	ND	ND
BI_15		0.19	2.8	10
BI_16		0.78	3.2	>33
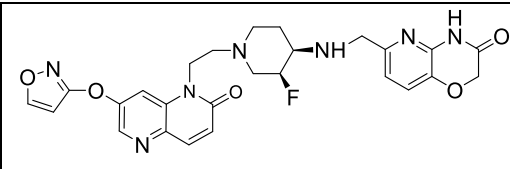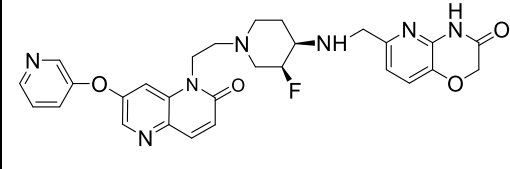
Compound	Structure	Mtb MIC (μM)	AZ LogD 7.4[a]	hERG IC$_{50}$ (μM)
Rifampicin	-	0.031	ND	ND
Moxifloxacin	-	0.15	ND	ND

ND- Not determined

Table 5.4: *In vitro* biological evaluation of the synthesized derivatives **HAR_1-HAR_22**

Compound	Structure	Mtb MIC (μM)	AZ LogD 7.4[a]	hERG IC$_{50}$ (μM)
HAR_1		0.19	4.0	>33
HAR_2		0.19	2.4	>33
HAR_3		0.25	2.41	>33
HAR_4		0.03	0.71	>100
HAR_5		0.06	1.3	>100
HAR_6		0.03	1.28	>100
HAR_7		0.06	1.18	82
HAR_8		0.06	0.99	>100

HAR_9		0.06	0.9	>100
HAR_10		0.06	1.22	155
HAR_11		0.25	0.82	>224
HAR_12		0.25	0.97	>100
HAR_13		0.25	0.76	>100
HAR_14		0.06	1.2	>100
HAR_15		0.25	1.45	79
HAR_16		0.25	1.07	>100
HAR_17		0.5	1.06	>100
HAR_18		0.5	1.6	>100
HAR_19		1.0	0.86	>100
HAR_20		0.25	1.54	>100

HAR_21		0.25	0.76	>100
HAR_22		0.25	1.45	78

5.5 Discussion

5. 5.1 Evaluation of *Mtb* DNA gyrase inhibition and mechanism of inhibition

Representative compounds from there series (**AP**, **BI** and **HAR**) were further investigated using inv vitro mycobacterial gyrase inhibition assay (Both Mtb DNA gyrase supercoiling and Msm GyrB ATPase assays) to link the *Mtb* MIC to gyrase inhibition (*Mtb* DNA gyrase supercoiling assay **Table 5.5**). Aslo to understand the inhibition at a molecular level vis a vis the fluoroquinolones, key compound from the synthesized set was evaluated in a cleavable complex assay (**Figure 5.4**). Most of the compounds with MIC against *Mtb* also inhibited the supercoiling activity of *Mtb* gyrase and inactive against *Msm* GyrB ATPase activity, thus confirming their mode of inhibition through inhibition either *Mtb* GyrA subunit or holo enzyme.

Compounds from **AP** and **HAR** series with aminopiperidine linker inhibited *Mtb* DNA gyrase supercoiling in submicromolar range and displayed potent MIC against *Mtb*, whereas compounds belonging to **BI** and **HAR** series with piperidine linker inhibited supercoiling activity in single-digit micromolar range with potent *Mtb* MIC. Compounds, which are in inactive against *Mtb* MIC were also inactive against the enzyme (IC$_{50}$ > 50 μM).

Table 5. 5: Mycobacterial gyrase inhibition profile for compounds from **AP**, **BI** and **HAR** series

119

Compound name	Mtb Gyrase SC IC$_{50}$ (μM)	Msm GyrB ATPase IC$_{50}$ (μM)	Mtb MIC (μg/ml)
AP_1	1.05	>100	1
AP_2	0.15	>100	0.13
AP_3	0.11	>100	0.13
AP_4	>15	>100	>100
AP_5	0.25	>100	0.03
AP_7	0.14	>100	0.03
AP_9	0.065	>100	<0.01
AP_16	0.25	>100	0.03
AP_18	0.35	>100	0.06
AP_19	0.24	>100	0.06
AP_22	0.17	>100	0.05
BI_1	1	>100	0.19
BI_9	2	>100	0.03
BI_15	0.9	>100	0.06
HAR_2	1.9	>100	0.19
HAR_10	0.14	>100	0.06
HAR_11	0.173	>100	0.25
HAR_22	0.8	>100	0.25
Moxifloxacin	12.5	ND	0.06

ND-Not determined

In order to rule out any contribution of *Mtb* GyrB inhibition to the observed *Mtb* MICs, the same set of compounds were screened against *Mycobacterium smegmati*s (*Msm*) GyrB as a surrogate for *Mtb* GyrB enzyme (Hameed, P.S. *et al.,* 2013). The lack of inhibitory activity of these compounds against the *Msm* GyrB clearly indicated that these compounds were inhibitor of either the holoenzyme (GyrA2B2 complex) or GyrA subunit.

FQs trap the DNA gyrase bound to double strand-cleaved DNA in a ternary complex; thereby resulting in the formation of linearised DNA in the cleavable complex assay as shown with moxifloxacin (**Fig. 5.4b**). In contrast, the titration of compound **AP_7** showed an increased formation of single-strand cleaved (nicked) plasmid with increasing compound concentration (**Fig. 5.4a**, **Fig 5.4c**). We propose that the chemical scaffold described in our work, arrests the reaction at the single-strand cleavage (or nick) and hence, is the primary mode of inhibition by trapping this as ~70% of reaction product. A small fraction of the enzyme-DNA complex may "proceed" through to the double-stranded cleavage, thereby resulting in a linear product as visualized on the gel. This level one must note is rather small (20%) just above the basal level of 10% of intact DNA. A much smaller increase in the formation of linear DNA was seen primarily at lower concentrations which saturated at 20% of the total DNA in the reaction (basal level of intact DNA ~ 10%). This suggests that the primary mechanism of inhibition of the enzyme-DNA complex by compound **AP_7** appears to be via trapping the transiently single-strand cleaved DNA as it represents ~ 70% of product formed. This is different from the mechanism of inhibition of FQs which form in classical "cleavable complex".

Another phenomenon observed was that these inhibitors were equipotent in inhibition of the enzyme (IC_{50}) and bacterial cell growth (MIC) as compared to the FQs (e.g. moxifloxacin), which exhibit MIC several orders of magnitude lower than the enzyme inhibition. This phenomenon observed with the FQs has been explained by the downstream effects of double-stranded lesions in the chromosomal DNA resulting in an SOS response of the cell leading to a more rapid inhibition/kill. This data suggests that the mechanism of action of the N-linked quinolones and naphthyridones inhibitors could be different from that of the FQs.
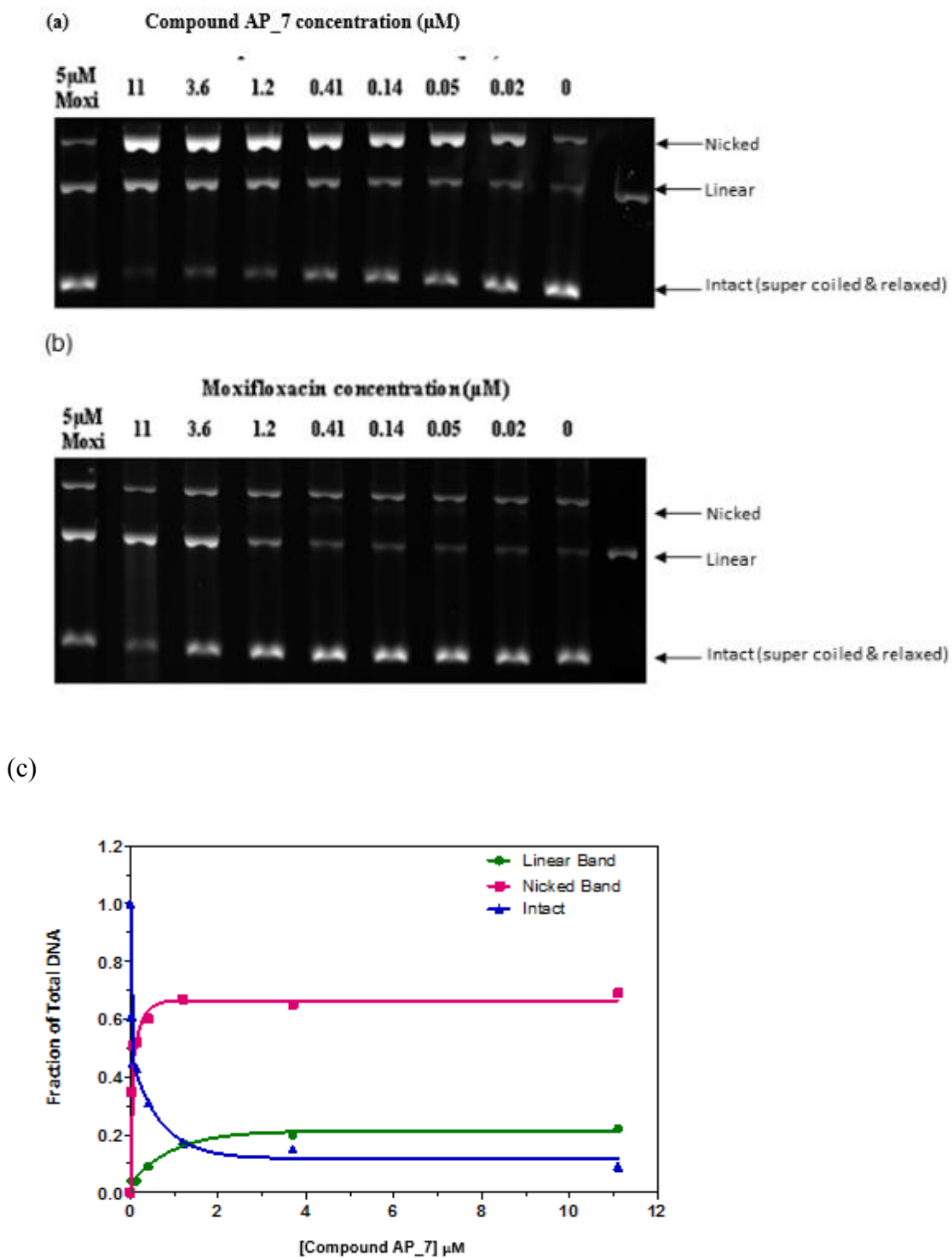
Figure 5.4: *Mtb* DNA gyrase cleavable complex assay for (a) compound **AP_7** and (b) moxifloxacin. A titration was performed with varying concentrations of compound **AP_7** and moxifloxacin. (c) Plot representing the relative fractions of nicked, linear and supercoiled DNA to the total DNA in the sample is shown.

5.5.2 Structure activity relationship (SAR) and homology modelling of aminopiperidine series

The mechanism of inhibition and the binding mode of NBTIs, methoxyquinoline-3-carbonitrile (GSK299423) for the antibacterial series has been reported (Bax, B.D. *et al.*, 2010). From the crystal structure studies of methoxyquinoline-3-carbonitrile (GSK299423), one can infer that the LHS portion of the NBTIs binds to DNA substrate, whereas the RHS portion interacts with the protein dimer interface of GyrA subunits. The binding site of NBTIs is distinct from the FQ binding and they are reported to be active against FQ-resistant strains of *S. aureus.* However, the mode of binding of NBTIs to the *Mtb* GyrA subunit is not known. As the active site of DNA gyrases are highly conserved across the bacterial species (Tretter, et al., 2010), we assumed that the binding mode could be similar to what has been reported for *S. aureus* DNA gyrase.

The biological profiles of initial lead compounds with both biclyclic and monocyclic RHS shown in **Table 5.6**

Table 5.6: Properties of the initial lead compounds (**AP_1, AP_2, AP_3**) and the novel compounds   with a monocyclic RHS (**AP_4** and **AP_ 5**)

Properties	AP_1	AP_2	AP_3	AP_4	AP_5
Mtb MIC (μM)	1	0.13	0.06	>15	0. 03
Mtb Gyrase supercoiling IC$_{50}$ (μM)	1.05	0.150	0.110	>100	0.25
Msm GyrB ATPase IC$_{50}$ (μM)	>100	>100	>100	>100	>100
LogD pH7.4	0.7	0.8	0.4	1.1	1.3
hERG IC$_{50}$ (μM)	44	21	ND	5.3	26
Caco-2: Papp A−B/B−A (1×10^{-6} cm/s)	1.9/38.3	1.1/25	2.0/12.6	17.1/9.1	13.6/7.4

As shown in **Table 5.6**, the compounds **AP_1**, **AP_2** and **AP_3** displayed low micromolar or *Mtb* MIC along with potent IC50 in the *Mtb* DNA gyrase super coiling (SC) assay. Specific

activity of the *Mtb* enzyme was too low to set up a specific assay for ATPase activity of *Mtb* gyrB (Hameed, P.S. et *al.*, 2013). Therefore, we have used *Mycobacterium smegmatis* (*Msm*) GyrB as a surrogate for the *Mtb* enzyme. None of the initial leads inhibited the ATPase activity of *Msm* GyrB suggesting that the holoenzyme (GyrA2B2 complex) or GyrA was inhibited. Initial leads inhibited the hERG channel and had poor Caco2 permeability. Further medicinal chemistry optimization efforts were primarily focused on improving the *Mtb* MIC, Caco2 permeability and reducing the hERG liability. During lead optimization, we tracked the SAR based on *Mtb* MIC assuming that the mechanism of gyrase inhibition was retained across newly synthesized compounds in this series.

Medicinal chemistry optimization and new compound design were shown in **Figure 5.5**
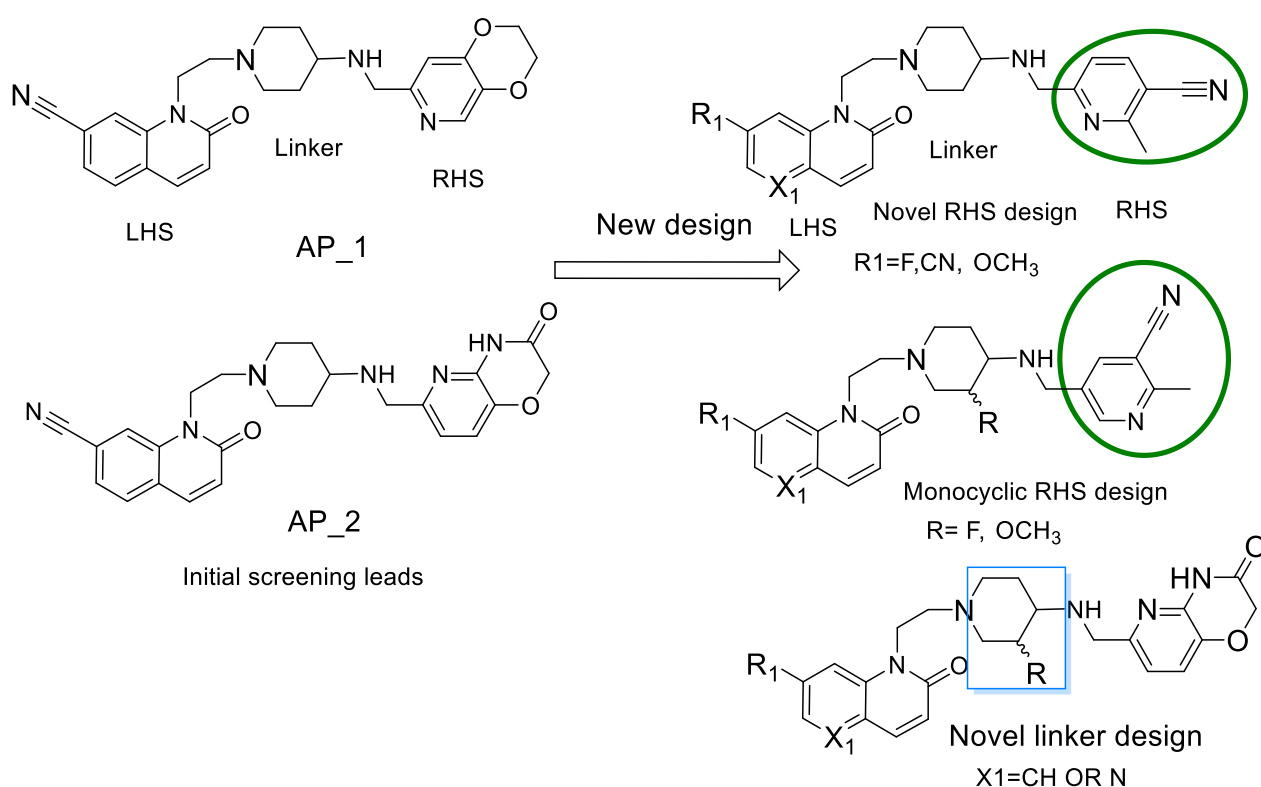
Figure 5.5: Structures of initial leads (**AP_1** & **AP_2**) and new compound design

We hypothesized that reducing the number of hydrogen bonding groups with optimal logD in the range of 1 to 2 or modulating pKa of basic aminopiperidine linker would improve the Caco-2 permeability and maintain MIC. Based on the above hypothesis, we have proposed new design set of molecules in **Figure 5.5**. To validate this hypothesis, we have designed compounds **AP_4** and **AP_5** having di-substituted pyridines with hydrophilic and electron withdrawing cyano substitution were designed by opening the bicyclic RHS ring. A shape

based overlay of the newly designed analogs (**AP_4** & **AP_5**) with the initial leads (**AP_1** and **AP_2** in **Fig.5.6**) using ROCS tool suggested that the overall shape of molecules on the LHS or the linker region was similar.
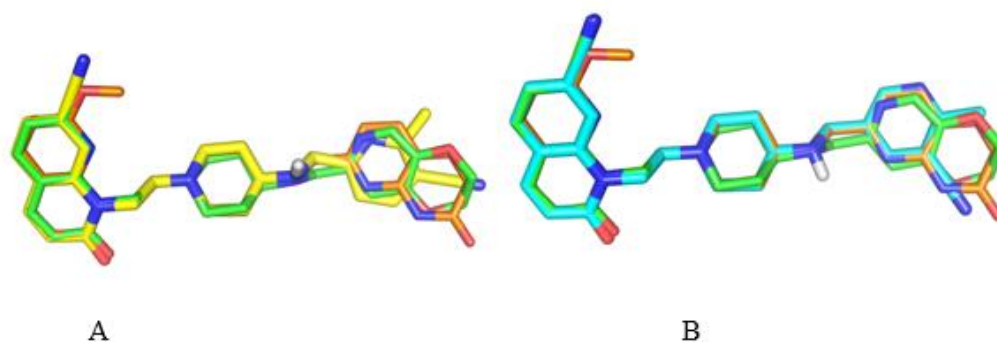
Figure 5.6: Overlay of the initial leads with compounds containing a novel monocyclic RHS; **AP_4** (Yellow) on **AP_1** (Green) and **AP_2** (Orange) (A) and **AP_5** (Cyan) on **AP_1** and **AP_2** (B).

The RHS fragment with the 3-pyridyl ring in compound **AP_5** fully occupies the shape of the bicyclic RHS (**AP_1** and **AP_2**) thereby, suggesting that their binding mechanism could be similar. In the case of compound **AP_4**, the RHS with 2-pyridyl ring did not fully occupy the shape of bicyclic RHS ring (**AP_1** and **2**) of the initial leads. Hence, compound **AP_4** may have different behavior with respect to the enzyme potency. Based on this hypothesis, compound **AP_4** and **AP_5** were synthesized and tested. Compound **AP_5** maintained good enzyme potency and MIC, whereas as compound **AP_4** lost both these activities

In order to explain the difference in potency observed for **AP_4** and **AP_5**, understand the binding modes and explain the activity trend for newly synthesized compounds, we took computational modelling help. Firstly we have docked representative compounds from aminopiperidine series (**AP_4** and **AP_5**) into the published crystal structure of *S. aureus* DNA bound GyrA subunit (PDB ID: 2XCS) as no co-crystal structure of *Mtb* Gyrase with NBTIs were reported. Subsequently, an *Mtb* DNA gyrase subunit A (*Mtb* GyrA) homology model was built on 2XCS as a template using MOE. FRED docking tool was used understand the binding interactions.

Figure **5.7**, **5.8** and **5.9** shows the possible binding modes of compound **AP_4** and **AP_5** in the DNA bound GyrA subunit of *S. aureus* and in the *Mtb* GyrA model, respectively. Docking analysis suggested that the LHS quinolone of compound **AP_4** and **AP_5** were positioned between the two base pairs of DNA as observed for NBTIs, whereas the RHS pyridine binding showed a subtle difference with respect to the methyl group orientation.The methyl substitution in the RHS of compound **AP_5** was oriented towards the hydrophobic region occupied by Ala68, Val71, Gly72, and Met121 of the DNA bound GyrA subunit of *S. aureus* (Ala74, Val77, Ala78 and Met127 in the Mtb GyrA respectively) making several van der Waals contacts. The methyl group also makes a stronger interaction with the carbonyl of Ala74 and methyl of Ala78 in *Mtb*. On the contrary, the methyl group of pyridine RHS in compound **AP_4** oriented away from the hydrophobic region (**Figure. 5.7**) and the nitrile group was in close proximity to Ala 74. Additionally, the -NH group of amino piperidine ring in compound AP_5 makes a key interaction with the carboxylate group of Asp83 of the *S. aureus* DNA bound GyrA (Asp 89 in *Mtb* GyrA). This observation was consistent with the binding mode of GSK299423 (Bax *et al*, 2010). On the other hand, -NH group's hydrogen in compound **AP_4** was 4.1 Å unit away from the oxygen atom of the carboxylate group in Asp83 (in the homology model of *Mtb* GyrA ,it was 4.7 Å away from Asp89) which is unlikely to make a strong hydrogen bonding interaction with the Asp83 residue. Thus, the combination of loss of hydrophobic interaction and a weak hydrogen bonding contact with the Asp 83 may partially explain the loss of potency for compound **AP_4**.

Addtionally, both the new compounds with monocyclic RHS (**AP_4** and **AP_5**) showed improved Caco-2 permeability over the bicyclic RHS analog (**AP_1** and **AP_3**).This validated our hypothesis (in design part) that lowevring of hydrogen bonding group and polar surface area (PSA) with optimal logD for oral absorption (1 to 2) would result in improved caco2 perameability and inturn increased oral absorption.

Although, compounds **AP_4** and **AP_5** had similar logD (1.1 to 1.3), compound **AP_5** showed moderate hERG inhibition (IC_{50} 26 µM), whereas compound **AP_4** was more potent (hERG IC_{50} 5.3 µM) against the hERG channel. The improved hERG selectivity seen for compound **AP_5** could be due to the substitution pattern of CH_3 and cyano groups on the RHS ring. Based on the promising profile of compound **AP_5**, we fixed 2-methyl-3-cyano pyridine as the RHS and started exploring the SAR on the LHS part.
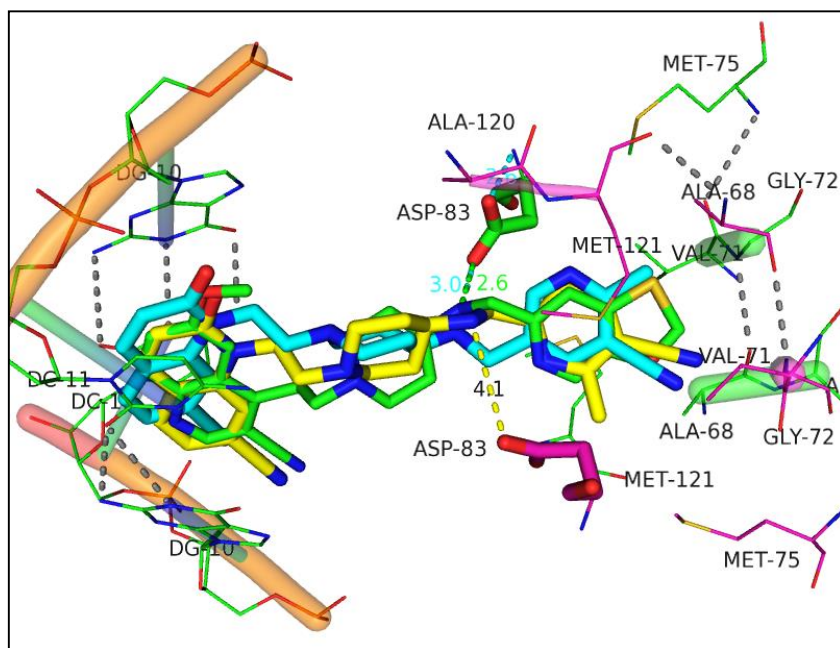
Figure 5.7: Docking pose of compound **AP_4** (yellow) & **AP_5** (cyan) in the crystal structure

S. aureus DNA gyrase bound to **GSK299423** (Baxter,B.D. *et al.*, 2010).
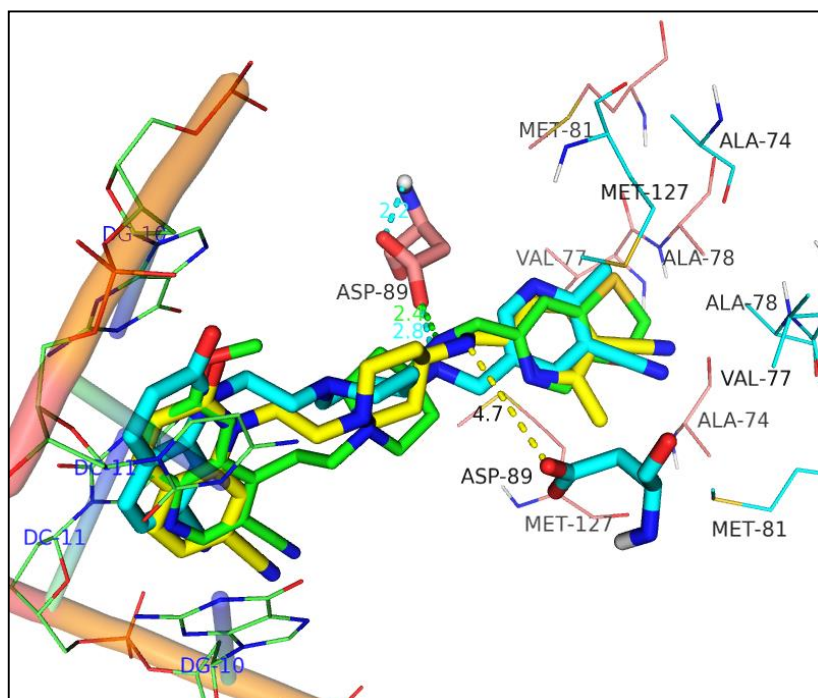
Figure 5.8: Docking pose of compound **AP_4** (yellow) & **AP_5** (cyan) on to the homology model of *Mtb* DNA gyrase subunit A
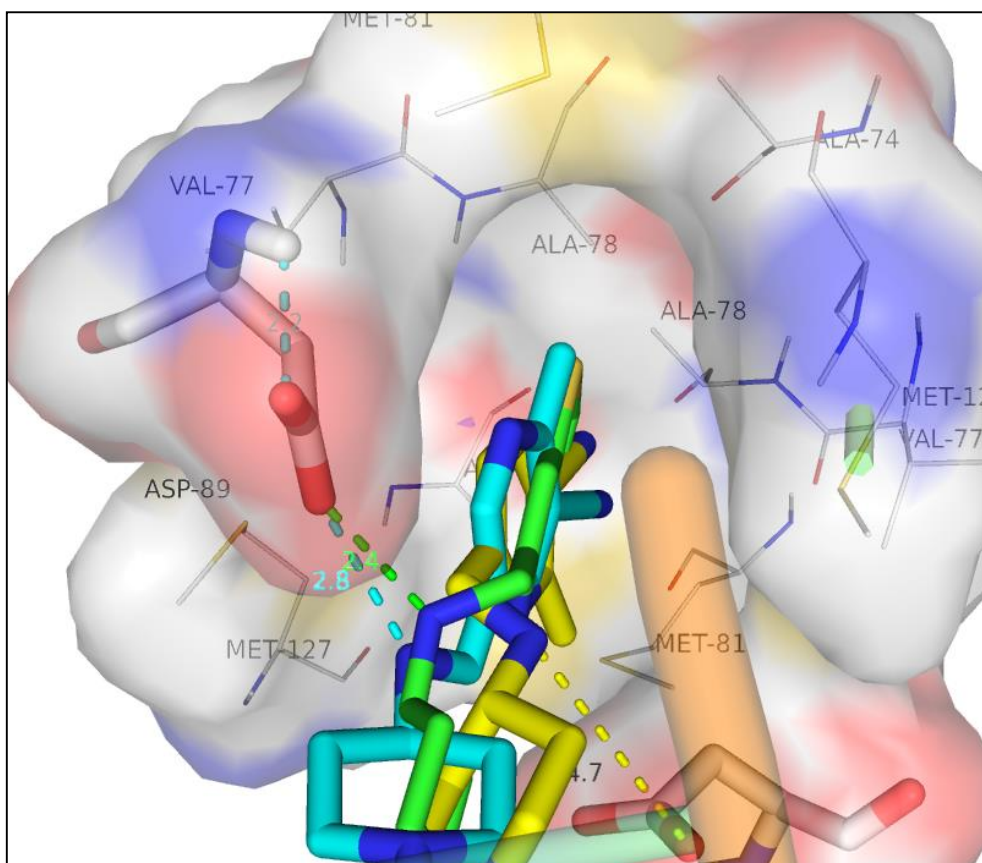
Figure 5. 9: Molecular surface of the active site depicting the RHS of compound **AP_4** and **AP_5.** The LHS part is not shown in **figure 5.9** for clarity purpose.

Replacement of the LHS cyanoquinolone ring with 1,5-naphthyridone resulted in a 2-3 fold improvement in the hERG liability, while maintaining the MIC and Caco-2 permeability (compound **AP_6** and **AP_7** in Table 5.2). Compound **AP_7** showed a 4-fold improvement in MIC (0.03 µM) as compared to the starting lead **AP_2**. Moving the methoxy group to the 6-position of 1, 5 naphthyridone LHS weakened the MIC (compound **AP_7** and **AP_7a** shown as match pair in **Table 5.2**), whereas converting compound **AP_7a** to a 1, 5 naphthyridine dione form (compound **AP_8**) completely abolished the antimycobacterial activity, suggesting that the substitution at 7-position of the LHS ring was essential for retaining MIC. The replacement of 1, 5 naphthyridone LHS ring with a 5-cyano-7-methoxy quinolone LHS (compound **AP_9**) improved the *Mtb* MIC to <0.01 µM at the cost of hERG selectivity. The best MIC observed for compound **AP_9** could be due to the improved binding to enzyme (super-coiling assay IC$_{50}$ 0.065 µM) or better cell permeability driven by higher lipophilicity. Changing the alkyl bridge of the RHS into an amide was tolerated for both the Mtb MIC and hERG selectivity (compound **AP_7** vs **AP_10** in **Table 5.2**). To further improve the hERG selectivity, we explored a pyrido

pyrazinone ring in the LHS (compound **AP_12** & **AP_13** in **Table 5. 2**). Compound **AP_15** with a pyrido[2,3-b]pyrazin-2(1H)-one improved the hERG inhibition (IC_{50}>100 μM) and compound **AP_12** with a pyrido[2,3-b]pyrazin-3(4H)-one lost the hERG selectivity (IC_{50} 13 μM). The higher hERG potency observed for compound **AP_12** could be due to the high logD and the enhanced pi-stacking interaction with the hERG channel. Overall, the reduction of hERG liability for this series tracked well with reduced lipophilicity (lower logD) as reported earlier for the antibacterial N-linked aminopiperidine series (Reck,F. *et al.,* 2011).

Modulation of the pKa of aminopiperidine linker through a substitution at the 3-position of piperidine moiety with fluoro substitution lowered the hERG inhibition (Reck,F. *et al.,* 2012). Adopting a similar strategy, a 2-3 fold improvement in hERG inhibition was achieved by introducing a flouro or methoxy group at 3-position of the aminopiperidine in *cis* configuration (compounds **AP _14**, **AP_15**, **AP_16** and **AP_17** in **Table 5.2**). The compounds with *trans* configuration were not synthesized due to synthetic complexity. It was interesting to note that that the linker modification did not affect *Mtb* MIC and the Caco-2 permeability. Replacing the monocyclic pyridine RHS with a bicyclic RHS along with a fluoro substituted linker also showed a similar trend in the hERG selectivity (**AP_18**-**AP_21** in **Table 5.2**) without compromising the *Mtb* MIC. It was also observed that a fluoro-substituted linker modification with a pyridoxazinone RHS and 6-fluoro 1, 5 naphthyridone LHS combination retained the Caco-2 permeability (**AP_18** & **AP_19** in **Table 5.2**). This could be due to the better permeability of the fluoro-substituted linker and the LHS part.

In order to understand the binding mode of an optimized lead, we docked **AP_18** in the *Mtb* GyrA model. **Figure 5.10** shows the possible binding modes of compound **AP_18** in the *Mtb* GyrA model. Docking analysis suggested that the LHS napthyridone of compound **AP_18** were positioned between the two base pairs of DNA as observed for monocyclic leads (compound **AP_5**) and antibacterial NBTIs. Also, the compound **AP_19** made critical interaction with Asp89, indicated tha smaller substitution on piperidine ring was not affected the critical interactions.The RHS bicyclic ring system fits well into hydrophobic pocket and makes stronger aliphatic interactions with the methyl group of Ala78 (stick model) in *Mtb*. This observation was consistent with the binding mode of NBTI (**GSK299423**).

Figure 5.10. Probabale binding mode of compound **AP_18** (stick model, pink) in *Mtb* GyrA homology model (dimer interface, residues colored in cyan and orange, residue labels in black). For comaprision, the Sau GyrA (2XCS) with bound inhibitor is also shown.

5.5.3 Structure activity relationship study (SAR) of benzimidaolze series (BI_1 to BI_16)

Based on design hypothesis and scaffold hopping approach described in section **4.1.2**, we designed compounds with benzimidzole (**BI_1** and **BI_2**, **Table 5.6**), indole (**IN_1** and **IN_2**, **Table 5.6**) and oxindole (**OI_1**, **Table 5. 6**) as novel RHS.

The newly designed compounds (**BI_1**, **BI_2**, **IN_1**, **IN_2** and **OI_1**) were docked into 2XCS and a *Mtb* DNA gyrase subunit A (*Mtb* GyrA) homology model to understand the binding interactions. Figure 4.5 depicts the possible binding modes of compound **BI_1**, **IN_1**, **IN_2** and **OI_1** in the *S. aureus* DNA bound GyrA subunit and in the *Mtb* GyrA model (**Figure 5.11**).

5.11a

5.11b

Figure 5.11(a and **b)**: Docking pose of compound **BI_1** (cyan), **IN_1** (yellow), **IN_2** (orange), and **OI_1** (pink) on to the crystal bound structure of GSK299423 (green) to *S. aureus* DNA gyrase.
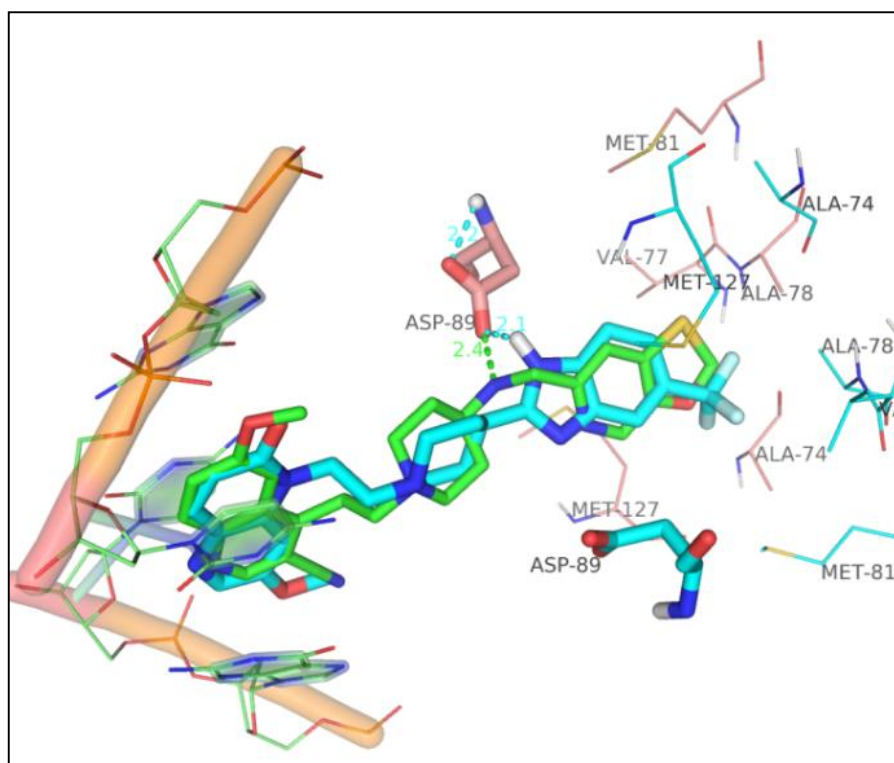
Figure 5.12: Docking pose of compound **BI_1** on to the homology model of *Mtb* DNA gyrase subunit A.

The H-bonding contacts with Asp83 (Asp89 in the case of *Mtb* GyrA model) and hydrophobic pocket occupied by Ala68, Val71, Gly72, and Met121 of *S. aureus* DNA bound GyrA (Ala74, Val77, Ala78 and Met127 in *Mtb* GyrA, respectively) were key interactions in the NBTIs binding site. The binding mode for benzimidazole derivative **BI_1** suggests that the hydrogen of N-1 atom of benzimidazole ring is engaged in H-bonding interaction with the carboxylate of Asp83 (Asp89 in the case of Mtb GyrA model) and CF_3 group attached to C-5 position point towards the hydrophobic pocket (**Figure 5.12**). This is similar to the interactions observed for NBTIs. Thus, compound **BI_1** is likely to be active against *Mtb* gyrase. On the other hand, the ring NH group in compounds **IN_1**, **IN_2** and **OI_1** is not suitably placed to make the desired hydrogen bonding interaction with Asp 83 (Asp89 in the case of *Mtb* GyrA model) due to the adaptation of a different conformational orientation of indole (**IN_1**, **IN_2**) and oxindole (**OI_1**) rings in comparison to benimidazole ring (**BI_1**). Furthermore, the substituents attached to C-5 or C-6 position of bicyclic rings in compound **IN_1** and **OI_1** are likely to be pointing away from the hydrophobic pocket constituting Ala68, Val71, Gly72, and Met121 of *S. aureus* GyrA (Ala74, Val77, Ala78 and Met127 in *Mtb* GyrA, respectively). The CF_3 group attached to C-6 in compound IN_2 is likely to pick up the hydrophobic interaction. In all cases,

the naphthyridone ring assembled between the two base pairs of DNA, similar to the reported binding mode of NBTIs.

Based on these observations, we synthesized compounds (**BI_1**, **BI_2**, **IN_1**, **IN-2** and **OI_1**) with different RHS and tested for *Mtb* gyrase inhibition. The biological activities*, in vitro* safety and logD of these novel leads are shown in **Table 5.7**.

Table 5.7: Profile of compounds with novel benzimidazole, indole and oxindole based RHS

Compd	Mtb MIC (μM)	Mtb Gyrase SC IC_{50} (μM)	Msm GyrB ATPase IC_{50} (μM)	hERG IC_{50} (μM)	LogD pH7.4
BI_1	0.19	1	>100	1	4
IN_1	100	>50	>100	2	3.3
IN_2	50	>50	>100	1.8	4
OI_1	100	>50	>100	4.8	2.8

Frome **table 5. 7**, it was evident that compound **BI_1** with benzimidazole RHS inhibited *Mtb* DNA gyrase supercoiling in the single-digit micromolar range and displayed potent MIC against *Mtb*. Compounds with indole (**IN_1** and **IN_2**) and oxindole (**OI_1**) RHS, were inactive against the enzyme (IC_{50} > 50 μM) and showed weak *Mtb* MIC (50-100 μM). As predicted by docking studies, compounds **IN_1-2** and **OI_1** are expected to be inactive against the *Mtb* gyrase, as these compounds are unable to pick up the critical interaction with Asp89. Hence, the observed lack of *Mtb* gyrase inhibition for compound **IN_1**, **IN_2** and **OI_1** were in agreement with the results from the docking studies.

BI_1

Mtb MIC: 0.19
Mtb Gyrase SC IC$_{50}$: 1 μM
hERG IC$_{50}$: 1 μM
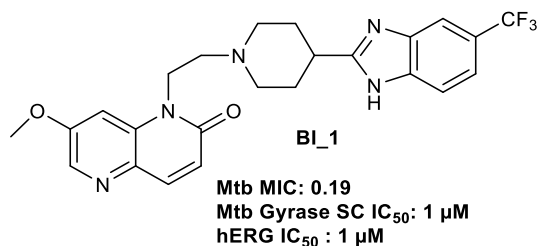
Figure 5.13: Chemical structure and biological profile of lead molecule **BI_1**.

Encouraged by the potent *Mtb* activity observed for compound **BI_1 (Figure 5.13)**, we envisaged the SAR requirements for the newly identified benzimidazole RHS and we used MIC as an activity indicator to track the SAR. We assumed that the mechanism of gyrase inhibition was similar across the newly synthesized compounds with benzimidazole RHS. Piperidine-based linker was found to be optimal for *Mtb* MIC. A substitution of piperidine with piperazine led to the weakening of *Mtb* MIC by 15-fold (compound **BI_1** versus **BI_2**, **Table 5. 3**). Removing the substitution at the C-5 position of benzimidazole resulted in the loss of *Mtb* MIC by 25-fold, thereby proving the essentiality of hydrophobic group at the C-5 position (compound **BI_2** versus **BI_3**, **Table 5.3**). Similarly, changing OCH$_3$ to F at the C-7 position of LHS resulted in the loss of *Mtb* MIC by 4-8 fold, suggesting that a bulky substitution may be essential for the MIC activity (**BI_2** versus **BI_4**, **BI_1** versus **BI_5**, **BI_6** versus **BI_8**, and **BI_10** versus **BI_11** as match pairs, **Table 5.3**). As suggested by modelling studies, the RHS benzimidazole-binding region was more hydrophobic in nature; additionally the electron withdrawing hydrophobic group like CF3 strengthened the H-bonding interaction of ring NH with Asp 89. In order to expand the hydrophobic pocket SAR further, we varied substitutions at the C-5 position and introduced additional substitution at the C-6 position of benzimidazole RHS. Replacement of CF$_3$ group by Cl at the C-5 position retained the *Mtb* MIC (compound **BI_1** versus **BI_5**), whereas CN substitution weakened MIC by 20-fold (compound **BI_1** versus **BI_8**, **Table 5.3**). This data suggested that electron withdrawing hydrophobic group at the C-5 position was essential for conferring potent Mtb MIC for this series. Introduction of other hydrophobic substituents such as methyl or fluorine enhanced the potency by 4-fold (compound **BI_7** versus **BI_9** and **BI_10**, **Table 5.3**). Addition of a nitrogen at the 8 position of LHS ring as pyrido[2,3-b]pyrazin-2(1H)-one (compound **BI_13**) or moving nitrogen to 4-position of LHS as 1,4 quinoxalinone (compound **BI_12**) was broadly tolerated for potency. Compound **BI_15** showed moderate improvement in reducing hERG inhibition (hERG IC$_{50}$ 10 μM as against 1.4 μM for compound **BI_10**). This could be due to a slight reduction in logD or disturbance of pi-stacking of LHS group to hERG channel. Furthermore, changing Cl to CN

134

at the C-5 position of benzimidazole RHS with both piperidine and piperazine linker retained the *Mtb* MIC but showed >4-fold improvement towards hERG selectivity (**BI_10** versus **BI_15** and **BI_16**, **Table 5.3**). The mitigation of hERG liability observed for compound **BI_15** and **BI_16** might be due to lowered logDs and disturbing the pi-stacking interaction of RHS group to the hERG channel.

5.5.4 LHS exploration and new structural handle for hERG selectivity (HAR_1 to HAR_16)

To expand SAR scope of benzimidaozle series and identify additional structural handle for hERG selectivity, we explored suitably substituted polar rings as ether attachment at the C-5 position of LHS that could lower logD. This resulted in identification of new structural handle for selectivity while retaining *Mtb* MIC. Herein, we report the new finding and discussion SAR and selectivity pattern for newly identified heteroaryl LHS series (HAR series, **Table 5.4**).

BI_7
Mtb MIC: 0.25
cLogD/PSA: 3.37/64
hERG IC$_{50}$: 1 µM

HAR_1
Mtb MIC: 0.19
cLogD/PSA: 4/129
hERG IC$_{50}$: >33µM

LHS exploration

BI_1
Mtb MIC: 0.19
cLogD/PSA: 4/69
hERG IC$_{50}$: 1 µM

HAR_2
Mtb MIC: 0.19
cLogD/PSA: 2.4/129
hERG IC$_{50}$: >33µM
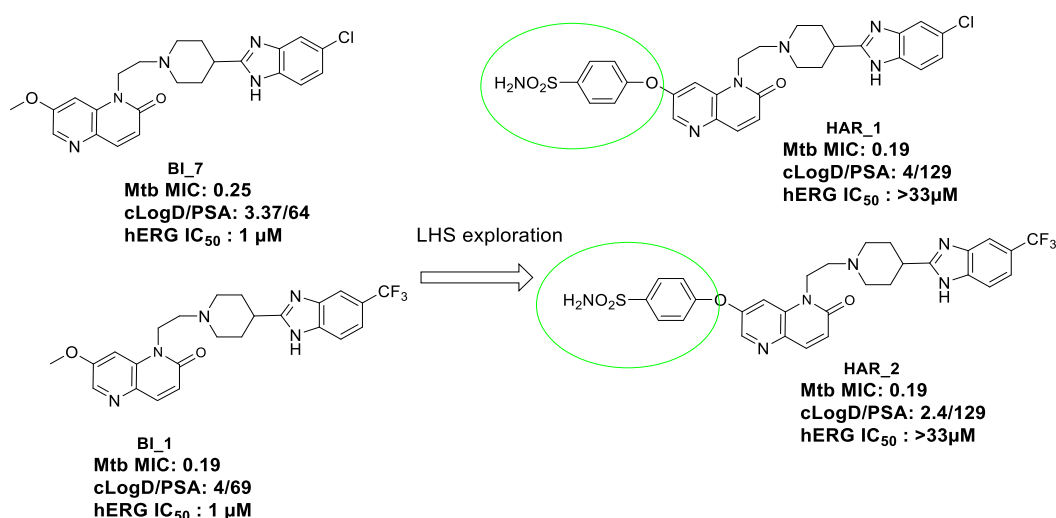
Figure 5.14: LHS exploration and new structural handle for hERG selectivity

Encouraged by the improved hERG selectivity for compounds **HAR _2** and **HAR_1** with 4-sulphamido phenyl substitution (**Figure 5.14**), we further expanded the SAR with various RHS combination to validate this hypothesis (**Table 5.4**).

As shown in **Table 5.4**, moving from a benzimidazole LHS to a pyrido oxazinone RHS ring or a mono cyclic pyridine ring system (compound **HAR_4** to **HAR_10**, **Table 5.4**) consistently showed good hERG selectivity, while retaining *Mtb* MIC. Introduction of an additional methyl group in the LHS naphthyridone did not affect the hERG selectivity and maintained *Mtb* MIC

(compound **HAR_5** and **HAR_6**, **Table 5.4**). Thus, the large polar bulky substitution at the C-7 position does not change the potency and hERG selectivity among the compounds reported in **Table 5. 4**

In order to understand the effect of bulky polar substitutions on NBTIs binding to *Mtb* GyrA subunit, we docked compound **HAR_1** and **HAR_6**. The possible binding modes of compound **HAR_1** and **HAR_6** in the *Mtb* GyrA homology model are depicted in **Figure 5.15**. The H-bonding contacts with Asp89 and occupation of hydrophobic pocket surrounded by Ala74, Val77, Ala78 for RHS part of compound **HAR_1** and **HAR_5** were well maintained as reported earlier for NBTIs. The additional bulky phenoxy sulfonamide did not disturb the positioning of LHS group between the two base pairs of DNA. Additionally, the phenoxy sulfonamide group pointing towards the Asp89 residue may be involved in making additional hydrogen bonding contacts.
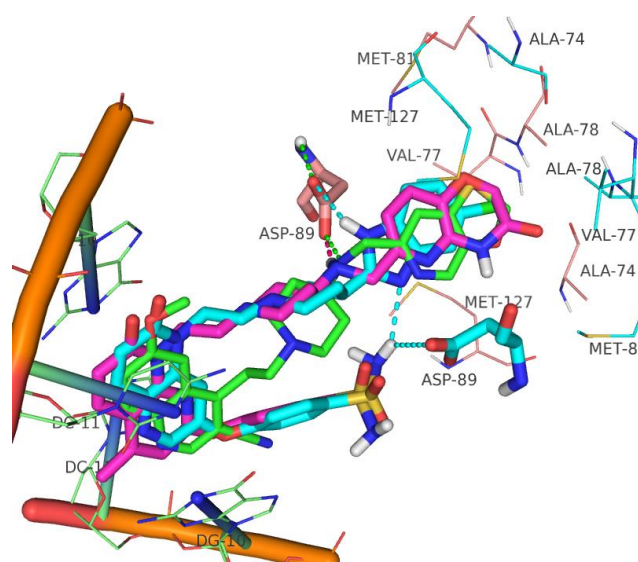
Figure 5.15: Docking pose of compound **HAR_1** (cyan), **HAR_5** (pink) and **NBTI** (green) on to the homology model of Mtb DNA gyrase subunit A.

Based on the findings from the SAR study that pyridoxazinonone ring appears to be the best in terms of providing hERG selectivity and ease of synthesis for pyridoxazinone RHS, we fixed pyridoxazinone ring as the RHS and explored a variety of substituents extending from the LHS naphthyridone as well in the linker part to improve and expand the scope of SAR for hERG selectivity. The results of this modifications were presented in **Table 5.4**

136

We hypothesized that the sulphonamide moiety in the R_1 ring may pose permeability issues in terms of achieving good oral bioavailability due to increased polarity (high polar surface area) and increased hydrogen bonding group. Hence, we started exploring the SAR without sulphonamide group in the R_1 ring. Replacement of the phenoxy sulphonamide group at the C-7 position of LHS by a 3-pyridyloxy group maintained *Mtb* MIC and hERG selectivity (Match pair: compound **HAR_4** vs compound **HAR_10**, **Table 5.4**). Furthermore, to expand the scope of SAR, we introduced other heterocyclic rings like pyrimidine and isoxazole as a bioisostere of pyridine at the R_1 position. These modifications retained hERG selectivity with a 4-fold loss in *Mtb* MIC (compound **HAR_11** and **HAR_12** versus **HAR_10**, **Table 5.4**). A similar trend in *Mtb* MIC and hERG selectivity was observed, following replacement of a 1,8-naphthyridone LHS with a 1,5- naphthyridone LHS (compound **HAR_13**, **HAR_14** and **HAR_15**, **Table 5.4**). The substitution of an aromatic isoxazole ring with a saturated heterocycle like a tetrahydrofuran ring retained the *Mtb* MIC and hERG selectivity (**HAR_ 13** *vs* **HAR_16** and **HAR_17**, **Table 5.4**). Further introduction of flexibility at R_1 position through a methylene bridge retained the hERG selectivity, albeit with a 4-fold loss in *Mtb* MIC compared to direct pyridyloxy compound (**HAR_10** vs **HAR_18-HAR_20**, **Table 5.4**). Overall, the substitutions at the R_1 position with a bulky polar group showed good hERG selectivity. This data suggested that R_1 substituents at the C-7 position of the LHS ring was amenable for chemical diversity

In order to identify compounds with good oral pharmacokinetic properties, we introduced a fluoro substitution in the linker portion of compound **HAR_13** and **HAR_14** to result in compound **HAR_21** and **HAR_22** respectively. This modification resulted in marginal loss in hERG selectivity for **HAR_22**, while retaining the *Mtb* MIC.

Inorder to highlight the improved hERG selectivity handle identifuied through heteroaryl ether modification for both aminopiperidine and benzimidazole RHS series, the scatter plot of hERG IC_{50} versus AZ logD presented in **Figure 5.16**.
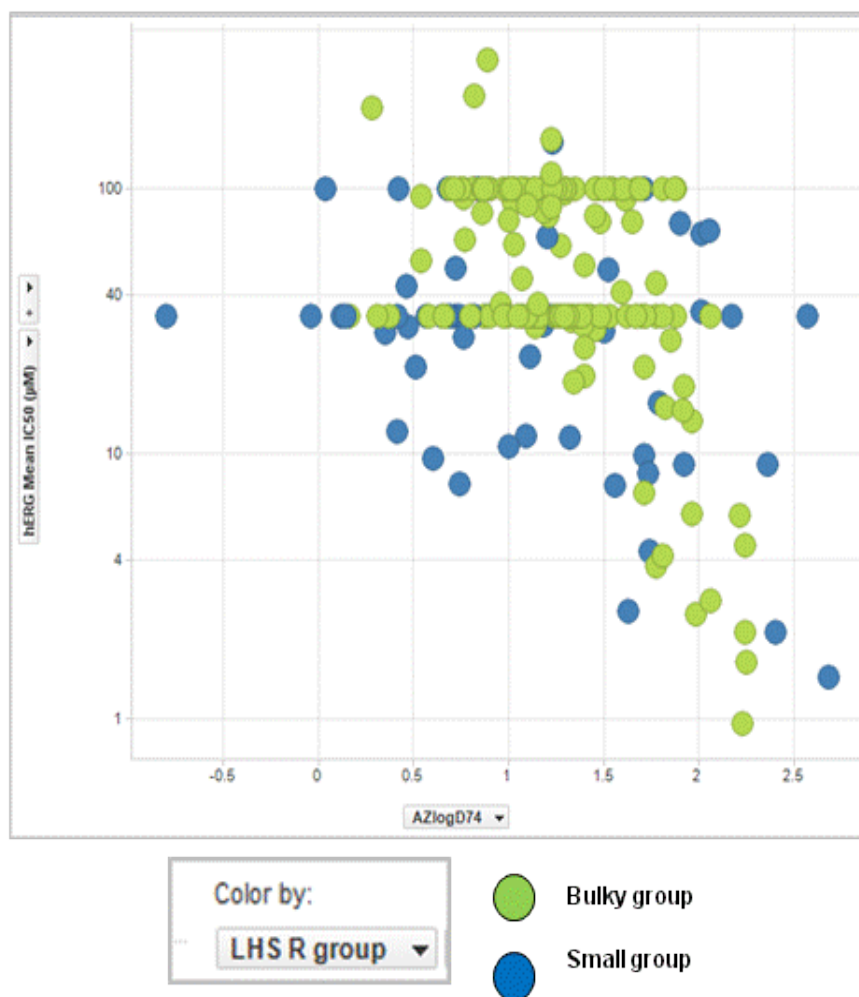
Figure 5.16: hERG IC$_{50}$ (-log scale) vs AZ logD

The above scatter plot for hERG IC$_{50}$ suggested that calculated lipophilicity (AZ logD) of < 1.5 is ideal for achieving good hERG selectivity for compounds with bulky substitutions at R$_1$ position of LHS ring (green encircled in **Figure 5.16**). This trend is not true for compounds with smaller substitutions at R$_1$ positions (blue encircled in **Figure 5.16**). This data clearly indicates that apart from logD, the polar substituents at R$_1$ position does play a critical role in improving the hERG selectivity.

5.5.5 Bactericidal activity of N-linked quinolone and naphthyridone against replicating *Mtb* in broth (Kill kinetic assay)

The advanced compounds from this series of chemical class was further investigated for bactericidal activity in a time dependent kill kinetic assay

Detailed time course kill studies were performed to understand the influence of varying drug concentrations over a period of 10 days. As shown in **Fig.5.17**, compounds **AP_18** and **AP_19** displayed a >3-log reduction in the colony forming units (CFU) over a period of 10 days. The extent of kill increased with both the concentration and time, a property displayed by fluoroquinolones against *Mtb* (Shandil, R. *et al.*, 2007).
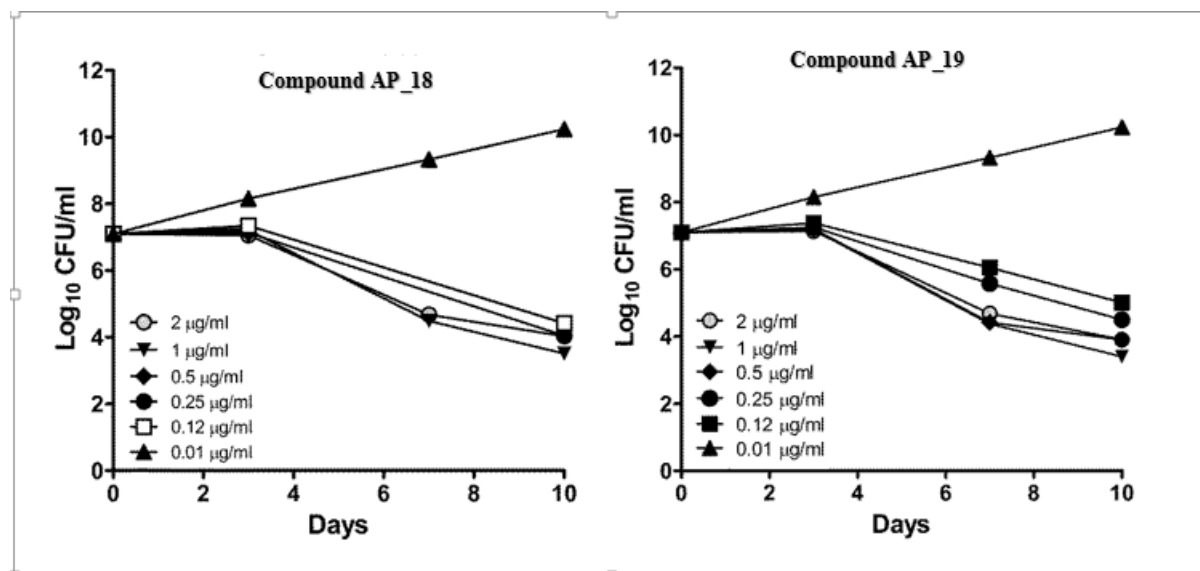
Figure 5.17: Compound **AP_18** and **AP_19** display a concentration as well as time-dependent killing of replicating Mtb grown in broth

This data highlighted the cidality of aminopiperidine series against *mycobacterium tuberculosis*.

5.5.6 Resistance frequency and mutation mapping to aminopiperidines (AP_3 and AP_16)

In order to measure the resistance frequency, spontaneous resistant mutants of Mtb were selected on agar plates containing varying concentrations of compound **AP_3** and **AP_16** (**Table 5.9**). Resistant mutants to compound **AP_3** arose at a frequency of 8.2×10^{-7} at 8X MIC as compared to 2×10^{-7} seen for ciprofloxacin at 8X MIC. In contrast, resistant mutants to compound **AP_16** arose at a frequency of 3.5×10^{-8} at ~ 10X MIC (8.7×10^{-9} at ~20X MIC), which is similar to the observed frequency for moxifloxacin (2.3×10^{-8}) at a similar multiples of the MIC.

Table 5.8: Mutation resistance frequency profile for aminopiperidines

Compound	Mtb MIC (μg/ml)	Mutant selection concentration (μg/ml)	Mutation Frequency
AP_3	0.13	0.5	2.9×10^{-6}
AP_3	0.13	1	8.2×10^{-7}
AP_16	0.06	0.5	3.5×10^{-8}
AP_16	0.06	1	8.7×10^{-9}
Ciprofloxacin	0.5	4	1.9×10^{-7}
Ciprofloxacin	0.5	8	1.9×10^{-7}
Moxifloxacin	0.06	0.25	2.6×10^{-8}
Moxifloxacin	0.06	0.5	2.3×10^{-8}

Compounds from across three series (**AP**, **BI** and **HAR**) were tested for their MIC against resistant mutants selected using **AP_3**, **AP_16** and moxifloxacin. As shown in **Table 5.8**) to the **AP_2** or **AP_16**-resistant mutant strains, while showing no change in their MIC against the moxifloxacin-resistant isolate. Interestingly, moxifloxacin retained its wild-type MIC against the compound **AP_3**-resistant clone, but its MIC increased ~16X versus the compound **AP_16**-resistant clone. Ciprofloxacin and ofloxacin retained their MIC on the **AP_3** resistant clone, but their MIC increased 16X and 8X against the compound **AP_16**-resistant clone. The aminopiperidines retained their MIC against moxifloxacin-resistant mutants, whereas MIC for three FQs increased by >16-fold (**Table 5.9**). Isoniazid and rifampicin retained their wild-type MIC against all the resistant clones tested; indicating that the resistant clones had a specific mutation in the gyrase gene.

Table 5.9: MIC modulation activity study against mutants resistant to compound **AP_3** and **AP_16** and Moxifloxacin

Compound Number	MIC (µg/ml)			
	Mtb H37Rv Wild-type	Cpd AP_3^R mutant (A74V)	Cpd AP_16^R Mutant (D89N)	Moxi^R mutant (G88N)
AP_3	0.13	2	>2	0.03
AP_16	0.06	1	>1	0.03
AP_5	0.06	>2	>2	0.06
AP_19	0.13	>2	>2	0.06
BI_1	0.25	50	25	0.5
BI_9	0.06	100	25	0.06
HAR_10	0.13	8	>100	0.5
HAR_11	0.25	50	>100	0.13
HAR_22	0.25	50	>100	0.5
Moxifloxacin	0.06	0.06	1	4
Ciprofloxacin	0.25	0.25	4	8
Ofloxacin	0.5	1	4	16
Isoniazid	0.06	0.06	0.03	0.06
Rifampicin	0.015	0.008	0.015	0.008

The entire *gyrA* gene of 6 spontaneous resistant clones from each compound were sequenced. The multiple sequence alignment of the mutated and the wild-type genes confirmed mutations in the *gyrA* gene. These mutations were clustered around the N-terminal domain of the GyrA protein spanning amino acid position 74 to 104. Compound **AP_3** resistant mutants had a A74V amino acid change. Interestingly, the compound **AP_16** resistant clone 16.4 showed a different mutation: D89N in the vicinity of the amino acid 88 which is critical for mediating resistance to moxifloxacin (McGrath, *et al*., 2014). The mutation in the moxifloxacin resistant clone was G88N, which is consistent with earlier observation that moxifloxacin resistance maps to G88N in the laboratory setting as well as in the clinic. (McGrath, *et al.,* 2014).

Figure 5.18: *In vitro* resistance to aminopiperidines (**AP_3, AP_16**) maps to the *gyrA* gene in *Mtb*

5. 5. 7 Structure property relationship for the *in vivo* clearance and oral bioavailability in rat

In general, a majority of compounds from AP and HAR series showed good solubility (>500 µM) at pH 7.4. However, the benzimidazoles series showed very poor solubility (<10 µM) at pH 7.4 The initial lead compound **AP_3** from AP series with a bicyclic RHS fragment showed 11% oral bioavailability in rats, probably due to poor Caco-2 permeability and high clearance. High clearance for compound **AP_3** (~ 2.5 times higher than rat liver blood flow), suggested an extra-hepatic route of elimination in the rats (**Table 5.10**). Replacement of the bicyclic RHS fragment with a monocyclic 2-methyl-3-cyanopyridine fragment in compound **AP_5 & AP_9** improved the oral bioavailability. Replacing the quinolone LHS ring with 1, 5, naphthyridone and introduction of fluoro substitution in the linker region also showed a similar trend (compounds **AP_7**, **AP_15** and **AP_16** in **Table 5.10**). The methoxy substitution in the amino piperidine linker with monocyclic RHS (compound **AP_17**) showed moderate clearance with good bioavailability (73%). Modification of the bicyclic pyrido-oxazinone RHS with 1, 5-napthyridone and a fluoro linker combination resulted in moderate to high in-*vivo* clearance with >50% oral bioavailability (compound **AP_18** and **AP_19** and **AP_20**, **Table 5. 10**). Good bioavailability (>50%) of compounds **AP_16** to **AP_20** with moderate to high clearance could be due to the saturation of clearance mechanism. Compounds from benzimidazole RHS series (**BI_15** and **BI_16**, **Table 5.10**) exhibited low to moderate *in vivo* clearance but the oral bioavailability was found to be very low (1 to 3%) for both compounds.This could be due to poor oral absorption associated with low solubility and poor intestinal permeability of these compounds. No compounds from HAR series were profiled for rat oral bioavailability due to low to moderate Caco2 permeability observed for the series.

Table 5.10: Structure property relationship for oral bioavailability

Compound	LogD	PSA (Å^2)	Caco-2: Papp A−B/B−A (1× 10^{-6} cm/s)	Rat Clearance (ml/min/kg)	Rat F (%)
AP_3	0.4	105	2.0/12.6	187	11
AP_5	1.31	82	13.6/7.4	41	>100
AP_9	1.71	91	10/4.7	10	59
AP_7	1.07	83	10.5/8.3	32	>100
AP_15	0.92	74	17.7/15.4	30	>100
AP_16	1.29	83	13.6/7.4	42	52
AP_17	0.99	92	11.7/9.9	54	73
AP_19	0.47	97	8.1/12.3	63	>100
AP_18	0.47	97	7.6/11.2	87	87
BI_15	3.2	93	0.4/28.1	35.5	1.1
BI_16	3.3	96	1.5/24.1	32.2	3.3
HAR_22	0.76	120	4.3/8.9	ND	ND

5. 5. 8. *In vivo* efficacy, pharmacokinetic and pharmacodynamic (PK-PD) relationship:

Inorder to demonstrate invivo proof of principle (invivo efficacy) for the series, compounds with good MIC, cidality and pharmacokinetic profile were selected. This study helped to establishing *in vivo* proof of concept in a murine model of TB and understanding the PK-PD relationship for advanced compounds from AP series. The PK profile in healthy mice suggested that the treatment with ABT (1-aminobenzotriazole) before giving the first dose and twice daily dosing were essential to maintain adequate plasma concentrations of the compound to drive efficacy. The data for five compounds from aminopiperidine series, representing both monocyclic and bicyclic RHS, tested in the acute murine model of TB are shown in **Fig.5.19**. Compound **AP_7** with a monocyclic RHS showed the best efficacy. It reduced the bacterial burden in lungs to below the limit of quantification at 20 mg/kg dose. Compounds with a bicyclic RHS were relatively less efficacious (**AP_18**, **AP_19** & **AP_21**). The best efficacy in this class was observed for compound 18: a 1.2 log reduction in the bacterial CFUs at 160 mg/kg. The % time of dosing interval for free plasma concentration to be above the MIC was > 50 for all the compounds profiled (**Table 5.11**). However, the free AUC/MIC ratio for compound **AP_7** was nearly eight times lower than for compound **AP_21**.

Table 5. 11: Pharmacokinetic and pharmacodynamic parameters in mice.

Compound ID	MIC (μg/ml)	Fraction unbound in mouse plasma	Dose (mg/kg)	free AUC/MIC	% free T > MIC
AP_5	0.062	0.43	20	159	58
AP_7	0.062	0.23	20	54	58
AP_18	0.125	0.32	80	129	70
AP_19	0.125	0.44	80	175	58
AP_21	0.062	0.48	160	434	83
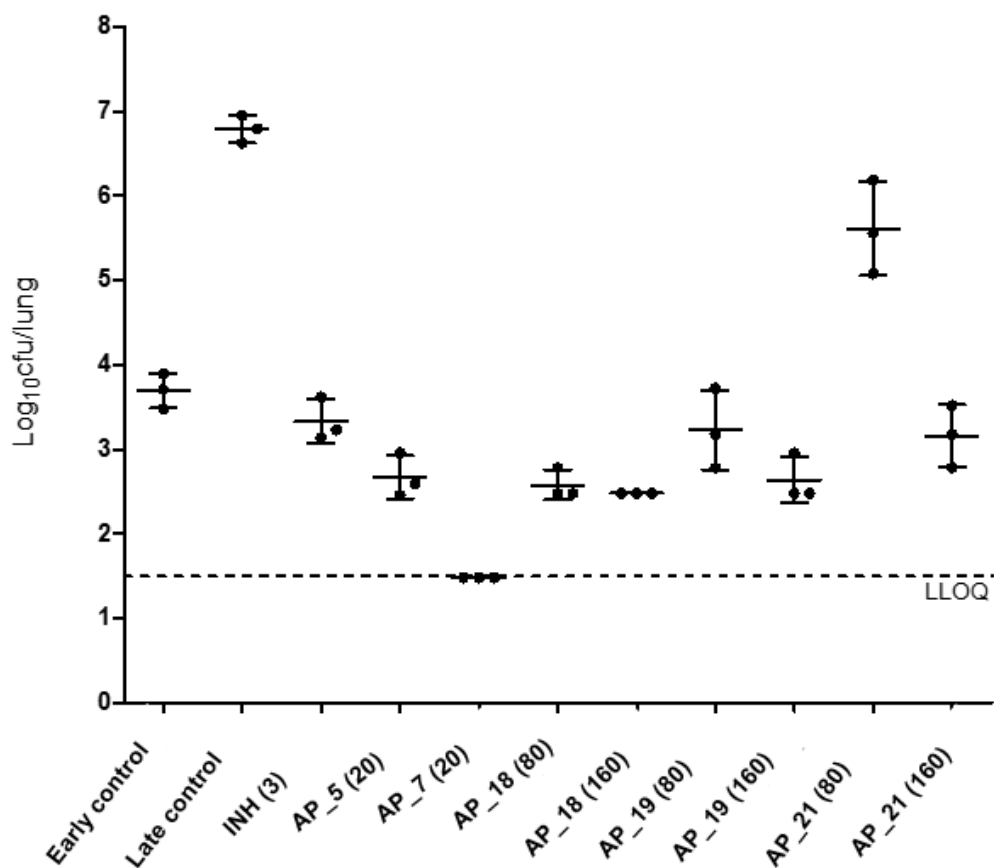
Fig.5.19: Efficacy after 20 days of daily treatment with compound **AP_5**, **AP_7**, **AP_18**, **AP_19** and **AP_21** in the acute model. Numbers in the bracket indicate the dose (mg/kg). The dotted line indicates the lower limit of quantitation (LLOQ) for the lung CFUs. The mean and standard deviation are shown for each dose group.

5.5.9 Highlights of the study

In present work, we report synthesis and various biological profiling of total of sixty three compounds from novel n-linked quinolone and napthyridones with three subseries against *Mycobacterium tuberculosis* drug sensitive strains, *Mtb* DNA gyrase, hERG, physciocehmical, pharmacokinetic and pharmacodynamics studies. The study also involves computational modelling to understand the binding modes of newly synthesized compounds. The synthesized compounds from aminopiperidine (**AP**) series showed improved potency (MIC), hERG selectivity and improved intestinal permeability (Caco2) leading improved oral bioavailablity as compared to hit/lead molecules. The scaffold morphing effort on monocyclic RHS based aminopiperidines resulted in identification of novel piperazinyl/piperidinyl benzimidazole (**BI**) based with potent MIC with expanded chemical diversity. However, this sub series (**BI**) had

shown potent hERG liability. To mitigate hERG liability for **BI** series, left hand side exploration of napthyridones with bulky polar substations provided new structural handle to improve hERG selectivity while retaining *Mtb* MIC with a new sub series called heteroaryl ether (HAR) series. This new structural handle identified for hERG selectivity not known in the literature for antibacterial NBTIs series as general belief is that small substituents on LHS ring favour antibacterial activity. This may provide further avenue to improve hERG selectivity for antibacterial series if the renewed attempt are made in the new direction. Representative compounds from all three sub series inhibited *Mtb* DNA gyrase supercoiling activity and shown no cross resistant activity against moxifloxacin resistant mutant, thus confirming gyrase mechanism of inhibition, which is distinctly different from fluroquinolone menchanism. The representative advanced compounds from all three synthesized sub series shown in **Figure.5.20**, **5.21** and **5.22**.

Compound **AP_7** and **AP_19** were found to be the most advanced compounds with potent *Mtb* MICs and IC$_{50}$ against *Mycobacterium tuberculosis* Gyrase. These two compounds also shown improved hERG selectivity, oral bioavailability and efficacious in the acute mouse TB model. (**Figure 5.20**).
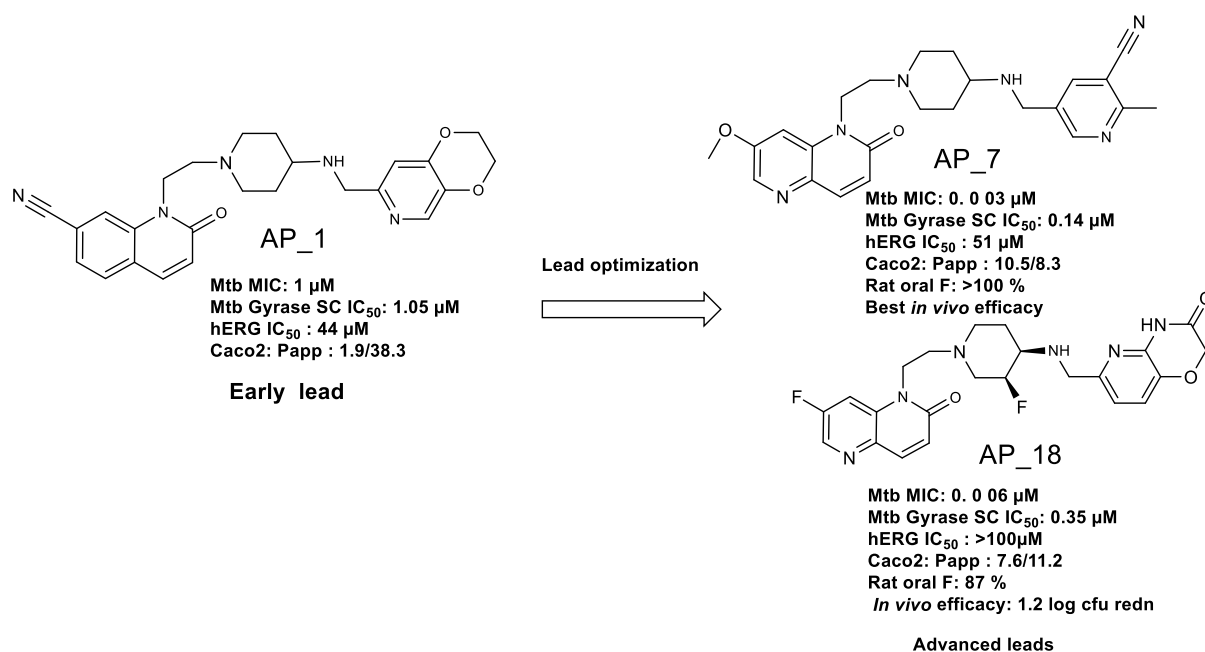
Figure 5.21: Chemical structures and biological activity of the advanced compounds from **AP** series (**AP_6** and **AP_18**)

From the scaffold morphing effort, **compound BI_15** emerged as the most active compound exhibiting *Mtb* gyrase inhibition with an IC_{50} of 0.9 μM and *Mtb* MIC of 0.06 μM. Compound **BI_15** had shown moderate hERG selectivity index of 166 compared to the starting lead (hERG SI: 5.2 for **BI_I**, **Figure 5.21**).

BI_1

Mtb MIC: 0.19 μM
Mtb Gyrase SC IC_{50}: 1 μM
hERG IC_{50} : 1 μM

Scaffold morphed hit

Hit expansion

BI_15

Mtb MIC: 0. 06 μM
Mtb Gyrase SC IC_{50}: 0.9 μM
hERG IC_{50} : 10μM
Lead
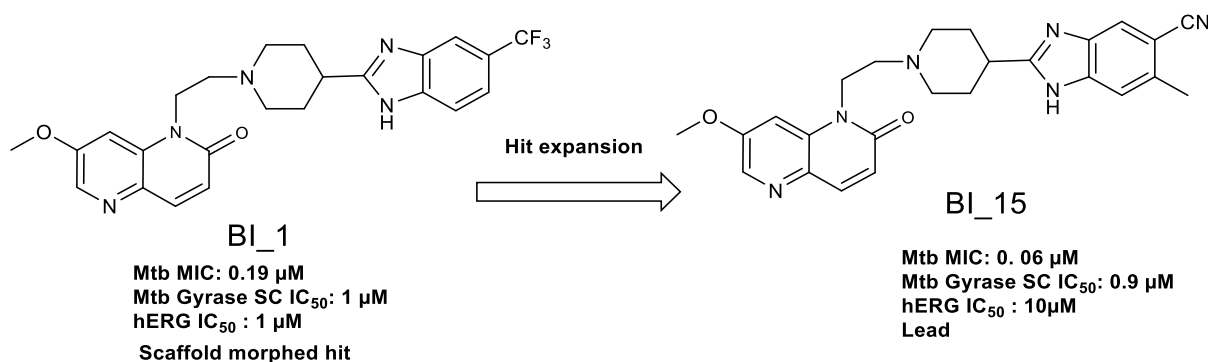
Figure 5.21: Chemical structures and biological activity of the lead compound from **BI** series (**BI_15**)

A series of twenty one heteroaryl ether derivatives synthesized through LHS exploration and screened against *Mycobacterium tuberculosis H37Rv strain* and hERG selectivity. In our study, most of the synthesized compounds showed improved hERG selectivity while retaining Mtb MIC as compared to lead molecules. Compound **HAR_10** found to have the best hERG selectivity index (2583 fold over Mtb MIC) with *Mtb* MIC of 0.06 μM and gyrase IC_{50} of 0.104 μM (**Figure 5.22**).

BI_7
Mtb MIC: 0.25
Mtb Gyrase SC IC$_{50}$: 1 µM
hERG IC$_{50}$: 1 µM
hERG selectivity index : 4

LHS exploration

HAR_3
Mtb MIC: 0.25
hERG IC$_{50}$: >33µM
hERG selectivity index : >132

AP_2
Mtb MIC: 0.19
Mtb Gyrase SC IC$_{50}$: 0.15 µM
hERG IC$_{50}$: 21 µM
hERG selectivity index : 110

HAR_10
Mtb MIC: 0.06
Mtb Gyrase SC IC$_{50}$: 0.104 µM
hERG IC$_{50}$: 155 µM
hERG selectivity index : 2583
Leads with improved hERG selectivity

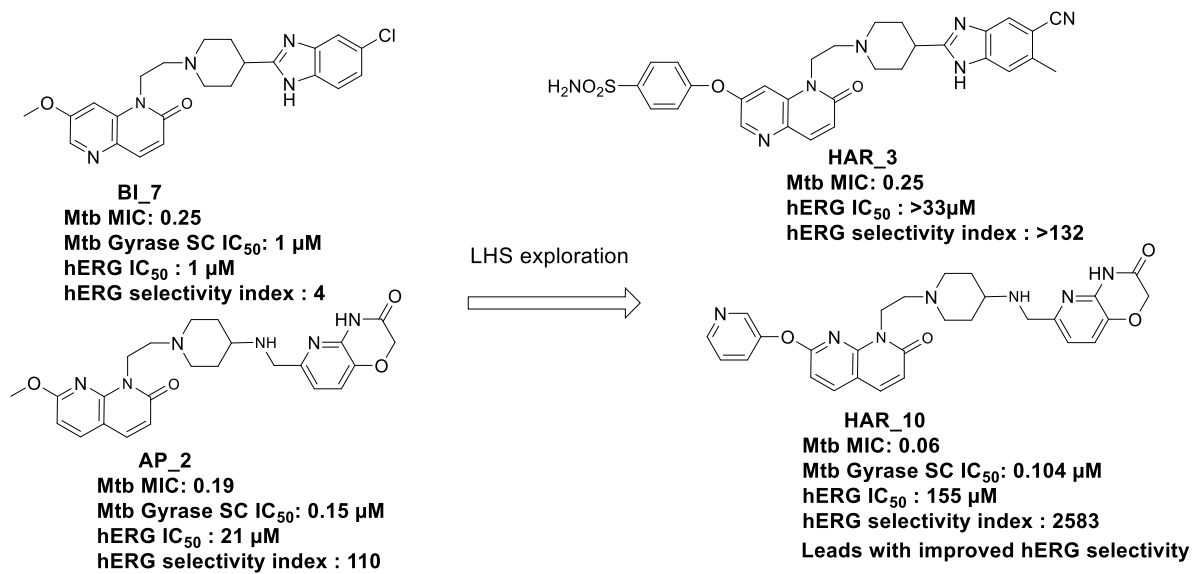**Figure 5.22:** Chemical structures and biological activity of the lead compound from **HAR** series (**HAR_3** and **HAR_10**)

148

Tuberculosis caused by *Mycobacterium tuberculosis* (*Mtb*), continues to be a global threat claiming 1.5 million lives each year. For treating drug susceptible TB, the World Health Organisation (WHO) recommends a regimen containing four drugs administered for six months. The global emergence of multi drug resistant (MDR) and extremely drug resistant (XDR) strains of *Mtb* have greatly impeded the TB control and eradication efforts. Patients with MDR or XDR-TB require treatment with a combination of 6-8 drugs for a period of 8-24 months. Hence, novel TB agents with newer mechanism of action will augment the TB treatment. The attractiveness of DNA gyrase as a high quality antibacterial target has been validated by the clinical success of several generations of FQs to treat serious bacterial infections. The widespread emergence of FQ-resistant bacterial strains is likely to reduce the clinical value of FQs in the near future. The clinical benefit of combining FQs in the drug regimen to treat TB have been demonstrated in preclinical animal models as well as in TB patients. Numerous reports have highlighted the emergence of *Mtb* strains resistant to FQs, thereby limiting the life of these drugs in treating TB. The existing body of evidence around the clinical safety and efficacy of FQs, provides an opportunity to identify novel GyrA inhibitors. It is envisaged that a novel GyrA inhibitor class would have a distinct binding mechanism compared to the binding mode of FQs. This novel class of compounds would serve as an attractive treatment option to tackle drug-resistant forms of *Mtb*.

All 63 synthesized derivatives were first evaluated for their antimycobacterial activity against *Mtb* in a whole cell assay (*Mtb* MIC), hERG inhibition as a step towards the derivation of structure-activity relationships and lead optimization for potency and selectivity. Also, representative active compounds from each series of chemical class were further evaluated for *Mtb* gyrase inhibition and crossresistant studies to ensure novel MOA for the series. The compounds were further subjected to Caco2 permeability assay, pharmacokinetic and pharmacodynamics profiling to demonstrate oral bioavailability and *in vivo* efficacy for the series. Additionally, all the synthesized derivatives were further evaluated for their predicted lipophilicity (AZ logD) using a proprietary AstraZeneca developed software.

In summary, screening of a focused antibacterial library followed by lead optimization effort led to the identification of a novel class of N-linked aminopiperidine-based alkyl quinolone and naphthyridone compounds with excellent *Mtb* MIC, improved pharmacokinetic properties and significantly reduced hERG liability. These compounds inhibited the *Mtb* DNA gyrase with a novel mode of inhibition which conferred the ability to retain their MIC against FQ-resistant clinical isolates of *Mtb*. Compound **AP_7** with monocyclic RHS and compound **AP_18** with bicyclic RHS displayed the best efficacy in an acute model of murine TB. Our lead optimization efforts led to a significant improvement in the properties that are suitable for an oral route of administration.

Additionally, the medicinal chemistry efforts by scaffold morphing of NBTIs provided a novel chemical series (benzimidazole) with enough structural diversity to optimize the safety and improve pharmacokinetic properties of this series. Compound (**BI_15**) from benzimidazole series displayed best *Mtb* MIC of 0.06 µM with moderate hERG selectivity

Also, exploration of polar bulky substitutions at the C-7 position of naphthyridone ring established a structure activity relationship to mitigate the hERG ion channel binding activity, while retaining potent antimycobacterial activity. Compound **HAR_10** from LHS SAR exploration shows great promise with excellent hERG selectivity with *Mtb* MIC of 0.06 µM and also provides future diercetion for further optimization of hERG selectivity.

In conclusion, the N-linked aminopiperidine lead series represents an attractive class of gyrase inhibitors with a potential to treat drug-susceptible as well as drug-resistant TB including FQ-resistant strains of *Mtb*. Assessment of the *in vivo* safety is essential before optimizing this class of compounds towards the development of a novel anti-TB drug.

Further optimization of the **BI** and **HAR** series towards improving oral bioavailability and evaluation of *in vivo* safety is warranted in order to progress the series towards developing a candidate drug to treat tuberculosis.

In conclusion, the aminopiperidine based N-linked quinolone and naphthyridone class of compounds identified among three series described here represents an attractive class of gyrase inhibitors with a potential to treat drug-susceptible as well as drug-resistant TB including FQ-resistant TB. Assessment of the *in vivo* safety is essential before optimizing this class of compounds towards the development of a novel anti TB drug.

Future perspectives

The bacterial type II topoisomerases are ubiquitous enzymes present in all bacteria but are absent in humans. DNA gyrase belong to the type II topoisomerase family and essential for maintaining various topological forms of DNA and cell survival. Inhibition of DNA gyrase by moxifloxacin is validated by both preclinical efficacy amd clinical efficacy. However, emergence of resistance against fluoroquinolones (moxifloxacin) limit their usage in the clinic. Hence, targeting *Mtb* DNA gyrase with novel mechanism provides a potential opportunity for the development of novel anti-tubercular agents. The present study focused on developing promising *Mycobacterium tuberculosis* GyrA inhibitors as potential anti-tubercular agents with reduced cardiac ion channel liability (hERG selectivity) and improved oral bioavailability. This approach offers an excellent opportunity to address the ever increasing problem of mycobacterial resistance and to develop an effective treatment for TB.

The present study describes the development of three chemical series with good chemical diversity as potential DNA GyrA inhibitors. The synthesized compounds display excellent antimycobacterial activity, hERG selectivity and good oral bioavailabity. The ability to retain antimycobacterial activity against a lab generated moxifloxacin-resistant mutant with a concomitant loss of potency against NBTIs resistant mutant suggest a mechanism of action similar to NBTIs.

Representative molecules from the synthesized set were found to be effective in an acute mouse model of TB with bactericidal effect observed *in vivo*. Although these results are encouraging, further lead optimization is required to achieve an adequate safety profile to ensure that the dose to humans would be in an acceptable range.

The advancement of any of the candidate molecules presented in this thesis along a drug development track will require a substantial investment in medicinal chemistry, preclinical saftey evaluation and clinical studies.

References

World Health Organization. Global tuberculosis control. WHO 2014 report: http://www.who.int/tb/publications/global_report/en/

Zumla, A.; Raviglione, M.; Hafner, R.; von Reyn, C. F. Tuberculosis. *N Engl J Med*. **2013**, 368, 745-755.

Zumla, A.; Nahid, P.; Cole, S.T Advances in the development of new tuberculosis drugs and treatment regimens. *Nat Rev Drug Discov*. **2013**, 12, 388-404.

World Health Organization. Multidrug and extensively drug-resistant TB (M/XDR-TB); WHO 2013 http://www.who.int/tb/challenges/mdr/MDR_TB_FactSheet.pdf

Champoux, J.J. DNA topoisomerases: structure, function, and mechanism. *Annu. Rev. Biochem.* **2001**, 70, 369-413

Corbett, K. D.; Berger, J. M. Structure, molecular mechanisms, and evolutionary relationships in DNA topoisomerases. *Annu. Rev. Biophys. Biomol. Struct*. **2004**, 33, 95-118.

Coates,W.J.;Gwynn,M.N.; Hatton, I. K.; Masters, P. J.; Pearson, N.D.; Rahman, S. S.; Slocombe, B.; Warrack, J. D. Patent Application WO 99/37635 A1, **1999**.

Black M. T.; Stachyra, T.; Platel , D.; Girard, A. M.; Claudon, M.; Bruneau, J. M; Miossec, C. Mechanism of action of the antibiotic NXL101, a novel nonfluoroquinolone inhibitor of bacterial type II topoisomerases. *Antimicrob. Agents Chemother*. **2008**, 52, 3339−3349.

Ballell, L.; Barros, D.; Brooks, G.;Castro Pichel, J.;Dabbs, S.; Daines, R.A.;Davies, D.T.; Fiandor Roman, J. M.; Giordano, I.; Hennessy, A. J.; Hoffman, J. B.; Jones, G. E.; Miles, T. J.; Pearson, N. D.; Pendrak, I.; Remuinan Blanco, M. J.; Rossi, J. A.; Zhang, L. Patent Application WO 2008/009700 A1, **2008.**

Brown, P.; Dabbs, S.; Davies, D. T.; Pearson, N. D. Patent Application WO 2008/116815 A1, **2008**.

Barfoot, C.; Davies, D. T.; Miles, T.; Pearson, N. D. Patent Application WO 2008/152603, **2008.**

Brown, P.; Dabbs, S.; Hennessy, A. J. Patent ApplicationWO2009/087153 A1, **2009**.

Giordina, I.; Hennessy, A. J. Patent Application WO 20010/043714, A1, **2010.**

Press release, June 30, 2008. http://www.novexel.com/.

Hafner R., Cohn J.A., Wright D.J., Dunlap N.E., Egorin M.J., Enama M.E., Muth K., Peloquin C.A., Mor N., Heifets L.B. Early bactericidal activity of isoniazid in pulmonary tuberculosis. *Am. J. Respir. Crit. Care Med.* **1997**, *156*, 918-923.

Mayer, C.; Janin, Y. L. Non-quinolone inhibitors of bacterial type IIA topoisomerases: a feat of bioisosterism. *Chem Rev*. **2014**, 114, 2313-2342.

Koul A., Arnoult E., Lounis N., Guillemont J., Andries K. The challenge of new drug discovery for tuberculosis. *Nature* **2011**, *46*9, 483-490.

Haydel S.E. Extensively drug-resistant tuberculosis: a sign of the times and an impetus for antimicrobial discovery. *Pharmaceuticals* **2010**, *3*, 2268-2290.

Singh, S.B.; Kaelin, D.E.; Wu, J.; Miesel, L..; Tan, C.M.; Meinke, P.T.; Olsen, D.; Lagrutta, A.; Bradley, P.; Lu J.; Patel S.; Rickert, K.W2.; Smith R. F.; Soisson, S.; Wei, C.; Fukuda, H4.; Kishii, R4.; Takei, M.; Fukuda, Y. Oxabicyclooctane-linked novel bacterial topoisomerase inhibitors as broad spectrum antibacterial agents. *ACS Med Chem Lett*. **2014,** 5,609-614.

Cole, S. T.; Brosch, R.; Parkhill, J.; Garnier, T.; Churcher1, C.; Harris, D.; Gordon, S. V.; Eiglmeier, K.; Gas, S.; Barry, C. E., III;Tekaia, F.; Badcock, K.; Basham, D.; Brown, D.; Chillingworth, T.;Connor, R.; Davies, R.; Devlin, K.; Feltwell, T.; Gentles, S.; Hamlin, N.; Holroyd, S.; Hornsby, T.; Jagels, K.; Krogh, A.; McLean, J.; Moule, S.; Murphy, L.; Oliver, K.; Osborne, J.; Quail, M. A.; Rajandream, M.-A.; Rogers, J.; Rutter, S.; Seeger, K.; Skelton, J.; Squares, R.; Squares, S.; Sulston, J. E.; Taylor, K.; Whitehead, S.; Barrell, B. G. Deciphering the biology of Mycobacterium tuberculosis from the complete genomesequence. *Nature* **1998**, 393, 537−544.

Sharma U. Current possibilities and unresolved issues of drug target validation in Mycobacterium tuberculosis. *Expert Opin. Drug. Discovery* **2011**, 6, 1171-1186.

Burman, W. J.; Goldberg, S.; Johnson, J. L.; Muzanye, G.; Engle, M.; Mosher, A. W.; Choudhari, S.; Daley, C. L.; Munsiff, S. S.; Zhao, Z.; Vernon, A.; Chaisson, R. E. Moxifloxacin versus ethambutol in the first 2 months of treatment for pulmonary tuberculosis. *Am. J. Respir. Crit. Care Med.* **2006**, 174, 331−338**.**

Conde, M. B.; Efron, A.; Loredo, C.; De Souza, G. R.; Graca, N. P.; Cezar, M. C.; Ram, M.; Chaudhary, M. A.; Bishai, W. R.; Kritski, A. L.; Chaisson, R. E. Moxifloxacin in the initial therapy of tuberculosis: A randomized, phase 2 trial. *Lancet* **2009**, 373, 1183−1189.

Diacon, A. H.; Dawson, R.; von Groote-Bidlingmaler, F.; Symons, G.; Venter, A.; Donald, P. R.; van Niekerk, C.; Everitt, D.; Winter, H.; Becker, P.; Mendel, C. M.; Spigelman, M.K. 14 day bactericidal activity of PA-824, bedaquiline, pyrazinamide, and moxifloxacin combinations: A randomized trial. *Lancet* **2012**, 380, 986-993

Duong, D. A.; Nguyen, T. H.; Nguyen, T. N.; Dai, V. H.; Dang, T. M.; Vo, S. K.; Do, D. A.; Nguyen, V. V.; Nguyen, H. D.; Dinh, N. S.; Farrar, J.; Caws, M. Beijing genotype of Mycobacterium tuberculosis is significantly associated with high-level fluoroquinolone resistance in Vietnam. *Antimicrob. Agents Chemother*. **2009**, 53, 4835−4839.

Drlica, K.; Malik, M.; Kerns, R. J.; Zhao, X. Quinolone-mediated bacterial death. *Antimicrob. Agents Chemother*. **2008**, 52, 385−392.

Bisacchi, G S.; Dumas, J. Recent advances in the inhibition of bacterial type II topoisomerases. In Annual Reports In Medicinal Chemistry; Macor, J. E., Ed.; Academic Press: Burlington, MA, **2009**; Vol. 44, pp 379−396.

Shirude, P. S.; Hameed, S. Nonfluoroquinolone-based inhibitorsof mycobacterial type II topoisomerase as potential therapeutic agentsfor TB. In Annual Reports in Medicinal Chemistry; Desai, M. C., Ed.; Academic Press: Burlington, MA, **2012**; Vol. 47, pp 319−330.

Bax, B. D.; Chan, P. F.; Eggleston, D. S.; Fosberry, A.; Gentry, D.R.; Gorrec, F.; Giordano, I.; Hann, M. M.; Hennessy, A.; Hibbs, M.; Huang, J.; Jones, E.; Jones, J.; Brown, K. K.; Lewis, C. J.; May, E. W.; Saunders, M. R.; Singh, O.; Spitzfaden, C. E.; Shen, C.; Shillings, A.;

Theobald, A. J.; Wohlkonig, A.; Pearson, N. D.; Gwynn, M. N. Type IIA topoisomerase inhibition by a new class of antibacterial agents. *Nature* 2010, 466, 935−940.

Tretter,E.M.; Schoeffler,A.J.; Weisfild,S.R.; Berger,J.M. Crystal structure of the DNA gyrase GyrA N-terminal domain from Mycobacterium tuberculosis. *Proteins* **2010**, 78, 492-495.

Breault, G.; Eyermann, C. J.; Geng, B.; Morningstar, M.; Reck, F. Preparation of quinolinones and analogs for the treatment of multi-drug resistant bacterial infections. WO2006134378, **2006**.

Janelle,C. P.; Mark, C.; Geng, B.; Aydon, G.A.; Reck, F. Preparation of 2-quinolinone and 2-quinoxalinone derivatives as antibacterial agents. WO2008071961, **2008**.

Breault, G.; Vincent, G.; Reck, F. Preparation of naphthyridines as bactericides for treating bacterial infections. WO2008071964, **2008**.

Geng, B.; Morningstar, M.; Reck, F. Preparation of piperidines for the treatment of bacterial infections. WO2008071981, **2008**.

Reck, F.; Alm, R.; Brassil, P.; Newman, J.; DeJonge, B.; Eyermann, C. J.; Breault, G.; Breen, J.; Comita-Prevoir, J.; Cronin, M.; Davis, H.; Ehmann, D.; Galullo, V.; Geng, B.; Grebe, T.; Morningstar, M.; Walker, P.; Hayter, B.; Fisher, S. Novel N-linked aminopiperidine inhibitors of bacterial topoisomerase type II: broad-spectrum antibacterial agents with reduced hERG activity. *J. Med. Chem.* **2011**, 54, 7834−7847.

Reck, F.; Alm, R.; Brassil, P.; Newman, J.; Ciaccio, P.; McNulty ,J.; Barthlow, H.; Goteti,K.; Breen, J.; Comita-Prevoir, J.; Cronin, M.; Ehmann, D.; Geng, B.; Godfrey, A.; Fisher, S. Novel N-Linked aminopiperidine inhibitors of bacterial topoisomerase type II with reduced pKa: Antibacterial agents with an improved safety profile. *J. Med. Chem.* **2012**, 55, 6916−6933.

Alemparte-Gallardo, C.; Ballell-Pages, L.; Barros-Aguirre, D.; Cacho-Izquierdo, M.; Castro-Pichel, J.; Fiandor Roman, J. M.; Hennessy, A. J.; Pearson, N. D.;Remuinan-Blanco, J. M. Naphthyridin-2(1H)-one compounds as antibacterial agents and their preparation, pharmaceutical compositions and use in the treatment of tuberculosis. WO 2009090222, **2009**.

Alemparte-Gallardo, C.; Barfoot, C.; Barros-Aguirre, D.; Cacho-Izquierdo, M.;Fiandor Roman, J. M.; Hennessy, A. J.; Pearson, N. D.; Remuinan-Blanco, M. J. Preparation of tricyclic nitrogen containing compounds as antibacterials. WO2009141398, **2009**.

Alemparte-Gallardo, C.; Barros-Aguirre, D.; Cacho-Izquierdo, M.; Fiandor-Roman, J. M.; Lavandera Diaz, J. L.; Remuinan-Blanco, M. J. Naphthyridin-2(1H)-one compounds as antibacterials and their preparation and use for the treatment of bacterial infections. WO2010081874, **2010**.

Miles, T.J.; Hennessy, A. J.; Bax, B.; Brooks, G.; Brown, B.S.; Brown, P.; Cailleau, N.; Chen, D.; Dabbs, S.; Davies, T. D.; Esken, J.M; Giordano, L.; Hoover, J.L; Huang, J.; Jones, G. E.; Sukmar, S.K.K; Spitzfaden, C.; Markwell, R. E.; Mlingthorn, E.A.; Rittenhouse, S.; Gwynn, M.N; , Pearson, N. D. Novel hydroxyl tricyclics (e.g., GSK966587) as potent inhibitors of bacterial type IIA topoisomerases. *Bioorg. Med. Chem. Lett*. **2013**, 23, 5437–5441.

Barrows, D. Recent advances in TB drug development, 40th IUATLD Meeting, Cancun, Mexico, **Dec2009**. (b) Presentations, Dec2009. http://www.newtbdrugs.org/eventfiles/p4/Novel%20Mtb%20DNA%20Gyrase%20inhibitors_The%20Union_40th.pdf.

Eric A, V.; Hao, Y.; Susan V, D.; Stacie A, C.; Hayao, M.; Ilaria, G.; Alan J, H.; Richard M, G.; Jeffery L, W. Target-directed synthesis of antibacterial drug candidate GSK966587. *Org. Lett*. **2010**, 12, 3422−3425.

Lluis, B.; David, B.; Gerald, B.; Julia, C.P.; Steven, D.; Robert A.D.; David Thomas,D.; Jose Maria, F.R.; Ilaria,G.; Alan Joseph,H. Derivatives and analog of N-ethylquinolones and N-ethylazaquinolones as antibacterial agents and their preparation. WO2008009700, **2008**.

Brooks, G.; Dabbs, S.; Davies, T. D.; Hennessy, A. J.; Jones, G. E.; Markwell, R. E.;Miles, T. J.; Owston, N. A.; Pearson, N. D.; Peng, T. W. The design of efficient and selective routes to pyridyl analogues of 3-oxo-3,4-dihydro-2H-1,4-(benzothiazine or benzoxazine)-6-carbaldehydes. *Tetrahedron Lett.* **2010**, 51, 5035–5037.

Hameed P.S.: Shanbhag, G.; Shinde, V.; Chinnapattu, M.; Manjrekar, P.; Puttur, J.; Patil, V.; Ugarkar, B. Short and efficient synthesis of oxazinone and thiazinone containing bicyclic heteroaromatic aldehydes. *Syn.com.***2013**, 43, 3315–3321.

Shandil, R.K.; Jayaram, R.; Kaur, P.; Gaonkar, S.; Suresh, B.L.; Mahesh, B.N; Jayashree, R; Nandi, V.; Bharath, S; Balasubramanian, V. Moxifloxacin, ofloxacin, sparfloxacin, and ciprofloxacin against Mycobacterium tuberculosis: evaluation of in vitro and pharmacodynamic indices that best predict in vivo efficacy. *Antimicrob. Agents. Chemother.* **2007**, 51,576-82.

Brvar, M.1.; Perdih, A.; Renko, M.; Anderluh, G.; Turk, D.; Solmajer, T. Structure-based discovery of substituted 4,5'-bithiazoles as novel DNA gyrase inhibitors. *J.Med.Chem.* **2012**, 55, 6413-6426.

Shirude, P. S.; Madhavapeddi, P.; Tucker, J. A.; Murugan, K.; Patil, V.; Basavarajappa, H.; Raichurkar, A. V.; Humnabadkar, V.; Hussein, S.; Sharma, S.; Ramya, V. K; Narayan, C. B.; Balganesh, T. S.; Sambandamurthy, V. K. Aminopyrazinamides. Novel and specific GyrB inhibitors that kill replicating and nonreplicating Mycobacterium tuberculosis. *ACS Chem. Biol.* **2013**, 8, 519−523.

Kale, M. G.; Raichurkar, A.; Hameed, S. P.; Waterson, D.; McKinney, D.; Manjunatha, M. R.; Kranthi, U.; Koushik, K.; Jena, L.; Shinde, V.; Rudrapatna, S.; Barde, S.; Humnabadkar, V.; Madhavapeddi, P.; Basavarajappa, H.; Ghosh, A.; Ramya, VK, Guptha, S.; Sharma, S.; Vachaspati, P.; Mahesh Kumar, K. N.; Giridhar, J.; Reddy, J.; Panduga, V.; Ganguly, S.; Ahuja, V.; Gaonkar, S.; Naveen Kumar, C. N.; Ogg, D.; Tucker, J. A.; Bori-ack-Sjodin, A. P.; de Sousa, S. M.; Sambandamurthy, V. K.; Ghorpade, S. R. Thiazolopyridine ureas as novel antitubercular agents acting through inhibition of DNA gyrase B. *J. Med. Chem.* **2013**, 56, 8834-8848.

Hameed, S. P.; Solapure, S.; Mukherjee, K.; Nandi, V.; Waterson, D.; Shandil, R.; Balganesh, M.; Sambandamurthy, V. K.; Raichurkar, A.; Deshpande, A.; Ghosh, A.; Awasthy, D.; Shanbhag, G.; Sheikh, G.; McMiken, H.; Puttur, P.; Reddy, J.; Werngren, J.; Read, J.; Kumar, M.; Ramaiah, M.; Chinnapattu1, M.; Madhavapeddi, P.; Manjrekar, P.; Basu, R.; Gaonkar, S.; Sharma, S.; Hoffner, S.; Humnabadkar, V.; Subbulakshmi, V.; Panduga, V. Optimization of pyrrolamides as mycobacterial GyrB ATPase inhibitors: structure-activity relationship and in vivo efficacy in a mouse model of tuberculosis. *Antimicrob. Agents Chemother.* **2013**, 58, 6-70.

Kale, R.R.; Kale, M.G.; Waterson, D.; Raichurkar, A.; Hameed, S.P.; Manjunatha, M. R.; Kishore Reddy, B.K; Malolanarasimhan, K.; Shinde, V.; Koushik, K.; Jena, L. K.;

Menasinakai, S.; Humnabadkar, V.; Madhavapeddi, P.; Basavarajappa, H.; Sharma, S.; Nandishaiah, R.; Mahesh Kumar, K.N.;, Ganguly, S.; Ahuja, V.; Gaonkar, S.; Naveen Kumar, C. N.; Ogg, D.; Boriack-Sjodin, P. A.; Sambandamurthy, V. K, de Sousa, S. M.; Ghorpade, S.R. Thiazolopyridone ureas as DNA gyrase B inhibitors: optimization of antitubercular activity and efficacy. *Bioorg. Med. Chem. Lett*. **2014**, 24, 870–879.

ROCS 3.2.0.4: OpenEye Scientific Software, Santa Fe, NM. http://www.eyesopen.com.

Hawkins, P.C.D.; Skillman, A.G.; Nicholls, A. Comparison of shape-matching and docking as virtual screening tools. *J. Med. Chem*. **2007**, 50, 74-82.

Molecular operating environment (MOE), 2013.08; Chemical computing croup inc., 1010 Sherbooke St. west, Suite #910, Montreal, QC, Canada, H3A 2R7, 2013.

FRED 2.0: OpenEye scientific software, Santa Fe, NM. http://www.eyesopen.com.

McGann, M. FRED pose prediction and virtual screening accuracy. *J. Chem. Inf. Model*. **2011**, 51, 578-596.

McGrath, M.; Gey van Pittius, N. C.; Sirgel, FA. Van Helden, P.D.; Warren, R. M. Moxifloxacin retains anti-mycobacterial activity in the presence of gyrA mutations. *Antimicrob. Agents Chemother*. **2014**, 58, 2912-2915.

Jayaram, R.; Gaonkar, S.; Kaur, P.; Suresh, B. L.; Mahesh, B. N.; Jayashree, R.; Nandi, V.; Bharat, S.; Shandil, R. K.; Kantharaj, E.; Balasubramanian, V. Pharmacokinetics-pharmacodynamics of rifampin in an aerosol infection model of tuberculosis. *Antimicrob. Agents Chemother*. **2003**, 47, 2118–2124.

Huitric, E.; Verhasselt, P.; Andries, K.; Hoffner, S.E. In vitro Antimycobacterial Spectrum of a Diarylquinoline ATP Synthase Inhibitor. *Antimicrob. Agents Chemother*. **2007**, 51, 4202-4204.

Dickinson J.M., Mitchison D.A. Experimental models to explain the high sterilizing activity of rifampin in the chemotherapy of tuberculosis. *Am. J. Respir. Crit. Care Med.* **1981**, *159*, 1580-1584.

Girling D.J. The role of pyrazinamide in primary chemotherapy for pulmonary tuberculosis. *Tubercle* **1984**, *65*, 1-4

Dorman S.E., Chaisson R.E. From magic bullets back to the Magic Mountain: the rise of extensively drug-resistant tuberculosis. *Nat. Med.* **2007**, *13*, 295-298.

Mukherjee J.S., Rich M.L., Socci A.R., Joseph J.K., Virú F.A., Shin S.S., Furin J.J., Becerra M.C., Barry D.J., Kim J.Y., Bayona J., Farmer P., Fawzi M.C., Seung K.J. Programmes and principles in treatment of multidrug-resistant tuberculosis. *Lancet* **2004**, *363*, 474-481.

Chan E.D., Strand M.J., Iseman M.D. Treatment outcomes in extensively resistant tuberculosis. *New Engl. J. Med.* **2008**, *359*, 657-659.

Hopewell P.C., Pai M., Maher D., Uplekar M., Raviglione M.C. International standards for tuberculosis care. *Lancet Infect. Dis.* **2006**, *6*, 710-725.

Migliori G.B., De Iaco G., Besozzi G., Centis R., Cirillo D.M. First tuberculosis cases in Italy resistant to all tested drugs. *Euro. Surveill.* **2007**, *12*, E070517- E070517.

Velayati A.A., Masjedi M.R., Farnia P., Tabarsi P., Ghanavi J., Ziazarifi A.H., Hoffner S.E. Emergence of new forms of totally drug-resistant tuberculosis bacilli: super extensively drug-resistant tuberculosis or totally drug-resistant strains in iran. *Chest* **2009**, *136*, 420-425.

Udwadia Z.F., Amale R.A., Ajbani K.K., Rodrigues C. Totally drug-resistant tuberculosis in India. *Clin. Infect. Dis.* **2012**, *54*, 579-581.

Parida S.K., Axelsson-Robertson R., Rao M.V., Singh N., Master I., Lutckii A., Keshavjee S., Andersson J., Zumla A., Maeurer M. Totally-drug resistant tuberculosis and adjunct therapies. *J. Intern. Med.* **2014**. Published online Jan 18. DOI:10.1111/joim.12264.

Cohen J. Approval of novel TB drug celebrated-with restraint. *Science* **2013**, *339*, 130-130.

Zumla A.I., Gillespie S.H., Hoelscher M., Philips P.P., Cole S.T., Abubakar I., McHugh T.D., Schito M., Marurer M., Nunn A.J. New antituberculosis drugs, regimens, and adjunct therapies: needs, advances, and future prospects. *Lancet Infect. Dis.* **2014**, *14*, 327-340.

Andries K., Verhasselt P., Guillemont J., Göhlmann H.W., Neefs J.M., Winkler H., Gestel J.V., Timmerman P., Zhu M., Lee E., Williams P., Chaffoy D., Huitric E., Hoffner S., Cambau E.,

Truffot-Pernot C., Lounis N., Jarlier V. A diarylquinoline drug active on the ATP synthase of *Mycobacterium tuberculosis*. *Science* **2005**, *307*, 223-227.

Makarov V., Manina G., Mikusova K., Mollmann U., Ryabova O., Saint-Joanis B., Dhar N., Pasca M.R., Buroni S., Lucarelli A.P., Milano A., De Rossi E., Belanova M., Bobovska A., Dianiskova P., Kordulakova J., Sala C., Fullam E., Schneider P., McKinney J.D., Brodin P., Christophe T., Waddell S., Butcher P., Albrethsen J., Rosenkrands I., Brosch R., Nandi V., Bharath S., Gaonkar S., Shandil R.K., Balasubramanian V., Balganesh T., Tyagi S., Grosset J., Riccardi G., Cole S.T. Benzothiazinones kill *Mycobacterium tuberculosis* by blocking arabinan synthesis. *Science* **2009**, *324*, 801-804

Pethe K., Bifani P., Jang J., Kang S., Park S., Ahn S., Jiricek J., Jung J., Jeon H.K., Cecjetto J., Christophe T., Lee H., Kempf M., Jackson M., Lenaerts A.J., Pham H., Jones V., Seo M.J., Kim Y.M., Seo M., Seo J.J., Park D., Ko Y., Choi I., Kim R., Kim. S.Y., Lim S., Yim S-A., Nam J., Kang H., Kwon H., Oh C-T., Cho Y., Jang Y., Kim J., Chua A., Tan B.H., Nanjundappa M.B., Rao S.P.S., Barnes W.S., Walker J.R., Alonso S., Lee S., Kim J., Oh S., Oh T., Nehrbass U., Han S-J., No Z., Lee J., Brodin P., Cho S.N., Nam K., Kim J. Discovery of Q203, a potent clinical candidate for the treatment of tuberculosis. *Nat. Med.* **2013**, *19*, 1157-1160.

Zhang D., Lu Y., Liu K., Liu B., Wang J., Zhang G., Zhang H., Liu Y., Wang B., Zheng M., Fu L., Hou Y., Gong N., Lv Y., Li C., Cooper C.B., Upton A.M., Yin D., Ma Z., Huang H. Identification of less lipophilic riminophenazine derivatives for the treatment of drug-resistant tuberculosis. *J. Med. Chem.* **2012**, *55,* 8409-8417.

Aubry A., Pan X.S., Fisher L.M., Jarlier V., Cambau E.Caws M.; *Mycobacterium tuberculosis* DNA gyrase: interaction with quinolones and correlation with antimycobacterial drug activity. *Antimicrob. Agents Chemother*. **2004**, 48, 1281−1288.

Baka E., Comer J. E. A., Takács-Novák K., Study of equilibrium solubility measurement by saturation shake-flask method using hydrochlorothiazide as model compound. *J. Pharm. and Biomed. Anal*. **2008**, 46, 335-341.

Berthod A.; Hydrophobicity of ionizable compounds. A theoretical study and measurements of diuretic octanol–water partition coefficients by countercurrent chromatography.Anal. Chem. **1999**, 71, 879–888.

Tavelin S., Taipalensuu J., Söderberg L., Morrison R., Chong S., Artursson P.; Prediction of the oral absorption of low-permeability drugs using small intestine-like 2/4/A1 cell monolayers. *Pharm Res.* **2003**, 20, 397-405.

Appendix

List of Publications

From this work

Hameed, P. S.; Patil, V.; Solapure, S. M.; Sharma,U.; Madhavapeddi, P.; Raichurkar, A.; Murugan Chinnapattu, M.; Manjrekar, P.; Shanbhag,G;   Puttur,J.; Shinde, V.; Menasinakai, S.; Rudrapatana , S.; Achar, V.; Awasthy,D.; Nandishaiah, R.; Humnabadkar, V.; Ghosh, A.; Narayan, C.; Ramya V K.; Kaur, P.; Sharma, S.; Wirngren, J.; Hoffner, H.; Panduga, V.; Naveen Kumar, C. N.; Reddy, J.; Mahesh Kumar, K. N.; Ganguly, S.; Bha-rath,S.; Mukherjee, K.; Arora, U.; Gaonkar, S.; Coulson, M.; Waterson, D.; Sambandamurthy, V. K.; de Sousa, S. M. Novel N-linked aminopiperidine based gyrase inhibitors with improved hERG and *in vivo* efficacy against Mycobacterium tuberculosis. *J. Med. Chem.* **2014**, 57, 4889-4905.

Hameed, P.S; Raichurkar, A.; Madhavapeddi, P.; Menasinakai, S.; Sharma, S.; Kaur, P.; Nandishaiah, R.; Panduga, V.; Reddy, J.; Sambandamurthy, V. K.; Sriram, D. Benzimidazoles: novel mycobacterial gyrase inhibitors from scaffold morphing. *ACS Med Chem Lett*. **2014**, 5, 820-825

Hameed P.S.; Manjrekar, P.; Raichurkar, A.; Shinde, V.; Puttur, J.; Shanbhag, G;   Murugan Murugan Chinnapattu, M.; Patil, V.; Rudrapatana , S.; Sharma, S.; Naveen Kumar, C. N.; Nandishaiah, R.; Madhavapeddi, P.; Sriram, D. Solapure, S. M.; Sambandamurthy, V. K. Left hand side exploration of novel bacterial topoisomerase inhibitors to improve selectivity against hERG binding [Communicated to *ACS Med Chem Lett*.)

Other publications

Hameed P, S., et *al.* **"**Triaminopyrimidin**e** is a fast killing and long acting antimalarial clinical candidate"**.** *Nat Commun.* **2015**, 6, 6715. . Published online Jan 31. DOI:10.1038/ncomms7715

Hameed, P. S. *et al*. Aminoazabenzimidazoles, a novel class of orally active antimalarial agents. J Med Chem. **2014**, 57, 5702-5713.

Ramachandran, S.; **Hameed, P. S**. *et al*. Aminoazabenzimidazoles, a novel class of orally active antimalarial agents. J Med Chem. **2014**, 57, 6642-6652.

Hameed, P. S. *et al*. Pyrazolopyrimidines establish MurC as a vulnerable target in *Pseudomonas aeruginosa* and *Escherichia coli*. *ACS. chem.bio*. **2014**, 9, 2274–2282.

Hameed, P. S. *et al*. Optimization of pyrrolamides as mycobacterial GyrB ATPase inhibitors: structure-activity relationship and in vivo efficacy in a mouse model of tuberculosis. *Antimicrob. Agents Chemother*. **2013**, 58, 61-70.

Hameed, P. S. *et al*. Short and efficient synthesis of oxazinone and thiazinone containing bicyclic heteroaromatic aldehydes. *Syn.com*. **2013**, 43, 3315–3321

Kale, M. G.; Raichurkar, A.; **Hameed, S. P**. *et al.* Thiazolopyridine ureas as novel antitubercular agents acting through inhibition of DNA gyrase B. *J. Med. Chem*. **2013**, 56, 8834-8848.

Kale, R.R.; Kale, M.G.; Waterson, D.; Raichurkar, A.; **Hameed, P.S**. *et al*. Thiazolopyridone ureas as DNA gyrase B inhibitors: optimization of antitubercular activity and efficacy. *Bioorg. Med. Chem. Lett*. **2014**, 24, 870–879,

Shirude, P. S.; **Hameed, S**. Nonfluoroquinolone-based inhibitorsof mycobacterial type II topoisomerase as potential therapeutic agentsfor TB. In Annual Reports in Medicinal Chemistry; Desai, M. C., Ed.; Academic Press: Burlington, MA, **2012**; Vol. 47, pp 319−330.

Hameed, P. S. *et al*. Design and Synthesis of Triazolopyrimidine−Acylsulfonamides as Novel Anti-Mycobacterial leads acting through inhibition of Acetohydroxyacid Synthase [AHAS]. *Bioorg. Med. Chem. Lett*. **2014**, 24, 870–879.

Shirude, P. S.; Shandil, R.; Sadler, C.; Naik, M; Hosagrahara, V.; **Hameed, S**. *et al*. Azaindoles: noncovalent DprE1 inhibitors from scaffold morphing efforts, kill Mycobacterium tuberculosis and are efficacious in vivo. *J. Med. Chem*. 2014, 56, 9701–9708.

Shirude P.S., Madhavapeddi P., Naik M., Murugan K., Shinde V., Nandishaiah R., Bhat J., Kumar A., **Hameed, S**. *et al*. Methyl-Thiazoles: A novel mode of inhibition with the potential to develop novel inhibitors targeting InhA in Mycobacterium tuberculosis. *J. Med. Chem*. **2013**, 56, 8533-8542

Humnabadkar, V.; Prabhakar, K.R; Narayan. A.; Sharma, S.; Guptha, S.; Manjrekar, P.; Chinnapattu, M.; Ramachandran, V. ; **Hameed, P.S**.; Ravishankar, S.; Chatterji, M. DP-N-Acetylmuramic Acid L-Alanine Ligase (MurC) Inhibition in a tolC Mutant Escherichia coli Strain Leads to Cell Death. *Antimicrob. Agents Chemother*.**2014**. 58, 6165-617, 2014.

Srivastava, A.; Ramachandran, S.; **Hameed, P. S** *et al*. Identification and Mitigation of a Reactive Metabolite Liability Associated with Aminoimidazoles. *Chem Res toxicol*. **2014**, 27, 1586−1597, 2014

BIOGRAPHY OF SHAHUL HAMEED P

Mr. Shahul Hameed completed his Bachelor of Pharmacy from Tamilnadu Dr. M.G.R Medical University, Chennai, Tamilnadu, and Master of Science (M.S. Pharm.) in Medicinal chemistry from National Institute of Pharmaceutical Education and Research (NIPER), S.A.S Nagar, Mohali, Punjab. He has more than a decade of drug discovery research experience in an industrial set-up with broad background in chemistry, pharmaceutical sciences and medicinal chemistry. His medicinal chemistry expertise includes lead identification and optimization of both anti-bacterials and anti-malarial projects and achieved critical milestones including delivering a clinical candidate for malaria (MMV243). He has been appointed as an AstraZeneca sponsored research fellow at Birla Institute of Technology and Science, Pilani, Hyderabad campus from 2010-2015 under the supervision of Prof. D. Sriram. He has published many scientific papers in well-renowned international journals (two from the current work).

BIOGRAPHY OF Professor D. SRIRAM

D. Sriram is presently working in the capacity of Professor at Department of Pharmacy, Birla Institute of Technology and Science, Pilani, Hyderabad campus. He received his Ph.D. in 2000 from Banaras Hindu University, Varanasi. He has been involved in teaching and research for last 15 years. He has 235 peer-reviewed research publications to his credit. He has collaborations with various national and international organizations such as Karolinska Institute, Sweden; National Institute of Immunology, New Delhi; Institute of Science and Technology for Tuberculosis, PA, Brazil etc. He was awarded the Young Pharmacy Teacher of the year award of 2006 by the Association of Pharmacy Teachers of India. He received ICMR Centenary year award in 2011. He has guided 6 Ph.D. students and 14 students are pursuing Ph.D. currently. His research is funded by agencies like the UGC, CSIR, ICMR, DBT and DST.